UNIVERSITY OF LIVERPOOL

DEVELOPMENT OF A SYNTHETIC SUBSTRATE FOR CONJUNCTIVAL CELL TRANSPLANTATION

Thesis submitted in accordance with the requirements of the University of Liverpool for the degree of Doctor in Philosophy

by

Aruni Kumari Makuloluwa

June 2017

ABSTRACT

The conjunctiva is a translucent mucous membrane consisting of epithelial cells and goblet cells (GCs). It protects the eye from external insults and prevents desiccation of the ocular surface by producing mucins of the tear film. Severe scarring due to injuries and diseases could lead to its anatomical and functional impairment. Moreover, the success of a limbal or a corneal transplant is dependent on the presence of a healthy ocular surface and a tear film. Various grafts and substrates employed to replace the damaged conjunctiva to date, have advantages and disadvantages peculiar to the material. Therefore, there is scope for the development of a better substrate for conjunctival cell transplantation. Understanding the protein composition of the extracellular matrix (ECM) of the conjunctiva that regulates cellular functions, could guide the development of a substrate. The aims of the present study, therefore, were to determine the role of ECM proteins on the growth of conjunctival cells and to investigate cell growth and behaviour on surface modified poly-epsilon-lysine (PεK) hydrogels.

The ECM proteins of a conjunctival epithelial cell line, HCjE-Gi cell line, were isolated using 1% ammonium hydroxide. The protein composition of the cell-secreted ECM from days 1 to 42 was determined using immunofluorescence and mass spectrometry experiments. The growth of cells on cell-secreted ECM of days 3 to 28 over seven days was determined by immunocytochemistry (ICC). The maximum adsorption of type IV collagen, laminin 111 and fibronectin onto tissue culture polystyrene (TCP) was determined using indirect enzyme-linked immunosorbent assays. The adhesion and growth of cells over seven days on TCP with pre-adsorbed type IV collagen, laminin 111, fibronectin and α-2-Heremans Schmid-glycoprotein (α-2-HS-GP) were determined by ICC. The expression of stem cell (SC) and GC protein markers over fourteen days on TCP with pre-adsorbed proteins were determined by ICC. The cell adhesion, growth and expression of MUC5AC protein over fourteen days on PεK hydrogels with and without pre-adsorbed proteins were determined by ICC staining.

Type XVIII collagen, a structural collagen, was present in the ECM of HCjE-Gi cells *in vitro*. The peptides of chains that give rise to laminin 332 were the most abundant glycoproteins present in the ECM. The peptide abundance of α-2-HS-GP was highest in the day 1 ECM, whereas that of fibronectin, nephronectin and vitronectin were highest in the day 7 ECM. Perlecan and agrin were the most abundant proteoglycans in the ECM. The day 7 ECM contained the highest proportion of growth factors and their binding proteins. The proportion of proteases and their inhibitors increased and decreased, respectively, with time. The adsorption of type IV collagen and fibronectin onto TCP reached a saturation point when pre-adsorbed from 5µg/mL solutions, whereas the adsorption of laminin 111 onto TCP reached a saturation point when pre-adsorbed from a 0.5µg/mL solution. Type IV collagen and fibronectin increased the adhesion, and type IV collagen, α-2-HS-GP and cell-secreted ECM of days 3 and 5 increased the growth of HCjE-Gi cells. The expression of SC and GC protein markers reduced and increased, respectively, *in vitro*. Azelaic and suberic acid cross-linked PεK hydrogels supported the adhesion and growth of HCjE-Gi cells *ex vivo*. However, pre-adsorption of proteins onto PεK hydrogels did not affect the adhesion or the growth compared to those without pre-adsorbed proteins. There was evidence of GC differentiation on azelaic acid cross-linked PεK hydrogels with and without pre-adsorbed proteins and on suberic acid cross-linked PεK hydrogels with pre-adsorbed fibronectin.

PεK hydrogels are a promising substrate for the *ex vivo* expansion of conjunctival cells for conjunctival cell transplantation purposes. Functional peptides of ECM proteins identified to enhance the growth and differentiation of conjunctival cells may be employed to develop a substrate for conjunctival cell transplantation in the future.

ACKNOWLEDGEMENTS

I would like to express my deepest gratitude to Professor Rachel Williams, Professor Stephen Kaye and Dr Rosalind Stewart for giving me the opportunity to undertake PhD studies and for their continuous guidance and encouragement throughout the last three years. I would also like to extend my gratitude to Dr Kevin Hamill for his constant support and invaluable advice throughout my PhD studies.

I would like to thank Professor Ilene Gipson for the gift of the HCjE-Gi cell line. I would like to extend my appreciation to Andy Gallagher and SpheriTech Ltd for their advice and assistance with the hydrogels. I would also like to acknowledge Professor Rob Beynon and Dr Deborah Simpson at the Centre for Proteome Research of the University of Liverpool for helping me with the mass spectrometry experiments.

A very special thank you to all the students and staff at the Eye and Vision Science Department for their support and friendship over the last four years.

Finally, I would like to thank my parents and my sisters for their kind words of encouragement and support over the years. Without you I would not have been able to complete my PhD studies. Thank You.

TABLE OF CONTENTS

LIST OF FIGURES AND TABLES

CHAPTER 1: INTRODUCTION

CHAPTER 2: THE ROLE OF EXTRACELLULAR MATRIX PROTEINS ON CELLULAR FUNCTIONS OF HCjE-Gi CELLS

ABBREVIATIONS

α-2-HS-GP	α-2-Heremans Schmid-glycoprotein
ΔNp63	Isoform ΔN of tumour protein p63
AA	Azelaic acid
ABCG2	ATP-binding cassette sub-family G member 2
ADAM(s)	A disintegrin and metalloproteinase
ADAMTS(s)	A disintegrin and metalloproteinase with thrombospondin motifs
ADM	Adrenomedullin
AM(s)	Amniotic membrane(s)
ANOVA	Analysis of variance
AVP-NPII	Vasopressin-neurophysin 2-copeptin
BCAM	Basal cell adhesion molecule
BM(s)	Basement membrane(s)
BSA	Bovine serum albumin
CCDC 80	Coiled-coil domain-containing protein 80
CD	Cluster of differentiation
CO_2	Carbon dioxide
CXCL	C-X-C motif chemokine
DAPI	4',6-Diamidino-2-Phenylindole, Dilactate
dH_2O	Distilled water
Dkk 1	Dickkopf-related protein 1
DTT	Dithiothreitol
ECM(s)	Extracellular matrix (matrices)
EDCI	1-(3-Dimethylaminopropyl)-3-ethylcarbodiimide HCl
EDDR 1	Epithelial discoidin domain-containing receptor 1
EDTA	Ethylenediaminetetraacetic acid
EGF	Epidermal growth factor
EHS	Engelbreth-Holm-Swarm
ELISA	Enzyme-linked immunosorbent assay
FGF	Fibroblast growth factor
FGFBP 1	Fibroblast growth factor binding protein 1
GAG(s)	Glycosaminoglycan(s)
GC(s)	Goblet cell(s)

GDF	Growth differentiation factor
GF(s)	Growth factor(s)
GGT 3	Gamma-glutamyltranspeptidase 3
GP(s)	Glycoprotein(s)
HAI 1	Hepatocyte growth factor activator inhibitor type 1
HCjE-Gi cells	Human conjunctival epithelial cell line – Gipson laboratory
HSPG(s)	Heparan sulphate proteoglycan(s)
hTERT	Human telomerase reverse transcriptase
HTRA1	High-temperature requirement A1
ICC	Immunocytochemistry
IF	Immunofluorescence
IGFBP(s)	Insulin-like growth factor binding protein(s)
ITI	Inter-alpha-trypsin inhibitor
KSF	Keratinocyte serum-free
LC-MS/MS	Liquid chromatography–mass spectrometry/mass spectrometry
LSCD	Limbal stem cell deficiency
LSCM	Laser scanning confocal microscopy
LTBP(s)	Latent transforming growth factor β binding protein(s)
LYPD 3	Ly6/PLAUR domain-containing protein 3
MIF	Migration inhibitory factor
MMP(s)	Matrix metalloproteinase(s)
MT-SP 1	Membrane type serine protease 1
MUC(s)	Mucin(s)
NBF	Neutral buffered formalin
NH_4HCO_3	Ammonium bicarbonate
NH_4OH	Ammonium hydroxide
NHS	N-Hydroxysuccinimide
NMM	4-Methylmorpholine
OS	Ocular surface
PAI	Plasminogen activator inhibitor
PBS	Phosphate buffered saline
PBST	PBS containing 0.1% Tween 20
PCL	Poly(ε-Caprolactone)
PDGF-A	Platelet derived growth factor A

PεK	Poly-epsilon-lysine
PG(s)	Proteoglycan(s)
PL	Phospholipase
PLGA	Poly(lactide-*co*-glycolide)
pNPP	*p*-nitrophenylphosphate
RISC	Retinoid-inducible serine carboxypeptidase
RT	Room temperature
SA	Suberic acid
SAA 1	Serum amyloid A-1
SC(s)	Stem cell(s)
SJS	Stevens-Johnson syndrome
SPARC	Secreted protein acidic and rich in cysteine
TAC(s)	Transient amplifying cell(s)
TACST 2	Tumour-associated calcium signal transducer 2
TCP	Tissue culture polystyrene
TE	Tissue engineering
TFA	Trifluoroacetic acid
TFPI 2	Tissue factor pathway inhibitor 2
TGFβ	Transforming growth factor β
TGFβ ig-h3	Transforming growth factor β-induced protein ig-h3
TIMP(s)	Tissue inhibitor(s) of matrix metalloproteinases
TIN Ag-like	Tubulointerstitial nephritis antigen-like
UEAI	Ulex europaeus agglutinin I

1 INTRODUCTION

1.1 THE EYE

1.1.1 ANATOMY AND PHYSIOLOGY

The eyes are specialised organs responsible for the perception of vision (figure 1.1).(1) They are protected within two bony cavities in the skull. The adult eye (volume 6.5mL) has an antero-posterior diameter of 21-26mm and a transverse diameter of approximately 24mm.(1, 2) It is made up of corneo-scleral, uveal and neural layers.(1) These surround the lens and three intraocular compartments (anterior chamber, posterior chamber and vitreous cavity). It can be approximated by a smaller anterior sphere comprising the cornea that contributes to one-sixth of the total circumference of the eye, whereas a larger posterior sphere making up the sclera accounts for the remainder of the circumference. The transparent cornea is the major refracting surface of the eye and transmits light rays to be focused on the retina. The opaque and fibrous sclera protects the intraocular tissues and maintains the shape of the eye. The uveal layer consists of the iris, ciliary body and choroid. The iris forms a central circular aperture, pupil, which controls the amount of light entering the eye. The ciliary body and the zonules alter the refractive power of the lens, thus allowing the eye to focus on either near or distant objects.(1, 2) The vascular choroid nourishes the outer retina.(1) The neural layer (neurosensory retina and retinal pigment epithelium) converts light energy into electrical impulses that are relayed, via the visual pathway, to the higher cortical centres in the brain to be processed to form an image.(1)

The anterior chamber is between the cornea and the anterior surface of the iris, whereas the posterior chamber is between the posterior surface of the iris and the lens.(1, 2) The ciliary processes of the ciliary body produce aqueous humour at a rate of 2-4µL per minute, which is secreted into the posterior chamber.(1) From here, the aqueous humour flows through the pupil into the anterior chamber and is removed chiefly via the Schlemm's canal that is adjacent to the trabecular meshwork, to maintain a stable intraocular pressure. The vitreous cavity between the posterior surface of the lens and the inner surface of the neurosensory retina occupies two-thirds of the volume of the eye. The vitreous humour, predominantly consisting of water, acts as a shock absorber and maintains the position of the neurosensory retina as well as the shape of the eye. The ocular appendages, namely the eyelids, the conjunctiva and the lacrimal apparatus, all aid towards the principal function of the eye, which is photoreception.(1)

The human eye

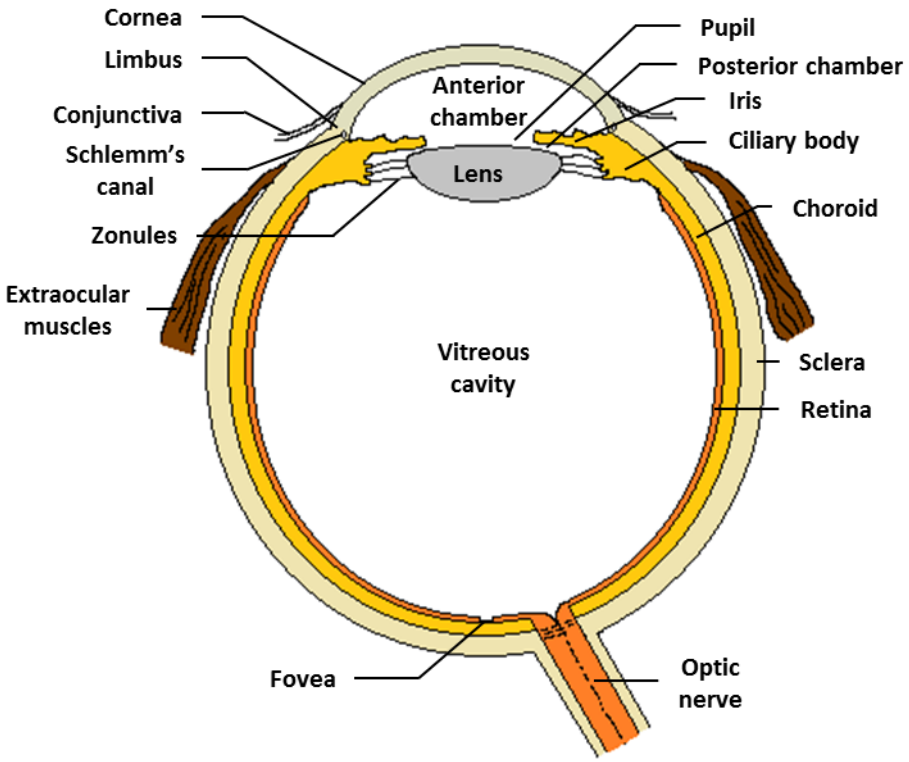

Figure 1.1: The human eye. The cornea transmits light rays from the environment, which then travel through the anterior chamber, the crystalline lens and the vitreous cavity to focus on the neurosensory retina, where the photoreceptors (rods and cones) convert light energy into electrical impulses that are transmitted to the brain to be processed to form an image. **(Adapted from: Forrester JV, Dick AD, McMenamin PG, Roberts F, Pearlman E. The Eye: Basic Sciences in Practice. 4th ed. UK: Elsevier; 2016. Figure 1.10, Schematic diagram of the human eye in horizontal section; p. 14)**

1.1.2 EMBRYOLOGY

The ocular tissues originate from two of the three primitive embryonic layers: the ectoderm and the mesoderm (table 1.1).(3) The ectoderm is divided into the surface ectoderm and its derivative, neural crest cells, and the neural ectoderm. The eye commences its development approximately on day 22 of a human embryo (figure 1.2).(1) Optic sulci appear as shallow pits on the inner surface of the neural ectoderm prior to their closure to form the neural tube or the future forebrain.(1, 3) The optic sulci out-pocket towards the surface ectoderm to form optic vesicles.(1, 3) On day 25, the hollow optic vesicles become surrounded by mesenchymal cells (neural crest cells and mesoderm), except at the apex adjacent to the surface ectoderm.(1) The disk-shaped neural ectoderm, called the retinal disk, is positioned posterior to the surface ectoderm. On day 27, the portion of the surface ectoderm that is adjacent to the neural ectoderm increases in thickness to form the lens placode, which overlaps the formation of the optic stalk that connects the developing eye to the forebrain. The optic vesicle invaginates further to form an optic cup with two layers of cells: the inner cell layer that will become the neurosensory retina, and the outer cell layer that will develop to be the retinal pigment epithelium. By day 29, the lens placode also invaginates to form a lens vesicle, which will eventually separate from the surface ectoderm to form the future lens. The surface ectoderm will give rise to the corneal epithelium (day 35 to day 42), whereas waves of mesenchymal cells form the stroma and the endothelium of the cornea (day 49).(1, 4) The surface ectoderm also gives rise to the future conjunctival epithelium, ocular adnexal gland epithelia, lacrimal gland and eyelid epidermis.(1)

The inferior aspect of the developing optic vesicle consists of a groove called the optic fissure, where the hyaloid vessels enter to nourish the developing eye.(1) Approximately on day 44, the optic fissure will close enclosing the hyaloid vessels within the canal of the optic stalk. The proximal ends of the hyaloid vessels will eventually persist as the central retinal artery and vein that nourish the inner portion of the neurosensory retina. By the end of the embryonic period (day 56), the eye is approximately 1.5-2.0mm in diameter with a double-layered retina derived from the neural ectoderm, lens and ocular surface epithelia derived from the surface ectoderm, and mesenchyme-derived corneal stroma, corneal endothelium, choroid and sclera.(1)

Embryological origins of the ocular tissues

SURFACE ECTODERM	NEURAL CREST CELLS	NEURAL ECTODERM	MESODERM
Conjunctival epithelium	Corneal stroma	Neurosensory retina	Vitreous
Corneal epithelium	Corneal endothelium	Retinal pigmented epithelium	Extra-ocular muscles
Epithelia of adnexal glands	Trabecular meshwork endothelium	Ciliary epithelium	Vascular endothelium
Lacrimal gland	Iris stroma	Iris pigmented epithelium	
Lens	Choroidal stroma	Iris dilator and sphincter muscles	
Eyelid epidermis	Ciliary muscles	Optic nerve fibres and glia	
	Scleral fibroblasts		
	Vitreous		
	Optic nerve meninges		

Table 1.1: Embryological origins of the ocular tissues.

Embryology of the human eye

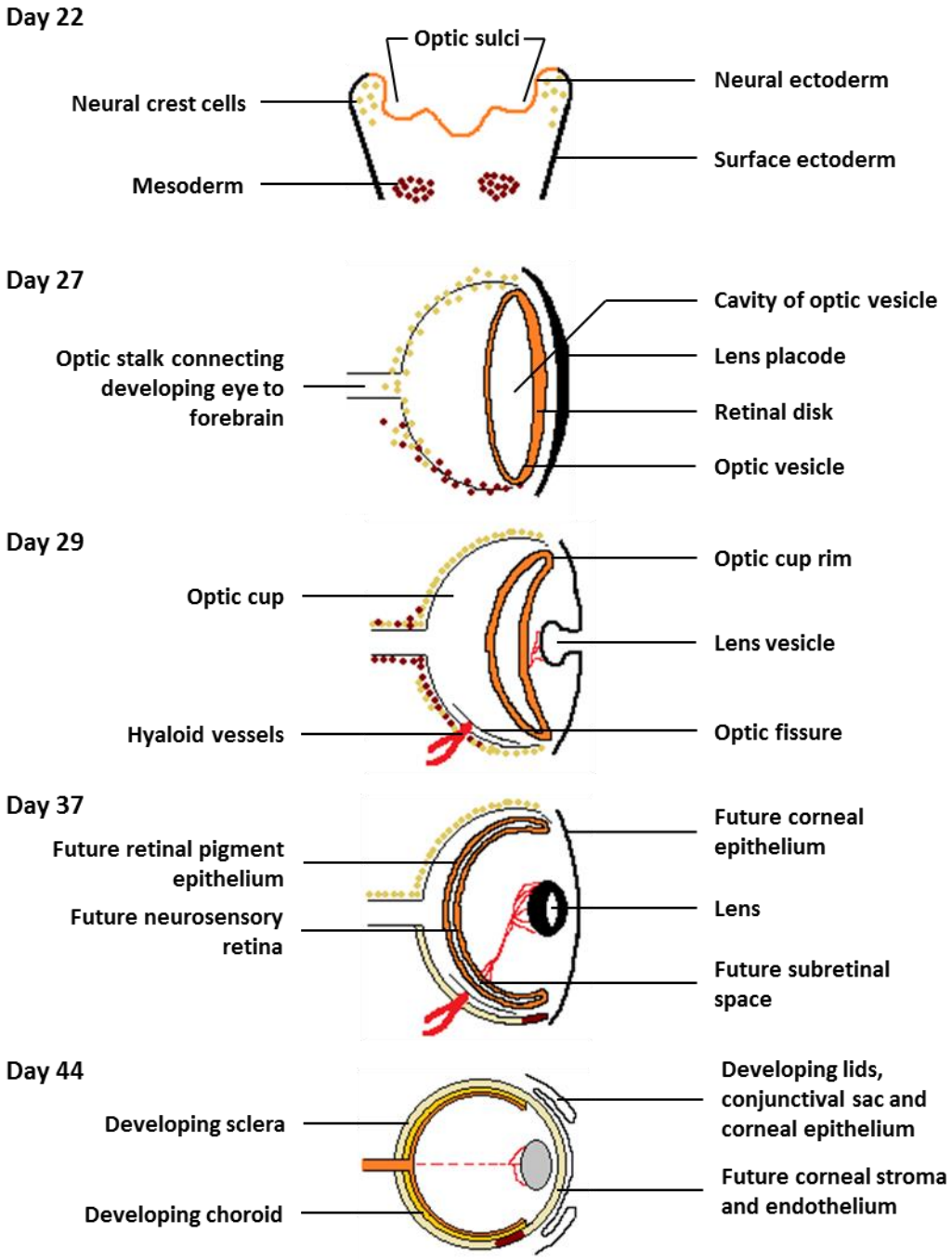

Figure 1.2: Embryology of the human eye. **(Adapted from: Forrester JV, Dick AD, McMenamin PG, Roberts F, Pearlman E. The Eye: Basic Sciences in Practice. 4th ed. UK: Elsevier; 2016. Figure 2.1, Diagrammatic summary of ocular embryonic development from day 22 to week 8; p. 104-5)**

1.2 THE OCULAR SURFACE

1.2.1 ANATOMY AND PHYSIOLOGY

The ocular surface (OS), as described by Thoft in 1978, consists of the external anterior segment of the eye, which includes the cornea, conjunctiva, lacrimal gland and the eyelids.(5) This definition was further expanded by Gipson in 2007, who took into account the embryological origins and functions of the OS, to describe it as the integrated unit of '*surface and glandular epithelia of the cornea, conjunctiva, lacrimal gland, accessory lacrimal glands, meibomian glands and their apical (tears) and basal (connective tissue) matrices; eyelashes with their associated glands of Moll and Zeis; those components of the eyelids responsible for the blink and the nasolacrimal duct*'.(5, 6) The rationale for this definition was that all the tissues of the OS are linked to each other by a continuous epithelium that originated from the surface ectoderm (table 1.1) and that they are all linked via the vascular, nervous, immune and endocrine systems to give rise to the OS system (figure 1.3).(5, 6)

The external appearance of the OS (figure 1.4) includes the transparent cornea in the centre surrounded by the sclero-conjunctival areas, seen as the white of the eye.(5) The transition zone between the cornea and the conjunctiva is known as the limbus. A tear film forms a smooth and transparent layer over the external surface of the OS.(1) The upper and lower eyelids meet at the medial and lateral canthi at the angles of the palpebral fissure.(5) Due to its exposure to the environment, the cornea responsible for the refraction and transmission of light rays into the eye; is particularly prone to injury, disease and desiccation.(6) Thus, the primary function of the OS system is to protect the cornea and maintain its smooth refractive surface. The OS system has evolved to entail a variety of protective structures and mechanisms.(7) The bony orbit and eyelids protect the eye from traumatic injuries. The tear film provides physical and chemical protection against desiccation and pathogens. The epithelial cells of the OS consist of a variety of defence mechanisms of the innate and adaptive immune systems. Damage to one or more components of the OS system can give rise to secondary dysfunction of the other components of the system and subsequent pathology.(6, 8)

The ocular surface system

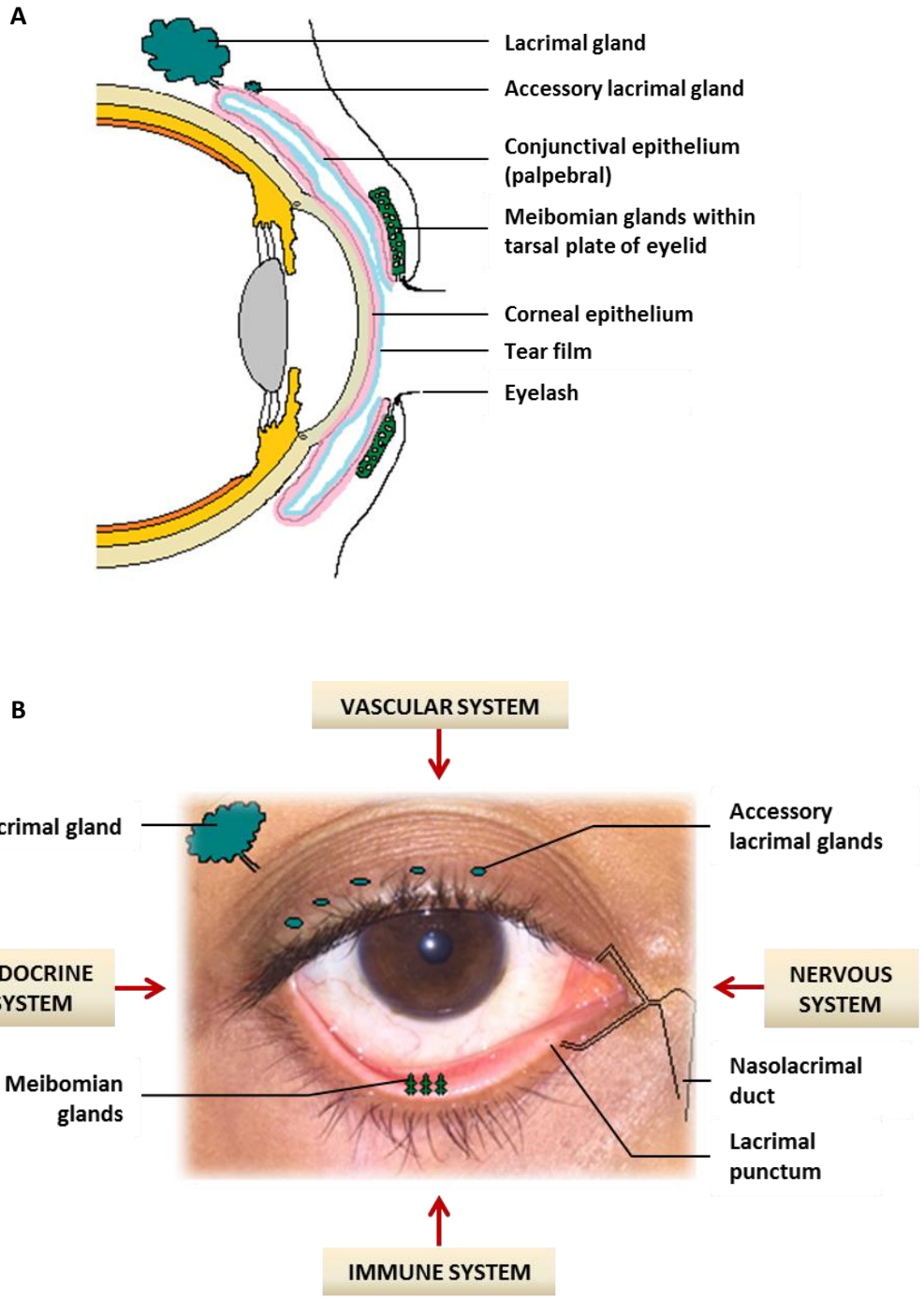

Figure 1.3: The ocular surface system. A sagittal section of the ocular surface system showing the continuous epithelia of the ocular surface (pink) and the overlying tear film (blue) (A), which are linked via the vascular, nervous, immune and endocrine systems (B). **(Adapted from: Gipson IK. The ocular surface: the challenge to enable and protect vision: the Friedenwald lecture. Invest Ophthalmol Vis Sci. 2007;48(10):4390-8. Figure 1, Diagrams depicting the Ocular Surface System; p. 4392)**

Surface anatomy of the human eye

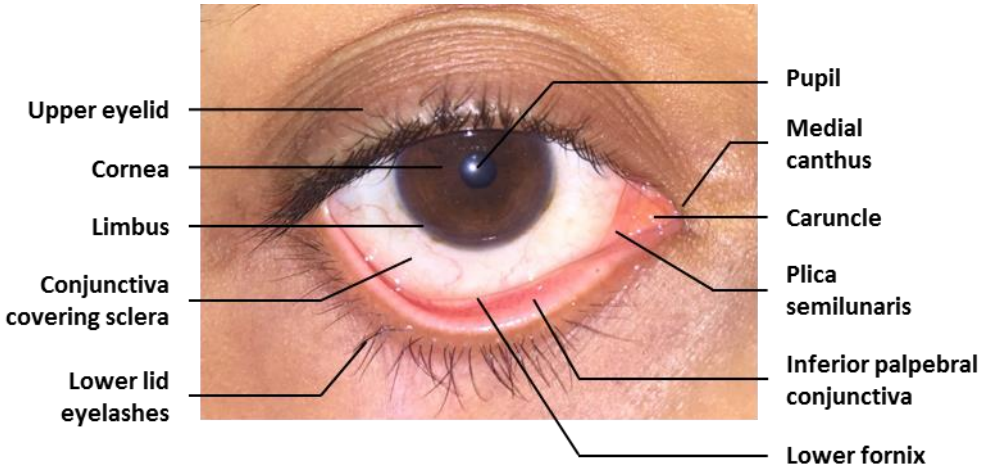

Figure 1.4: Surface anatomy of the human eye.

1.2.1.1 CORNEA

Gross structure and functions

The cornea is a transparent, avascular tissue in the centre of the OS (figure 1.4).(5) When viewed anteriorly it is ovoid in shape with a vertical diameter of approximately 10.6mm and a horizontal diameter of approximately 11.7mm.(1) The central radius of the anterior surface of the cornea is approximately 7.8mm with the curvature reducing peripherally.(1) The cornea accounts for two-thirds of the total refractive power of the eye and transmits light into the eye to be detected by the photoreceptors in the retina.(6) In addition, it functions to protect the delicate inner structures of the eye and as a support for the overlying tear film.(9) Due to its avascular nature, the cornea receives nutrition from the tear film and the aqueous humour in the anterior chamber.(1)

Histology

The cornea has a central thickness of approximately 520µm and the thickness increases to 670µm towards the periphery.(1) Histologically, it consists of five distinct layers: epithelium, Bowman's layer, stroma, Desçemet's membrane and the endothelium (figure 1.5).(1) The corneal epithelium is a 50-60µm thick stratified and non-keratinised epithelium.(1, 5) It has five to seven layers of epithelial cells of varying morphology: two to three layers of superficial flattened squamous cells, several layers of wing cells and a monolayer of columnar basal cells.(5) The apical surfaces of the superficial cells have microplicae that holds the glycocalyx of the OS.(1) The cells in all layers are linked by tight junctions, which is demonstrated clinically by the lack of fluorescein staining observed on a healthy corneal epithelium.(4) Additionally, the basal cell layer is connected to the underlying basement membrane (BM) via hemidesmosomes and to the stroma via anchoring fibrils.(1) Abnormal or lack of these cellular and extracellular components lead to epithelial defects and recurrent epithelial erosions.(4) The epithelium lacks melanocytes.(1) The main functions of the epithelium are to maintain a smooth OS for refraction and to act as a physical barrier to injury and entry of pathogens.(10)

Bowman's layer is a 8-12µm thick modified acellular layer of the stroma.(1) It consists of randomly arranged type I, III, V and VI collagen fibrils that are 20-30nm in diameter.(1) The anterior margin is well delineated from the BM of the epithelium, whereas the posterior margin merges with the stroma.(1) The Bowman's layer ends abruptly at the limbus.(1) When damaged, the Bowman's layer does not regenerate but leads to scar tissue formation.(4) In contrast, the corneal stroma is made up of 2µm thick 200-250 flattened

layers of collagenous lamellae orientated parallel to the surface of cornea.(1) The adjacent lamellae are orientated right angles to each other, except in the anterior stroma, where the lamellae are orientated more obliquely. The major type of collagen in the stroma is type I collagen with small amounts of type III, V and VI collagens.(1) Each collagen fibre has a diameter of approximately 30nm, which is maintained by type V collagen that wraps around the type I collagen fibrils. Keratocytes, which are modified fibroblasts, lie between the collagenous lamellae in a corkscrew pattern at an average density of 2-2.4x10^4 cells/mm^3.(1) These cells are linked via gap junctions. Glycosaminoglycans (GAGs), predominantly keratan sulphate and chondroitin sulphate, regulate the inter-fibrillary distance between the collagen fibres, and this together with the regular diameter of the fibres help to maintain a transparent cornea.(1, 5) As in the epithelium, the stroma lacks blood and lymphatic vessels.(1) Sensory nerve fibres from the long ciliary nerve (ophthalmic and sometimes maxillary divisions of the trigeminal nerve) enter the cornea peripherally just below the anterior one-third of the stroma.(1) As they travel towards the centre, approximately 1mm from the limbus, the nerve fibres lose the perineurium and the myelin sheath, thus contributing to the maintenance of the overall transparency of the cornea. The nerve fibres change direction to travel towards the epithelium, pierce the Bowman's layer to form the sub-epithelial plexus. Some fibres travel through the epithelial cell layers to form the intra-epithelial plexus that terminate in the superficial layer. These sensory nerve fibres are Aδ and C fibres that carry information regarding pain and temperature.(1) There are seven thousand sensory receptors per square millimetre in the epithelium of the human cornea.(1) Damage to the stroma leads to remodelling of the stroma by myo-fibroblasts and subsequent scar tissue formation.(4)

Desçemet's membrane, a modified BM of the corneal endothelium, is a 8-12µm thick layer that increases with age.(1, 5) It has an anterior banded region produced by the endothelial cells before birth, and a posterior non-banded region secreted after birth.(1, 4) It contains the major proteins found in BMs, type IV collagen, laminin and other glycoproteins.(1) The Schwalbe's line demarcates the transition zone between the Desçemet's membrane and the cortical zone of the trabecular meshwork.(1, 4) The posterior-most layer of the cornea, the endothelium, is a monolayer of cells involved in the active transport of fluid from the corneal stroma to the aqueous humour, thus maintaining the hydration of the corneal stroma and its transparency.(1) The cells (approximately 18-20µm in diameter and 5-6µm in height) are arranged in a hexagonal array with numerous lateral inter-digitations as well as gap and tight junctions.(1, 4) Additionally, there are Na^+/K^+-ATPase pumps in the cell

membranes that are involved in the active transport of fluid across the endothelium.(4) The endothelium has an approximate cell density of 3-4x10^3 cells/mm^2 at birth, reducing to 2.5x10^3 cells/mm^2 in middle age and 2x10^3 cells/mm^2 in old age.(1) The endothelium has a low regenerative capacity and when cells are lost, they are replaced by spreading of adjacent cells that are heterogeneous in size and shape.(1) When the cell density reduces below 800 cells/mm^2, the role of fluid transport becomes disrupted and the stroma becomes oedematous with subsequent reduction or loss in transparency of the cornea.(1) A minimum endothelial cell density of 1.5x10^3 cells/mm^2 of the donor cornea is required when considering potential use in corneal transplantation.(1) Lack of antigen presenting cells in the central cornea and its avascular nature allow for the successful transplantation of donor corneas.(1)

Histology of the cornea

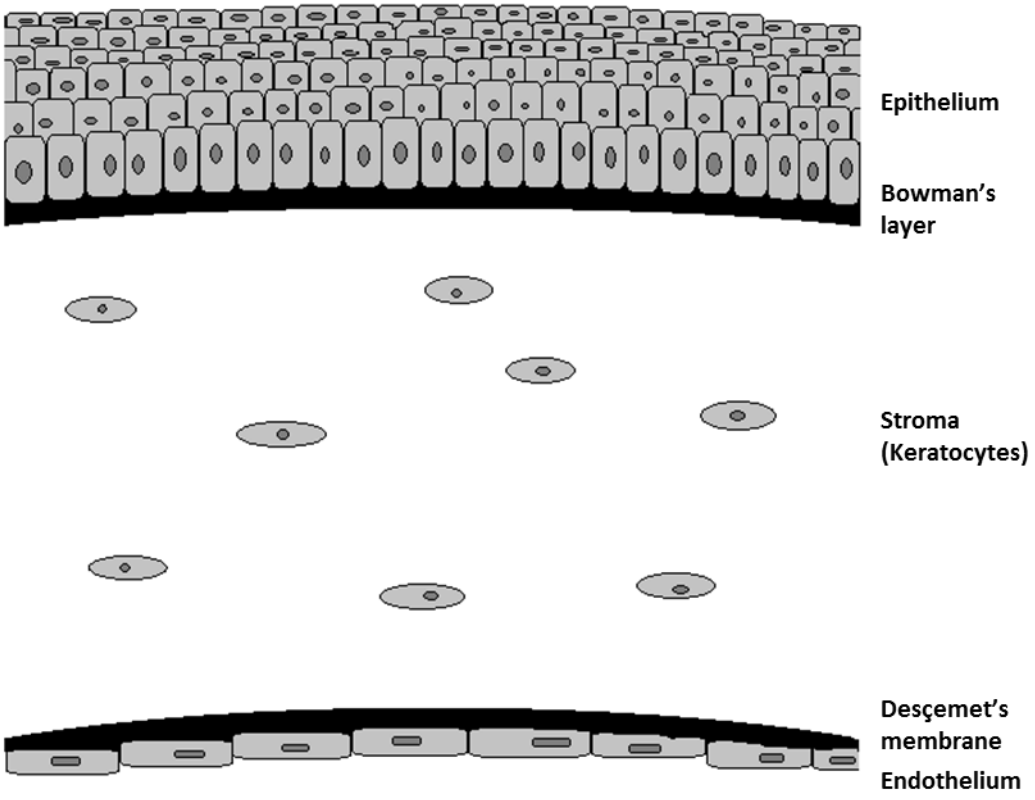

Figure 1.5: Histology of the cornea. The cornea consists of five distinct layers: epithelium (superficial, wing and basal cells), Bowman's layer, stroma, Desçemet's membrane and endothelium.

1.2.1.2 LIMBUS

Gross structure and functions

The limbus is a 1.5-2.0mm wide transition zone between the conjunctiva and the cornea.(11) The surgical limbus appears as a blue-grey zone around the transparent cornea on external examination of the OS (figure 1.4).(1) The line in between these two zones represents the site of Schwalbe's line and incisions made here will pass anterior to the trabecular meshwork and the Schlemm's canal, thus giving a safe access site into the anterior chamber for surgery involving the anterior segment of the eye.(1, 5) The limbus plays numerous roles: source of stem cells for wound healing and nourishment of the cornea, immunosurveillance and hypersensitivity responses of the OS, and aqueous humour outflow and regulation of the intraocular pressure.(1)

Histology

The limbus consists of an uneven stratified squamous epithelium, a BM and an underlying loosely arranged connective tissue stroma.(9) Anatomically, the limbus is described as the transition zone where the regularly arranged corneal collagen lamellae become randomly arranged scleral lamellae (figure 1.6).(1) This is in contrast to the definition used by pathologists, who describe this region as a block of tissue bordered by two lines: one line passing through Schwalbe's line and the junction of the corneal and conjunctival epithelia (stratified non-keratinised corneal epithelium becomes stratified non-keratinised conjunctival epithelium with goblet cells), and a second line drawn perpendicularly from the scleral spur to the tangent of the OS.(1) Immunocompetent cells, such as major histocompatibility complex class II-positive dendritic cells, mast cells, plasma cells and lymphocytes, as well as vascular capillaries and lymphatics that are absent in the cornea appear in the connective tissue of the limbus and conjunctiva.(1)

The limbus

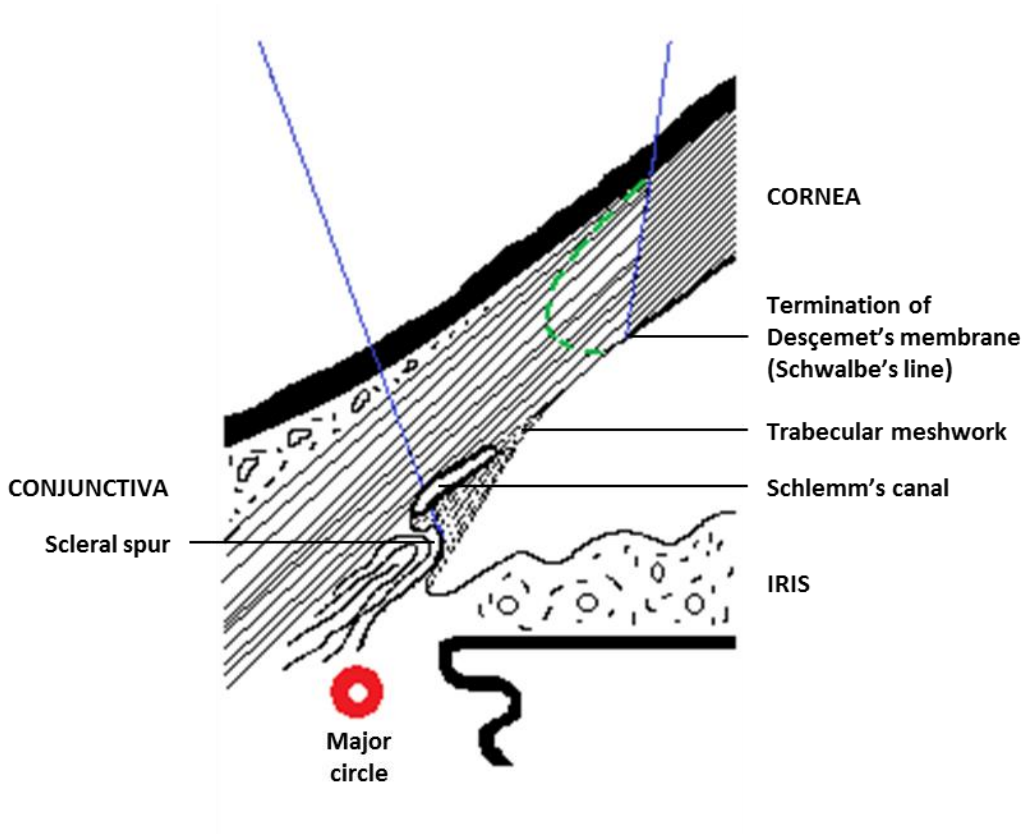

Figure 1.6: The limbus. Solid blue lines represent the limbus as described by pathologists and the green dotted line represents the limbus as described by anatomists. **(Adapted from: Fundamentals and Principles of Ophthalmology. Basic and Clinical Science Course. San Francisco: American Academy of Ophthalmology; 2011-2012. Figure 2.7, Anterior chamber angle and limbus, depicting the concept of the limbus; p. 49)**

1.2.1.3 CONJUNCTIVA

Gross structure and functions

The conjunctiva is a thin and translucent mucous membrane that overlies the sclera (figure 1.4).(5) It extends from the limbus to cover the majority of the OS, extends over the posterior surfaces of the eyelids and ends at the muco-cutaneous junctions (figure 1.7).(1, 5) Grossly, the conjunctiva is divided into three regions: bulbar, forniceal and palpebral conjunctiva.(5) The palpebral conjunctiva, attached to the tarsal plate, lines the posterior aspect of the eyelids.(1) The epithelium of the conjunctiva in this region is continuous with that of the nasal cavity via the lacrimal puncta that open into the inferior meatus (figure 1.3). The bulbar conjunctiva covers the majority of the OS and the forniceal conjunctiva is the region in between the bulbar and palpebral conjunctivae.(1) The superior and inferior forniceal conjunctivae meet at the canthi to form a *cul de sac*.(1) The total surface area of the conjunctiva is greater than the area that the conjunctiva is in contact with the eyeball and eyelids.(8) The surplus tissue forms folds in the forniceal region, and this together with the loosely attached conjunctival tissue to fascial sheaths of extraocular muscles, allow the free movement of the eyeball.(1, 8) Moreover, the lacrimal gland and accessory lacrimal glands empty into the superotemporal fornix.(1) There are specialized regions in the medial conjunctiva called plica semilunaris and the caruncle (figure 1.4).(1) These are highly vascular regions of the conjunctiva, the former is rich in goblet cells (GCs) and immunocompetent cells, whereas the latter contains accessory lacrimal and sebaceous glands.(1) The conjunctiva contains its own pool of stem cells for epithelial and GC renewal.(9) The conjunctiva functions as a physical barrier against injury and pathogens, as well as an immunological defence barrier against pathogens.(12-14) The GCs secrete mucins that contribute to the overlying tear film.(1) Overall, it is an important structure of the OS that functions to prevent desiccation of the epithelia and protect the eye from external insults.(14)

Histology

Histologically, the conjunctival epithelium is a stratified, non-keratinised epithelium with approximately six cell layers at the limbus and may increase to up to twelve cell layers at the fornices (figure 1.8).(5, 12) It is replaced by a keratinised, stratified squamous epithelium of the skin at the muco-cutaneous junction.(12) The cells of the epithelium are arranged into superficial, intermediate and basal cell layers.(1) The thickness of the bulbar conjunctival epithelium, as examined by laser scanning confocal microscopy (LSCM) *in vivo*, was found to be approximately 40% thinner than that of the cornea (approximately 33µm),

the superior conjunctival epithelium being significantly thinner than that in other regions.(15) LSCM studies have shown that the density of superficial cells in the bulbar conjunctiva is 221.2 ± 78.2x10^3 cells/cm^2, whereas that in the basal cell layer is 236.8 ± 74.1x10^3 cells/cm^2.(15) A similar study by Messmer et al. however, gave values that were approximately double these values, although an explanation for this was not clear.(15) The basal cell density in the superior palpebral conjunctiva was 297.9 ± 51.0x10^3 cells/cm^2.(16) As in the cornea, the superficial cells of the conjunctiva have microplicae that support the glycocalyx of the tear film.(1) The conjunctiva consists of muco-secretory GCs, which together with the epithelial cells lie on a BM.(8, 13) The density of GCs in the bulbar conjunctiva as studied by LSCM is 11.1 ± 5.8x10^3 cells/cm^2; the nasal bulbar conjunctiva having significantly higher number of GCs than the rest of the conjunctiva.(15) Studies on the palpebral conjunctiva showed higher GC densities, 105.0 ± 49.5x10^3 cells/cm^2 superiorly and 197.2 ± 86.2x10^3 cells/cm^2 inferiorly.(16) However, other studies have demonstrated that the largest densities of GCs are found within the forniceal regions of the conjunctiva and the plica semilunaris.(1, 8, 17) In contrast to the corneal epithelium, the conjunctival epithelium contains melanocytes, major histocompatibility complex class II-positive dendritic cells and lymphocytes.(1)

The conjunctival stroma is divided into two major layers: superficial adenoid layer and a posterior fibrous layer.(15) The adenoid layer contains conjunctiva associated lymphoid tissues, a type of mucosa associated lymphoid tissue, consisting of immune cells, such as T and B lymphocytes, plasma cells, macrophages and dendritic cells, all of which serve a role in the immune defence system of the OS.(5) The fibrous layer of the conjunctival stroma is highly vascular receiving branches from the anterior ciliary arteries and palpebral arteries and their accompanying veins.(1, 5) The lymph from the medial and lateral aspects of the conjunctiva drains into submandibular nodes and superficial pre-auricular nodes, respectively.(5) Innervation is from the ophthalmic and maxillary divisions of the trigeminal nerve and consists of sensory and autonomic nerve fibres. (1, 5)

Gross anatomy of the conjunctiva

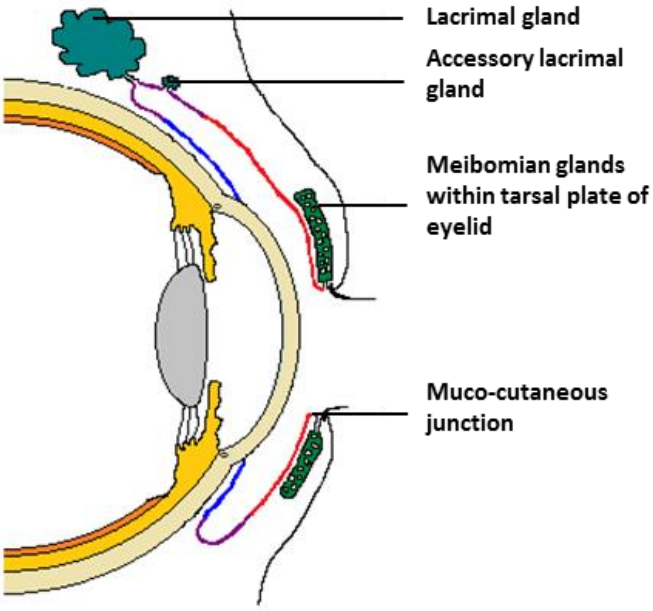

Figure 1.7: Gross anatomy of the conjunctiva. The conjunctiva is divided into palpebral (red), forniceal (purple) and bulbar (blue) conjunctivae. **(Adapted from: Fundamentals and Principles of Ophthalmology. Basic and Clinical Science Course. San Francisco: American Academy of Ophthalmology; 2011-2012. Figure 1.31, The conjunctiva consists of bulbar, forniceal and palpebral portions; p. 30)**

Histology of the conjunctiva

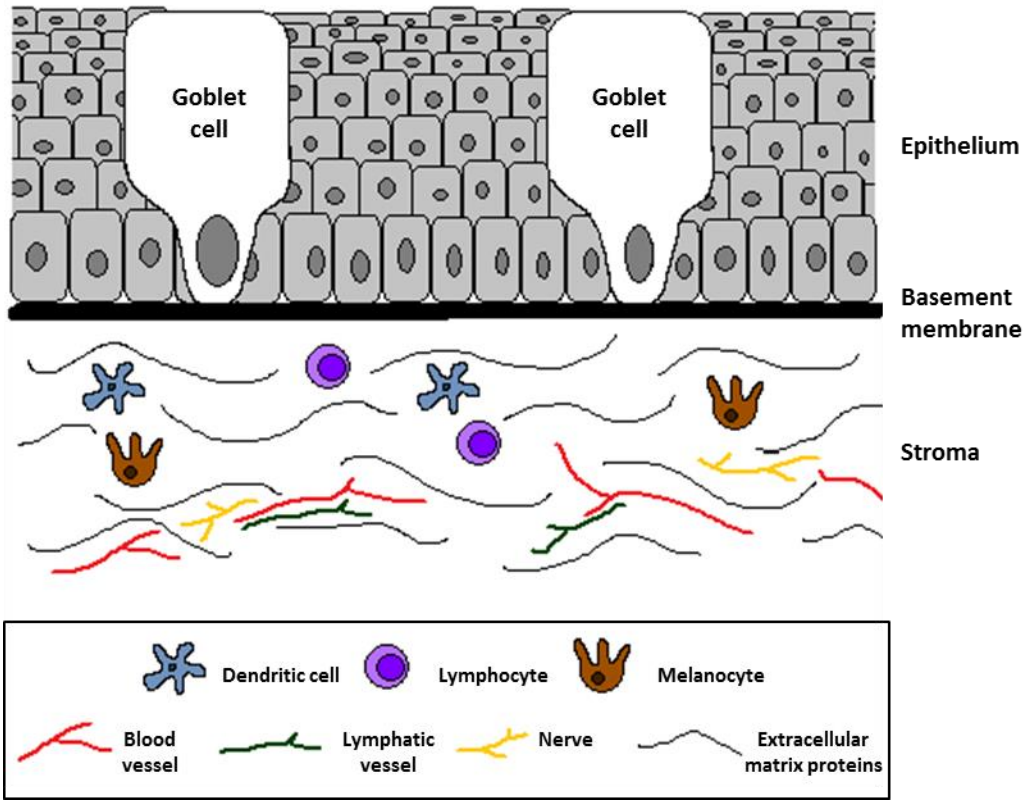

Figure 1.8: Histology of the conjunctiva. The conjunctival epithelium consists of stratified epithelial cells (superficial, intermediate and basal cells) and goblet cells, which lie on a basement membrane. The underlying stroma consists of extracellular matrix proteins, dendritic cells, lymphocytes, melanocytes, blood vessels, lymphatic vessels and nerves. The immunocompetent cells and melanocytes may also be present within the epithelium.

1.2.1.4 TEAR FILM

The traditional model of the tear film consisted of three distinct layers: lipid layer secreted by the meibomian glands in the tarsal plates of eyelids, aqueous layer secreted by the lacrimal gland and the accessory lacrimal glands, and the mucous layer secreted by the GCs of the conjunctiva and the epithelial cells of the cornea and conjunctiva.(5) Currently, a two layer model combining the mucous and the aqueous layers is described, where secreted mucins of the mucous layer co-exist with the aqueous layer (figure 1.9).(6) The thickness of the tear film has been studied with no conclusive results; the majority of the studies have shown the thickness to be between 3 and 10μm in humans, whereas one study using confocal microscopy has shown it to be 40μm.(18, 19) This variation is thought to be due to the dynamic nature of the tear film during blinking, humidity of the environment, as well as patient factors, such as age and sex.(19) In addition, the inconsistencies between the results could be due to the different measurement methods employed, and if the microplicae of the cells and the glycocalyx were taken into account in the measurement process.(19)

The lipid layer consists of polar and neutral lipids of melting point 35°C so that it takes the liquid form on the OS.(1) The hydrophobic neutral lipids are found anteriorly where they provide a barrier to foreign bodies. The hydrophilic polar lipids bind to lipocalin in the aqueous layer, thus providing stability to the tear film by lowering the surface tension, and allow spreading of the tear film during blinking to prevent formation of hydrophobic areas on the OS. The lipid layer has multiple other functions, such as preventing evaporation of tears, providing a transparent optical medium for light transmission, preventing spill-over of tears at lid margins and preventing migration of skin lipids onto the OS.(1) The aqueous layer consists of more than one thousand and five hundred proteins, as recognised by proteomic analysis, and electrolytes.(1) The electrolytes maintain a constant osmolality and a pH that allow maintenance of epithelial integrity.(20) The major types of proteins found in the aqueous layer are antimicrobials, such as lysozyme, lactoferrin, lipocalin, defensin and transferrin, as well as immunoglobulin A, a component of the adaptive immune system.(1, 18) Thus, the proteins in the aqueous layer play a major role in the protection of the OS.

The mucous layer that gives the tear film its viscosity, consists of the glycocalyx of the epithelial cells and secreted mucins.(1) Mucins are glycoproteins that take the shape of a bottle-brush, where the hairs of the brush are multiple O-glycosylated short oligosaccharide chains on a protein ‘handle’ containing threonine and serine residues.(1) The heavy

glycosylation make the mucins highly negatively charged, thus are hydrophilic.(20) The mucins interact with hydrophobic, hydrophilic and charged molecules to form the mucous layer.(1) To date, there are nineteen types of mucins identified in the human that are categorized into two groups named, secreted and membrane-associated mucins.(6) Five out of seven secreted mucins (MUCs 2, 5AC, 5B, 6 and 19) are called gel-forming mucins, which form large polymers that may be 600kDa in size, due to the presence of cysteine-rich domains.(6) The small soluble secreted mucins (MUCs 7 and 9) lack these domains. The secretory mucins collect debris, which are removed via the nasolacrimal duct during blinking. Additionally, MUC7 mainly produced by the lacrimal gland, has also been found to have antimicrobial properties. The membrane-associated mucins functioning mainly as an anti-adhesive layer have a short cytoplasmic tail, a transmembrane domain, and most have a large highly O-glycosylated extracellular domain.(6, 20) These extracellular domains found in the apical membranes of epithelial cells extend up to 500nm above the surface to form a heavily glycosylated hydrophilic layer on the surface of the eye, the glycocalyx, that forms a thick barrier to pathogens and provide lubrication allowing smooth movement of the eyelids over the OS.(6, 20) In addition, MUCs 1 and 4 serve as cell-signalling glycoproteins.(6) The membrane-associated mucins may be secreted into the aqueous layer via the action of metalloproteinases.(1)

MUCs 1 and 16 are expressed uniformly throughout the human OS.(6) MUC4 is also expressed on the OS; however, its expression increases towards the conjunctiva. Moreover, the gel-forming mucin, MUC5AC, produced by the conjunctival GCs is also present in the human tear film. Studies on mouse eyes have shown that MUC5AC appear on day seven following birth coinciding with the appearance of conjunctival GCs, whereas the membrane-associated mucins appear on day fourteen coinciding with eyelid opening.(6) Vitamin A has been shown to be important for the regulation of MUCs 4, 16 and 5AC.(6) The GCs also produce trefoil factor family peptides 1 and 3 that have anti-apoptotic properties.(21) The basal and reflex tear secretion is mainly by the accessory lacrimal glands and the lacrimal gland, respectively, which are under parasympathetic nervous control.(1) Overall, the tear film functions to protect and lubricate the OS and prevent desiccation of the epithelia (figure 1.10).(1, 5) Moreover, the physiological process of blinking gives rise to a smooth refractive surface by continuous replenishment of tears that is removed by the lacrimal system.(6) Lastly, the tear film provides nutrients and removes metabolic waste products produced by the avascular cornea.(5)

The tear film

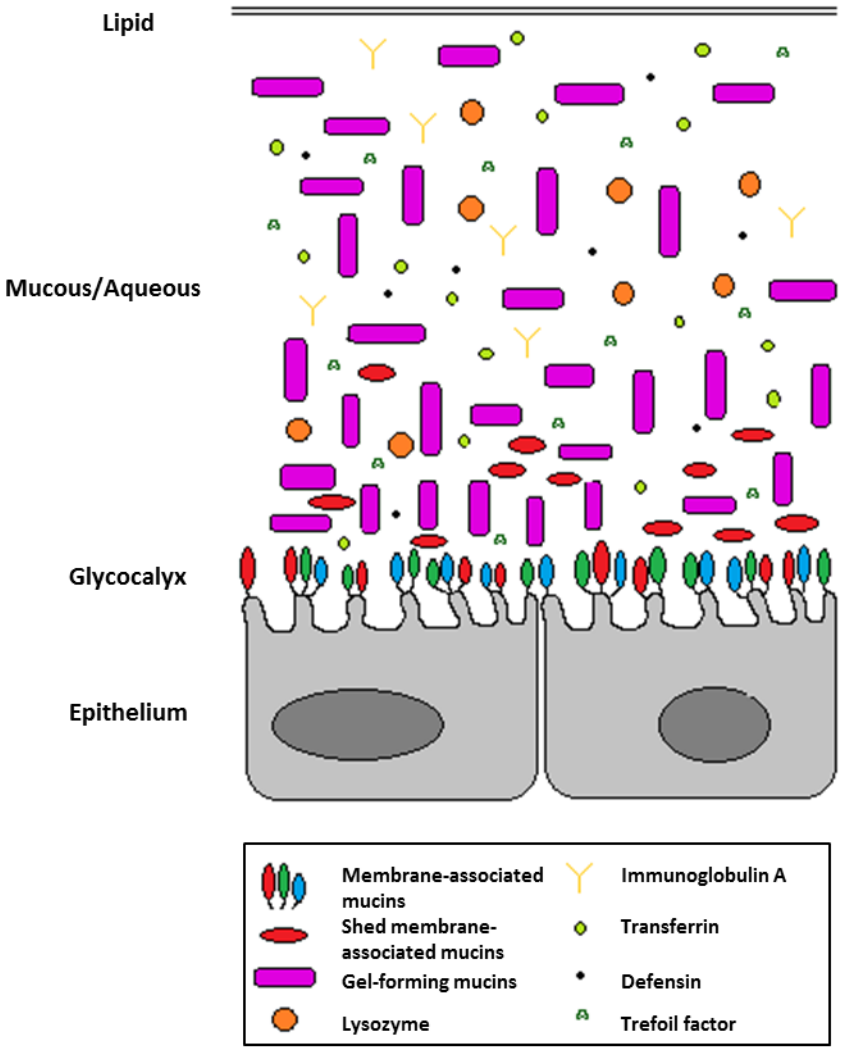

Figure 1.9: The tear film. The two layer model of the tear film and their components that overlie the ocular surface epithelia and the glycocalyx. **(Adapted from: Gipson IK. Distribution of mucins at the ocular surface. Exp Eye Res. 2004;78(3):379-88. Figure 5, Diagram of the gel-forming and membrane-associated mucins superimposed on an electron micrograph of the apical portion of a goblet cell and adjacent cells of the conjunctiva; p. 384)**

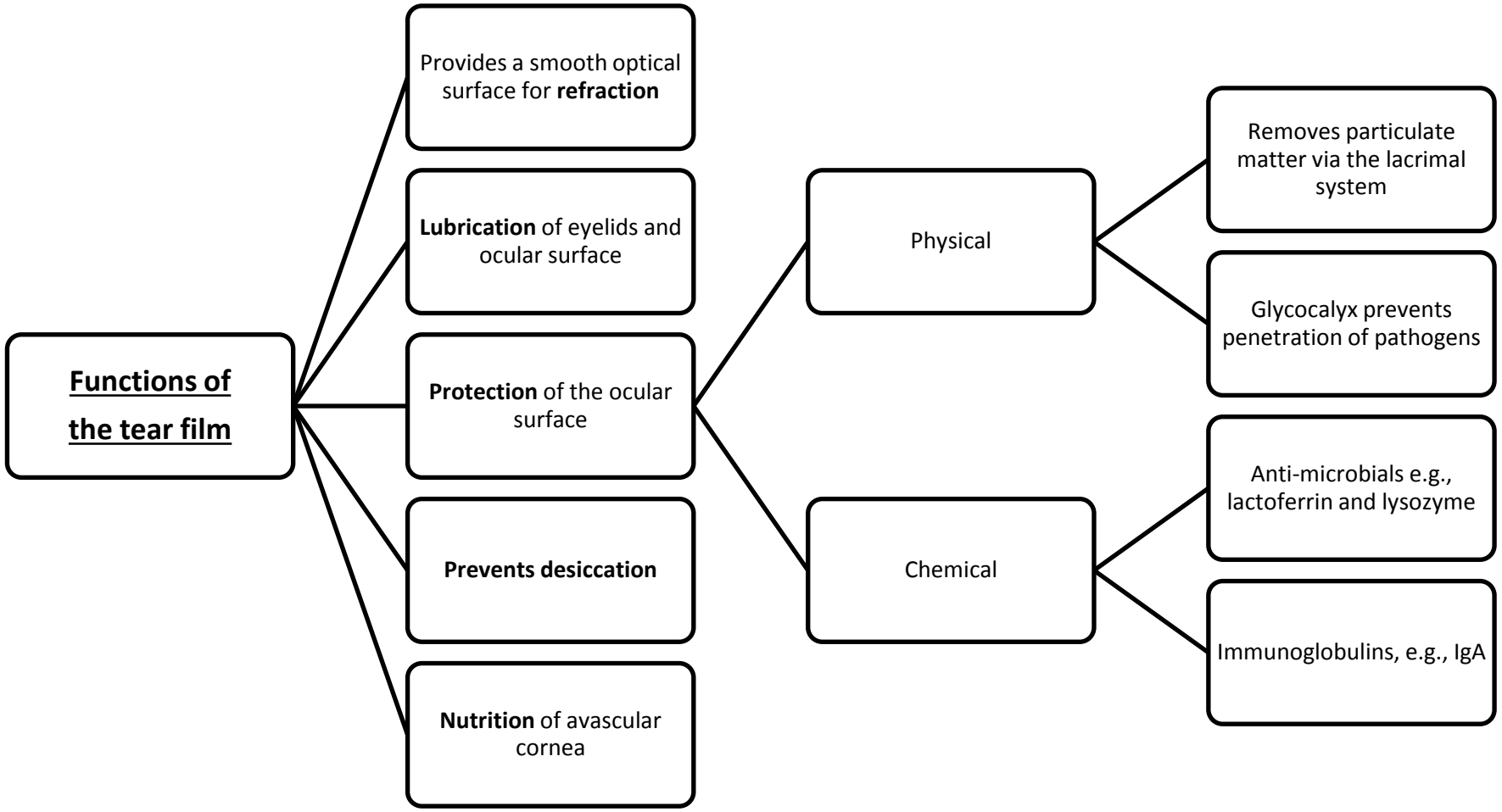

Figure 1.10: Functions of the tear film.

1.2.2 EPITHELIAL RENEWAL

Stem cells (SCs) are cells that have the proliferative capacity to self-renew and are able to differentiate into different types of cells.(22) Within all self-renewing tissues, such as that of the OS, hair follicle and haematopoietic system, there are populations of SCs that give rise to two daughter cells with each mitotic division.(9) One cell remains as a SC to maintain the SC pool and the other becomes a transient amplifying cell (TAC); the young TACs are able to divide more times than the mature TACs. Once the TACs reach the end of their proliferating capacity they become post-mitotic differentiated cells. There is increasing evidence that the TACs can resume a SC phenotype in the presence of appropriate stimuli.(9) The niche, a specialised microenvironment, consists of extracellular proteins, as well as specific anatomical and functional features, that regulate the self-renewal, proliferation and activation of SCs.(23, 24) The extracellular component include, extracellular matrix (ECM) proteins and signalling molecules secreted by cells and blood vessels, that act to stimulate cells in an outside-in mechanism.(11) SC niches are able to de-differentiate progenitor cells from one tissue into a different cell type of another tissue, for example, corneal progenitor cells can be differentiated into epidermal cells of the skin when cultured on an embryonic dermal niche, thus providing evidence of these niches as a modulator of the plasticity of progenitor cells.(23)

To date, an exclusive SC marker is undefined, however, the combination of morphological, biochemical and cell kinetic criteria aid in the identification of SCs.(9, 11) Morphologically they are characterised as small cells with a high nucleus to cytoplasm ratio.(22) They may be heavily pigmented in sun-exposed areas of the body to protect themselves against damage from ultraviolet light.(9) SCs are thought to have unique distribution patterns within tissues and are able to proliferate and undergo neoplastic transformation in response to certain stimuli.(9) Biochemically, they express specific protein markers that are identified by immunocytochemistry (ICC): nuclear isoform ΔN of tumour protein p63 (ΔNp63) and transmembrane ATP-binding cassette sub-family G member 2 (ABCG2) are expressed by adult SCs.(11, 22) SCs are thought to lack specific cell-cell junction proteins expressed by cells that have undergone terminal differentiation, such as connexin 43 of gap junctions and desmoglein 3 of desmosomes.(11) Lastly, SCs are known to have long cell cycles that allow maintenance of their proliferative capacity and reduce errors that may be caused by DNA replication.(9) Thus, they are known as slow-cycling or label-retaining cells.(9) In comparison to TACs, SCs can proliferate for more generations producing larger and tightly packed colonies.(25)

The epithelia of the cornea and the conjunctiva originate from separate pools of SCs that reside in the limbus and conjunctiva, respectively (sections 1.2.1.2 and 1.2.1.3).(9, 12) A study looking at the gene expression of epithelial cells of the OS has shown more than two-hundred transcripts that were unique to the conjunctiva and more than one-hundred transcripts that were unique to corneo-limbal cells.(25) These finding demonstrate the presence of unique genes that determines the phenotype of the different tissues of the OS. For example, the epithelial cells of the OS express different keratin pairs and are able to produce different phenotypic SC epithelial cysts in athymic mice injected with either corneal or conjunctival epithelial cells.(9) The cysts with a corneal epithelial phenotype consisted of a stratified epithelium with basal, wing and superficial cells, whereas those with a conjunctival phenotype produced cysts that consisted of both epithelial cells and GCs.(9) It is essential that the epithelia are able to maintain adequate numbers of self-renewing SCs throughout a person's life to ensure homeostasis of the OS.(22)

The SCs of the cornea reside in the epithelia of the anatomically protected inter-palisade ridges of palisades of Vogt of the limbus.(11) These specialised niches are abundant in immunocompetent cells and melanocytes and are therefore highly pigmented.(23) The limbal palisades that extend upwards into the BM, are fenestrated allowing close association of the limbal epithelial cells and the underling stroma.(23) The limbal stroma consists of a dense vascular and neuronal supply providing the cells with nutrients and growth factors.(11) The limbal cells express transmembrane proteins, integrin α_9 and N-cadherin, that allow interaction of these cells with specific extracellular proteins.(23) The limbal BM is made up of α_2 and β_2 chains of laminin, and α_1 and α_2 chains of type IV collagen that are absent in the corneal BM, which may confer the ability of the limbus to maintain SCs.(23) Other ECM proteins, γ_3 chain of laminin, fibulin 2, type XVI collagen, secreted protein acidic and rich in cysteine (SPARC), tenascin C and agrin have also been found in the limbal ECM in close association with SC populations.(24) Additionally, the BM sequester specific concentrations of growth factors and cytokines optimal for the maintenance of SCs.(23) SCs in the basal epithelium of the limbus differentiate into TACs that proliferate and migrate from this specialised niche centripetally and apically towards the central cornea to undergo terminal differentiation into corneal epithelial cells.(11) The corneal epithelium is thought to take one to two weeks to differentiate following which the superficial cells are desquamated into the overlying tear film.(10) During wound healing of the corneal epithelium, the SCs are able to proliferate and differentiate spontaneously to repair any damage to its integrity.(1)

The conjunctiva is also a self-renewing tissue with its own population of SCs that are essential for the maintenance of the OS system.(9, 12, 13) Conjunctival SCs are able to differentiate into non-secretory and muco-secretory conjunctival epithelial cells throughout life, thus are bi-potent.(13) Stewart et al., carried out studies on human conjunctival tissue as a whole.(14) They showed the presence of SCs throughout the conjunctiva with the medial canthal and inferior forniceal areas having the highest colony forming efficiency and highest expression of SC markers in cultured primary cells, as well as in fixed tissue. In fixed tissue, the highest amount of staining was observed in the basal cells. Although there is a lack of literature regarding the conjunctival SC niche, there are certain features of these SC-rich conjunctival regions that are similar to other SC niches: the medial canthus and inferior fornix provide greater physical protection, and the medial canthal region is highly vascularised, richer in GCs, melanocytes and immune cells, compared to other regions of the conjunctiva.(14)

1.3 CONJUNCTIVAL INJURY AND DISEASE

Despite the existence of multiple defence mechanisms of the OS, due to its exposure to the environment, the conjunctiva is prone to injury and entry of pathogens.(6) The conjunctiva may be damaged by chemical and physical injuries (thermal and ionising radiation injuries), mechanical trauma or iatrogenic injury during ophthalmic surgeries.(26) Damage may also be caused by microbial infections or systemic autoimmune diseases, such as mucous membrane pemphigoid and Sjögren's syndrome.(26) Stevens–Johnson syndrome (SJS) is a systemic disease that is a type III hypersensitivity reaction involving abnormal immune complex deposition secondary to drugs or infections.(26) Whatever the mechanism of injury, the wound healing response is activated involving several steps: inflammation due to the recruitment of neutrophils, macrophages and lymphocytes, fibroblast activation and ECM protein deposition and lastly, remodelling by uniaxial alignment of collagen fibres leading to a fibrous scar and wound contracture.(8, 27)

Severe scarring may lead to anatomical and functional impairment of the conjunctiva.(28) Chronic inflammation leads to squamous metaplasia of the epithelium with keratinisation of the OS and loss of GCs.(27) Deficiencies in mucin production lead to loss of lubrication and symptoms of dry eyes (pain, irritation and redness). The deposited keratin layer rubs against the OS leading to mechanical irritation, further aggravating the inflammation and symptoms. Scarring may obstruct the outflow systems of the lacrimal and accessory lacrimal glands, leading to a reduction in the aqueous component of the tear film and exacerbation of symptoms of dry eyes.(27) Anatomically, scarring between the palpebral and bulbar conjunctiva will give rise to symblepharon formation, which will affect the tear reservoir due to shortening of the fornices (figure 1.11).(27) The subsequent abnormal anatomy of the eyelids and eyelashes will further aggravate the disease process due to abnormal blinking, blink-related mechanical trauma to the OS and greater evaporation of tears due to defects in eye closure.(19) Inappropriate scar formation may also affect the free movement of the eyeball.(8) In severe cases, there may be limbal SC deficiency (LSCD) with corneal epithelial defects, stromal scarring and conjunctivalisation of the cornea, which will eventually lead to impairment of vision.(21) In cases where a limbal or a corneal transplantation is required, the presence of ongoing inflammation of the OS and tear deficiency, will affect the success of the transplant.(8, 22) Thus, it is imperative that the health of the conjunctiva is restored prior to repair of the limbus or the cornea. When considering management of OS disorders, it is essential that the OS system as a whole is taken into account in preference to targeting a single component of the system.(6)

Scarring of the conjunctiva

Figure 1.11: Scarring of the conjunctiva. Severe conjunctival scarring and shortening of fornices secondary to mucous membrane pemphigoid. **(From: Professor S. B. Kaye, St Paul's Eye Unit, Royal Liverpool University Hospital)**

1.3.1 CURRENT MANAGEMENT

1.3.1.1 MEDICAL MANAGEMENT

Appropriate management of conjunctival injuries and diseases is required to prevent subsequent complications that may arise due to severe scarring. Moreover, it is important that a stable and healthy OS is present for potential limbal and corneal transplantation procedures in the future. The management includes anatomical and/or functional restoration of the OS. Initial therapy in most cases is aimed at adequate symptom control with analgesics, and prevention of progression of the damage.(14) To prevent ongoing damage to the OS, chemical injuries should be treated with ample irrigation, drugs should be stopped in cases of SJS and infections should be treated with appropriate antimicrobial medication.(26) Autoimmune diseases are treated with numerous topical and systemic immunosuppressive agents and although good control of inflammation is observed, the serious adverse effects to other organs lead to poor patient compliance.(29) As previously mentioned, the scarring caused by injuries and diseases can have significant effects on the tear film leading to symptoms of dry eyes. Thus, early detection and treatment with frequent lubrication with preservative-free artificial tears is essential.(30) A limitation of artificial tears is that they lack many of the integral components of the natural tear film, such as vitamin A and growth factors.(30) Punctal occlusion of the lacrimal drainage system is carried out in cases where there is a patent system without significant scarring, to preserve the natural and artificial tear volume on the OS.(30) Additionally, minor surgical procedures such as removal of abnormally positioned eyelashes and correction of abnormally positioned eyelids should be carried out where indicated to prevent mechanical damage to the OS.(26) Symblepharon rings may be used to prevent formation of symblephara in the acute phase.(26) Generally, all the medical treatment options described above are palliative giving short-term relief and do not replace the damaged tissue with healthy tissue.

1.3.1.2 SURGICAL MANAGEMENT

When there is extensive scarring, medical management may not be optimal to avoid the long-term consequences of the injury or disease. In these cases the management may require a surgical intervention to remove the damaged tissue and replace with a suitable tissue graft, in an attempt to restore the integrity of the OS.(8) The choice of surgery depends on the amount of conjunctiva damaged, whether the damage is unilateral or bilateral, and if the whole of the OS is involved requiring restoration of the limbus and the

cornea.(27) Surgery also depends on the chief function of OS that is lost requiring restoration. For example, in cases where there is fornix shortening, grafts that are flexible and cause less wound contracture are ideal, whereas in cases where there is tear or mucus deficiency, a graft that supports GCs is required.(28) In many indications the ideal graft has been found to be conjunctival autografts.(28) An autograft is a piece of healthy tissue obtained from a patient that is used to replace damaged tissue in the same patient.(31)

Conjunctival transplantation using autografts were first described by Thoft in 1977 for reconstruction of a unilateral chemical injury.(32, 33) The autografts contain conjunctival epithelial cells, GCs and their BM, thus are able to restore the normal architecture of the tissue and their function.(34) They are used for conjunctival defects that are small and unilateral.(8, 27) Although transplantation of allogenic conjunctival tissue from living relatives may be an option in cases of bilateral disease, this is associated with risks of microbial disease transmission, such as viral (hepatitis B and C and human immunodeficiency virus), bacterial and fungal infections.(35) Despite the use of immunosuppressive agents, this procedure carries the risk of donor tissue rejection.(35) Kwitko et al. has shown this risk to be 25% when grafts were obtained from living donors in the presence of incompatible human leukocyte antigen donor pairs, and suggested that identical or haplo-identical pairs were adequate for transplantation purposes.(36) Daya et al. showed that the post-operative use of immunosuppressive agents did not change the incidence of graft rejection, however, the presence of severe inflammation pre-operatively increased the incidence of early graft rejection.(37) Rejection can occur as early as one month or up to two years post-operatively.(36, 37) Additionally, the immunosuppressive agents used post-operatively are also associated with adverse effects including systemic infections.(35)

Conjunctival autografts are the gold standard treatment following excision of pterygia (a fibrovascular growth of tissue on the OS) that other treatment options are compared to in most clinical trials.(32) The main complication following excision of pterygia is recurrence. When the scleral bed is left bare following excision unacceptable recurrence rates (60%) were observed, whereas when reconstructed with a conjunctival autograft, recurrence rates were substantially lower (2-39%).(27, 32) The recurrence rates have also shown to be less with the use of limbal-conjunctival autografts, especially in cases of recurrent pterygia in high-risk regions, where the inclusion of the limbal autograft is thought to restore the barrier function of the limbus preventing conjunctival tissue from migrating onto the

cornea.(38) Conjunctival autografts have been studied with plasma derived fibrin glue instead of sutures that may be associated with higher rates of inflammation.(39) Lower recurrence rates and post-operative inflammation were observed with the use of fibrin glue. It creates a network of cross-linked fibrin from fibrinogen in the presence of thrombin, thus holding the graft in place. Moreover, fibrin glue is associated with a shorter surgical time and lower post-operative discomfort. It also requires less surgical expertise although some training is required since there is a chance of wound dehiscence and graft displacement if not applied appropriately.(39) The disadvantages of fibrin glue are higher cost, risk of viral disease transmission (parvovirus B19, hepatitis and human immunodeficiency virus) and anaphylaxis.(40) Autologous blood and electro-cautery pen have been investigated in place of fibrin glue, although further studies are required to prove any benefit compared to fibrin glue or sutures.(39, 40) Limitations of conjunctival autografts and living-donor allografts include lack of sufficient amounts of tissue to cover large defects, lack of remaining healthy tissue for future glaucoma surgery and risks of damage to the donor site with potential fibrosis and scarring.(27, 41)

1.3.2 SUBSTRATES FOR CONJUNCTIVAL CELL AND TISSUE TRANSPLANTATION

Regenerative medicine is increasingly popular in the field of medicine as a potential treatment to replace damaged tissues.(42) Within this field, tissue engineering (TE) provides a promising method by which prospective tissue constructs may be formed that can replace damaged tissue.(42) This may be done by developing biological substitutes to be used as grafts or by implanting a biomaterial scaffold containing *ex vivo* cultured cells and/or biological molecules to accelerate the regeneration of new tissue, which can replace the damaged tissue and maintain the anatomical structure and functions of the original tissue.(8, 42, 43) *Ex vivo* expansion of cells enable formation of confluent sheets of cells from small biopsies, which is important when there is a lack of heathy tissue due to injury or disease.(35) In cases of limbal allograft transplantation, up to 50% of healthy limbal tissue may be resected placing the donor eye at risk of developing LSCD.(44) Moreover, transplantation of *ex vivo* expanded conjunctival tissue has been shown to result in faster re-epithelialisation, reduce post-operative inflammation, and subsequent rapid healing reduces the risks of scleral necrosis and secondary infection and perforation.(45) This concept was first introduced by Rheinwald and Green in the 1970s, when they used *ex vivo* expanded epidermal cell sheets in the management of thermal skin burns.(46) Following that, Pellegrini et al. successfully transplanted an autologous corneal epithelial sheet to

restore a damaged human cornea in 1997.(46) Since then TE has become increasingly popular in the management of OS diseases. The success of a tissue construct depends on three factors: the source of cells and the presence of SCs, the carrier substrate and the presence of growth factors.(33) The substrate provides the initial support for the cultured cells and physical and biological cues for growth of cells.(47) Additionally, it facilitates the delivery of cultured cells to the site of interest and provides a three-dimensional scaffold for the formation of new tissue.(48) During regeneration, the substrate may be replaced by secreted ECM proteins of the cells.(47) A large number of studies have been carried out to investigate various biological and synthetic substrates that are optimal for the *in vitro* culture of epithelial cells.

Characteristics of an ideal substrate for conjunctival cell and tissue transplantation:

1. Thin and porous material that allow interaction between the graft and the underlying host tissue allowing rapid exchange of nutrients and metabolic waste products in and out cells, respectively.(8, 35, 43)
2. Flexible and able to conform to different surfaces, especially the conjunctival fornices.(8, 35)
3. Optimal mechanical properties that allow easy handling and suturing, however, are similar to that of the natural tissue as it guides cellular functions.(35, 43)
4. Biocompatible, that is, the material is tolerated without causing inflammation or rejection by the host's immune system.(8, 35)
5. Support the adhesion, migration and proliferation of epithelial cells and mucus-producing GCs.(8)
6. Presence of SCs to ensure long-term survival of the transplant.(21)
7. Biodegradability is desired but not essential. If the substrate is biodegradable, it is important that this occurs in a controlled manner to ensure that the substrate remains until the transplanted tissue incorporates into the surrounding tissue of the host by producing ECM proteins. If the substrate breaks down too quickly the transplanted cells will also be lost prior to them forming strong adhesions with the underlying tissue, thus the scaffolds lose their cell carrier function.(43, 45, 49) If the substrate is biodegradable, it is important that the by-products are not toxic.
8. Low *in vivo* shrinkage.(35)

The various biological and synthetic substrates that have been studied for TE of the conjunctiva to date, and their advantages and disadvantages will be discussed in the next sections (table 1.2).

1.3.2.1 BIOLOGICAL SUBSTRATES

Biological or natural substrates are generally biodegradable and contain biologically active domains that support various cellular functions, however, they lack superior mechanical properties and may elicit an immunological reaction *in vivo*.(49)

1.3.2.1.1 AMNIOTIC MEMBRANE

Amniotic membrane (AM) is the innermost layer of the placenta that has been used in ophthalmology for many years, mainly as a BM substitute for reconstruction of damaged OS tissue.(50) It was first used in skin transplantation by Davis in 1910.(51) The first ophthalmological use was in 1940 when De Rotth used both AM and the chorion of the placenta to reconstruct the conjunctiva following lysis of symblepharon secondary to a chemical burn.(51-53) However, for unknown reasons, there is no mention of its ophthalmological use in the literature until 1993, when Batlle et al. used AM as a conjunctival substitute to repair fornices, and Kim and Tseng (1995) used preserved AM to reconstruct the cornea in rabbits with total LSCD.(41, 44) Since then, AM has been a popular substrate used in the reconstruction of damaged OS tissue and in TE for the *ex vivo* expansion of epithelial cells.(51) AMs are obtained from placentas delivered via Caesarean section, due to the risks of microbial contamination following vaginal delivery.(44) The donor mothers undergo serology investigations prior to delivery and six months after delivery to rule out the presence of infectious agents, such as human immunodeficiency virus and hepatitis B and C.(50) These allogenic membranes are then cryopreserved and stored under sterile conditions for up to one to two years for use in transplantation.(50) Although cryopreservation devitalises the epithelial cells, it has been shown to preserve the biological properties of the native tissue.(50)

<u>Histology</u>

The AM is a translucent membrane that consists of cuboidal-columnar epithelial cells with microvilli on their apical surface, a thick BM and an underlying almost acellular stroma.(50, 51) The thickness of AM varies greatly from 20µm to 500µm.(50) The epithelial cells obtain nutrients from the surrounding tissue, via diffusion, and produce energy, mainly via anaerobic glycolysis.(51) The BM is a permeable barrier to macromolecules.(50, 51) AM, which provides protection to the fetus, contains a collagen-rich stroma that imparts elasticity and ability to withstand external forces.(51) Blood vessels, lymph vessels and nerves are absent in the stroma.(51)

Biological properties (Figure 1.12)

AM is known to support the adhesion, growth and differentiation of epithelial cells and prevent apoptosis of cells.(44, 50) This is thought to be mainly due to the BM, the composition of which closely resembles that of the OS.(44) One study showed that the isomers of α chains of type IV collagen in the BM of AM are similar to that in the conjunctiva, suggesting that AM may be more suitable for culture of conjunctival cells than corneal cells.(53) In contrast, other studies have shown the BM of AM to be similar to that of the limbus and cornea, indicating its suitability in the culture of limbal and corneal epithelial cells.(24, 54) Studies have shown the ability of AM to produce a well-differentiated corneal epithelium with progressive reduction in progenitor cells during *ex vivo* expansion of limbal epithelial cells suggesting that the AM lack specific limbal ECM components that contribute to the maintenance of SCs.(24)

The AM, derived from the epiblast (source of all germ layers of the embryo), is thought to contain pluripotent cells that have the capacity to differentiate into any cell type of the human body.(51) However, during the preservation process the cells become unviable. Moreover, the AM contains various growth factors that are important for wound healing.(50, 51) The anti-inflammatory properties of AM are due to the inhibition of pro-inflammatory cytokines by expressing interleukin 1 and 10 receptor antagonists, the ability to trap inflammatory cells within the stroma and the presence of pro-apoptotic properties against neutrophils.(50, 51) Fetal hyaluronic acid inhibits transforming growth factor β (TGFβ) signal transduction and proliferation of fibroblasts, thus it has anti-scarring properties beneficial in reconstructing damaged OS tissue.(44, 50) Moreover, AM provides a physical barrier to pathogens and produces antimicrobial molecules, such as β-lysin and lysozyme.(44, 51) Its anti-angiogenic properties, due to the presence of endostatin and thrombospondin 1, are beneficial in inhibiting neovascularisation of the cornea.(51) Although an allogenic material, tissue rejection following transplantation is very rare due to the low expression of human leukocyte antigens by amniotic epithelial cells in fresh AM, as well as the lack of immunogenicity due to devitalised epithelial cells in cryopreserved AM.(50, 51) Thus, there is no requirement for immunosuppression of patients following transplantation and this avoids complications that are associated with its use. Additionally, the transparency, easy surgical handling, and the ability to preserve membranes for a long period of time make AM a popular substrate for use in ophthalmology.(44, 52) Other beneficial non-biological properties of AM are, that they are readily available and are associated with few ethical issues.(51)

Use in reconstruction of the ocular surface

AM is a useful alternate to autologous conjunctival tissue in the reconstruction of the conjunctiva, especially where there is limited availability of tissues due to bilateral disease, where a large graft is required and when the conjunctiva needs to be preserved for future filtration surgery in glaucoma patients.(44) AM has been used in the reconstruction of the conjunctiva and fornices following various injuries and diseases, including chemical burns, autoimmune diseases, and defects following excision of pterygia and tumours.(50) The primary aims are to promote epithelialisation and to reduce the inflammation, so that a healthy anatomical and functional OS is restored to ensure the success of subsequent limbal and corneal transplantation. Different surgical procedures and techniques are used to apply the AM for OS reconstruction. AM may be used as a graft that is sutured BM side up, and therefore provides a BM substitute to which neighbouring OS epithelial cells can migrate on to and close an epithelial defect.(50) It may be used as a single layer graft to close epithelial defects or as a multilayer graft to close deep corneal ulcers.(44) The graft may last for months or even years and will gradually be integrated into the surrounding host tissue.(50) Chemical injuries lead to severe inflammation and breakdown of the epithelium; an AM used as a patch sutured either BM side up or stromal side up is useful in reducing the surrounding inflammation, especially in the acute stages, and aid in rapid re-epithelialisation.(50, 53) When the patch covers the whole of the OS including the fornices, it can be used to prevent symblepharon formation due to its anti-scarring properties.(44) It acts as a biological shield against mechanical damage that may be caused during blinking by abnormally positioned eyelashes and eyelids.(44) It is only a temporary treatment and requires weekly replacement, as the preserved AM becomes depleted of the anti-inflammatory molecules.(50) A combination of these methods are used in cases of severe ulcers where the graft promotes epithelialisation, whereas the patch protects the graft and the rest of the OS.(50) With advances in TE, AM has also become a popular substrate for the *ex vivo* expansion of epithelial cells of the OS. The AM provides a BM substitute that supports the growth of conjunctival epithelial cells and GCs.(44)

Studies investigating AM as grafts have shown a success rate (complete and partial) of 92-92.5% with complete re-epithelialisation within one to three weeks, even when large grafts were used.(41, 55) Recurrence of primary pterygia following resection has been shown to be higher than when autologous conjunctiva is used, however, with extensive removal of fibrovascular tissue, a recurrence rate of 3% has been reported.(44, 53) In addition to the advantages described above, AM transplantation to cover epithelial defects following

tumour resection is beneficial since recurrence of the tumour can be clinically monitored due to the transparent nature of the AM.(44) Similarly, it can also be used to reconstruct epithelial defects following symblepharon lysis, although the outcome is poor in the presence of ongoing inflammation.(44) Prabhasawat et al. observed a failure rate of 23.1% following symblepharon lysis secondary to multiple surgeries for pterygia, which is thought to be due to increased fibroblastic activity that invade the graft and cause shrinking of the graft, scar formation and recurrence of the symblephara.(41) In these cases, success was only seen once a limbal allograft was transplanted. Another important factor that determines the success of AM grafts is the vascular supply; when AM was used as scleral grafts for scleral necrosis secondary to β irradiation or mitomycin C (anti-scarring effects) use during surgery for pterygia, there was a tendency for the graft to rapidly melt and dissolve over the ischaemic scleral bed.(41) Success was obtained when the AM was transplanted with a conjunctival flap that restored the vascular supply. Other prognostic factors that lead to poor outcomes following AM transplantation are the presence of dry eye syndrome, total destruction of SCs and use of immunosuppression.(55) AM has also been used as an adjunct in glaucoma surgery to reduce scarring during filtration surgery, to repair leaking blebs and to cover valve procedures.(44) Whatever the indications for AM transplantation, all studies have shown that AM was associated with significant reduction in pain. Although the exact mechanism of this is not yet determined, the biological effects, such as anti-inflammatory properties and the ability to act as a physical barrier to trauma caused by abnormally positioned eyelids and eyelashes, may contribute to this process.

AM has also been used to reconstruct corneas that are damaged due to persistent epithelial defects, LSCD, corneal ulcers and corneal perforations with a success rate of 85.7%.(44, 55) As described previously, the success of a corneal transplant depends on the presence of a healthy OS with SCs. AM transplantation has been successful in managing patients with partial LSCD, however, in total LSCD, this is an adjunct treatment to limbal SC transplantation, since AM can only optimise the function of existing SCs.(44) In such cases, it is better to culture autologous limbal SCs *ex vivo* on AM and transplant the AM with an intact epithelial cell sheet to the OS.(44)

Limitations

Risks of transmission of microbial infections persist if the donors are not screened adequately or if the AMs are not processed or stored under sterile conditions.(44) Some diseases, such as Creutzfeld-Jacob disease, do not have screening tests, thus it is impossible to completely rule out all microbes that may be transmitted on to the host.(53) Incidence of microbial infections has been reported to be 1.6-8% in the literature, most being due to growth of gram positive bacteria.(44) Another limitation is the early degradation of the graft prior to complete re-epithelialisation and integration into the host tissue, especially in the presence of host inflammation, that may require further surgery.(44, 56) AM is not a standardised product and carries inter- and intra-donor variations affecting clinical results.(52) If the AMs are not processed and stored properly there is also further possibility for there to be alterations to the constituents.(52) AM is prone to contraction in the presence of active inflammation, thus may not be a suitable substrate in cases where there is shortening of fornices due to inflammatory autoimmune disorders and recurrent pterygia.(21) Moreover, AM has failed to show adequate repopulation of GCs despite the addition of biomolecules, such as retinoic acid, air-lifting, co-culture with fibroblasts or culture on the stromal side of AM.(8) As previously described, the preserved AM does not have SCs, thus an adequate source of SCs in the remainder of the OS is a prerequisite for successful and complete epithelialisation. Lastly, the cost of preserved AM may limit the availability of grafts in developing countries.(8)

Biological properties of amniotic membrane

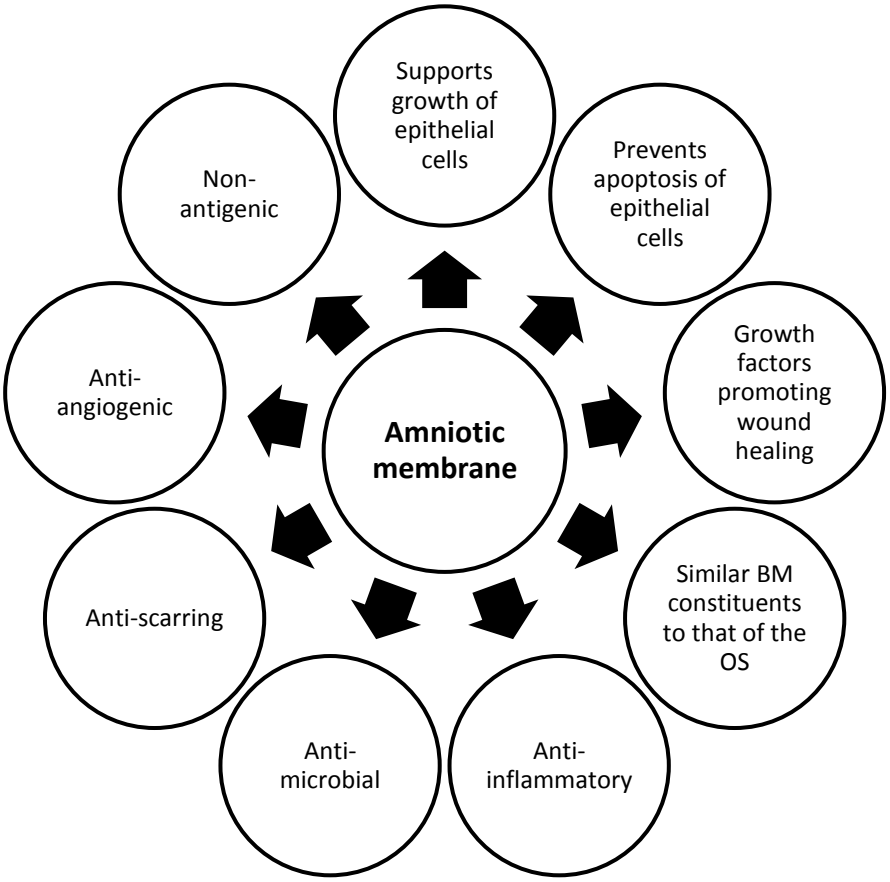

Figure 1.12: Biological properties of amniotic membrane.

1.3.2.1.2 AUTOLOGOUS MUCOSAL MEMBRANES

Autologous mucosal membranes (figure 1.13) of the nasal and oral cavities are employed as alternatives to conjunctival autografts avoiding the use of allogenic ocular tissue.(27, 46) Nasal mucosa consists of non-keratinising epithelial cells and mucus producing GCs.(34) It was first used by Naumann et al. in 1990 to repair a OS with severe mucus deficiency syndrome.(34) A study by Kuckelkorn et al. used mucosa of the inferior concha to reconstruct fornices in seventeen patients with symblepharon or ankyloblepharon secondary to chemical and thermal burns.(34) The middle concha is used as a surgical landmark during nasal surgery and is in close proximity to the olfactory receptors and the base of the skull, thus carries more surgical risks. Moreover, larger grafts can be obtained from the inferior than the middle concha. After an average follow-up time of twenty months, complete or partial success was seen in 76% of the cases with no complications to the donor site. There was evidence of presence of GCs in 35% of the patients up to eighteen months.(34) Another study carried out nasal mucosal grafts in fifty-five eyes; thirty-eight eyes with chemical, thermal or radiation-related injury and seventeen eyes with systemic mucosal diseases.(57) The major complication observed was persistent or recurrent symblepharon formation in 24% of the cases, which was predominantly in patients affected by systemic diseases. More than 90% of the patients reported improved symptoms of dry eye and ocular pain, and 42% had improved vision. There was evidence of GCs in the grafts up to ten years post operatively. Only 26% of the corneal transplants remained transparent during follow-up and the transplant survival at two years was 21% for those with chemical and thermal burns, whereas 0% for those with systemic mucosal diseases. Thus, nasal mucosa presents a viable option for cases where there is bilateral conjunctival damage and when there is severe loss of GCs with mucus deficiency.

Although the above studies have shown the presence of GCs clinically, one study that biopsied the mucosal graft only observed a few glands in the sub-mucosa.(58) However, this study had a small sample size of five eyes. The limitations of nasal mucosal grafts are difficulty obtaining sufficient amounts of tissue to cover large defects and complexity of surgery requiring partial resection of the inferior or middle nasal turbinate, removal of bone or cavernous tissue and thinning of the mucosa.(21) Although all mucosal grafts carry the risk of morbidity to the donor site, it is a rare complication.(21) Nasal septal cartilage has also been investigated, which has been found to be a useful graft in the reconstruction of the posterior lamellar of eyelids where the tarsus is absent, although these grafts have lower number of GCs.(28) More recently, mucosa from the floor of the nasal cavity has

been investigated, where larger grafts may be obtained, although similar to the septum, the number of GCs was less.(59) This procedure is thought to carry fewer risks, such as bleeding, compared to surgery involving the nasal turbinates.

Oral mucosal grafts for the reconstruction of the conjunctiva has involved obtaining tissue from the hard palate, buccal or labial mucosa.(28) Grafts from the hard palate are thicker and more difficult to harvest. However, they contract the least and are more suitable for the reconstruction of fornices. Split-thickness oral mucosal grafts have been found to contract more than full-thickness grafts, thus are not suitable to reconstruct fornices. Oral mucosal tissue do not contain GCs, therefore are not suitable in cases of mucus deficiency.(28) Kheirkhah et al. operated on thirty-two eyes with high grade symblephara secondary to chemical and thermal injuries and autoimmune diseases.(60) They used oral mucosal grafts with AM and intra-operative mitomycin C to reconstruct the OS. They observed restoration of deep fornices in 84% of the cases after an average follow-up time of sixteen months. Fu et al. demonstrated the use of inferior labial mucosal grafts in reconstructing lid margins.(61) Of the twenty-two eyes, there was complete success in 68% of the eyes, with improvement in symptoms in 77% and increased visual acuity in 59% of the patients after an average follow-up time of sixteen months. The authors showed that these mucosal grafts increased the height of the lid margin allowing complete closure of the palpebral fissure, and that the grafts were able to stop the ingrowth of the keratinised epithelium of the skin. When harvesting oral mucosal grafts, it is recommended to obtain a graft that is 20% larger than the defect to prevent post-operative shrinkage.(61) A study comparing the histology of the mucosal grafts post-transplantation showed that the hard palate grafts used to reconstruct posterior eyelid surfaces had an epithelium similar to that in the donor site with evidence of keratinisation, whereas buccal mucosa used in one patient had a non-keratinised squamous epithelium.(58)

Nasal and oral mucosal cells have also been cultured *in vitro* to obtain epithelial sheets that can be used to reconstruct the OS. Kobayashi et al. co-cultured human nasal mucosal epithelial cells with human mesenchymal SCs on denuded AM and subsequently transplanted epithelial sheets onto conjunctival defects in rabbits.(62) They reported the presence of a stratified conjunctival epithelium with expression of conjunctival cell differentiation markers keratins 4 and 13, junctional proteins, BM-related proteins, progenitor cell marker tumour protein p75, and MUCs 1, 16 and 5AC, two weeks post-operatively. Moreover, a significantly higher level of MUC5AC was observed in cultured

nasal mucosal cells than in cultured conjunctival cells. Madhira et al. showed that buccal mucosal cells from healthy volunteers cultured on AM without a feeder layer gave rise to a stratified non-keratinised epithelium.(63) The cells were smaller and slower to grow compared to conjunctival and limbal cells, although presence of a feeder layer was shown to give a more rapid growth *in vitro*.(63, 64) The cells expressed differentiation markers keratins 3, 4 and 13, with evidence of progenitor cells, however, no GCs were observed.(63) Hori et al. showed mRNA expression of MUCs 1, 4 and 16 in cultured oral mucosal cells obtained from healthy volunteers that were co-cultured with a feeder layer on temperature-responsive dishes.(65) Further studies are required to investigate the protein expression of these mucins, if the expression is similar when grafts are taken from patients with systemic mucosal diseases and if the expression is maintained *in vivo* post-transplantation. Although the presence of cell-cell junctions were observed in cultured cells, a study by Satake et al. investigating the barrier function of the transplanted stratified mucosal epithelial sheets showed that the epithelia were highly permeable to molecules less than 1kDa, in contrast to conjunctival epithelia and pathological corneal epithelia, questioning their barrier function.(63, 66)

Studies investigating the oral mucosa as a substitute for conjunctival tissue are limited due to the lack of GCs, which is in contrast to studies on reconstruction of the limbus and cornea. Autologous oral mucosal cells cultured on AM have been used to reconstruct the OS with LSCD secondary to various causes. There was re-epithelialisation of the cornea within one week following surgery in all the studies. Successful outcomes where there was no evidence of corneal epithelial defects, corneal vascularisation, conjunctival inflammation or symblepharon formation, were seen in 66-70% of the cases with improved visual acuity in 67-100% of the cases, during the follow-up period that lasted up to four years in one study.(46, 64, 67) Patients who had failed outcomes had an initial diagnosis of SJS, which is characterised by chronic inflammation of the OS, tear deficiency and lid abnormalities.(64, 67) These results further demonstrate the importance of controlled inflammation of the OS prior to transplantation. However, the failed outcomes in cases of SJS may be due to the systemic disease affecting all mucosal surfaces including that in the oral cavity. All studies reported evidence of peripheral neovascularisation between the AM and the corneal stroma, suggesting that this may be due to either pro-angiogenic or lack of anti-angiogenic factors in the transplanted tissue.(46, 64, 67) Interestingly, the neovascularisation peaked between three and six months, declining thereafter and remained stable after one year. The blood vessels did not encroach on to the visual axis in any of the cases.

Advantages of autologous mucosal membranes

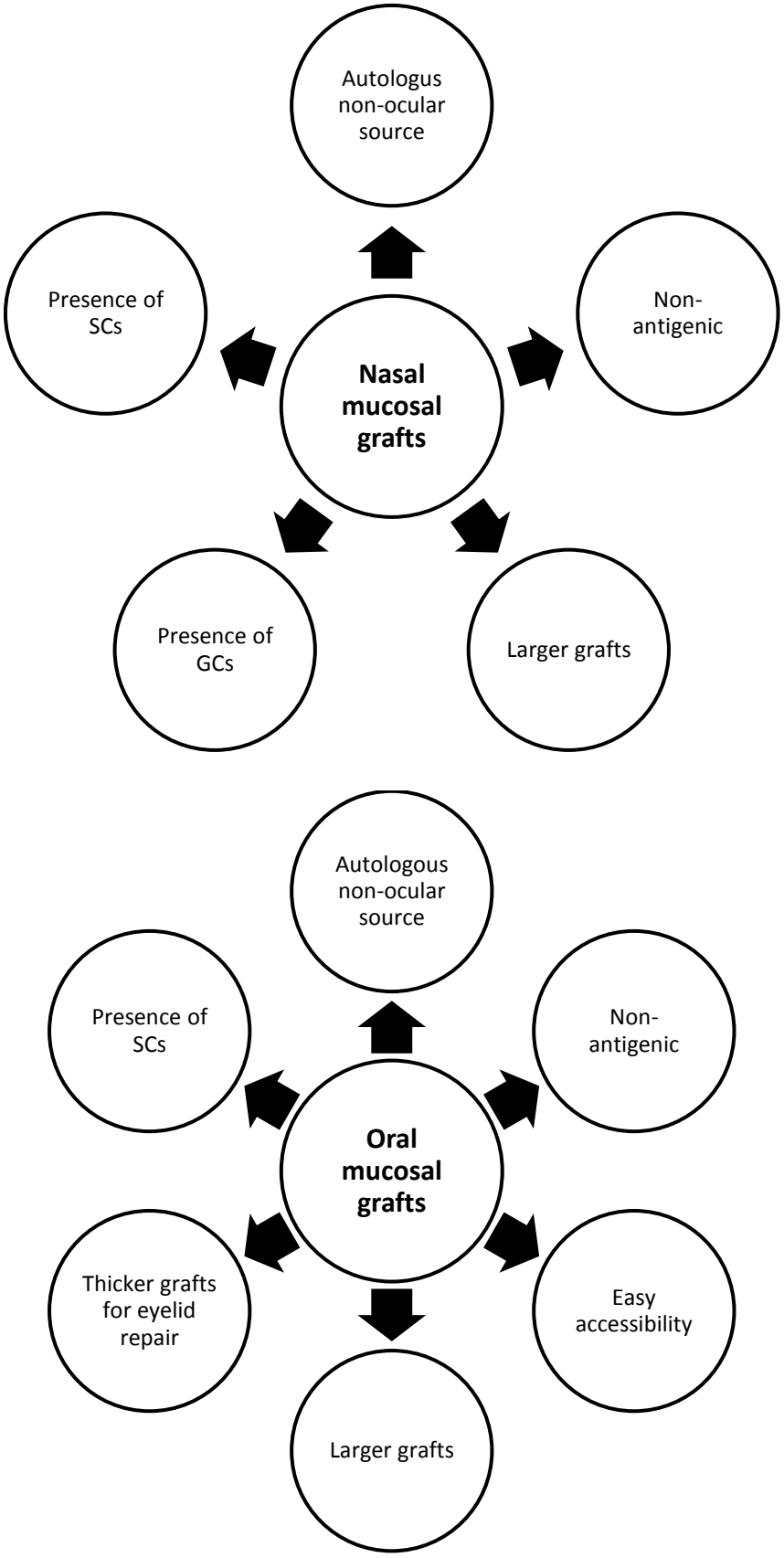

Figure 1.13: Advantages of autologous mucosal membranes as conjunctival grafts.

1.3.2.1.3 OTHER BIOLOGICAL SUBSTRATES

Safinaz et al. studied the use of autologous fibrin in *ex vivo* expansion of autologous conjunctival cells.(45) The epithelial cell sheets were then transplanted on to conjunctival epithelial defects in rabbits and monitored for six weeks. The rate of re-epithelialisation was found to be comparable with AM. Although there was less stratification with both fibrin and AM substrates compared to the native tissue, there was evidence of GC differentiation. Thus, fibrin may be an alternative substrate to AM that is cheap and tolerated in animals. Although fibrin is highly degraded, this may be controlled with protease inhibitors to increase the graft survival.(45)

An elastin-like polymer produced from bioengineered *Escherichia Coli* has been investigated for growth of conjunctival epithelial cells.(68) These polymers contain four domains: two elastin-derived, one fibronectin and one proteolytic domain that is active when released. Conjunctival epithelial cells adhered significantly more on polymer treated glass coverslips than untreated glass coverslips and tissue culture treated coverslips. The proliferation of conjunctival cells on polymer treated glass coverslips was significantly higher on culture day five compared to the untreated coverslips, but was similar to those on tissue culture treated coverslips. All the cells expressed keratin 7, a conjunctival cell differentiation marker, and junctional proteins. The authors suggested that this increased biological activity may be particularly due to the cell adhesion peptide REDV found in the fibronectin domain that may be interacting with the cell integrins.(68)

Borrelli et al. investigated keratin films made of human hair and gelatin (a softening agent) as a substitute for corneal epithelial and stromal defects.(69) *In vivo* studies in rabbits showed that the corneas were mostly transparent with no epithelial defects and induced a minimal inflammatory reaction. The keratin films were degraded within four weeks of transplantation. A limitation of this study was that the phenotype of the transplanted cells was not investigated, especially since the keratin found in hair is not found in epithelial cells of the OS and this may affect the biological characteristics of the cells.(31) Although keratin has good biomechanical strength, these may be too stiff for use as an OS substitute, especially in the conjunctival fornices. (8, 31)

1.3.2.2 SYNTHETIC SUBSTRATES

As described above, the use of biological substrates are limited due to limitations in availability of sufficient healthy tissue, inconsistent tissue composition, risks of microbial disease transmission and risks of immunological rejection by the host. Therefore, there is much scope for investigating synthetic substrates for use in conjunctival transplantation. Although a large amount of literature exists regarding the use of biological substrates as conjunctival grafts or substrates for conjunctival cell and tissue transplantation, there is very limited literature regarding the use of synthetic substrates. To date, synthetic substrates investigated for use in TE include synthetic polymers, for example, poly(ε-Caprolactone) (PCL) and poly(lactide-*co*-glycolide) (PLGA), which are approved by the Food and Drug Administration for specific applications in humans.(31, 70) There are numerous advantages to employing synthetic substrates in TE (figure 1.14) and due to the limitations of biological substrates, there is much scope for exploring non-biological options.(35, 70) The disadvantages of using synthetic substrates are lack of structure similar to that *in vivo* and lack of tissue-specific extracellular environment that guide cellular functions.(71)

Ang et al. investigated PCL membranes in the cultivation of rabbit conjunctival epithelial cells.(35) They stretched the membranes to produce 6μm thick membranes that were treated with sodium hydroxide. The sodium hydroxide made the surface more hydrophilic by converting the ester groups on the membrane to hydroxyl and carboxyl groups.(35) Wettability as well as surface chemistry, charge, roughness and rigidity affect the attachment of cells onto a synthetic substrate.(72) The stretching process gave the PCL membranes superior characteristics: the stretched membranes were transparent, had higher surface roughness with a fibrillary structure, higher tensile strength and were more flexible than un-stretched PCL membranes.(35) In comparison to human AM, the stretched PCL membranes had higher tensile strength but were stiffer. The stretched PCL membranes were able to support the growth of rabbit conjunctival cells expressing conjunctival cell differentiation markers keratins 4 and 19. The sodium hydroxide treated membranes had a greater number of proliferating cells with cell morphology similar to that on AM and demonstrated more stratification than untreated membranes. Both treated and untreated stretched PCL membranes supported the growth of GCs that was comparable to that on AM, although numbers were significantly less than that in the native rabbit conjunctiva. The authors showed that the cells were able to synthesise ECM proteins and form hemidesmosomes important for the attachment of the cells to the ECM. When these PCL membranes were transplanted onto immune-deficient mice, the cells underwent further

stratification and differentiation.(35) The disadvantages of this material is that it may be difficult to integrate into the host and its uniaxially aligned fibrillar architecture may be predisposed to scar formation.(8)

Sharma et al. used PCL membranes that were treated with helium-oxygen plasma to culture human corneal and limbal epithelial cells *in vitro*.(73) Plasma consists of partially ionised gas containing ions, electrons, neutral particles and free radicals.(73) In the presence of oxygen, the active species on plasma coated membranes form functional groups that are hydrophilic.(73) This treatment also made the membranes more transparent, which is important for corneal reconstruction.(73) The treated and untreated PCL membranes were able to support the growth of corneal and limbal cells, however, the treated membranes supported better adhesion and proliferation of cells. In addition, the corneal cells were able to maintain their differentiated phenotype and the limbal epithelial cells expressed SC markers. Shin et al. carried out animal studies to investigate the biocompatibility and biodegradability of the PCL membranes *in vivo*.(74) They showed that PCL membranes without cells induced an inflammatory reaction similar to AM when transplanted on to the OS of rabbits and re-epithelialised within two weeks with GC differentiation. Moreover, the authors showed that when the PCL membranes carrying a layer of conjunctival cells were transplanted on to abdomen of mice, the membranes were absorbed and replaced by surrounding host tissue within five weeks.(74)

The other synthetic substrate that has been studied for use in conjunctival transplantation is PLGA. Lee et al. studied the growth of corneal epithelial cells on PLGA and PLGA treated with type I collagen alone or with hyaluronic acid *in vitro* and *in vivo*.(75) Type I collagen is a hydrophilic protein containing RGD sequence domains that support attachment of cells, whereas hyaluronic acid is a GAG that is present in ECMs. The treated and untreated membranes were flexible that could be easily handled during surgery. However, these membranes were not transparent, although this is not a problem in the case of conjunctival transplantation.(31) All the surface modifications enhanced cell attachment and proliferation compared to untreated PLGA, with the combination of type I collagen and hyaluronic acid having a greater effect than type I collagen alone.(75) The PLGA that was treated with type I collagen and hyaluronic acid were transplanted on to conjunctival defects in rabbits. The conjunctival defects completely re-epithelialised and started to stratify four weeks post-operatively, although this was much slower than that observed with the ungrafted wounds. The ungrafted wounds contracted significantly more than the

grafted wounds with forniceal shortening. The collagen fibres were arranged regularly in the ungrafted wounds, whereas the grafted wounds showed random collagen orientation similar to the native tissue. The random pattern may be due to the presence of type I collagen and/or the porous structure of the PLGA that allowed the randomly aligned deposition of collagen fibres by the fibroblasts.(75) The PLGA grafts had a slower degradation time than PCL, which were found to be undegraded even at four weeks post-operatively.(75) Degradation of synthetic substrates depends on their chemical structure and presence of hydrolytically unstable bonds.(72) Rates of degradation of PLGA can be altered depending on their glycolic acid content, for example, 50:50 and 85:15 poly(DL-lactide-*co*-glycolide) have degradation times of two to four months and six to twelve months, respectively.(76) Moreover, the addition of carbonate units increases the degradation time as observed with 70:30 PGLA:poly(L-lactide-*co*-1,3-trimethylene carbonate), which takes one to two years to degrade.(76)

As described above, when investigating synthetic substrates it is important that the surface is hydrophilic as the ECM proteins secreted by the cells have higher affinity for binding to a hydrophilic surface than a hydrophobic surface.(73) The integrins on the cell membranes will then interact with specific domains on the ECM proteins to allow cell adhesion and growth. Other characteristics important for supporting culture of cells on synthetic substrates are the pore size and the number of pores, which affects attachment and spreading of cells as well as the diffusion of nutrients.(73) This is important when substrates with cells are transplanted *in vivo,* to ensure that the nutrients and waste products can diffuse from and to the vascular supply in the connective tissue stroma, respectively. Although many of the synthetic substrates may have superior mechanical properties than biological substrates that allow easy handling, lack of elasticity may limit their use in reconstructing fornices.(21) Moreover, the studies so far have been carried out in animals with wounds that were made surgically, therefore warranting further studies regarding the degradation times in the presence of active inflammation *in vivo*.(21)

Advantages of synthetic substrates

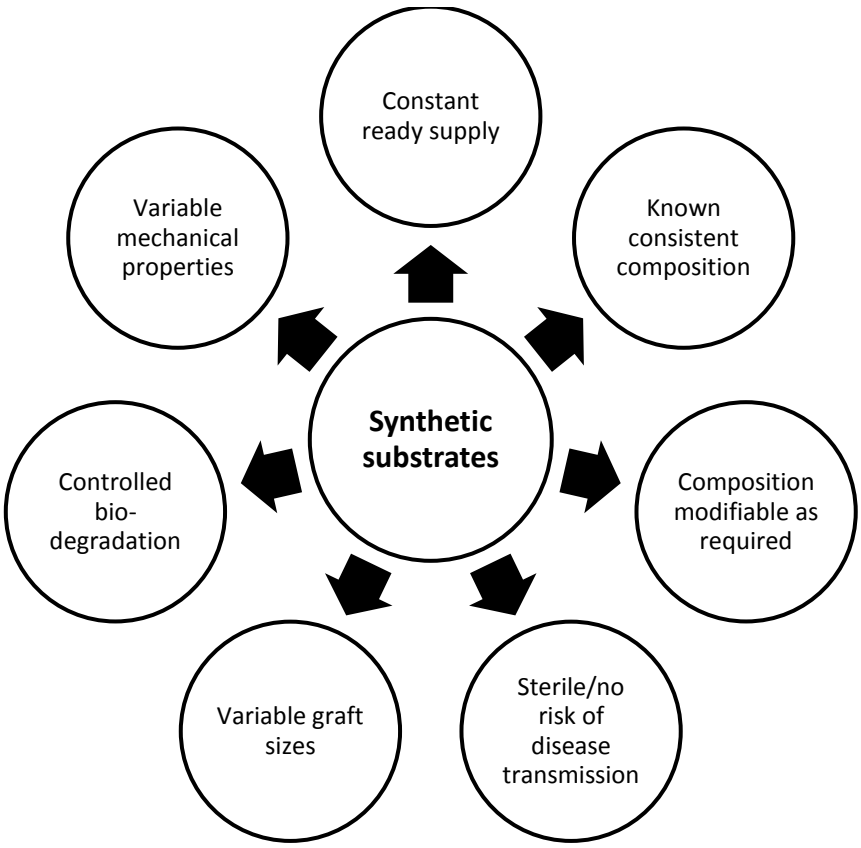

Figure 1.14: Advantages of synthetic substrates for use in tissue engineering.

Comparison of substrates investigated for tissue engineering of the conjunctiva

	Amniotic membrane	Autologous nasal mucosa	Autologous oral mucosa	Autologous fibrin	Elastin-like polymer	Keratin films	Surface modified PCL	Surface modified PLGA
Transparent	Yes					Yes	Yes	No
Suitable thickness	Yes (20-500µm)		Varies depending on the site of the oral cavity				6µm thick (stretched substrates)	
Flexibility and surgical handle-ability	Good					Good biomechanical strength but may be too stiff	High tensile strength and flexible (stiffer than amniotic membrane)	Yes
Biocompatible	Yes, non-antigenic	Yes, non-antigenic	Yes, non-antigenic	Yes, non-antigenic			Yes	Yes
Risk of microbial disease transmission	Potential risk	Autologous product	Autologous product	Autologous product	Made from bio-engineered bacteria	No	No	No

	Amniotic membrane	Autologous nasal mucosa	Autologous oral mucosa	Autologous fibrin	Elastin-like polymer	Keratin films	Surface modified PCL	Surface modified PLGA
Support epithelial cell growth	Yes	Yes	Yes	Yes	Yes	Yes but unknown phenotype	Yes	Yes
Support goblet cell differentiation	Yes but lower than native tissue	Yes	No	Yes			Yes but lower than native tissue	
Support maintenance of stem cells	No	Yes	Yes				Yes	
Biodegradability	Biodegradable			Highly degraded but could be controlled		Degrade within four weeks *in vivo*	Degrade within five weeks *in vivo*	Slower than PCL (undegraded at four weeks)
Low *in vivo* shrinkage	Prone to *in vivo* shrinkage		Prone to *in vivo* shrinkage				May be prone to scar tissue formation	

	Amniotic membrane	Autologous nasal mucosa	Autologous oral mucosa	Autologous fibrin	Elastin-like polymer	Keratin films	Surface modified PCL	Surface modified PLGA
Accessibility	Readily available	Complex surgery – limited size of donor tissue	Yes depending on the site of the oral cavity	Readily available	Readily available	Readily available	Readily available	Readily available
Standardised product	No	Autologous product	Autologous product		Yes	Yes	Yes	Yes
Risk to donor site	n/a	Yes	Yes	n/a	n/a	n/a	n/a	n/a

Table 1.2: Comparison of substrates investigated for tissue engineering of the conjunctiva.

1.4 EXTRACELLULAR MATRIX AND BASEMENT MEMBRANE

1.4.1 STRUCTURE AND FUNCTIONS

The ECM is a non-cellular component of tissues consisting of biomolecules secreted by the resident cells.(42, 77) There are two forms of ECMs: the BM and the interstitial matrix.(42) The BM, also known as the basal lamina, was first observed by histologists as an electron-dense sheet-like structure basolateral to all cell monolayers, separating them from the underlying stroma, on transmission electron microscopy.(77, 78) Since then, BMs have been found in all tissues, specifically on the basal side of epithelial cells (figure 1.15), adjacent to vascular endothelial cells and Schwann cells of peripheral nerves and encircling smooth, cardiac and skeletal muscle fibres.(79) The BM, consists of large insoluble proteins that are highly cross-linked by undergoing self-assembly, which is guided by cellular receptors.(77) Transmission electron microscopy studies have measured the thickness to be between 50 and 100nm containing two layers, lamina lucida (approximately 25nm) and lamina densa (approximately 50nm).(1, 78) The ocular lens capsule, tracheal BM and Desçemet's membrane of the cornea are exceptions to this where the thickness is in the micrometre range.(79) However, recent studies involving atomic force microscopy show that the BMs are two-folds thicker than previously measured using transmission electron microscopy.(79) BMs are formed during the embryonic period to establish polarity in the epiblast.(80) In humans, the BM of the cornea is first detected during gestation weeks eight and nine, and the epithelium is seen to be separated from the underlying stroma by week sixteen.(81) In contrast to BMs, the interstitial matrix is a three-dimensional amorphous gel surrounding the cells and acts as the 'glue' that holds the cells in place within tissues.(42) This form of ECM is mainly found surrounding cells of mesenchymal origin, such as adipocytes, chondrocytes, myoblasts and osteoblasts.(43) The protein profile of the interstitial matrix may differ from that of BMs, having more collagen, elastin and fibronectin.(42) Additionally, interstitial matrices are less dense and more porous than BMs. The ECM is an integral structure in eukaryotic tissues that regulates their development, function and homeostasis.(80)

Functions of the ECM:

1. Structural support for cells.(77, 78)
2. Anchorage site for cells by providing ligands to cell receptors.(78)
3. Divides different types of tissues of an organ into compartments.(77)
4. Provides a semi-permeable selective barrier, for example in the kidneys, the proteins of the glomerular BM provide charged molecules required for appropriate filtration of blood and the mechanical strength to sustain this function.(78)
5. Contributes to the mechanical properties of tissues by providing tensile strength.(77, 82)
6. Individual proteins have multiple binding sites for cell surface receptors that initiate intracellular signalling pathways influencing cellular processes, such as cell migration, proliferation and differentiation, thus are involved in the outside-in signalling of cells.(11, 42, 78) Studies have shown that when conjunctival epithelial cells have been cultured on substrates containing ECM proteins of the cornea, these cells differentiate to express cornea-specific protein markers, displaying the ability of ECM proteins to govern the differentiation of cells.(83) In addition, specific proteins are responsible for the self-renewal, maintenance and activation of SCs.(11)
7. Provides a reservoir of growth factors and cytokines that influence behaviour of cells in both physiological and pathological states.(42, 78)

The basement membrane

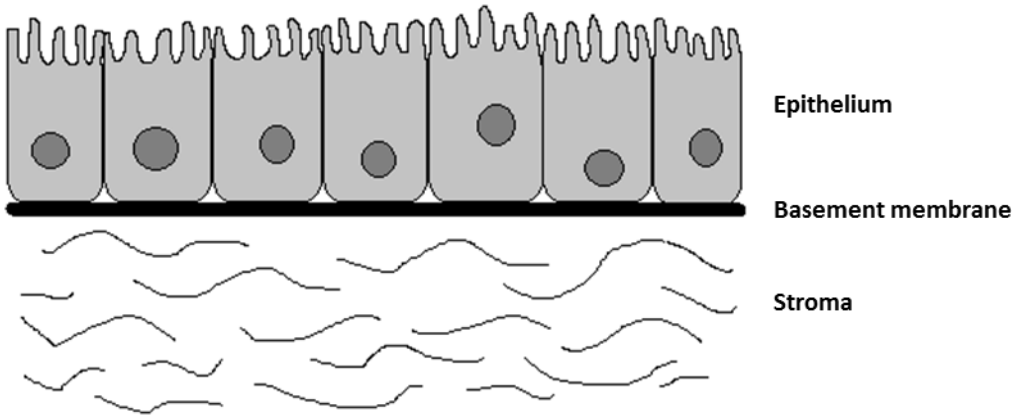

Figure 1.15: The basement membrane of epithelial cells. Epithelial cells sit on a basement membrane that separates them from the underling connective tissue stroma.

1.4.2 COMPONENTS OF THE EXTRACELLULAR MATRICES AND BASEMENT MEMBRANES

The composition of ECM/BMs are diverse, tissue-specific and dynamic.(78) The ECM composition has been studied largely by means of immunohistochemistry, in particular by investigating the BM of the mouse Engelbreth-Holm-Swarm (EHS) sarcoma in the 1980s.(79, 84) A major limitation of this is that the ECM of a tumour is different to that of a healthy tissue in their composition and structure, where the former is less cross-linked.(77, 78) Thus, it is important that these protein structures are studied in their physiological healthy states. Studies carried out since then have shown that the matrisome consisting of 1-1.5% of the mammalian proteome, is made up of more than three-hundred proteins, although this is not an exhaustive list.(82, 84) ECMs consist of structural proteins, such as collagens, glycoproteins (GPs) and proteoglycans (PGs).(42, 78) Additionally, cell receptors such as integrins, growth factors (GFs) and matrix metalloproteinases (MMPs) also constitute the ECM.(42) The multi-domain structures of the ECM proteins allow interaction with each other to form protein polymers.(78, 79)

Although all BMs in the human body may appear similar under electron microscopy, the combination of protein composition and their isomers is diverse and unique to each type of tissue, conferring tissue specificity and dictating their individual functions within an organ.(77, 78) Moreover, this heterogeneity is accounted for by the different amounts of each type of protein and their isomers, their splice variants and post-translational modifications giving rise to variable binding affinities to other proteins.(78) Isomers of type IV collagen and laminin are thought to account for the major differences between ECMs of tissues, whereas the specific composition of the other minor proteins adds to further tissue specificity and heterogeneity.(78, 85) The differences in assembly of the major and minor components of ECMs also confer tissue specificity.(85) For example, laminin α_1, α_3 and α_5 chains are predominantly present in epithelial BMs, whereas the α_2 chain is found mainly in BMs of skeletal and cardiac muscles and α_4 chain in vascular BMs.(78) Moreover, the mammalian kidney is an example where the composition of ECMs varies between the different types of tissues present within an organ, portraying the unique cellular function of that particular tissue: glomerular BM has been shown to consist of $\alpha_3\alpha_4\alpha_5$ protomers of type IV collagen, whereas Bowman's capsular BM consists of $\alpha_5\alpha_5\alpha_6$ and $\alpha_1\alpha_2\alpha_1$ protomers.(78) Thus, studying the unique composition of ECMs of different tissues and their structure could uncover information regarding the effects of cellular microenvironments on the regulation of the functionality of the resident cells.(77)

In addition to variations in composition between different types of tissues, the ECM is a dynamic structure in which the composition and assembly of proteins and the biomechanical properties differ for each tissue type depending on the physiological states, such as ageing, and pathological states.(78, 79) The constant remodelling of the ECM proteins may expose cryptic binding sites on the proteins allowing cells to interact with different domains of the same molecule to give rise to distinct cellular functions.(77) During ageing, there is an overall reduction in synthesis of proteins, especially type I collagen.(42) However, synthesis of proteins, such as fibronectin and MMPs, increase relative to the other proteins.(42) These differences during ageing have shown to alter the cellular functions, for example, the ECM laid down by fetal SCs was found to be superior to that laid down by adult SCs for chondrogenic cell proliferation and differentiation.(42) Moreover, there are higher levels of hyaluronic acid in ECM of fetal skin wounds than in adult wounds.(42) Increasing levels of hyaluronic acid in adult skin wounds have been shown to reduce scar formation by altering collagen synthesis and enhancing cell proliferation and migration.(42) Defects in BMs have been shown to give rise to various disease processes within the human body. One example is Alport syndrome, where mutations in type IV collagen α_5 chain gives rise to the loss of $\alpha_3\alpha_4\alpha_5$ protomers in the glomerular BM and replacement with $\alpha_1\alpha_1\alpha_2$ protomers that are unable to withstand the glomerular pressures with subsequent loss of structural integrity of the BM and kidney failure.(77, 78) Collagen proteins may also be affected by autoimmune diseases, such as Goodpasture syndrome of the kidneys, where there are auto-antibodies against type IV collagen α_3 chain in the glomerular BM.(77) These studies emphasise the importance of the correct combination of components and their assembly in the ECM of a given tissue.(77)

1.4.2.1 COLLAGENS

Collagens are the most abundant proteins in the human body, especially in connective tissues.(42) It is the main protein found within ECMs functioning as the principle structural protein providing tensile strength to tissues and serving a role in cellular processes, such as cell adhesion and migration.(42, 84) There are twenty-eight types of collagens in vertebrates that are grouped into three major categories: fibrillar (I, II, III, V, XI, XXIV, XXVII), fibril-associated collagens with interrupted triple helices (IX, XII, XIV, XVI, XIX, XX, XXI, XXII) and non-fibrillar collagens.(80, 86) The latter is further divided into network forming BM collagens (IV), microfibrillar (VI), anchoring fibrils (VII), short chain (VIII, X), multiplexins (XV, XVIII) and membrane-associated collagens with interrupted triple helices (XIII, XVII, XXIII). All collagens are made up of three α polypeptide chains that wind around each other to form a triple helix.(82)

1.4.2.1.1 TYPE IV COLLAGEN

Although type I collagen is the most abundant collagen in the human body, type IV collagen accounts for 50% of all BM proteins.(77, 78) It is first expressed on embryonic stage day 4.5 in mice.(78) Protomer, the basic building unit of collagens, consists of three α chains (each 400nm long, 170kDa) that form a triple-helix.(77, 78) These protomers interact with each other to form a network.(77) Each protomer consists of the triple helical collagenous domain consisting of Glycine-X-Y sequence, where X and Y amino acids are hydroxylysine and lysine or hydroxyproline and proline.(77, 78) The triple helical collagenous domain provide the collagen protomer with structural integrity, however, about twenty-two short sequence interruptions within this domain provide flexibility.(78) The C-terminal of the protomers have globular non-collagenous domains and the N-terminal consists of 7S domains containing interrupted Glycine-X-Y repeats.(78) The non-collagenous domain is hydroxyproline free but is rich in amino acids cysteine and lysine thought to be important for the self-assembly of type IV collagen.(77, 78) There are six types of type IV collagen α chains in mammals, which give rise to fifty-six possible combinations of protomers.(77, 78) Homology between these chains are thought to differ mostly in their non-collagenous domains.(78) The main *in vivo* combinations of type IV collagens are $\alpha_1\alpha_1\alpha_2$ and $\alpha_3\alpha_4\alpha_5$, where the former is found in most epithelial and endothelial BMs.(43, 78) The non-collagenous domains limit the random association between the α chains ensuring specific protomer combinations *in vivo*.(78) Early studies on EHS tumours have shown that correct formation of the type IV collagen network is essential for BM stability and assembly.(77)

1.4.2.1.2 OTHER COLLAGENS

Type XV collagen is a non-fibril forming collagen that forms homotrimers consisting of three α_1 chains observed in a variety of tissue ECMs with highest expression in the BMs of the heart and skeletal muscles.(77) Studies on type XV collagen deficient mice have shown normal development of blood vessels, however, the vessels were collapsed suggesting a vital structural role in the vasculature of these tissues.(77, 78) This collagen is highly homologous to type XVIII collagen in the BM.(77) Type XVIII collagen, a non-fibrillar type collagen-heparan sulphate PG (HSPG), is mainly found in epithelial and vascular endothelial BMs.(86) Both type XV and XVIII collagens are thought to be found at the interface between the BM and the underlying stroma, possibly forming connections between the two regions.(87) Type XVIII is made up of three α_1 chains that form a triple helix, which is interrupted by non-collagenous regions.(88) These non-triple helical domains provide a good degree of flexibility between the triple-helical regions and allow formation of collagen polymers.(88) Moreover, they provide binding sites for heparan sulphate side chains that interact with GFs and various receptors on cell membranes.(88) There are three isoforms, long, medium and short isoforms that differ in their N-termini non-collagenous regions and their tissue distribution.(89) The non-collagenous domain at the C-terminal consists of three regions: proximal region involved in formation of the triple-helix, hinge domain that is highly susceptible to proteases and distal globular domains.(88) These globular domains contain an anti-angiogenic fragment called endostatin.(77, 78) Endostatin has been shown to interact with integrin $\alpha_5\beta_1$, glypican, domain V of perlecan, nidogen and the laminin complex.(88) Proteolysis studies have shown that the non-collagenous domains of type IV collagen also have anti-angiogenic fragments, such as arrestin (α_1 chain), canstatin (α_2 chain) and tumstatin (α_3 chain).(77, 78) Type XVIII collagen is thought to play a role in the development of the vasculature of the retina, where a mutation is associated with Knoblach syndrome characterised by failed development of retinal vasculature and affected individuals have retinal degeneration and blindness.(77)

1.4.2.2 GLYCOPROTEINS

GPs are proteins that have covalently attached carbohydrates. There are approximately two-hundred GPs in the matrisome having various roles in individual tissues.(84)

1.4.2.2.1 LAMININS

Laminins are the most abundant non-collagenous proteins in BMs and is involved in a variety of cellular processes, such as adhesion and differentiation.(42, 78) Laminin trimers are the basic building unit of the laminin network.(77) Three polypeptide chains, α, β and γ form a trimeric three-pronged fork-like structure that is between 400 and 800kDa in size.(77, 78, 82) There are twelve genes encoding five α-chains, three β-chains and three γ-chains, which are able to form fifteen trimeric combinations of laminin and all have been found in BMs, laminin 111 ($\alpha_1\beta_1\gamma_1$ or laminin 1) being the most abundant type in BMs.(78, 80) The C-terminal of the α chain (400kDa, 160nm) consists of five homologous globular domains, which is the major site for cell attachment.(78) The β (200kDa, 60nm) and γ (200kDa, 40nm) chains lack these domains. The C-termini of all three chains form a triple α-helical coiled-coil ("handle" of the fork) and consists of domains I and II of the laminin trimer.(78) The short arms of the three chains ("prongs" of the fork) contain domains III, IV, V and VI.(78) Some α and β chains of laminin have short truncated arms.(78) The α chain mainly plays a role in cell adhesion, whereas the β and the γ chains are mainly involved in the self-polymerisation of laminin and binding to nidogen.(87) Laminin 111 is the first laminin detected in mice on embryonic stage day 4.5.(78) Laminin 511 ($\alpha_5\beta_1\gamma_1$ or laminin 10) has also been found to be important for the early embryonic development.(87) Among the first proteins of the ECM to be expressed in embryos, laminins have been shown to be important for differentiation where a defect in their expression can have fatal results in the embryo or they manifest as serious conditions affecting various organs.(42) Laminin γ_1 chain is shown to be a common component in all BMs, whereas other isoforms have a tissue-specific distribution.(85) Laminins 111, 211 ($\alpha_2\beta_1\gamma_1$ or laminin 2) and 121 ($\alpha_1\beta_2\gamma_1$ or laminin 3) have three short arms in which the N-termini provide the binding sites for self-polymerization to form a network.(43) On the other hand, laminins 411 ($\alpha_4\beta_1\gamma_1$ or laminin 8), 421 ($\alpha_4\beta_2\gamma_1$ or laminin 9) and 423 ($\alpha_4\beta_2\gamma_3$ or laminin 14) have only two short arms, which require other molecules for assembly, and laminin 332 ($\alpha_3\beta_2\gamma_2$ or laminin 5) has one short arm that bind to other laminins and proteins within the ECM.(43)

1.4.2.2.2 FIBRONECTIN

Fibronectin plays a role in cell adhesion, migration and the wound healing response to injury.(42, 82) It prevents terminal differentiation of keratinocytes by down-regulating the expression of involucrin.(48) The absence of fibronectin during embryonic development is found to be fatal in mice.(42) There are two forms of fibronectin, as a component in blood plasma, and as a cellular and extracellular protein produced predominantly by fibroblasts.(42) Fibronectin monomers are approximately 250kDa in size and are made up of repeating units of three types of modules: types I, II and III.(42, 82) Each monomer contains binding sites for integrins, collagen, heparin and other fibronectin monomers.(90) The FNIII10 repeat contains a RGD peptide sequence that is important for cell adhesion.(42, 82) Fibronectin is secreted as dimers by forming two disulphide bonds between C-termini of two monomers.(90) The dimers then interact with each other to form a multimeric fibronectin fibril mesh.(42, 82) The mesh provides a structural support for the cells to grow on.(90)

1.4.2.2.3 VITRONECTIN

Vitronectin, a cell adhesive protein, is predominantly found in loose connective tissue in healthy tissues, and like fibronectin, is deposited during wound healing responses where it contributes to the provisional matrix.(80, 91) Similar to fibronectin, vitronectin is also found in blood plasma.(48) It binds to integrins on cell membranes and extracellular collagen, heparin and plasminogen activator inhibitor.(48) Vitronectin knock-out mice have been shown to have delayed wound healing and a defective inflammatory response.(92)

1.4.2.2.4 NEPHRONECTIN

Nephronectin is a GP that has been found to be essential for the development of the urinary tract system, including the kidneys.(87) This is mediated by binding of the RGD peptide sequence on the protein to integrin $\alpha_8\beta_1$ on cell membranes.(87) Nephronectin has also been found in tissues of other organs, including the eyes and skin.(87)

1.4.2.2.5 THROMBOSPONDINS

The thrombospondin family consists of five isomers (1-5), of which 1 and 2 form homotrimers, whereas 3, 4 and 5 form homopentamers.(93) Thrombospondins 1 and 2 are approximately 400kDa in size and contain von Willebrand factor type C, anti-angiogenic and

epidermal GF (EGF)-like domains. They bind to multiple proteins in the ECM, including type I-V collagens, laminin, fibronectin and heparin. They modulate cell adhesion via integrin subunits β_1 and β_3. They bind to other cell membrane proteins, such as syndecans and cluster of differentiation 36 (CD36, also known as platelet glycoprotein 4). The interaction between CD36 and thrombospondin 1 leads to cell apoptosis. Moreover, thrombospondin 1 modulates the expression of other proteins within the ECM, such as GFs and MMPs. This together with CD36 mediated endothelial cell apoptosis gives rise to the anti-angiogenic properties of thrombospondin 1. In diabetic patients, the expression of thrombospondin 1 in the aqueous and vitreous humour has been shown to be reduced, which may explain the neovascularisation seen in these patients, thus plays a significant role in the growth of retinal blood vessels.(93) Thrombospondin 1 is important for normal wound healing responses of the cornea where it has been shown to be synthesised within four hours of injury supporting cell migration and inhibiting angiogenesis, thus ensuring transparency of the cornea.(93) Moreover, studies have shown the development of a chronic inflammatory response of the OS with age in thrombospondin 1-null mice that was absent at birth.(94) There was also a reduction in mucin producing GCs that may have contributed to the increased inflammation of the OS.(94) Thus, thrombospondin 1 has been associated with an immunomodulatory role on the OS.

1.4.2.2.6 NIDOGEN

Nidogen is a GP that accounts for 2-3% of all BM proteins.(78) Its core consists of three globular-like domains, where G1 is at the N-terminal and G3 is at the C-terminal of the core protein. A short rod separates G1 and G2 domains, whereas a longer rod separates G2 and G3 domains. Two genes encode for two isomers, each approximately 150kDa, nidogen 1 (30nm) and nidogen 2 (40nm).(78, 79) Both are found in all BMs of the human body, although nidogen 2 shows a more restricted expression, predominantly found in vascular BMs.(78) Their expression is first detected on embryonic stage day 10.5 in mice.(78) They mainly function as bridging proteins between the laminin and type IV collagen networks, however, they also bind to other proteins, such as perlecan, fibronectin and fibrinogen.(78) Studies have shown that laminin provides more than one binding site for nidogen 2 suggesting separate functions for the two isomers.(78) Double-null mice have been found to be peri-natally lethal, whereas mice lacking a single gene show that nidogen is not required for formation of BMs, however is essential for the correct functioning of BM, in particular that of the lungs and the heart.(78)

1.4.2.2.7 TENASCINS

Tenascins are GPs of the ECM, in particular within connective tissues where it plays a role in load bearing.(42) They are also found in ECMs of the brain and skin.(42) Tenascin C was discovered first following which four other isomers namely, tenascins Y, X, W and R were described.(42, 95) All types form trimers, except for tenascin C, which forms hexamers.(95) The tenascin C molecule contains a tenascin assembly domain, an EGF-like domain, a FNIII domain and a fibrinogen-like domain.(95) Although it has been suggested that tenascin is not present in normal adult tissue, this protein is found in the provisional matrix during development and pathological states, such as wound healing.(42) In particular, the absence of tenascin C has been shown to lead to impaired regeneration following an injury.(42) Tenascin C has been shown to enhance migration of fibroblasts to wound sites to lay down a provisional matrix made up of fibrin and fibronectin supporting the adhesion and migration of cells.(42) Substrate coating with tenascin C, however, has been shown to prevent cell adhesion.(42) Moreover, tenascin C has been shown to be associated with SC niches, especially in neural tissues where it appears to regulate GF activity.(11, 42) Moreover, on the OS, tenascin C was noted to be a component of the limbal SC niche.(24)

1.4.2.2.8 α-2-HEREMANS SCHMID-GLYCOPROTEIN

α-2-Heremans Schmid-glycoprotein (α-2-HS-GP), also known as Fetuin A (bovine homologue), is a GP found in humans and animals that belongs to the cystatin superfamily.(96, 97) Depending on the carbohydrate content, it has a molecular mass of 51-67kDa.(98) It was first detected in fetal and new born calf serum.(96) In humans, it is primarily produced by hepatocytes in adults where its production is regulated by systemic inflammation.(97, 99) However, it has been found in other organs, such as the brain and kidney, as well in the amniotic fluid of the fetus.(96, 99) In humans, the concentration of α-2-HS-GP is approximately five times higher in the fetus than that in the adult.(96) However, the concentration has been shown to be high around hair follicles and at epidermal-dermal junctions in adult skin tissue.(97) α-2-HS-GP has been shown to have various biological roles: roles in brain development, in bone remodelling and as an inhibitor of ectopic calcium deposition, inhibitor of TGFβ signalling and as an anti-inflammatory acute phase protein.(96, 99) Moreover, it has been shown to play a role in insulin resistance in type II diabetes by inhibiting insulin receptor tyrosine kinase. α-2-HS-GP, as a component of fetal calf serum, is known to support the attachment and migration of cells cultured *in vitro*.(96, 100)

1.4.2.3 PROTEOGLYCANS

PGs (approximately thirty-six in the matrisome) are made up of a protein backbone covalently attached to GAG side chains, where GAGs are linear anionic chains made up of repeating units of disaccharides.(82, 84) There are four types of GAGs, hyaluronic acid, heparan sulphate, keratan sulphate and dermatan/chondroitin sulphate.(82) The anionic GAG chains are able to bind to water and divalent cations, thereby acting as space-filling and lubricating components in the ECM.(82) These proteins maintain the hydration of the ECM, thus have a role in regulating the biomechanical properties, such as the thickness and stiffness of BMs.(79) Moreover, GAGs in particular heparan sulphate, bind to GFs and GF receptors to play a role in cell signalling and other biological functions.(82, 84) The PGs are categorised into large (aggrecan, versican), small leucine-rich (decorin, lumican), BM-associated (perlecan, agrin), and cell-surface associated (syndecan, glypican, CD44) PGs.(82, 84, 95) The cell surface-associated PGs act as receptors for other ECM proteins, such as GFs, fibronectin, thrombospondin and collagen.(48)

1.4.2.3.1 PERLECAN

Perlecan is a large HSPG with a core protein containing five domains (I-V) resembling "pearls on a string".(78) Domain I at the N-terminus is covalently linked to three GAG chains.(78) In humans, the core protein is approximately 470kDa and the addition of the GAG chains can give rise to a protein that is more than 800kDa.(88) The core protein consists of protein sequences that are shared by other ECM proteins and cell membrane receptors, which are evolutionarily related to having roles in metabolism of nutrients, cellular adhesion and growth.(88) Perlecan binds to laminin, type IV and XVIII collagens, fibronectin, thrombospondin, nidogen, heparin, GFs and integrins.(88) Mouse studies show its first expression on embryonic stage day 10.5 with predominant expression in the heart and major blood vessels.(78) It has also been detected in the connective tissue outside BMs, where it is thought to play a role in chondrogenesis.(78) The main functions of HSPGs are to bind to GFs and to connect the laminin and type IV collagen protein networks.(79)

1.4.2.3.2 AGRIN

Agrin is a 150kDa HSGP detected in muscular, neuromuscular and neural BMs.(78) They contain the globular domains of laminin, EGF domains and Kazal-type serine protease inhibitor domains.(80)

1.4.2.4 GROWTH FACTORS

The ECM acts as a reservoir for GFs.(82) GFs are proteins that modulate cellular functions, such as migration, proliferation and differentiation.(49) As previously mentioned PGs interact with GFs, such as fibroblast GF (FGF) and TGFβ, and other developmental control factors (Wnt factors).(42, 82) The ECM proteins are known to regulate controlled release and actions of GFs and conversely, GFs are involved in the remodelling of the ECM and tissues, especially during injury by activating ECM proteins.(42) For example, TGFβ is involved in the up-regulation of ECM-related genes and production of ECM proteins by interacting with latent TGFβ binding protein (LTBP), which in turn bind to fibrillins and to fibronectin-rich matrices.(82, 84)

1.4.2.5 MATRIX METALLOPROTEINASES

The ECM is dynamic and is constantly degraded and remodelled by the action of proteins, such as MMPs, a disintegrin and metalloproteinase (ADAM), a disintegrin and metalloproteinase with thrombospondin motifs (ADAMTS) and other proteases.(82) To ensure controlled action of these proteases, they are regulated at the transcription level and are held in a quiescent state within the ECM until activated.(42) There are also inhibitors, such as tissue inhibitors of MMPs (TIMPs).(42) There are more than twenty MMPs identified that were initially named according to substrate specificity, for example collagenases (MMPs 1, 8 and 13), gelatinases (MMPs 2 and 9), stromelysins (MMPs 3, 10 and 11), and matrylisins (MMPs 7 and 26).(95) However, MMPs were found to have overlapping substrate specificity.(42) MMPs are predominantly expressed in response to cytokines and GFs, and may be secreted or transmembrane.(95) Degradation and remodelling of the ECM proteins cause cryptic domains to be exposed causing changes to cell behaviour, for example type IV collagen binds to integrins $\alpha_1\beta_1$ and $\alpha_2\beta_1$ of endothelial cells leading to their proliferation and migration, however, when degraded by MMPs they bind to integrin $\alpha_v\beta_3$ inhibiting these processes.(77) In addition, MMPs also play a role in cleaving precursor proteins and releasing bioactive domains, such as GFs and anti-angiogenic molecules from the parent proteins.(82) Enzymes, such as heparanases and sulfatases, are also present within ECMs that degrade GAGs and alter the properties of PGs.(84)

1.4.3 ASSEMBLY OF THE BASEMENT MEMBRANE

Correct assembly of BM components is essential for normal development.(90) Abnormal assembly leads to fibrosis and formation of tumours, whereas delayed assembly gives rise to malformation of anatomical structures and chronic wounds.(90) Components of the BM contain all the essential information required to promote self-assembly via specific binding sites.(77) Type IV collagen and laminin form independent supra-structures via intermolecular self-assembly, forming the basic framework for the formation of a stable sheet-like BM (figure 1.16).(77, 78) This type IV collagen-laminin network has a pore size of approximately 10nm.(87)

Initially, laminin trimers are formed in the Golgi apparatus of cells where the three chains are linked by disulphide bonds.(78) Upon secretion, laminin self-assembles into a honeycomb-like structure by interaction of the VI domains at the N-termini of each chain, that is thought to be a calcium-dependent process.(78) The laminin polymer being the centrepiece of the BM is formed underneath the cells in association with cellular receptors and is thought to provide the main cell-binding activity, whereas the type IV collagen network is deposited later on the stromal side and provides a scaffold, which is considered the main stabilising structure.(77, 79) Protomers of type IV collagen are also formed in the Golgi apparatus of cells, where alignment of the non-collagenous domains at the C-termini of the three α chains initiates the formation of a triple helix.(78) These protomers are then secreted into the ECM where they self-assemble to form a network.(78) Initially, non-collagenous regions at the C-termini of two protomers interact with each other.(77, 78) The 7S domains at the N-termini of four protomers also associate with each other to eventually form a type IV collagen network.(77, 78) Studies on protomer $\alpha_3\alpha_4\alpha_5$ of type IV collagen have shown that the 7S domain localises to the stromal side, whereas its non-collagenous domain is found at the epithelial side co-localising with laminin.(79) The precise formation of this type IV collagen network is important for the integrity and the structural organisation of the remaining BM.(77) In contrast, studies have also shown that abnormal assembly of the laminin network initially leads to subsequent abnormalities in the assembly of the type IV collagen network.(77)

The other major proteins of the BM, perlecan and nidogen, are secreted as single molecules and do not undergo self-assembly to form supra-structures. Instead they act as bridging proteins between the laminin and type IV collagen superstructures, stabilising them and promoting structural integrity of the BM complex.(77, 78) Nidogen G3 domain binds to

domain III of the laminin γ chain, whereas the G2 domain binds to the triple-helical collagenous domain of type IV collagen.(78) The G2 domain also binds to perlecan and fibulin.(78) The perlecan core protein binds to the triple-helical collagenous domain of type IV collagen, whereas the GAG chains may interact with the non-collagenous domains of type IV collagen and globular domains of the laminin α chain.(78)

Fibronectin is secreted by cells as dimers by forming disulphide bonds between C-termini of two monomers.(90) Fibronectin dimers then bind to integrins that cause integrins to cluster leading to high concentrations of bound fibronectin locally.(90) This stimulates phosphorylation of cellular proteins that enhance cell contractility and the force generated causes the fibronectin to change its conformation exposing cryptic sites of the protein that allow self-assembly into fibrils.(80, 90) This is guided by fibrillar adhesions between the cells and fibronectin formed near the centre of the cells.(90) The fibronectin dimers interact with each other to give rise to fibrils that increase in length as well as thickness.(90) Fibronectin fibrils (10-1000nm in thickness) form linear and branched networks around the cells, which support the growth of cells.(42, 90)

Previous transmission electron microscopy studies showed the thickness of BMs to be less than 100nm posing limitations when modelling the large proteins within this thickness.(79) However, recent measurements using atomic force microscopy show that the BM is a thicker structure making it easier for modelling the protein distribution and architecture.(79) Specifically, this means that type IV collagen, which is 400nm long, does not have to be arranged in a flat and stretched-out configuration that limits its ability to stretch laterally. Lack of lateral elasticity of tissue would lead to functional defects during development. The current proposed theory is that having this protein in a meshed network would provide greater extensibility of BMs, essential for the development of tissues and organs that are constantly undergoing changes to their shape. The difference in the thickness of BM seen with transmission electron microscopy and atomic force microscopy is attributed to the high water content of BMs.(79) HSPGs with their GAG side chains have negative charges that bind ions and therefore large quantities of water. Transmission electron microscopy requires tissue samples to be dehydrated and therefore the measurements were taken without their normal water content. Studies done with and without GAG chains show that the BMs shrink by 50% in the absence of these side chains.(79)

Assembly of basement membrane proteins

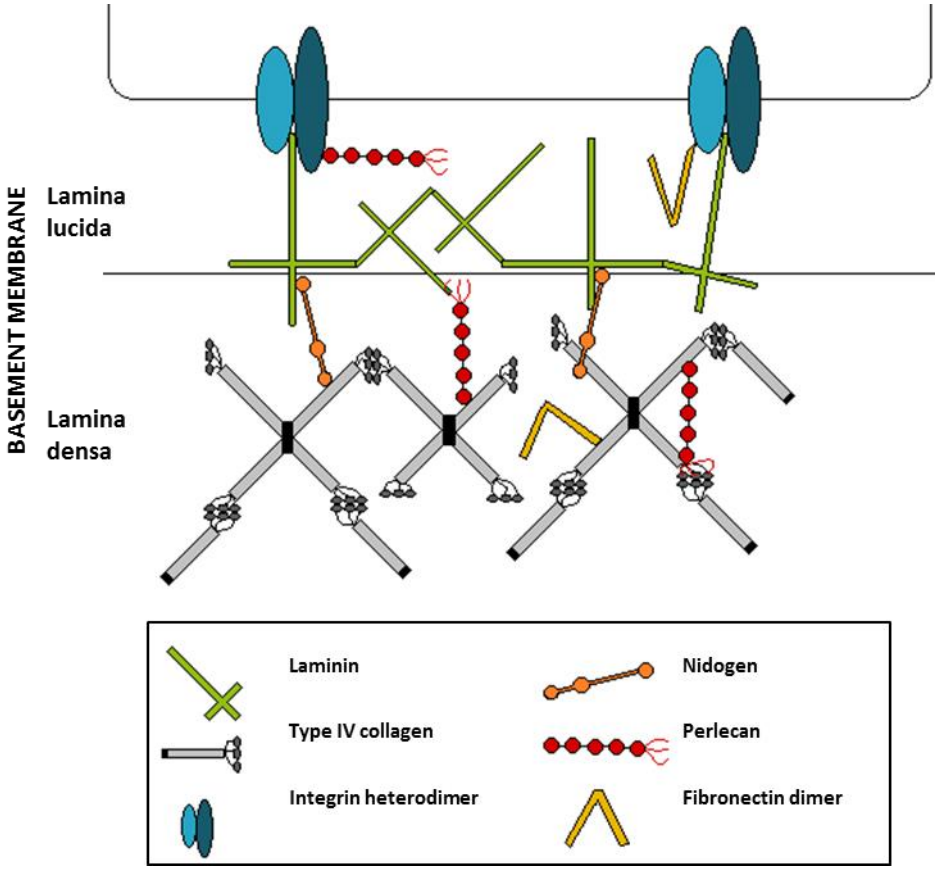

Figure 1.16: Assembly of basement membrane proteins.

1.4.4 CELLULAR RECEPTORS AND THEIR INTERACTIONS WITH BASEMENT MEMBRANE PROTEINS

BM proteins interact with cells via receptors on cell membranes.(82) Integrins, major cellular receptors for BM proteins, are heterodimeric proteins consisting of an α and a β chain, together forming a large extracellular domain, a transmembrane domain and short cytoplasmic domain.(82) In vertebrates, there are eighteen α chains and eight β chains that form twenty-four integrin heterodimers. Integrins are involved in the bi-directional signalling within tissue.(87) The main integrin that binds to BM proteins is β_1 that interacts with collagens, laminins and fibronectin.(82) Binding of integrins to BM proteins lead to outside-in signalling by activating intracellular phosphorylation cascades to regulate cell processes.(82) Similarly, the intracellular proteins can change the shape of integrins that affect their binding to specific BM proteins, thus are involved in inside-out signalling of cells.(82) Integrins involved with collagens are $\alpha_1\beta_1$ and $\alpha_2\beta_1$, which down-regulate the production of collagens through negative feedback and enhance the production of collagens, respectively.(42) Laminin 332 predominantly binds to integrin $\alpha_6\beta_4$, whereas laminin 511 is a ligand for integrin $\alpha_3\beta_1$.(87) Integrin $\alpha_5\beta_1$ is the main cellular receptor for fibronectin.(42) Other non-integrin receptors include proteoglycans, such as syndecans and CD44.(48) Both contain GAG side chains that bind to a variety of BM proteins to modulate intracellular signalling pathways.

Hemidesmosomes connect epithelial cells to their BM and the underlying stroma (figure 1.17).(101) Integrin $\alpha_6\beta_4$ and type XVII collagen on the basal aspect of epithelial cells interact with laminin 332 that connect cells and the BM, which in turn is connected to the stroma by type VII collagen anchoring fibrils.(101, 102) The β_4 subunit interacts with intracellular keratin by associating with type XVII collagen (bullous pemphigoid antigen 180), bullous pemphigoid antigen 230 and plectin.(102) Calcium is required for the formation of hemidesmosomes.(6) Focal adhesions mediate interactions between cells and BM proteins via integrins $\alpha_2\beta_1$, $\alpha_3\beta_1$ and $\alpha_5\beta_1$ (figure 1.17).(102) These connect BM proteins to the actin cytoskeleton via a combination of intracellular proteins, actinin, paxillin, vinculin and talin. Focal adhesions include signalling proteins, such as focal adhesion kinase, and are therefore involved in outside-in and inside-out signalling.(102) When BM proteins bind to integrins, the shape of the integrin changes and the cytoplasmic domain binds to focal adhesion complex proteins.(82) This causes the integrins to cluster, modulate activities of focal adhesion kinases and formation of focal adhesion complexes by organising the actin cytoskeleton.(82, 87) The cell-BM interactions via focal adhesion

complexes lead to changes in cell shape as well as modulation of intracellular signalling pathways by phosphorylation of proteins.(48) In general, hemidesmosomes mediate interactions between the BM and the keratin cytoskeleton, whereas the focal adhesions mediate interactions between the BM and the actin cytoskeleton.(102) However, hemidesmosomes are also thought to interact with the actin cytoskeleton, which is important for cell migration.(103) Abnormal or loss of hemidesmosomes or focal adhesions can lead to blistering diseases, where the epithelial cell layer detaches from the underlying stroma.(102)

1.4.5 MECHANICAL PROPERTIES OF BASEMENT MEMBRANES

As well as the chemical cues from BM proteins, their physical properties, such as rigidity, porosity and topography, also regulate cell processes.(82) These physical properties are sensed by integrins that activate specific intracellular signals, thereby modulating cellular processes. Focal adhesion complexes are formed by cells when cultured on stiff substrates, whereas dynamic adhesion complexes are observed on softer substrates.(42) Additionally, migrating cells also form dynamic adhesion complexes and once completed these complexes disassemble to form more stable focal adhesion complexes.(42) These focal adhesion complexes transmit signals from the BM to cells regarding the mechanical properties of the substrate. The cells respond by altering the ECM protein production, the cytoskeletal structure and re-organising the forces the cells exert on the outside environment. The specific assembly of proteins of the BM that account for the side-specific variations in their protein composition give rise to variations in their biomechanical properties.(79) Studies on human BMs show that the laminin-rich epithelial side of BMs are approximately twice as stiff as the collagenous stromal side. Cell adhesion experiments showed that the cells adhered more strongly and faster when cultured on the epithelial side in contrast to the stromal side. Epithelial cells are biomechanically weak and require a strong substrate for support. Rigidity of matrices also affect the differentiation of SCs, for example, mesenchymal SCs take an osteogenic path and a neurogenic path when cultured on stiff and soft matrices, respectively.(82) Changes in the composition and structure of BMs observed with advancing age also alter their biomechanical properties.(79) BM of many tissues deteriorate due to reduced amount of proteins formed by the cells and increased MMP activity that lead to breakdown of proteins.(42) These studies have shown reduced amount of collagen synthesis and an increase to the cross linking of this protein with ageing giving rise to undesirable mechanical properties of the BM.(42, 79)

Interactions between cell receptors and basement membrane proteins

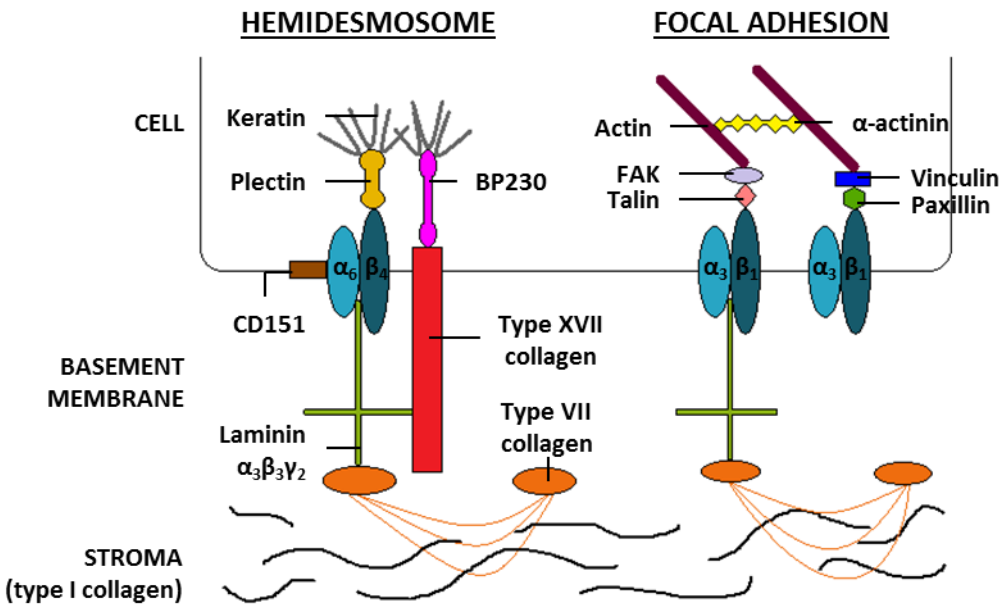

Figure 1.17: Interactions between cell receptors and basement membrane proteins. Hemidesmosomes and focal adhesion complexes form interactions between cells and the underlying basement membrane as well as the stroma; BP 230 - bullous pemphigoid antigen 230 and FAK – focal adhesion kinase.

1.4.6 BASEMENT MEMBRANE OF THE CONJUNCTIVA

Numerous studies have been done over the years to investigate the BM components of the OS, including the conjunctiva (table 1.3). All these are immunohistochemical studies looking at the distribution of the structural protein components. Type IV collagen is found throughout the OS with variations in the distribution of its isomers.(11) The chains α_1 and α_2 were present within limbal and conjunctival BMs, whereas the α_3 chain was present in the corneal BM with weaker staining in the limbal BM.(11) Type IV collagen chains α_5 and α_6 chains were found throughout the OS, however, the intensity was reduced in the conjunctiva compared to the rest of the OS.(11) The α_4 chain was absent within the BMs of the OS.(11) Other collagens found throughout the OS were type VII, XV, XVII and XVIII collagens.(11) A study by Maatta et al. however showed the absence of type XV collagen in the BM of normal corneas.(104) Type V collagen was found only in the corneal BM, whereas type XVI collagen staining was observed as a sub-epithelial band in association with the BM in the corneo-limbal transition zone.(11)

Laminin α_3, β_3 and γ_2 chains that make up laminin 332 were found in uniform distribution throughout the OS.(11) A study by Messmer et al. however showed staining for the β_3 chain in only 7% and γ_2 chain in 34% of the normal conjunctival samples.(85) Chains α_5, β_2 and γ_1 were found in the limbal and conjunctival BM and generally absent within the corneal BM.(11) Laminin chains α_1, α_2 and β_1 predominantly stained the limbal BM and the γ_3 chain was exclusively found within the BM of the limbus.(11) The absence of the α_2 and β_2 chains within the cornea was also shown by Ljubimov et al.(105) Whereas Schlotzer-Schrehardt et al. did not observe staining for α_1 chain in the conjunctiva, two other studies reported the presence of this chain in the conjunctival BM.(11, 85, 101) The differential distribution of isomers between studies, especially those of laminins, may be due to differences in the sites of tissue harvesting and specificity of antibodies used.(85) Laminin α_4 chain was absent throughout the OS.(11)

Other GPs found throughout the OS were nidogen (isomers 1 and 2), fibronectin and matrillins 2 and 4.(11) The staining for fibronectin was thicker and stronger in the BMs of the limbus and conjunctiva than compared to the corneal BM.(11, 83) Thrombospondin 4 was also present in patchy distribution throughout the OS, with intensity of staining increasing towards the conjunctiva.(11) The limbus specific GPs include SPARC and tenascin C, with some focal staining of the latter protein in the conjunctiva.(11) The corneo-limbal transition zone consisted of fibulin 2 (a calcium binding protein associated with BMs and

extracellular elastic fibres) and vitronectin, the latter however was mainly found as a sub-epithelial band in association with the BM.(11) The cornea specific components are fibrillins 1 and 2 (a component of elastic microfibrils) and thrombospondin 1.(11) A study involving corneal and conjunctival cell lines showed significantly higher production of thrombospondin 1 in the cornea, which was forty times higher than that in the conjunctiva.(106) The presence of thrombospondin 1, an anti-angiogenic protein, may contribute to the maintenance of the avascular cornea. Another study by Sekiyama et al. showed little or no expression of thrombospondin 1 mRNA and protein in the conjunctiva compared to the BM of the cornea and limbus, where high expression was particularly observed in the basal cells.(107) Perlecan was found throughout the OS, whereas agrin was predominantly found in the limbal BM compared to the rest of the OS.(11)

Basement membrane proteins of the ocular surface tissues

ECM component		Cornea	Limbus	Conjunctiva
Collagens	Type IV α_1	X	O	O
	Type IV α_2	X	O	O
	Type IV α_3	O	O/X	X
	Type IV α_5	O	O	O
	Type IV α_6	O	O	O
	Type V	O	X	X
	Type VII	O	O	O
	Type XV	O/X	O	O
	Type XVII	O	O	O
	Type XVIII	O	O	O
Glycoproteins	Laminin α_1	O/X	O	O/X
	Laminin α_2	X	O	O
	Laminin α_3	O	O	O
	Laminin α_5	O/X	O	O
	Laminin β_1	O/X	O	O
	Laminin B_2	X	O	O
	Laminin β_3	O	O	O
	Laminin γ_1	O/X	O	O
	Laminin γ_2	O	O	O
	Laminin γ_3	X	O	X/focal
	Nidogen 1+2	O	O	O
	Fibronectin	O	O	O
	Vitronectin	X/weak	Sub-BM	X
	Fibulin 2	X/O	O	X
	Fibrillin 1	O	X	X
	Fibrillin 2	O	O/X	X
	SPARC	X	O	X
	Tenascin C	X	O	X/focal
	Matrillin 2+4	O	O	O
	Thrombospondin 1	O	X	X
	Thrombospondin 4	X/Focal	Focal	Focal
Proteoglycans	Perlecan	O	O	O
	Agrin	X/weak	O	O/Weak

Table 1.3: Basement membrane proteins of the ocular surface tissues as summarised by integrating the literature to date; O – present and X – absent.

1.4.7 EXTRACELLULAR MATRIX AS A SUBSTRATE FOR CELL AND TISSUE TRANSPLANTATION

The dynamic composition of the ECM and its architecture regulate the growth and differentiation of cells by providing specific biological and physical cues.(42, 47) Gaining knowledge about the composition and structure of the ECM, as well as the functions of the various components of the ECM will benefit in investigating methods by which the ECM can be used in TE applications, in particular as substrates for cell and tissue transplantation.(42) Advantages of using ECM or ECM-mimicking substrates for TE are retained anatomical structure, reduced immunological response due to lack of cellular components, and retained ECM composition and architecture providing similar biological and physical cues to that *in vivo*.(72) There are various types of ECM-related substrates studied to date, namely, decellularised ECMs from cultured cells, tissues or organs, substrates with pre-adsorbed individual or a combination of ECM proteins, and substrates with attached functional peptides of ECM proteins. These methods are especially useful when studying synthetic substrates for TE, which lack tissue-specific biological niches that guide cellular functions.

ECM scaffolds may be obtained by decellularisation of cultured cells or cadaveric tissues or organs.(47) The goal of decellularisation is to remove all the cellular components and therefore all antigenic molecules, without altering the composition, the biological functions or the mechanical integrity of the remaining ECM to produce a physiologically active scaffold.(72) Decellularisation may be done using physical (agitation, sonication or freeze-thaw cycles), chemical (acid, alkali, detergents or hypo/hyper-tonic solutions) or enzymatic (proteases) methods.(47) Each method disrupts the ultrastructure of the ECM to variable extents, thus an optimal method or a combination of methods are used for each type of cultured cells, tissue or organ. The ECMs of various organs have been studied for the purposes of TE, for example that of the skin, bone, bladder, small intestine submucosa, heart and lungs.(47) Of these, Alloderm (acellular skin matrix) and CryoValve SG Pulmonary Valve (acellular human cardiac valve) are Food and Drug Administration-approved ECM-based products used clinically for therapeutic use.(47, 71)

Wen et al. transplanted allogenic acellular conjunctival ECM grafts onto iatrogenic conjunctival defects in rabbits, who observed a stratified conjunctival epithelium with evidence of GCs four weeks post-operatively.(108) In contrast, they observed a T cell mediated immune reaction in the group that was transplanted with allogenic conjunctival grafts containing cells. Zhao et al. studied porcine acellular conjunctival ECM as a substrate

for *ex vivo* expansion of rabbit limbal epithelial cells, as an alternative to the denuded AM.(56) They showed that both substrates had similar transparency, however, the conjunctival ECM was thicker (53μm vs 35μm) and had a higher tensile strength compared to denuded AM. Moreover, they showed that the denuded AM completely degraded within one hour of collagenase treatment *in vitro* and between one and two weeks *in vivo*. In comparison, conjunctival ECM was unchanged following collagenase treatment for one hour *in vitro* and degraded between three and four weeks *in vivo*. The conjunctival ECMs with cultured rabbit limbal epithelial cells were used to reconstruct rabbit LSCD models. Clinically, the eyes that were transplanted with conjunctival ECM with cultured epithelial cells showed the best outcome with no corneal haze or evidence of neovascularisation, whereas minimal corneal haze and limbal neovascularisation were observed in those transplanted with denuded AM containing cultured cells. Interestingly, there was moderate corneal haze and evidence of peripheral corneal neovascularisation involving 50% of the cornea or more in eyes that were treated with acellular conjunctival ECM without cultured epithelial cells. This may be due to the presence of angiogenic factors in the ECM of conjunctiva and the presence of limbal epithelial cells may remodel the ECM scaffold to one that is more suitable for growth and differentiation of corneal epithelial cells. Rabbits grafted with conjunctival ECM containing cultured limbal epithelial cells showed complete re-epithelialisation by day thirty with evidence of epithelial stratification, expression of corneal keratins and the absence of GCs. ECM obtained from decellularised tissues and organs have limitations: scarcity of donor tissue, variations of ECM composition and architecture between donors and different developmental stages, and immunological reactions and potential pathogen transfer if allogenic or xenogenic ECM scaffolds are used.(47, 109)

ECM produced by autologous cells would be a useful alternative to acellular autologous tissues and organs as they can be cultured *in vitro* and maintained under sterile conditions.(109) Autologous cells can be expanded from a small tissue biopsy and will prevent undesired immunological reactions once transplanted.(109) Isolation and use of cell-secreted ECM has been reported since the 1970s.(47) Cultured cell-secreted ECMs will have a similar protein composition to that *in vivo*, however, there may be alterations to its architecture.(47) ECM of tissues may be used to culture cells of a different tissue but this is not always successful due to tissue specific composition and architecture of the ECMs.(47) The ECM derived from native tissue has been shown to induce optimal cellular growth and function.(47)

Substrates pre-adsorbed with ECM proteins have been used to culture conjunctival epithelial cells, type I collagen being the most common, others being laminin, fibronectin, matrigel and gelatin-chitosan.(70) Type I collagen, the most abundant protein in stromal tissue, has been used to form hydrogels.(8) Zhou et al. studied vitrified type I collagen gels, where controlled evaporation of water produced gels with randomly aligned dense network of collagen fibrils.(8) They showed that these substrates supported the growth of rabbit conjunctival epithelial cells and GCs *in vitro* and *in vivo*. These gels have been shown to have suitable physical and mechanical properties for transplantation and also prevent scar formation and wound contracture.(8, 26) Zhu et al. showed that rabbit conjunctival epithelial cells cultured on membranes made up of gelatin (processed type I collagen) and chitosan (a GAG) exhibited similar morphology to those grown on tissue culture polystyrene and expressed the conjunctival differentiation marker keratin 4.(110) Fibronectin with or without type I collagen has been shown to support growth of conjunctival epithelial cells as monolayers, however, without GCs.(70) Matrigel, a mixture of laminin, type IV collagen, HSPG and GFs derived from the mouse EHS sarcoma, has been shown to promote aggregates of conjunctival epithelial cells with some evidence of GCs.(70)

ECM-mimicking substrates can be developed by attaching functional peptides of ECM proteins, which may be cell adhesive, sensitive to degradation enzymes or those that bind to GFs.(49) There are well-established small functional peptides of larger ECM proteins identified as motifs that guide specific cell functions.(43) The RGD sequence initially described on fibronectin is a well-known cell-binding domain. To date, other ECM proteins, such as laminin, thrombospondin and tenascin are known to contain this motif that binds to twelve types of integrins. It has been shown that cell adhesion on substrates can be enhanced by coating them with this peptide, however, when added as a solution into a cell culture system, inhibit cell adhesion by blocking the integrins. Laminin α_1 and β_1 chains contain peptide sequences IKVAV and YIGSR, respectively, which have roles in promoting endothelial cell adhesion and neuronal cell migration. Other functional peptides on ECM proteins are KQAGDV and REDV on fibronectin, DGEA and GFOGER on collagens, and VAPG on elastin.(49) These small ECM peptide sequences are easier to incorporate into scaffolds than the large ECM proteins, easy to produce in large scale and provide further consistency between substrates.(43, 49) In addition, these peptides are relatively more stable than the larger proteins, which may be subjected to denaturation and degradation *in vivo*.(49) However, the assumption when employing these small peptides are that they retain the biological functional specificity when isolated from the native protein.(49)

1.5 POLY-EPSILON-LYSINE HYDROGELS

Hydrogels are three-dimensional structures made of hydrophilic polymers that are either physically or chemically cross-linked.(49) These polymer gels are insoluble, however, swell in the presence of water.(49) They have good biocompatibility, are able to entrap and release biologically active molecules, and have high permeability to oxygen, nutrients and other water-soluble molecules.(49) The latter property is advantageous in TE involving the OS, especially the avascular cornea, where the epithelium depends on diffusion of oxygen from the environment. There are numerous methods of classifying hydrogels: their structure (crystalline or non-crystalline), constituents (homopolymer or co-polymer), origin of the constituents (natural, synthetic or hybrid), ionic charge (cationic, neutral or anionic) or type of cross-linking (chemical or physical).(49) The type and the degree of cross-linking determines the physical properties of the hydrogels, such as swelling properties and the elastic modulus.(49) As previously mentioned, synthetic substrates may be considered superior to biological substrates due to the ability to synthesise them with reproducible and constant composition and varying mechanical properties, which are important for TE. Synthetic polymers may be non-biodegradable or biodegradable.(49) Non-biodegradable polymers (poly(ethylene glycol) and poly(vinyl alcohol) based) need to maintain their physical and mechanical properties, where an optimal degree of cross-linking needs to be attained to ensure balance between strength and flexibility of the product.(49) Biodegradable polymers are mostly polyesters (poly(lactic acid), poly(glycolic acid) and poly(caprolactone) based) and polypeptides.(49) An optimal hydrogel for TE should model the biological and the physical properties of the ECM of the native tissue. Surface modification of synthetic polymers by attaching ECM-derived peptides is becoming increasingly popular as a method for manufacturing bioactive substrates for TE.

Poly-epsilon-lysine (PεK) is a homopolymer made up of ι-lysine amino acids that are linked by peptide bonds between their ε-amino and the α-carboxyl groups.(111) It is a naturally occurring, biodegradable and non-toxic polymer to humans and to the environment that is approved by the Food and Drug Administration as a food preservative.(111, 112) Industrially, PεK is produced by aerobic fermentation of bacteria, *Streptomyces albulus*, which produces residues that are 25-35 amino acids long.(111, 113) It is known to be stable in acidic and alkaline conditions, and at high temperatures, including at autoclaving temperatures of 120°C.(113) The homopolymer carries positive charges on their amino groups that are able to bind to biomolecules, including negatively charged cell surfaces of microbes by electrostatic adsorption.(111, 113) This antimicrobial property allows its use as

a food preservative and as a disinfectant.(111) Other uses of PεK are as an emulsifying agent and as a drug delivery carrier.(111)

SpheriTech Limited Company has developed a PεK-based hydrogel that could be employed as a substrate for TE of the OS. The homopolymer of PεK is chemically cross-linked with dicarboxylic acids that are also naturally-occurring products produced from oxidation of longer chain fatty acids in animals and plants.(112) These hydrogels are transparent with a high water content allowing adequate diffusion of oxygen. Moreover, these peptide-based hydrogels are able to form bonds with biomolecules, thus allowing surface chemistry to be altered to suit requirements. Physical properties, such as tensile strength and transparency, of these hydrogels can be altered by changing the density of PεK, cross-linking density and the type of dicarboxylic acid used for cross-linking.(112) Gallagher et al. carried out cytotoxicity studies on a corneal cell line over eight days that showed cytocompatibility of these hydrogels.(112) The advantageous properties of PεK hydrogels make them a potential substrate for use in TE of the OS, in particular in developing a conjunctival tissue substitute (figure 1.18).

Properties of poly-epsilon-lysine hydrogels

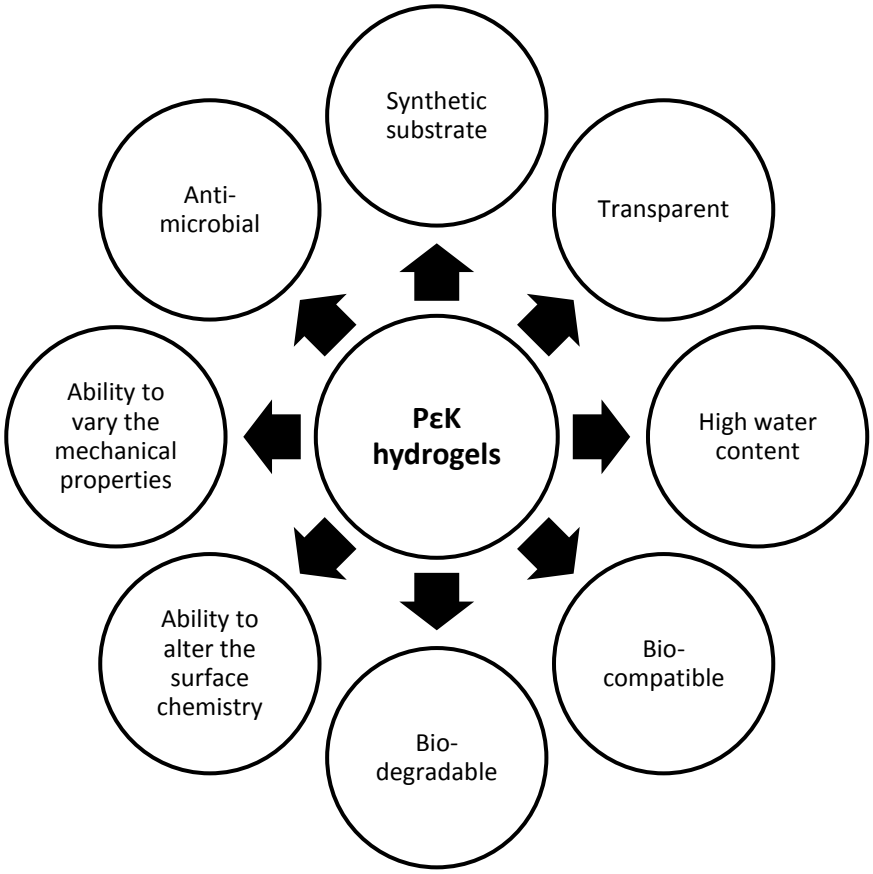

Figure 1.18: Properties of poly-epsilon-lysine hydrogels that are advantageous in tissue engineering of the conjunctiva.

1.6 HUMAN CONJUNCTIVAL EPITHELIAL CELL LINE (HCjE-Gi cells)

The immortalised Human Conjunctival Epithelial cell line – Gipson laboratory 2003 (HCjE-Gi cells) is a conjunctival epithelial cell line that consists of epithelial cells as well as GCs. Gipson et al. immortalised conjunctival epithelial cells derived from the supero-temporal bulbar conjunctival tissue from patients undergoing phacoemulsification surgery.(114) They first transduced cells with specific proteins that inactivated the cell cycle pathway by altering the functions of p16 and p53 proteins, thus allowing cells to bypass senescence. Then the cells were transduced to express human telomerase reverse transcriptase (hTERT), the catalytic subunit of telomerase. This allowed the cells to retain their telomeres and divide indefinitely (figure 1.19). In somatic cells, cell division results in telomere shortening and eventual senescence.(115) Telomeres are repetitive nucleotide sequences of DNA located at the ends of chromosomes that act as protective structures. Telomerase prevents telomere shortening by adding nucleotide sequences to telomeres by reverse transcribing the RNA template and compensating for the loss of telomeres with normal cell division. Expression of exogenous hTERT induces telomerase activity in the cells. Immortalisation of epithelial cells by preventing telomere shortening has been shown to give rise to indefinite replication ability without the loss of differentiation potential of cells.(114) This is in contrast to immortalisation with viral oncogenes, such as that of the Simian vacuolating virus 40, which disrupts differentiation pathways of cells. However, the alterations of the normal functioning of p16 and p53 proteins may affect the progress of differentiation. Toouli et al. showed that immortalisation of human mammary epithelial cells by hTERT expression resulted in fewer karyotypic and phenotypic alterations than did when immortalised by expression of Simian vacuolating virus 40 genes, however, it required the prior loss of $p16^{INK4a}$ expression.(115)

Primary cells have a finite proliferative capacity in culture *in vitro* and become senescent, thus are a limited resource.(115) This is overcome by using immortalised cell lines, which in theory gives rise to an unlimited number of divisions. However, a limitation of immortalised cell lines is the unknown extent to which the cells lose the differentiated characteristics of the native cells.(115) This raises concerns over the applicability of results observed *in vitro* to that observed *in vivo*. Although this is overcome by using primary cells in studies, they come with their own limitations. In addition to the limited proliferative potential, there is inter-donor variability with primary tissue giving rise to inconsistent results, whereas cell lines allow reproducibility of the observed results. There is limited availability of donor

tissue to obtain primary cells from and extensive optimisation experiments are required prior to employing them in studies.

OS epithelial cells share similar characteristics to other epidermal systems such as the skin. They are stratified epithelial cells in which the basal cells have features of low differentiation and high proliferative capacity, express tissue-specific keratins and contain populations of SCs for rapid renewal of epithelial cells.(25) They differ from epithelia of the skin by the lack of a cornified layer on the apical aspect of the superficial cells that is present in the skin. Under physiologic conditions, the epithelia of the OS have an abundance of tear retinoids that prevent the formation of a cornified layer that would affect the normal functioning of these cells.(25) Keratins (40-70kDa) are a group of intermediate filaments that contribute to the cytoskeleton of epithelial cells.(10, 22) Keratins 1 to 8 belong to the acidic group of keratins (genes expressed on chromosome 21), whereas keratins 9 to 20 (genes located on chromosome 17, except that for keratin 18 found on chromosome 21) belong to the neutral or basic group of keratins.(10) The epithelial cells produce more than one type of keratin that co-polymerise to form the keratin filament system.(21) The keratins are expressed in a tissue-specific manner, thus are used to characterise the phenotype of cells and are used as differentiation markers.(10, 21) In the epidermal keratinocytes, expression of keratins change from keratins 5 and 14 expressed by immature cells to keratins 1 and 10 expressed by mature cells.(22) Similarly, immature epithelial cells of the OS express keratins 5 and 14. When the corneal epithelial cells differentiate they are known to express the keratin pair 3 and 12, whereas the conjunctival epithelial cells express the keratin pair 4 and 13.(22)

Keratins 4 and 19 are differentiation markers of HCjE-Gi cells as suggested by the manufacturers of the cell line.(116) Keratin 4 is a marker of non-keratinised stratified epithelial cells, whereas keratin 19 is a marker of simple epithelial cells.(117) Gipson et al. showed that the HCjE-Gi cells expressed keratin 19 similar to that expressed by the native conjunctival tissue.(114) Ramirez-Miranda et al. showed that keratin 19 is expressed by the epithelial cells of the entire OS, the intensity reducing towards the central cornea, whereas keratin 13 is expressed by the suprabasal cells of the posterior limbus and by all the layers of the conjunctival epithelium.(118) They further showed that expression of keratins 12 and 13 are mutually exclusive suggesting that keratin 13 may be a more specific marker of conjunctival epithelial cells than keratin 19.

Gipson et al. reported that the HCjE-Gi cells do not undergo stratification to the same degree *in vitro* as that observed in the native conjunctival tissue.(114) Studies have shown that the expression of keratin 4 coincided with the deposition of α_2 and β_2 laminin chains, thus have been shown to be important for the differentiation of conjunctival epithelial cells.(119, 120) The conjunctival cell line HC0597 (virally transformed) has been used in previous studies since they express keratin 4 and deposit laminin 211 in culture, thus modelling the *in vivo* conjunctival cells.(120) Moreover, the expression of keratin 4 has shown to be rescued by culturing conjunctival cells on exogenous placental laminins that contain the β_2 chain of laminin.(119) However, the presence of GCs in this cell line has not been shown.

Gipson et al. also showed that the HCjE-Gi cell line expressed mucins that are expressed by the native conjunctival tissue, although the mRNA expression of these mucins was lower in the cell line.(114) They showed that only a very small number of HCjE-Gi cells differentiated into GCs expressing the GC protein, MUC5AC, after seven days in culture in the differentiation and stratification medium. The authors suggested that this could be due to three reasons: the immortalisation technique altered the GC differentiation pathway, only few SCs were present in the primary cultures that were available to be transduced with hTERT and these cells gave rise to the small population of GCs, or the culture niche is different to that of the native tissue that is required for GC differentiation.(114) To date and to our knowledge, this is the only conjunctival epithelial cell line that has been shown to differentiate into GCs.

Cell immortalisation by hTERT expression and maintenance of telomere lengths

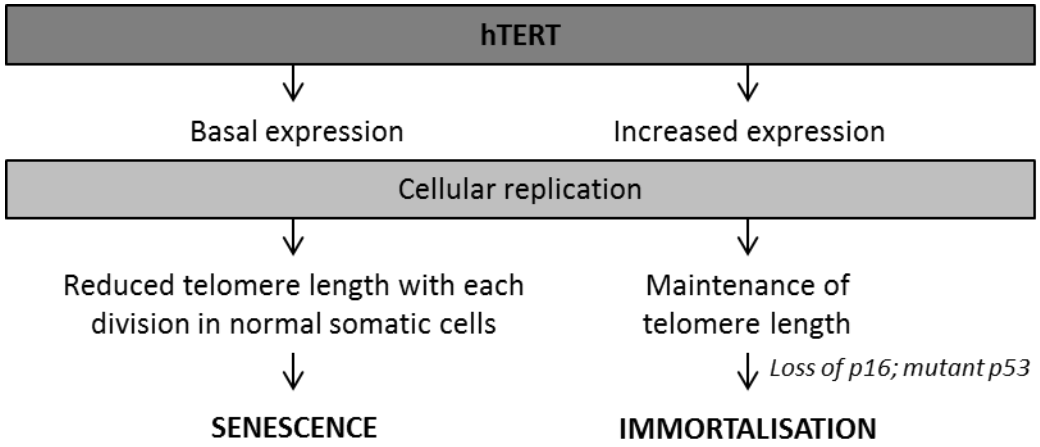

Figure 1.19: Cell immortalisation by hTERT expression and maintenance of telomere lengths. **(Adapted from http://jeb.biologists.org/content/218/1/59)**

1.7 HYPOTHESIS, AIMS AND OBJECTIVES

Hypothesis

The surface modification of PεK hydrogels with ECM proteins of the native tissue enables the growth and differentiation of conjunctival epithelial cells.

Aims and objectives

Aim 1: To establish the role of ECM proteins on the cellular functions of HCjE-Gi cells.

Objective 1: To identify and quantify the protein composition of the ECM secreted by HCjE-Gi cells over a culture period of six weeks.

Objective 2: To determine the adhesion and growth of HCjE-Gi cells cultured on pre-adsorbed proteins modelling the natural ECM composition over a culture period of seven days.

Objective 3: To determine the stem cell and goblet cell expression by HCjE-Gi cells cultured on pre-adsorbed proteins modelling the natural ECM composition over a culture period of fourteen days.

Aim 2: To establish the cellular response of HCjE-Gi cells cultured on surface modified PεK hydrogels.

Objective 1: To determine the adhesion of HCjE-Gi cells on PεK hydrogels with and without pre-adsorbed proteins.

Objective 2: To determine the growth and differentiation of HCjE-Gi cells on PεK hydrogels with and without pre-adsorbed proteins over a culture period of fourteen days.

2 THE ROLE OF EXTRACELLULAR MATRIX PROTEINS ON CELLULAR FUNCTIONS OF HCjE-Gi CELLS

2.1 AIMS AND OBJECTIVES

To establish the role of ECM proteins on the cellular functions of HCjE-Gi cells.

1. To identify and quantify the protein composition of the ECM secreted by HCjE-Gi cells over a culture period of six weeks.

2. To determine the adhesion and growth of HCjE-Gi cells cultured on pre-adsorbed proteins modelling the natural ECM composition over a culture period of seven days.

3. To determine the stem cell and goblet cell expression by HCjE-Gi cells cultured on pre-adsorbed proteins modelling the natural ECM composition over a culture period of fourteen days.

2.2 METHODS

2.2.1 HCjE-Gi CELL LINE

2.2.1.1 CELL CULTURE MEDIA

Culture and maintenance of the immortalised Human Conjunctival Epithelial cell line – Gipson laboratory 2003 (HCjE-Gi cells) involved several different media for culturing, sub-culturing, differentiation and stratification and cryopreservation.(116)

2.2.1.2 CELL CULTURE AND SUB-CULTURE

The immortalised HCjE-Gi cells was cultured in keratinocyte serum-free (KSF) media (table 2.1) in a humidifying incubator set at 37°C with 5% carbon dioxide (CO_2). The cells were maintained in 75cm^2 flasks (*Greiner 658175*) and fresh media was supplied three times a week.

Once the cell cultures were approximately 75% confluent in a flask, the KSF media was removed and 6mL of 1X Trypsin-Ethylenediaminetetraacetic acid (EDTA) solution (*Sigma T4174*; 2mL of stock mixed with 18mL sterile phosphate buffered saline) was added. The cells were incubated at 37°C for approximately ten to fifteen minutes until the cells rounded and detached spontaneously from the flask. Next, 6mL of neutralisation media (table 2.2) was mixed with the Trypsin-EDTA solution to stop the protein digestion. The solution was transferred into two 15mL tubes (*Greiner bio-one 188271*) in equal volumes and was centrifuged (*Thermo Scientific Heraeus Multifuge X1*) at 112 *x g* for five minutes. The supernatant in each tube was removed and the cell pellet was re-suspended in 1mL of KSF media. The cell suspension was mixed thoroughly prior to counting with a haemocytometer (*Fisher Scientific 12634546*). The cells were seeded in culture vessels at appropriate cell densities and volumes of KSF media, as required for subsequent experiments. All cell culture experiments were carried out inside a class II biosafety cabinet that was appropriately disinfected following the local guidelines.

2.2.1.3 DIFFERENTIATION AND STRATIFICATION

When required, the culture medium was switched to the differentiation and stratification medium (table 2.3) to induce differentiation and stratification of HCjE-Gi cells. This was done on culture day seven, when the cell layer was approximately 70-80% confluent.

2.2.1.4 CRYOPRESERVING AND THAWING FROZEN CELLS

The cells were sub-cultured as described above to obtain $2x10^6$ cell suspension in 1mL KSF media. An equal volume of 2X freezing media (table 2.4) at room temperature (RT) was added. The cell suspension was mixed and divided into two cryogenic vials (*Star Lab E3110-6122*) with $1x10^6$ cells per cryogenic vial. The cells were slow frozen initially in a Mr Frosty™ Cryo 1°C freezing container (*Thermo Scientific 5100-0001*) containing isopropanol (*Sigma I9516*), which was stored in a -80°C freezer (approximately 1-3°C/minute cooling rate) overnight. Then the cryogenic vials containing the cells were transferred into liquid nitrogen for storage. The dimethyl sulfoxide in the freezing media is a cryoprotective agent that reduces the freezing point and prevent rapid cooling of the media.(121) This reduces the risk of ice crystal formation that can lead to cell death.(121)

To thaw frozen cells, the cryogenic vial was immersed in a water bath set at 37°C for one to two minutes. The cell suspension was transferred into a 15mL tube, 7mL of neutralisation media was added slowly and the solution was mixed thoroughly. The cells were centrifuged at 1370 *x g* for four minutes and re-suspended in 1mL of KSF media. Next, the cell suspension was transferred into $75cm^2$ flasks (approximately $5x10^5$ cells per flask) with 8mL of KSF media, which were maintained inside a humidifying incubator (37°C, 5% CO_2). Fresh media was added the following day and then three times a week thereafter.

Components of the keratinocyte serum-free media

CELL CULTURE MEDIUM	SOURCE	VOLUME
1. Keratinocyte serum-free media 1X (include L-Glutamine)	*Life Technologies 37010-022*	500mL
2. Bovine pituitary extract (12.6mg/mL) Final concentration of 25µg/mL	*Supplied with the media bottle*	1.1mL
3. Human recombinant epidermal growth factor 1-53 (0.0395835µg/µL) Final concentration of 0.2ng/mL	*Supplied with the media bottle*	3µL
4. Calcium chloride (1M) Final concentration 0.4mM	*Sigma C4901*	200µL
5. Penicillin-Streptomycin (100X) Final concentration 1X	*Sigma P0781*	5.1mL
The media bottle was protected from light and stored at 4°C for approximately one month.		

Table 2.1: Components of the keratinocyte serum-free media used for culture of HCjE-Gi cells.

Components of the neutralisation media

NEUTRALISATION MEDIUM	SOURCE	VOLUME
1. Dulbecco's Modified Eagle's Medium/Nutrient Mixture F-12 Ham media (1:1 mix) with L-Glutamine, 15mM HEPES and sodium bicarbonate	*Sigma D8437*	500mL
2. Fetal bovine serum Final concentration 10%	*Biosera FB-1090*	55mL
3. Penicillin-Streptomycin (100X) Final concentration 1X	*Sigma P0781*	5.5mL

Table 2.2: Components of the neutralisation media used for sub-culture of HCjE-Gi cells.

Components of the differentiation and stratification media

DIFFERENTIATION AND STRATIFICATION MEDIUM	SOURCE	VOLUME
1. Dulbecco's Modified Eagle's Medium/Nutrient Mixture F-12 Ham media (1:1 mix) with L-Glutamine, 15mM HEPES and sodium bicarbonate	*Sigma D8437*	500mL
2. Fetal bovine serum Final concentration 10%	*Biosera FB-1090*	55mL
3. Penicillin-Streptomycin (100X) Final concentration 1X	*Sigma P0781*	5.5mL
4. Human recombinant epidermal growth factor 1-53 (0.0395835µg/µL) Final concentration of 10ng/mL	*Supplied with the KSF media (Life Technologies 37010-022)*	149µL
5. Calcium chloride (1M) Final concentration 1mM	*Sigma C4901*	500µL

Table 2.3: Components of the differentiation and stratification media.

Components of the freezing media

2X FREEZING MEDIUM	SOURCE	VOLUME
1. Dulbecco's Modified Eagle's Medium/Nutrient Mixture F-12 Ham media (1:1 mix) with L-Glutamine, 15mM HEPES and sodium bicarbonate	*Sigma D8437*	500mL
2. Dimethyl sulfoxide Hybri-Max Final concentration 20%	*Sigma D2650*	100mL
3. Fetal bovine serum Final concentration 20%	*Biosera FB-1090*	100mL
The solution was mixed and incubated at room temperature for two hours (or at 4°C overnight). The solution was filter sterilised, divided into plastic tubes and placed in -80°C to freeze-solid. The aliquots were stored in -20°C.		

Table 2.4: Components of the freezing media used for cryopreserving HCjE-Gi cells.

2.2.1.5 CHARACTERISTICS OF THE HCjE-Gi CELL LINE

The HCjE-Gi cells were cultured in ninety-six well plates (*Greiner bio-one 655180*) to determine their growth curve. The cells maintained in KSF media were cultured with initial seeding densities of $5x10^3$, $1x10^4$ and $1x10^5$ cells/cm^2. On culture days one, three, five and seven, the media was removed and the cells were washed three times with phosphate buffered saline (PBS) (*Thermo Scientific Oxoid BR0014G*; 1 tablet per 100mL distilled water (dH_2O)). The cells were then fixed with 100% ice cold methanol (*Fisher Scientific 11976961*) for two minutes and air dried. Methanol acts as a fixative as well as a permeabilising agent.(122) It dehydrates the cells, precipitates soluble proteins and solubilises cytoplasmic and transmembrane lipids. The cell nuclei were stained with 4',6-Diamidino-2-Phenylindole, Dilactate (DAPI) (*Life Technologies D3571*; 5mg/mL), diluted 1:30 000 in PBS, for five minutes at RT. DAPI binds to adenine-thymine nucleic acids in the minor groove of double stranded DNA to give rise to blue fluorescence. Images were taken with a 10X objective from five fixed positions within each well using a Nikon Eclipse Ti-E microscope (*Japan*). The number of nuclei per view (0.011cm^2) was determined using the Image-based Tool for Counting Nuclei plugin on Image J software (figure 2.1). The raw image was first converted into an inverted eight-bit image. An estimation of the width of cells and the minimum distance between the cells were entered into the plugin (20 and 10 pixels, respectively for images taken using a 10X objective). A threshold of 0.1 was entered and the plugin was set to detect dark peaks on the image. The mean number of nuclei per view was calculated to determine the number of cells per cm^2 in each well at each culture time point. The experiments were carried out in three sets of triplicates.

To determine the cell morphology, the cells were stained for the cytoskeletal microfilament, filamentous actin. The cells were seeded in ninety-six well plates at an initial seeding density of $1x10^4$ cells/cm^2 and were maintained KSF media. On culture days one and seven, the cells were washed three times in PBS and fixed with 10% neutral buffered formalin (NBF) (*Sigma HT501128*) for ten minutes at RT. NBF cross-links proteins to preserve the *in vivo* architecture of the cellular constituents.(122) Methanol is not suitable as a fixative agent in this case as it breaks down hydrogen bonds thereby destroying the tertiary structure of proteins.(122) The fixed cells were washed three times in PBS and permeabilised with 0.2% Triton X-100 (*Sigma-Aldrich T9284*) for fifteen minutes at RT. Permeabilisation with a non-ionic detergent solubilises lipids and disrupts the cell membranes allowing large molecules such as antibodies to enter the cell.(122) The cells were again washed three times in PBS and were stained with Alexa Fluor 488 Phalloidin

(*Life Technologies A12379;* 200units/mL), diluted 1:1000 in PBS, at 37°C for thirty minutes. Phalloidin, which binds to filamentous actin, is a method of visualising the cytoskeleton of cells. The cells were then stained with DAPI following three further washes. Images were taken with a 20X objective of a Nikon Eclipse Ti-E microscope.

Additionally, the expression of differentiation markers of HCjE-Gi cells, keratins 4 and 19, were evaluated. The cells were cultured in ninety-six well plates with an initial seeding density of $1x10^4$ cells/cm^2 for seven days with KSF media, and then switched to the differentiation and stratification media. The cells were cultured for a further seven days. On culture days one, seven and fourteen, the cells were washed three times in PBS and fixed with 10% NBF for ten minutes at RT. Next, the cells were permeabilised with 0.2% Triton X-100 for fifteen minutes at RT following three PBS washes. The samples were blocked with 10% goat serum (*Sigma G9023*) for one hour at RT. Goat serum contains an excess of charged proteins that bind to non-specific binding sites on cells, thus preventing antibodies (via the Fc region) from binding to these sites, which will give rise to background staining.(122) The cells were incubated with the primary antibodies (table 2.5A), diluted in 1% bovine serum albumin (BSA), overnight at 4°C. Following three washes with PBS containing 0.1% Tween 20 (*Sigma P1379*) (PBST), the cells were incubated with the appropriate secondary antibodies (table 2.5B), diluted in 1% BSA, for another one hour at 37°C and counterstained with DAPI. PBS containing Tween 20, a non-ionic detergent, was used for washes following antibody incubation to ensure more stringent washes and reduce further background staining. Images were taken with a 20X objective of a Nikon Eclipse Ti-E microscope. PBS was used instead of the primary antibody to ensure the specificity of the secondary antibodies. Mouse or rabbit immunoglobulins were used instead of the primary antibody as an isotype control to ensure the specificity of the immunoglobulins of the antibodies. Additionally, this study was repeated using a retinal pigment epithelial cell line (A19 cells) to ensure the specificity of the primary antibodies.

Image-based Tool for Counting Nuclei plugin on Image J

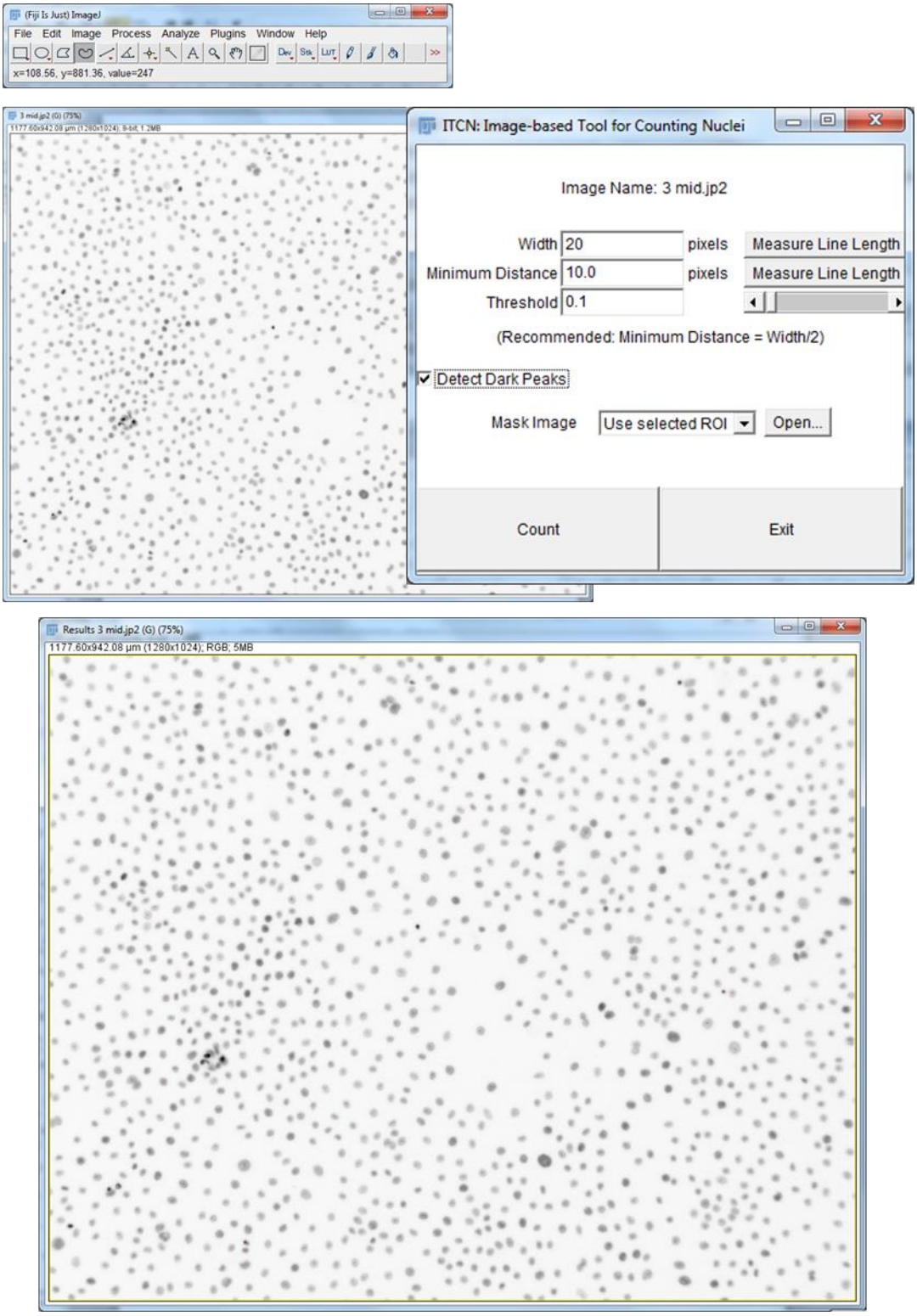

Figure 2.1: Image-based Tool for Counting Nuclei plugin on image J software used to count the number of nuclei.

Antibodies used to identify the expression of conjunctival cell differentiation markers by HCjE-Gi cells

A

PRIMARY ANTIBODIES	SOURCE	DILUTION
Keratin 4 mouse monoclonal [6B10] 1mg/mL	*Abcam ab9004*	1:100
Keratin 19 rabbit monoclonal [EP15804] 0.808mg/mL	*Abcam* ab*52625*	1:500

B

SECONDARY ANTIBODIES	SOURCE	DILUTION
Goat anti-mouse, Alexa Fluor 488 2mg/mL	*Life Technologies A-11029*	1:500
Goat anti-rabbit, Alexa Fluor 594 2mg/mL	*Life Technologies A-11012*	1:500

Table 2.5: Primary (A) and secondary (B) antibodies used to identify the expression of conjunctival cell differentiation markers by HCjE-Gi cells.

2.2.2 ISOLATION OF THE EXTRACELLULAR MATRIX

Ammonium hydroxide (NH_4OH) was used to remove the cells and isolate the underlying ECM.(123) NH_4OH disrupts the cell membranes and solubilises the cellular organelles leaving behind the adsorbed ECM proteins and the transmembrane proteins associated with the ECM. To determine the optimal NH_4OH concentration required, the cells were cultured in forty-eight well plates (*Greiner bio-one 677180*) with an initial seeding density of $1x10^4$ cells/cm^2 for seven days in KSF media. The media was removed and the cells were washed three times with PBS. NH_4OH solutions (*Fisher Scientific 10305220*, Ammonia solution 35%) of 0.1%, 0.2%, 0.5% and 1% concentrations were prepared. The cells were incubated with the different concentrations of NH_4OH solutions for 2.5, 5 or 10 minutes at 37°C. The NH_4OH solution was removed and the wells were washed vigorously three times with PBS. Images were taken using a bright-field microscope.

To ensure that the underlying ECM was not damaged with the NH_4OH treatment, the ECM was stained for the laminin α_3 chain. The samples treated with 0.1% NH_4OH for 2.5 minutes, 1% for 5 minutes and 1% for 10 minutes were fixed with 100% ice cold methanol for two minutes and air dried. Then, the samples were blocked with 10% goat serum for one hour at RT. Next, the samples were probed with a mouse monoclonal antibody against the laminin α_3 chain (prepared in Dr Kevin Hamill's Lab), diluted 1:200 in PBS, at 37°C for one hour. Following three PBST washes, secondary antibody goat anti-mouse Alexa Fluor 514 (*Life Technologies A-31555;* 2mg/mL), diluted 1:500 in PBS, was added and incubated at 37°C for one hour. The samples were washed three times in PBST and counterstained with DAPI for five minutes at RT. Images were taken using a 20X objective of a Nikon Eclipse Ti-E microscope.

2.2.3 IDENTIFICATION OF HCjE-Gi CELL-SECRTED EXTRACELLULAR MATRIX PROTEINS BY IMMUNOFLUORESCENCE STAINING

The HCjE-Gi cells were seeded at $1x10^4$ cells/cm^2 and maintained in KSF media. On culture days one, three, five, seven, fourteen, twenty-one, twenty-eight and forty-two, immunofluorescence (IF) staining was carried out to determine the presence or absence of four ECM proteins. The ECM was isolated by incubating the cells with 1% NH_4OH for five minutes at 37°C. The samples were fixed with 100% ice cold methanol for two minutes and air dried. Then, the samples were blocked with 10% goat serum for one hour at RT and then incubated with the primary antibodies (table 2.6A), diluted in PBS, at 4°C overnight.

Following three PBST washes, the samples were incubated with the appropriate secondary antibody (table 2.6B), diluted in PBS, for one hour at 37°C. The samples were counterstained with DAPI following a further three washes with PBST. Images were taken using a 20X objective of a Nikon Eclipse Ti-E microscope. The samples with the cells intact were used as positive controls. ECM samples with mouse or rabbit immunoglobulins instead of the primary antibodies were used to ensure the specificity of the immunoglobulins, whereas samples with PBS instead of the primary antibodies were used to ensure the specificity of the secondary antibodies used.

Antibodies used to identify the extracellular matrix proteins secreted by HCjE-Gi cells

A

PRIMARY ANTIBODIES	SOURCE	DILUTION
Type IV collagen rabbit polyclonal 1mg/mL	*Abcam ab6586*	1:100
Type XVIII collagen rabbit polyclonal 1mg/mL	*Invitrogen PA5-38894*	1:100
Laminin α_3 chain mouse monoclonal [RG13] 600µg/mL	*Prepared in Dr Kevin Hamill's Lab*	1:200
Fibronectin rabbit polyclonal 0.6mg/mL	*Sigma F3648*	1:400

B

SECONDARY ANTIBODIES	SOURCE	DILUTION
Goat anti-mouse, Alexa Fluor 488 2mg/mL	*Life Technologies A-11029*	1:500
Goat anti-rabbit, Alexa Fluor 594 2mg/mL	*Life Technologies A-11012*	1:500

Table 2.6: Primary (A) and secondary (B) antibodies used to identify the extracellular matrix proteins secreted by HCjE-Gi cells by immunofluorescence staining.

2.2.4 IDENTIFICATION AND QUANTIFICATION OF HCjE-Gi CELL-SECRETED EXTRACELLULAR MATRIX PROTEINS BY MASS SPECTROMETRY

HCjE-Gi cells were seeded in forty-eight well plates at a density of $1x10^4$ cells/cm^2 and were maintained in KSF media for a period of six weeks. On culture days one, seven, fourteen, twenty-eight and forty-two, the ECM was isolated using 1% NH_4OH. The samples were dried and stored at -20°C until all the samples were collected. The samples were given to the Centre for Proteome Research (University of Liverpool) to carry out mass spectrometric analysis.

On the day of the experiment, the samples were thawed to RT. First, 285µL of 0.052% (*w/v*) RapiGest surfactant (*Waters Corporation UK, 186001861*) reconstituted in ammonium bicarbonate (NH_4HCO_3) (*Sigma A6141*) was added to each sample well (final concentration 0.05%). The samples were incubated with the RapiGest solution for thirty minutes at RT on a plate shaker (*IKA-VIBRAX-VXR*) and then for ten minutes at 80°C. RapiGest is an anionic surfactant that improves in-solution protein digestion and peptide recovery by unfolding hydrophobic proteins that are resistant to proteolysis.(124) Then, the samples were cooled to RT and transferred into 1.7mL low bind tubes (*Corning 3207*) to prevent non-specific adsorption of proteins to the surface. Each well was rinsed with further 100µL of RapiGest and this was transferred to the same low bind tubes. The samples were then vortexed (*Heidolph Reax*) gently. Half the protein extract (192.5µL) was aspirated into new low bind tubes and 2.5µL of 60mM dithiothreitol (DTT) (*Melford Biolaboratories Ltd, MB1015*), reconstituted in 25mM NH_4HCO_3 (final concentration of 0.75mM), was added. The samples were vortexed and incubated at 60°C for ten minutes. The DTT is a reducing agent that converts disulphide bonds between cysteine residues into free sulfhydryl groups.(125) Next, 2.5µL of 180mM iodoacetamide (*Sigma-Aldrich I1149*), reconstituted in 25mM NH_4HCO_3 (final concentration of 2.25mM), was added and incubated for thirty minutes at RT in the dark. This acts as an alkylating agent that reacts with the sulfhydryl groups, preventing the formation of disulphide bonds and ensuring that trypsin is able to access its cleavage sites on proteins.(125) Lastly, 100ng/µL trypsin (Trypsin Gold Mass Spectrometry Grade, *Promega V5280*) was made by diluting 200ng/µL stock solution in 50mM acetic acid (*VWR 20103.320*) with an equal volume of 25mM NH_4HCO_3. The samples were incubated at 37°C overnight with 2.5µL of trypsin. Trypsin contains a catalytic triad of histidine-aspartate-serine. The negatively charged aspartate attracts positively charged lysine and arginine and cleaves peptides chains by targeting the carboxyl ends of these amino acids.

The following day, the samples were acidified by the addition of 1µL of trifluoroacetic acid (TFA) (*Biosolve 20234131*) to stop the protein digestion. The samples were incubated at 37°C for forty-five minutes and then centrifuged at 17 200 *x g* for thirty minutes. The clarified digests were transferred to fresh low-bind tubes and the centrifugation step repeated before transfer to total recovery vials for liquid chromatography–mass spectrometry/mass spectrometry (LC-MS/MS) analysis.

Data-dependent LC-MS/MS analyses were conducted by the Centre for Proteome Research (appendix 1). Due to the present study being a time course study with a concomitant increase in cell numbers throughout, the raw data were incorporated into downstream analyses. The raw peptide counts were divided by the total peptide count for each time point to determine the proportion of each protein within a sample.

2.2.5 GROWTH OF HCjE-Gi CELLS ON CELL-SECRETED EXTRACELLULAR MATRIX

The HCjE-Gi cells were cultured in forty-eight well plates at an initial seeding density of $1x10^4$ cells/cm^2 in KSF media. On culture days three, five, seven, fourteen, twenty-one and twenty-eight, the cell-secreted ECM was isolated using 1% NH_4OH. Following thorough washes with sterile PBS, the cells were re-seeded on the cell-secreted ECM at a density of $1x10^4$ cells/cm^2 with KSF culture media. HCjE-Gi cells cultured on tissue culture polystyrene (TCP) on the same well plate that were also treated with 1% NH_4OH, were used as controls. On culture days one, three, five and seven, the cells were fixed with 100% ice cold methanol and stained with DAPI. Images were taken with a 10X objective from five fixed positions of each well using a Nikon Eclipse Ti-E microscope and the number of nuclei per view was determined. The number of nuclei per view on cell-secreted ECM was divided by the number of nuclei of the corresponding view on TCP to obtain ECM:TCP cell number ratios (figure 2.2). The ECM:TCP cell number ratios per view for each culture day were used in the downstream analysis. All experiments were carried out in three sets of triplicates.

The arrangement of the well plates used to determine the growth of HCjE-Gi cells on cell-secreted extracellular matrix

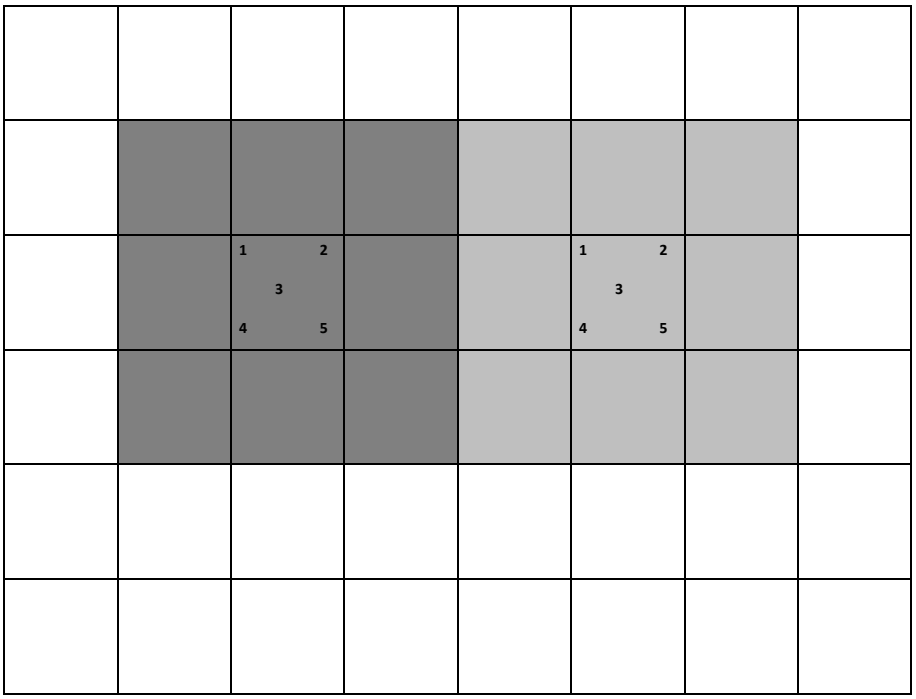

Figure 2.2: The arrangement of the well plates used to determine the growth of HCjE-Gi cells on cell-secreted extracellular matrix. Images were taken from five fixed positions of each well as shown. The number of nuclei per view on the cell-secreted ECM (dark grey) was divided by the number of nuclei of the corresponding view on tissue culture polystyrene (light grey) to obtain ECM:TCP cell number ratios that were used in the downstream analyses.

2.2.6 ADSORPTION OF PROTEINS ONTO TISSUE CULTURE POLYSTYRENE

An indirect enzyme-linked immunosorbent assay (ELISA) was carried out to determine the adsorption of proteins onto TCP. Type IV collagen, laminin 111 and fibronectin proteins were diluted in PBS to make solutions of protein concentrations 0.5, 1, 2, 5, 10 and 20µg/mL (table 2.7A). Type IV collagen protein was diluted in PBS as well as 0.5M acetic acid (*Sigma A6283*), as per manufacturer's instructions, to determine if there is a significant difference in the adsorption of type IV collagen when diluted in these solutions. Protein solutions were added into ninety-six well plates (100µL of protein solution per well) and incubated for one hour at 37°C. PBS or 0.5M acetic acid was added into control wells (0µg/mL protein). The wells were washed three times with PBS and non-specific binding sites were blocked with 2% goat serum for one hour at RT. The wells were washed three more times with PBS prior to incubating with the appropriate primary antibody (table 2.7B), diluted in PBS, at 37°C for one hour. The appropriate secondary antibodies conjugated with alkaline phosphatase (table 2.7C), diluted in PBS, were added and incubated for one hour at 37°C following a further three washes in PBS. Alkaline phosphatase yellow (*p*-nitrophenylphosphate (pNPP)) liquid substrate system for ELISA (*Sigma P7998*) warmed to 37°C was added as a substrate. A colour change from colourless to yellow was observed (figure 2.3) and the reaction was stopped with 1M sodium hydroxide (*BDH 102524X*) after one minute. The absorbance was read at 405nm on a plate reader (*FLUOstar OPTIMA, BMG LABTECH*). TCP that did not have pre-adsorbed proteins and were not probed with a primary antibody were used as a negative control. The background measurements from the negative control were subtracted from the raw readings. The experiments were carried out as three sets of triplicates.

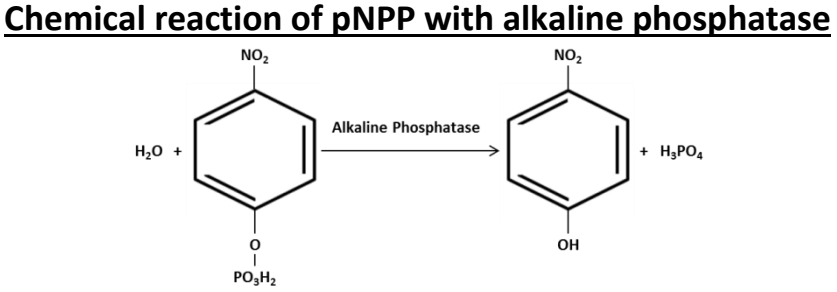

Figure 2.3: Chemical reaction of pNPP with alkaline phosphatase. pNPP is converted to p-nitrophenol (yellow end-product) when hydrolysed by alkaline phosphatase. **(Adapted from: http://www.sigmaaldrich.com/catalog/product/sigma/p7998?lang=en&region=GB)**

Reagents used to determine the protein adsorption onto tissue culture polystyrene

A

PROTEINS	SOURCE	DILUENT
Collagen IV from human placenta 1mg/mL	*Sigma C7521*	PBS or acetic acid
Laminin from EHS murine sarcoma 1mg/mL	*Sigma L2020*	PBS
Fibronectin from human plasma 1mg/mL	*Sigma F2006*	PBS

B

PRIMARY ANTIBODIES	SOURCE	DILUTION
Fibronectin mouse monoclonal [IST-4] 4.5mg/mL	*Sigma F0916*	1:5000
Type IV collagen mouse monoclonal [Col-94]	*Sigma C1926*	1:5000
Laminin rabbit polyclonal 0.5mg/mL	*Sigma L9393*	1:2500

C

SECONDARY ANTIBODIES	SOURCE	DILUTION
Goat anti-mouse – Alkaline Phosphatase 1.3mg/mL	*Sigma A3562*	1: 20 000
Goat anti-rabbit – Alkaline Phosphatase 1mg/mL	*Promega S3731*	1: 10 000

Table 2.7: Reagents used to determine the protein adsorption onto tissue culture polystyrene; proteins that were pre-adsorbed onto tissue culture polystyrene and their diluents (A), and the primary (B) and secondary antibodies (C) used in ELISA experiments.

2.2.7 ADHESION OF HCjE-Gi CELLS ON PRE-ADSORBED PROTEINS

Adhesion of HCjE-Gi cells on pre-adsorbed type IV collagen, laminin 111, fibronectin and α-2-HS-GP was determined as described below. Solutions containing 0.5-10µg/mL type IV collagen, 0.1-1µg/mL laminin 111, 0.5-10µg/mL fibronectin and 0.5-20µg/mL α-2-HS-GP (*Sigma* G0516, 1mg/mL) were prepared in PBS. Ninety-six well plates were pre-adsorbed with protein solutions by incubating for one hour at 37°C. HCjE-Gi cells cultured on TCP (0µg/mL protein) were used as controls. The wells were washed three times with PBS and HCjE-Gi cells were seeded at a density of $3x10^4$ cells/cm^2. The cells were incubated for three hours at 37°C and 5% CO_2, as per protocol by the Gipson lab.(116) The media was removed and washed once gently with PBS. The cells were fixed with 100% ice cold methanol for two minutes and air dried. Then, the cells were stained with DAPI for five minutes at RT and washed three times with PBS. Images were taken with a 10X objective from five fixed positions of each well using the Nikon Eclipse Ti-E microscope. The mean number of nuclei per view (0.011cm^2) was calculated to determine the number of cells per cm^2 in each well. The experiments were carried out in three sets of triplicates.

2.2.8 GROWTH AND DIFFERENTIATION OF HCjE-Gi CELLS ON PRE-ADSORBED PROTEINS

Solutions containing 0.5-10µg/mL type IV collagen, 0.1-1µg/mL laminin 111, 0.5-10µg/mL fibronectin and 0.5-20µg/mL α-2-HS-GP proteins were prepared in PBS. Ninety-six well plates were pre-adsorbed with protein solutions by incubating for one hour at 37°C. HCjE-Gi cells cultured on TCP (0µg/mL protein) were used as controls. The wells were washed three times with PBS and HCjE-Gi cells were seeded at a density of $1x10^4$ cells/cm^2 and maintained in a humidifying incubator (37°C, 5% CO_2). On culture days one, three, five and seven, KSF media was removed and the cells were washed three times with PBS. The cells were fixed with 100% ice cold methanol for two minutes and air dried. Then, the cells were stained with DAPI for five minute at RT and again washed in PBS. Images were taken with a 10X objective from five fixed positions of each well using the Nikon Eclipse Ti-E microscope. The mean number of nuclei per view was calculated to determine the number of cells per cm^2 in each well at each culture time point and a growth curve was drawn for each test condition. The experiments were carried out in three sets of triplicates. Additionally, on culture day seven, separate wells with cells cultured on pre-adsorbed proteins were fixed with 10% NBF and permeabilised with 0.2% Triton X-100 to evaluate the expression of conjunctival cell differentiation markers (keratins 4 and 19) as described in section 2.2.1.5.

2.2.9 EXPRESSION OF STEM CELL AND GOBLET CELL MARKERS BY HCjE-Gi CELLS ON PRE-ADSORBED PROTEINS

The expression of SC and GC markers by HCjE-Gi cells cultured on pre-adsorbed proteins was analysed using ICC. Ninety-six well plates were pre-adsorbed with type IV collagen from 2 and 10µg/mL solutions, laminin 111 from 0.5 and 1µg/mL solutions and fibronectin from 2 and 10µg/mL solutions. PBS was added to control wells (0µg/mL protein). HCjE-Gi cells were seeded at a density of $1x10^4$ cells/cm^2 and were maintained in KSF medium for seven days and switched to the differentiation and stratification medium for a further seven days. On culture days one, seven and fourteen, the cells were fixed in 10% NBF, permeabilised with 0.2% Triton X-100 and non-specific binding sites were blocked with 10% goat serum. The expression of two SC markers, ABCG2 and ΔNp63 localised in the cell membrane and the nucleus, respectively, were investigated. Similarly, the expression of two GC markers, MUC5AC and the co-expression of keratin 7 and Ulex Europaeus Agglutinin I (UEAI), were investigated. Keratin 7 is a cytoplasmic protein, whereas UEAI is a lectin that binds to glycoproteins and glycolipids in the cells. MUC5AC may be found intracellularly in the cytoplasm or extracellularly when secreted. The cells were incubated with primary antibodies (table 2.8A and B), diluted in 1% BSA, at 4°C overnight. The samples were washed with PBST prior to incubating with the appropriate secondary antibody (table 2.8C), diluted in 1% BSA, for one hour at 37°C. The samples that were probed for keratin 7 were counter-stained with UEAI, which was conjugated with fluorescein. Lastly, all the samples were counterstained with DAPI following three PBST washes. Images were taken from five fixed positions with a 20X objective of the Nikon Eclipse Ti-E microscope. The percentage of cells with positive staining for each protein per field of view ($0.003cm^2$) was determined. Next, the mean percentage of cells with positive staining per field of view at each time point for each substrate investigated was calculated. These experiments were carried out in one set of duplicates. Mouse or rabbit immunoglobulins and PBS were used instead of the primary antibody to ensure specificity of the immunoglobulins and secondary antibodies, respectively.

Antibodies used to identify the expression of stem cell and goblet cell markers by HCjE-Gi cells

A

PRIMARY ANTIBODIES	SOURCE	DILUTION
ABCG2 mouse monoclonal [BXP-21] 0.25mg/mL	*Millipore MAB4146*	1:100
ΔNp63 rabbit polyclonal [poly6190] 0.28mg/mL	*Biolegend 619002*	1:1000

B

PRIMARY ANTIBODIES	SOURCE	DILUTION
MUC5AC mouse monoclonal [45M1] 0.2mg/mL	*Abcam ab3649*	1:200
Keratin 7 mouse monoclonal [OV-TL 12/30] 0.2mg/mL	*Abcam ab9098*	1:200
Fluorescein labelled Ulex Europaeus Agglutinin I 2mg/mL	*Vector Laboratories FL-1061*	1:500

C

SECONDARY ANTIBODIES	SOURCE	DILUTION
Goat anti-mouse, Alexa Fluor 488 2mg/mL	*Life Technologies A-11029*	1:500
Goat anti-mouse, Alexa Fluor 594 2mg/mL	*Life Technologies A-11032*	1:500
Goat anti-rabbit, Alexa Fluor 488 2mg/mL	*Life Technologies A-11008*	1:500
Goat anti-rabbit, Alexa Fluor 594 2mg/mL	*Life Technologies A-11012*	1:500

Table 2.8: Primary antibodies used to identify the expression of stem cell (A) and goblet cell (B) markers by HCjE-Gi cells by immunocytochemistry and the corresponding secondary antibodies (C).

2.2.10 STATISTICS

All data were analysed using the SPSS Statistics 22 software.

One-way analysis of variance (ANOVA)

- Raw peptide abundances of proteins from ECM day 1 to 42
- Adsorption of proteins onto tissue culture polystyrene
- Adhesion of HCjE-Gi cells on pre-adsorbed proteins

Outliers were determined by inspection of boxplot diagrams. Shapiro-Wilk test was carried out to determine the normal distribution of the data, whereas Levene's test was undertaken to assess the homogeneity of variances. When outliers were present, analysis was done by excluding these to determine if there was a difference to the overall result. Data that did not assume normal distribution were included in the analysis, since one-way ANOVA is robust to deviations from normality when sample sizes are equal. Where homogeneity of variances was violated, results of Welch's ANOVA were reported. Tukey post hoc test was used when there was homogeneity of variances, whereas Games-Howell post hoc test was carried out when this assumption was violated. A significance level of $p < 0.05$ was set for all the experiments.

Two-way ANOVA

- Abundance of ECM and non-ECM peptides obtained by LC-MS/MS
- Peptide abundance of protein categories from ECM day 1 to 42
- Adsorption of type IV collagen diluted in acetic acid or PBS
- Growth of HCjE-Gi cells on pre-adsorbed proteins
- Expression of ΔNp63 and ABCG2 by HCjE-Gi cells on pre-adsorbed proteins
- Expression of MUC5AC and co-expression of keratin 7 and UEA1 by HCjE-Gi cells on pre-adsorbed proteins

Residual analysis was performed to test for the assumptions of two-way ANOVA. Outliers were determined by inspection of boxplot diagrams. Shapiro-Wilk test was carried out to determine the normal distribution of the data, whereas Levene's test was undertaken to assess the homogeneity of variances. When outliers were present, analysis was done by excluding these to determine if there was a difference to the overall result. Data that did not assume normal distribution were included in the analysis since two-way ANOVA is

considered robust to deviations from normality. Data that violated the assumption of homogeneity of variances were also included in the analysis since the sample sizes were equal, although small.

First, the data were analysed to determine if there was an interaction effect between the two independent variables. Analysis of the main effect for each independent variable was performed when there was no significant interaction effect between the two. If this was found to be significant, all pairwise comparisons were run, where the reported *p* values were Bonferroni-adjusted. When there was a significant interaction effect between the two independent variables, analysis of the simple main effect was performed. All pairwise comparisons were run for each simple main effect, where the reported *p* values were Bonferroni-adjusted. A significance level of $p < 0.05$ was set for all the experiments.

<u>Generalised linear model</u>

- Growth of HCjE-Gi cells on cell-secreted ECM proteins

A significance level of $p < 0.05$ was set for this experiment.

2.3 RESULTS

2.3.1 CHARACTERISTICS OF HCjE-Gi CELL LINE

2.3.1.1 GROWTH CURVE

A typical growth curve of cultured cells consists of four phases: lag phase, log phase, plateau phase and decline phase (figure 2.4).(126) The lag phase represents the time taken by the cells to recover following trypsinisation and adapt to the new culture conditions by re-assembling their cytoskeleton and secreting ECM proteins.(126) This phase ensures that the cells have adhered onto the substrate prior to entering a new cell cycle.(126) Moreover, new DNA and structural proteins are synthesised by the cells during this time.(127) The lag phase may last from a few hours to up to forty-eight hours.(128) The log phase is when there is an exponential increase in the cell number.(127) The time period taken for the cell number to double is known as the population doubling time and is characteristic for each cell line.(128) As the culture becomes confluent, the growth rate reduces and the cells enter the plateau phase.(128) This is due to the lack of nutrients, accumulation of metabolic waste products and lack of physical space.(127, 128) Certain types of cells may remain as a monolayer before entering the decline phase where there is a reduction in the cell number due to cell death, however, some cells may differentiate and become multi-layered with continued replenishment of nutrients.(128)

The growth curves of HCjE-Gi cells did not exhibit the typical sigmoid shape of a growth curve over the seven days in culture in KSF media (figure 2.5). When seeded at an initial seeding density of $5x10^3$ and $1x10^4$ cells/cm^2, only the lag and log phases of the growth curve were demonstrated. The HCjE-Gi cells had a lag phase of approximately 48 to 72 hours. The cells then entered the log phase of the growth curve where they proliferated exponentially between culture days three and seven. The population doubling time during this phase was 25.4 hours when seeded at a density of $5x10^3$, whereas the doubling time was 31.1 hours when seeded at a density of $1x10^4$ cells/cm^2. This is in keeping with the doubling times stated by the manufactures of this cell line.(116) When seeded at a density of $1x10^5$ cells/cm^2, the growth curve over the seven days represented the late stages of the log phase when the growth rate reduced with time before entering the plateau phase. By culture day seven, the cells seeded at initial densities of $1x10^4$ and $1x10^5$ cells/cm^2 were more than 80% confluent, whereas those seeded at $5x10^3$ cells/cm^2 was about 50% confluent (figure 2.6). A seeding density of $1x10^4$ cells/cm^2 was chosen for the subsequent experiments.

2.3.1.2 CELL MORPHOLOGY

On culture day one, the HCjE-Gi cells have commenced rebuilding their cytoskeleton as evidenced by the positive staining for the cytoskeletal microfilament, filamentous actin (figure 2.7). The cells spread to form discrete colonies of cells. Following seven days in culture in KSF media, the HCjE-Gi cells formed a monolayer of cells that resembled a cobblestone appearance in keeping with the epithelial cell morphology. The individual cells were polygonal in shape and were approximately 20-40µm in diameter. There were a few cells that were larger with a diameter of approximately 75-100µm. These cells are thought to be post-mitotic cells expressing the differentiation marker, involucrin (not done).(116)

2.3.1.3 EXPRESSION OF CONJUNCTIVAL CELL DIFFERENTIATION MARKERS

All the HCjE-Gi cells, which were cultured in KSF media for seven days and in the differentiation and stratification media for a further seven days, stained positive for keratin 19 from culture days one to fourteen (figure 2.8). Few cells stained positive for keratin 4 from day seven onwards. Qualitatively, there was no increase to the number of cells stained positive for keratin 4 after culturing the cells in the differentiation and stratification medium. However, culture of these cells in the differentiation and stratification medium did induce stratification of at least two layers of cells, which was observed during microscopy. Qualitatively, there was no significant positive staining observed in the negative controls used for these experiments demonstrating the specificity of the primary and secondary antibodies as well as the immunoglobulins of the antibodies (figure 2.9). A limitation of the present study is that I have not shown the lack of expression of corneal epithelial markers, keratins 3 and 12, or the expression of keratin 13 by the HCjE-Gi cells, which has been suggested to be a more specific marker of conjunctival epithelial cells than keratin 19.

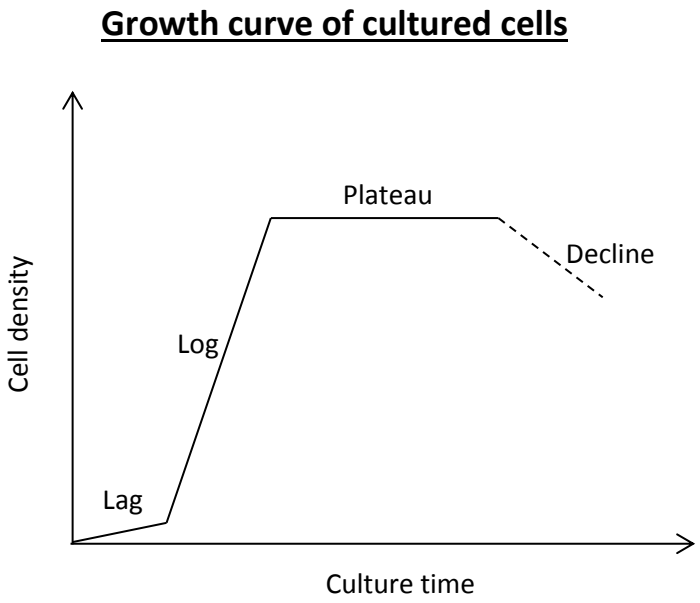

Figure 2.4: Growth curve of cultured cells. A schematic diagram illustrating the typical sigmoid shape of a growth curve of cultured cells with lag, log, plateau and decline phases.

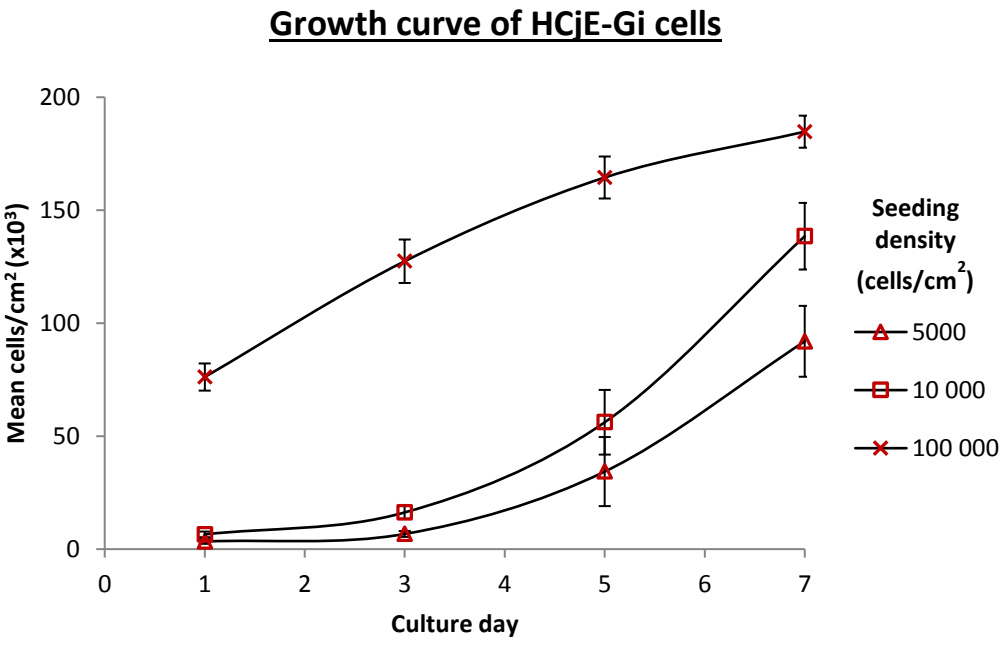

Figure 2.5: Growth curve of HCjE-Gi cells over seven days in culture in keratinocyte serum-free media. Data are presented as mean number of cells/cm² (x10³) ± 1SD, n = 9. A seeding density of 1x10⁴ cells/cm² was chosen for the subsequent experiments.

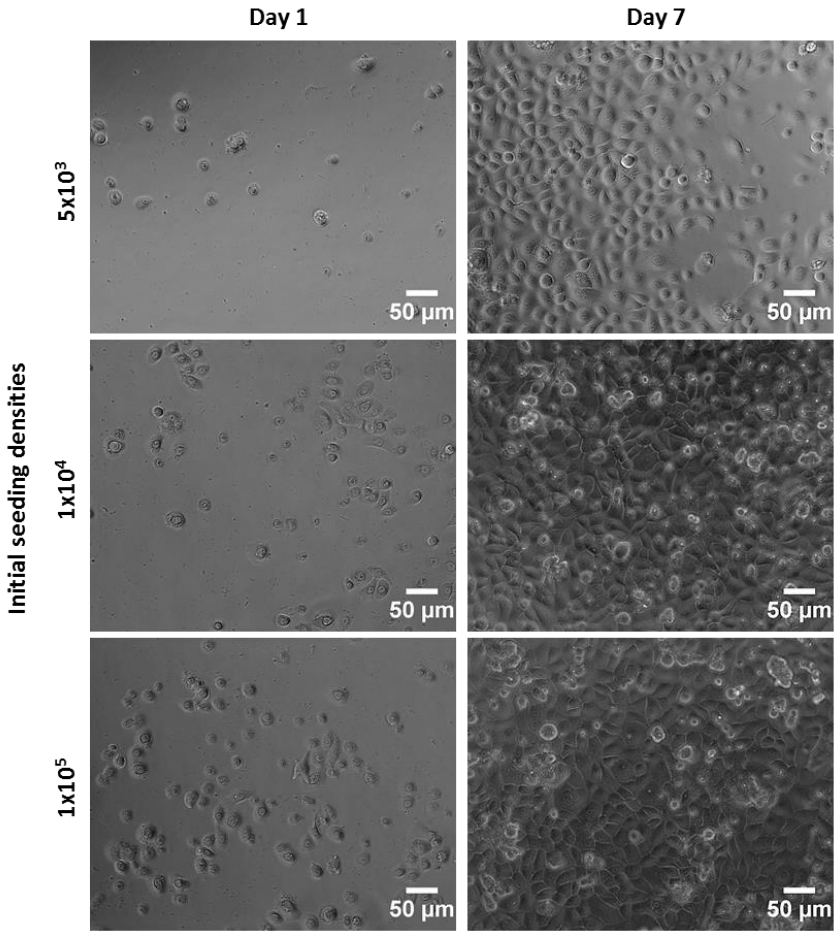

Figure 2.6: Phase-contrast images of HCjE-Gi cells on culture days one and seven in keratinocyte serum-free media. By culture day seven, the cells seeded at initial densities of $1x10^4$ and $1x10^5$ cells/cm^2 were more than 80% confluent, whereas those seeded at $5x10^3$ cells/cm^2 was about 50% confluent.

Cytoskeletal morphology of HCjE-Gi cells

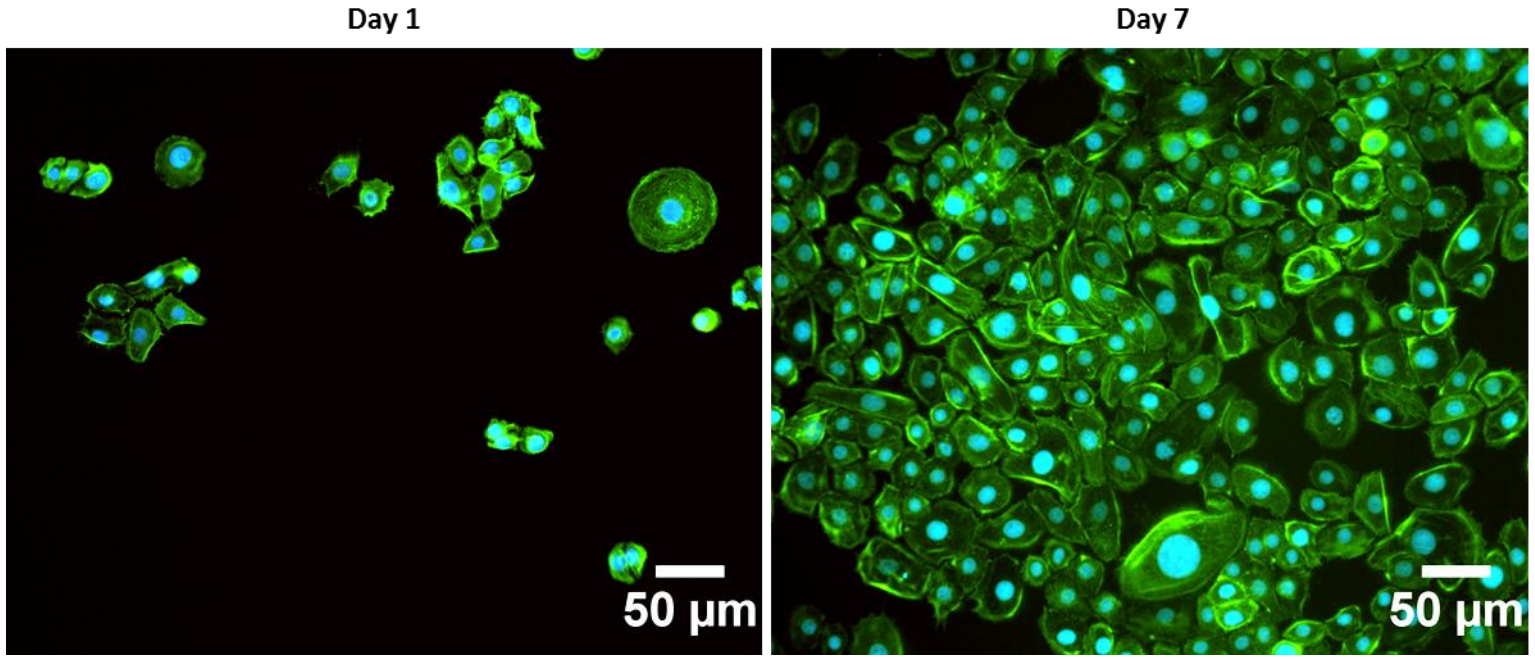

Figure 2.7: Cytoskeletal morphology of HCjE-Gi cells demonstrated by staining for filamentous actin on culture days one and seven in keratinocyte serum-free media (initial seeding density 1x10^4 cells/cm^2); Alexa Fluor® 488 Phalloidin (green) and DAPI (blue). Phalloidin, which binds to filamentous actin, is a reagent used to visualise the filamentous cytoskeleton of cells.

Expression of conjunctival cell differentiation markers by HCjE-Gi cells

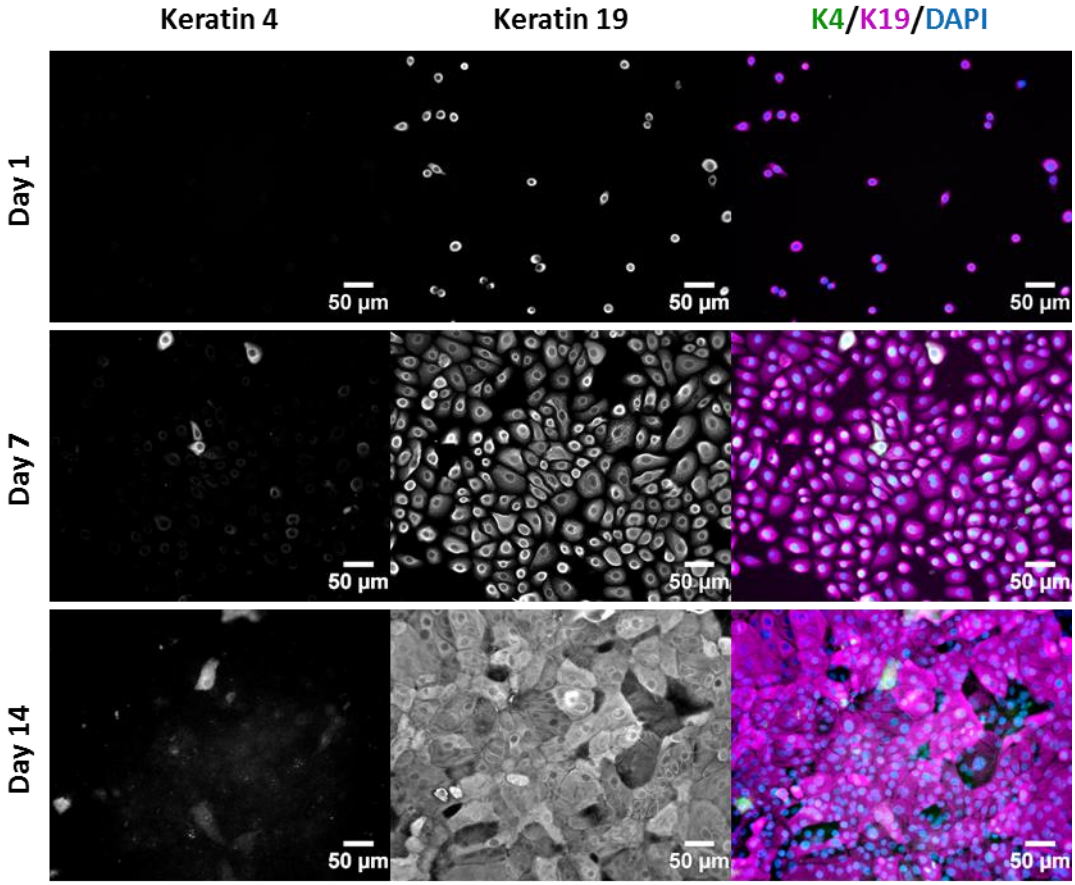

Figure 2.8: Expression of conjunctival cell differentiation markers by HCjE-Gi cells over a culture period of fourteen days (cultured in keratinocyte serum-free media for seven days and in the differentiation and stratification media for a further seven days). There was positive staining in all cells for keratin 19, a marker of simple epithelial cells, over the culture period, whereas only few cells stained positive for keratin 4, a marker of non-keratinised stratified epithelial cells, between culture days seven and fourteen. There was evidence of stratification by culture day fourteen as observed during microscopy; K4 - keratin 4 (green), K19 - keratin 19 (purple) and DAPI (blue).

Negative controls for immunocytochemistry

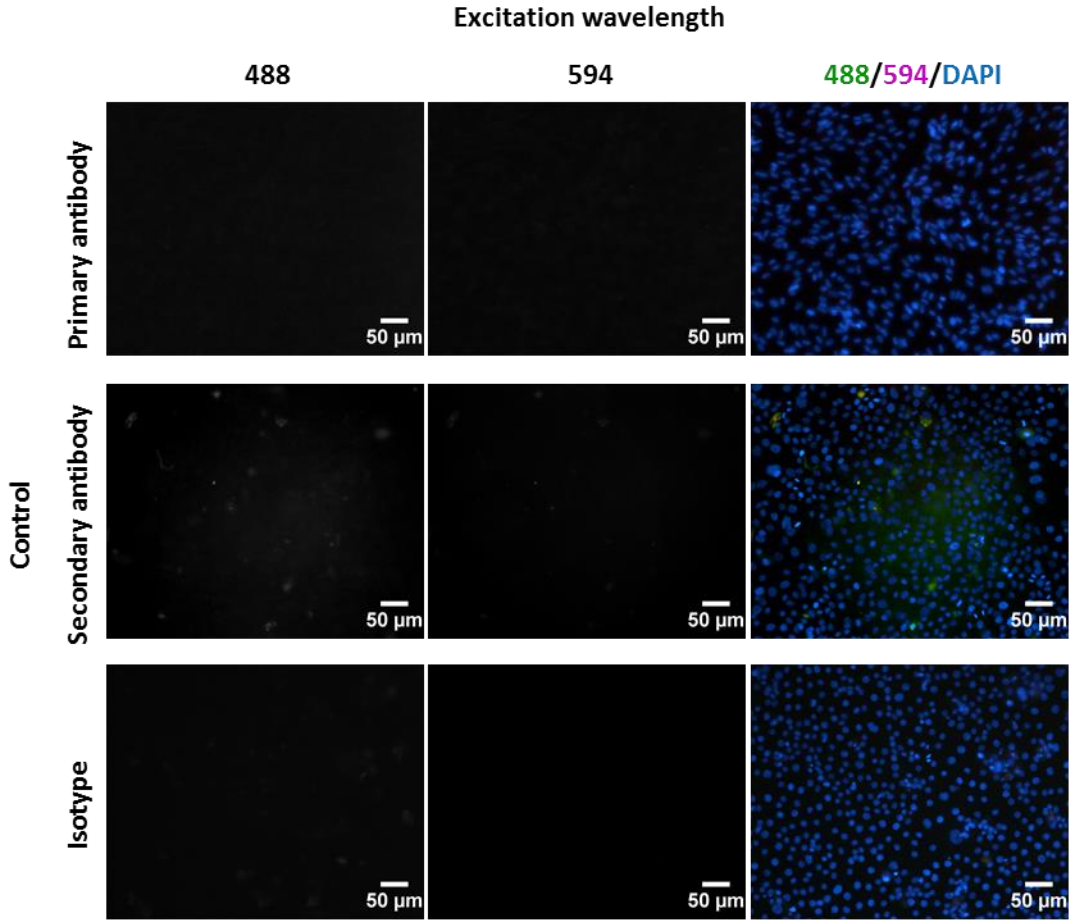

Figure 2.9: Negative controls for immunocytochemistry used to ensure the specificity of the primary antibodies (A19 cells, retinal pigment epithelial cell line), secondary antibodies and immunoglobulins of the antibodies. Qualitatively, there was no significant positive staining in any of the controls.

2.3.2 ISOLATION OF THE EXTRACELLULAR MATRIX

Treatment of HCjE-Gi cells with NH_4OH caused the cells to swell, round up and detach from the TCP (figure 2.10). The cells were still present when treated with NH_4OH concentrations of 0.1-0.5% for 2.5 minutes. Almost all the cells were completely removed when treated with 1% NH_4OH for 2.5 minutes, 0.5-1% for 5 minutes and 0.1-1% for 10 minutes. Vigorous washes were required to remove all the visible cell debris.

To ensure that the underlying ECM proteins were not altered following treatment with NH_4OH, the ECM obtained from samples treated with 0.1% NH_4OH for 2.5 minutes, 1% for 5 minutes and 1% for 10 minutes were stained for the ECM protein, laminin α_3 chain (figure 2.11). The samples were also counterstained with DAPI to ensure the absence of nuclei, therefore the absence of cells. The samples treated with 0.1% NH_4OH for 2.5 minutes were not completely decellularised, whereas those treated with 1% NH_4OH, for either 5 or 10 minutes, did not stain positive for DAPI. Qualitatively, the staining for laminin α_3 chain was similar in samples treated with 1% NH_4OH for either 5 or 10 minutes. Therefore, in the subsequent experiments, it was decided to treat cells with 1% NH_4OH for five minutes to successfully isolate the ECM and the transmembrane proteins associated with the ECM.

Optimisation of the ammonium hydroxide protocol to isolate the extracellular matrix

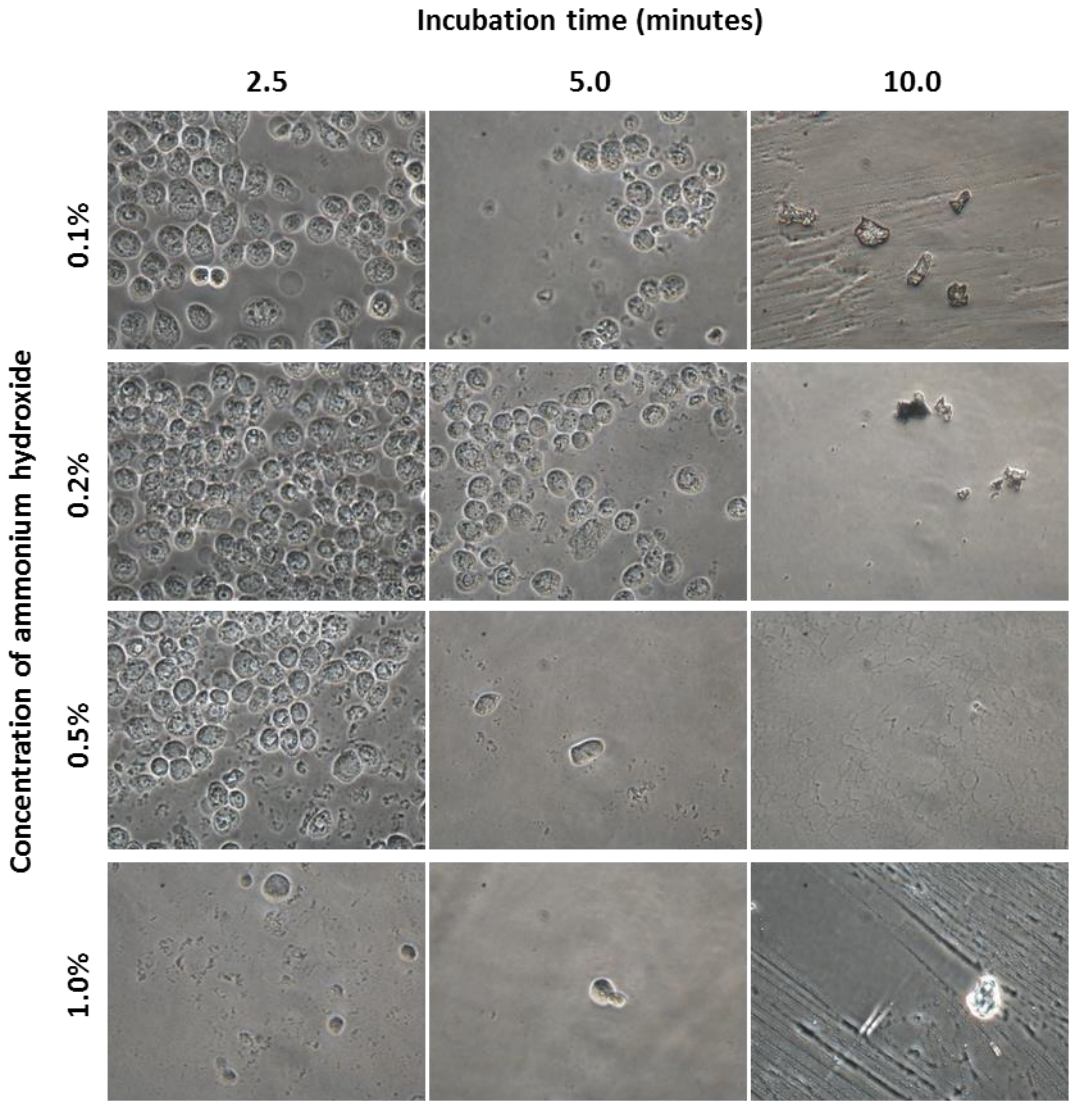

Figure 2.10: Optimisation of the concentration and incubation time of ammonium hydroxide to isolate the extracellular matrix. Almost all the cells were removed when the samples were treated with 1% ammonium hydroxide for 2.5 minutes, 0.5-1% ammonium hydroxide for 5 minutes and 0.1-1% ammonium hydroxide for 10 minutes. Vigorous washes with PBS were required to remove all the visible cell debris.

Immunofluorescence staining for laminin α_3 chain following ammonium hydroxide treatment

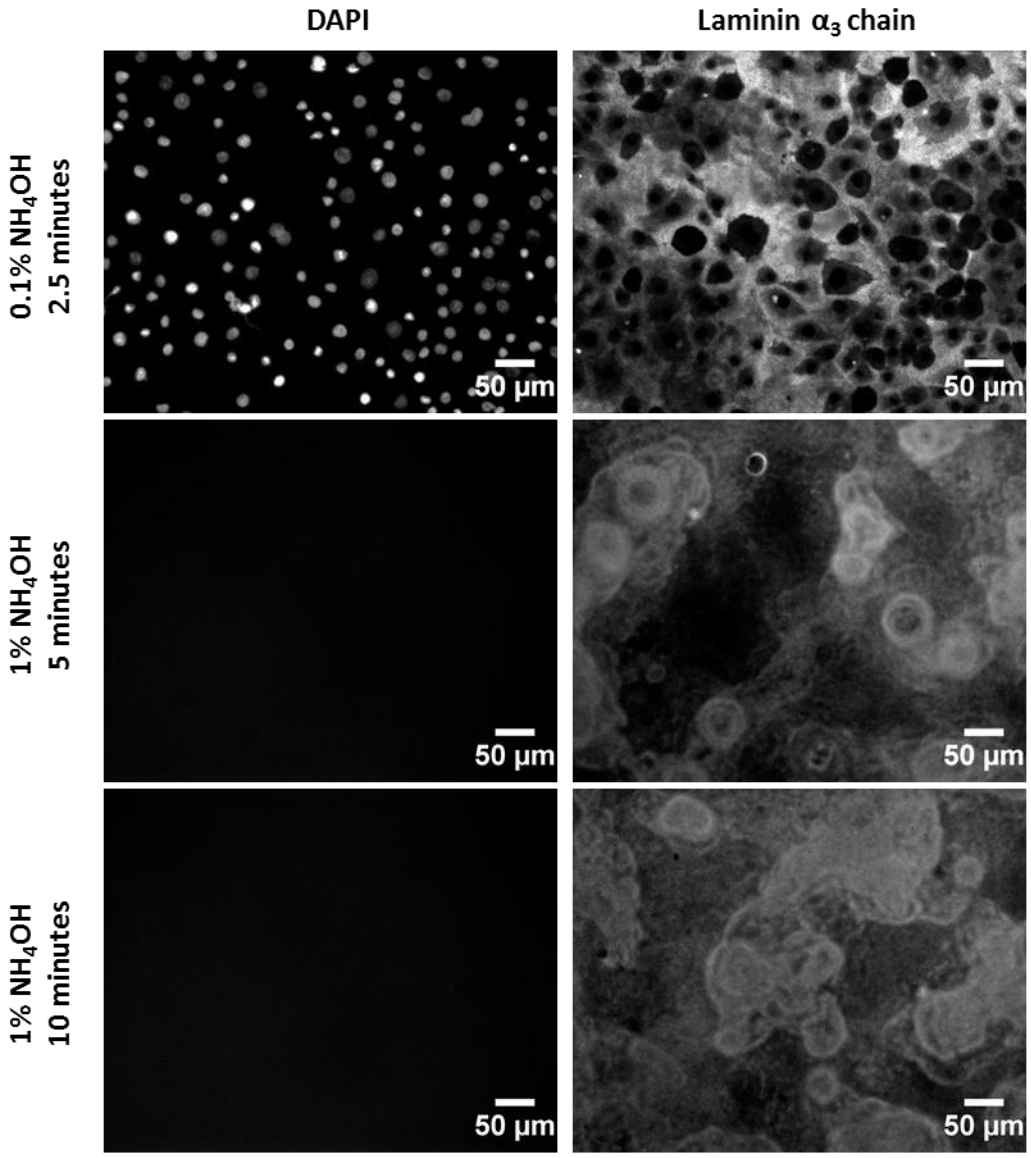

Figure 2.11: Immunofluorescence staining for the extracellular matrix protein, laminin α_3 chain, following ammonium hydroxide treatment. Nuclear staining was present when the cells were treated with 0.1% ammonium hydroxide for 2.5 minutes, however, this was absent when treated with 1% ammonium hydroxide for 5 or 10 minutes. Qualitatively, there was no difference in the staining for laminin α_3 chain when treated with 1% ammonium hydroxide for 5 or 10 minutes. The cells were treated with 1% ammonium hydroxide for five minutes at 37°C to isolate the extracellular matrix in the subsequent experiments.

2.3.3 IDENTIFICATION OF HCjE-Gi CELL-SECRETED EXTRACELLULAR MATRIX PROTEINS BY IMMUNOFLUORESCENCE STAINING

HCjE-Gi cells cultured for one, three, five, seven, fourteen, twenty-one, twenty-eight and forty-two days were treated with 1% NH_4OH to isolate the ECM and were stained for type IV collagen, type XVIII collagen, laminin α_3 chain and fibronectin (figures 2.12-2.19). Samples with cells that were not treated with NH_4OH were used as positive controls. Negative controls did not demonstrate significant staining that affected the accurate interpretation of the IF staining results (figure 2.20).

The protein expression for laminin α_3 chain was present from day one and continued to increase until day forty-two. During the culture period of six weeks, various staining patterns for laminin α_3 were observed. Initially, laminin was deposited in a rosette-like pattern with a few trail-like patterns between days one and seven. This has previously been described as the pattern of laminin deposition by stationary and migrating cultured keratinocytes, respectively.(129) With time, there was a mixture of these two patterns with larger rosettes and some areas of diffuse staining. In the positive controls, with the cells intact, a network of laminin around the cells was observed.

The antibody used to detect type IV collagen in the current study targeted the α_1 chain. Positive staining for type IV collagen was only evident from day twenty-one onwards and was present until day forty-two. The staining for type IV collagen co-localised with that of the laminin α_3 chain. The positive control demonstrated intracellular staining only. The antibody used to detect type XVIII collagen targeted the α_1 chain, specifically the endostatin domain at the C-terminal. Similar to type IV collagen, there was positive staining for type XVIII collagen from days twenty-one to forty-two. There was diffuse granular staining observed with no specific pattern or co-localisation with the laminin α_3 chain. The positive controls showed some weak staining intracellularly.

Fibronectin was present at the early time points, however, from day seven the staining reduced. A linear 'spike-like' staining pattern was observed, mainly around the staining for the laminin α_3 chain. The staining for fibronectin was observed intracellularly and extracellularly in the positive controls.

Day 1 extracellular matrix

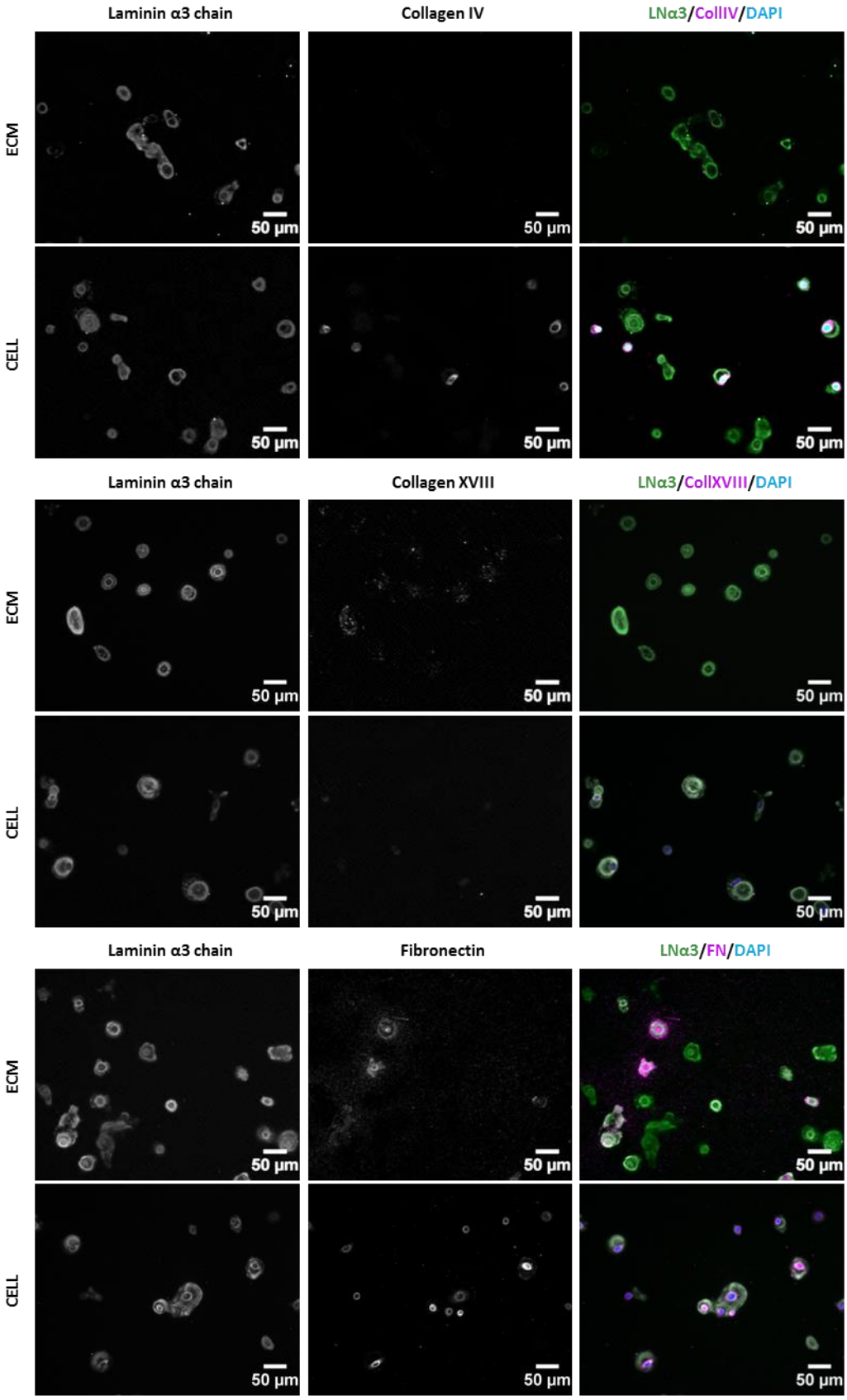

Figure 2.12: Day 1 extracellular matrix; LNα3 - laminin α_3 chain (green), CollIV – type IV collagen (purple), CollXVIII – type XVIII collagen, FN - fibronectin (purple), and DAPI (blue).

Day 3 extracellular matrix

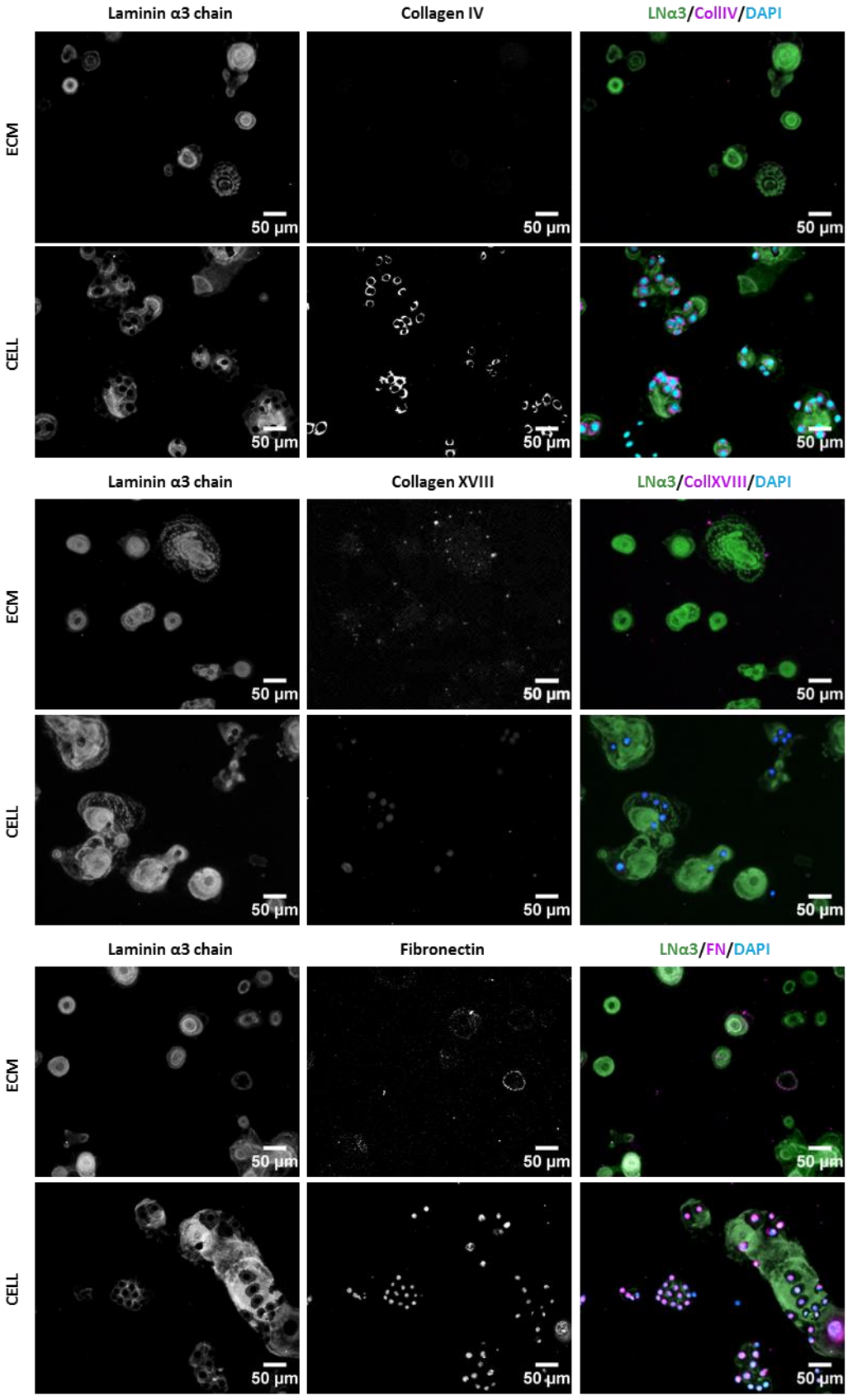

Figure 2.13: Day 3 extracellular matrix; LNα3 - laminin α_3 chain (green), CollIV – type IV collagen (purple), CollXVIII – type XVIII collagen, FN - fibronectin (purple), and DAPI (blue).

Day 5 extracellular matrix

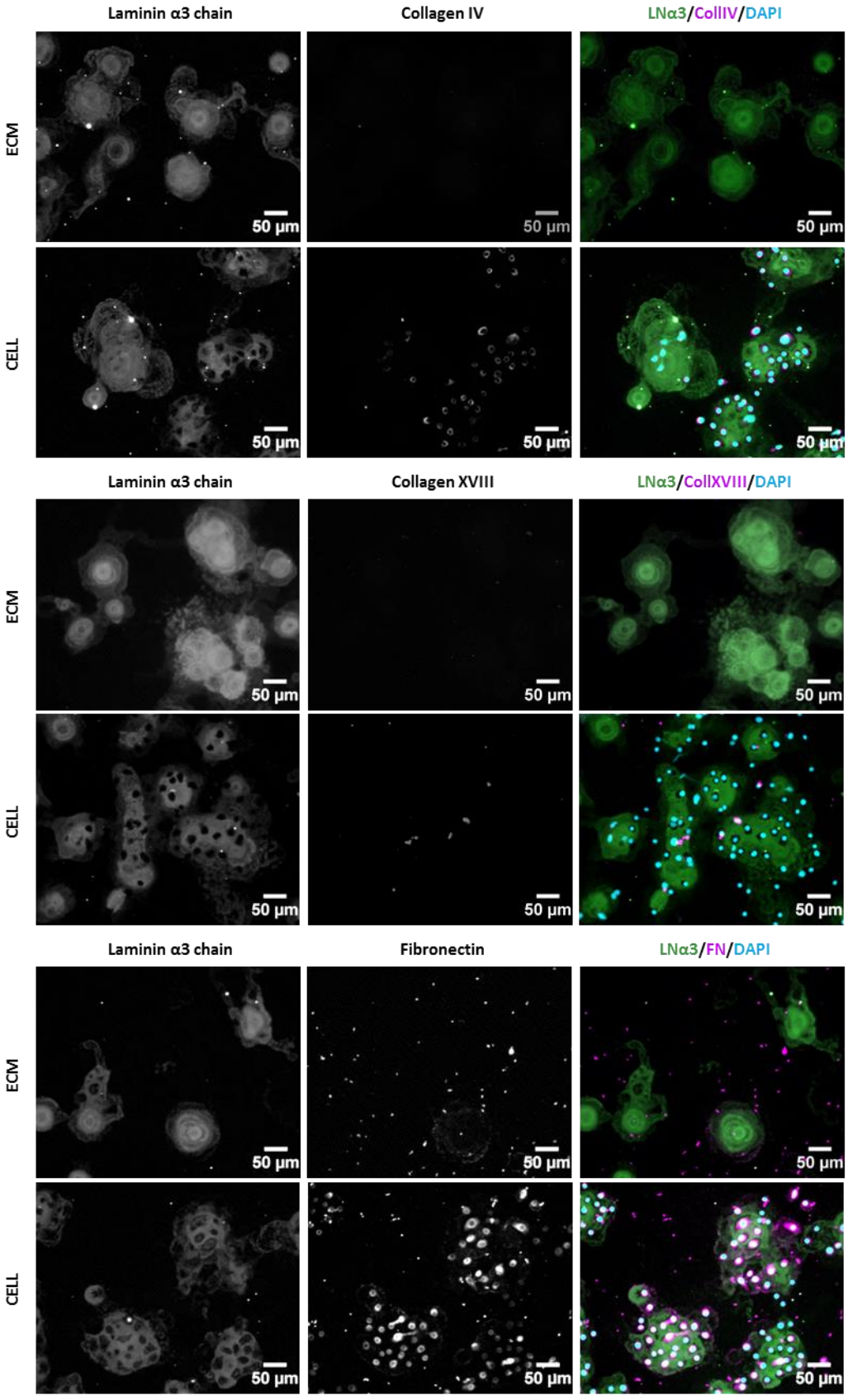

Figure 2.14: Day 5 extracellular matrix; LNα3 - laminin α_3 chain (green), CollIV – type IV collagen (purple), CollXVIII – type XVIII collagen, FN - fibronectin (purple), and DAPI (blue).

Day 7 extracellular matrix

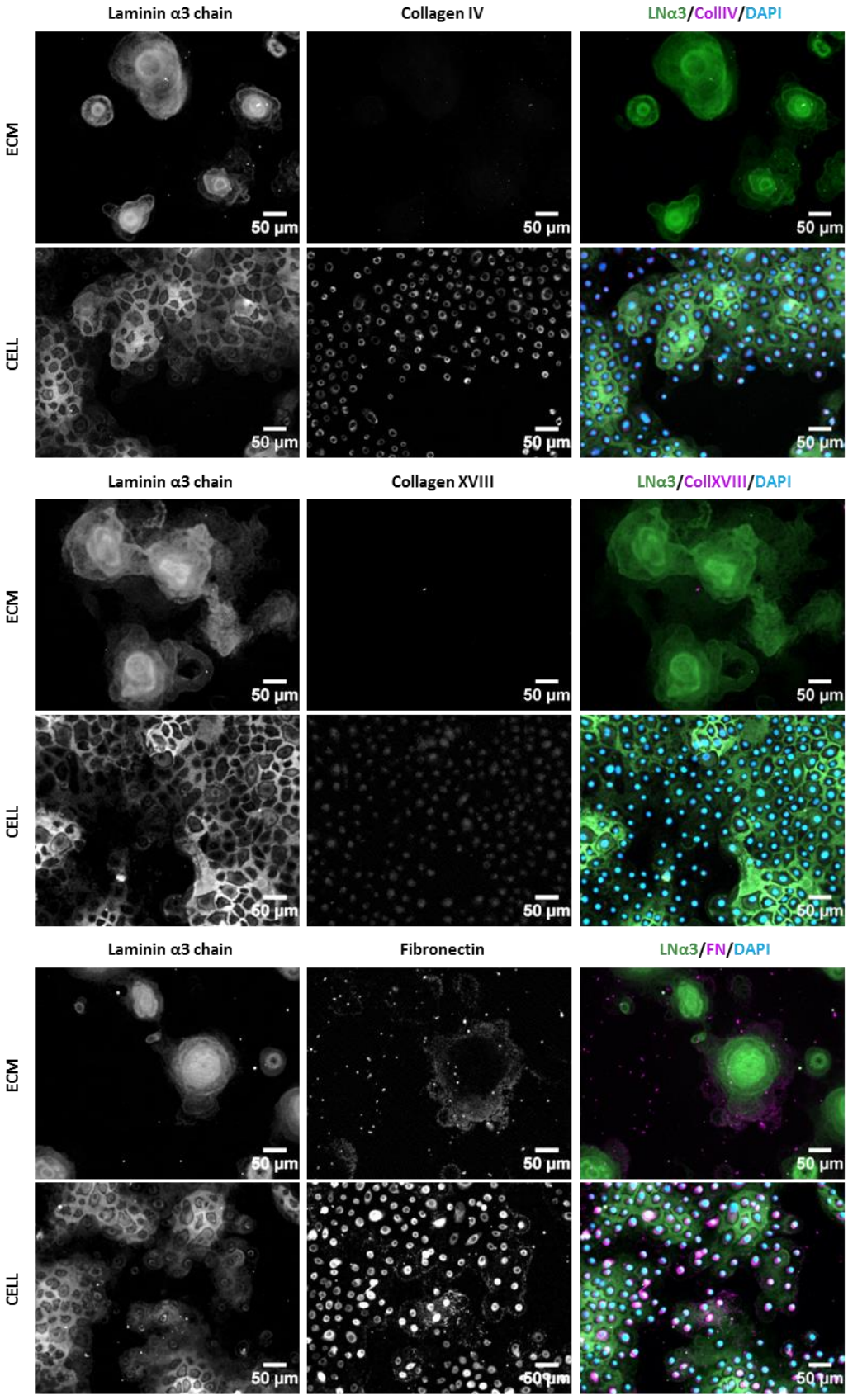

Figure 2.15: Day 7 extracellular matrix; LNα3 - laminin α_3 chain (green), CollIV – type IV collagen (purple), CollXVIII – type XVIII collagen, FN - fibronectin (purple), and DAPI (blue).

Day 14 extracellular matrix

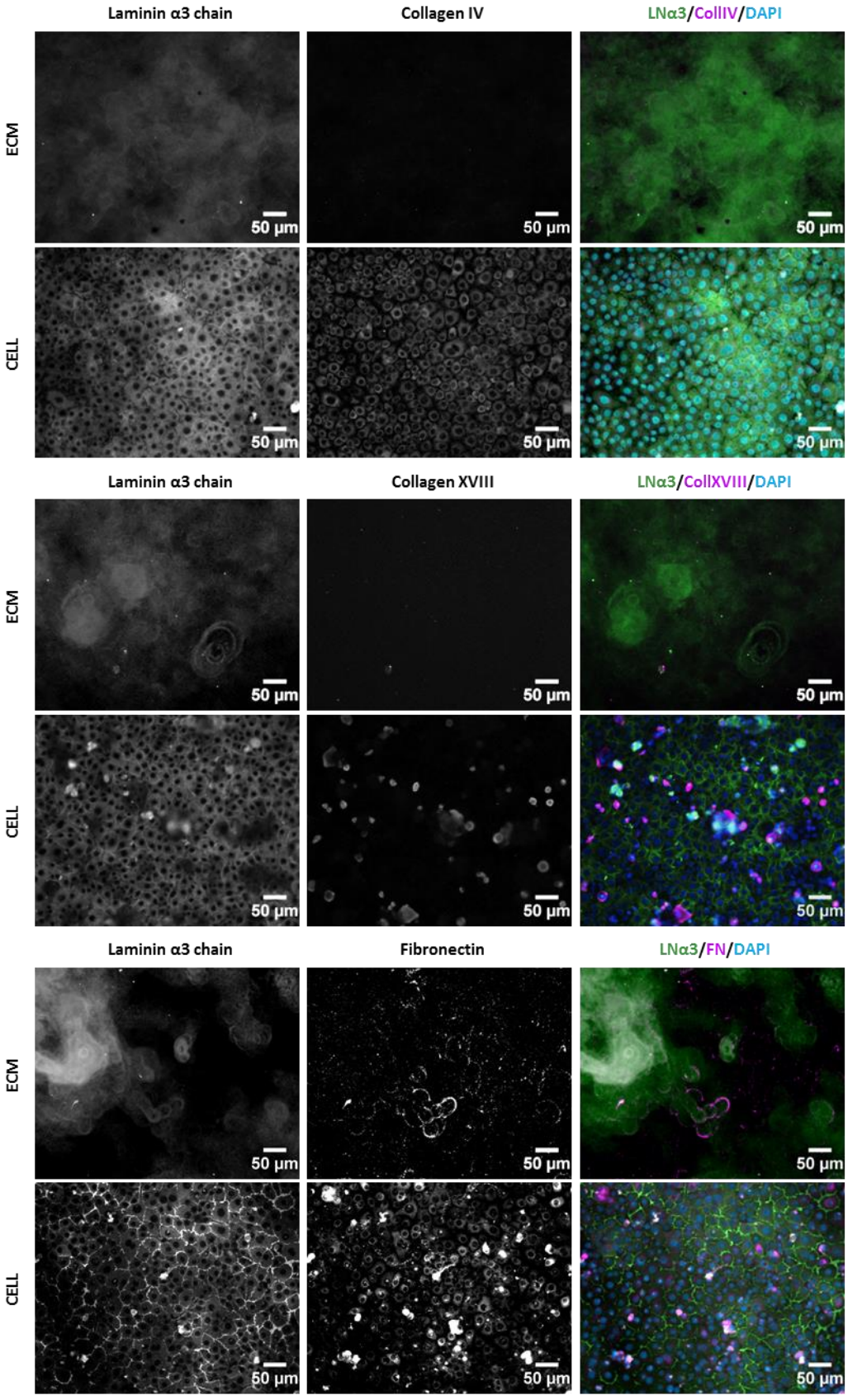

Figure 2.16: Day 14 extracellular matrix; LNα3 - laminin α_3 chain (green), CollIV – type IV collagen (purple), CollXVIII – type XVIII collagen, FN - fibronectin (purple), and DAPI (blue).

Day 21 extracellular matrix

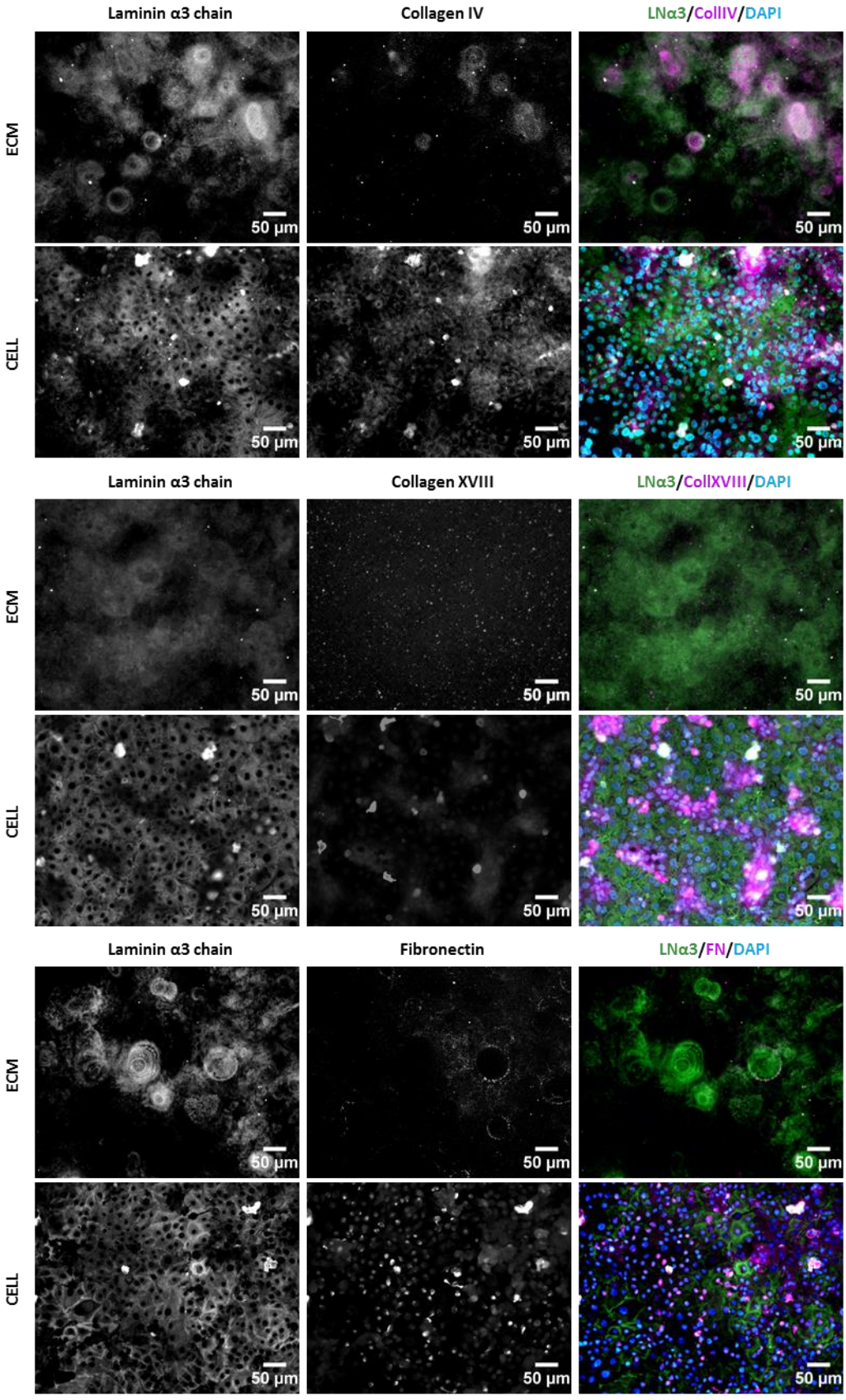

Figure 2.17: Day 21 extracellular matrix; LNα3 - laminin α_3 chain (green), CollIV – type IV collagen (purple), CollXVIII – type XVIII collagen, FN - fibronectin (purple), and DAPI (blue).

Day 28 extracellular matrix

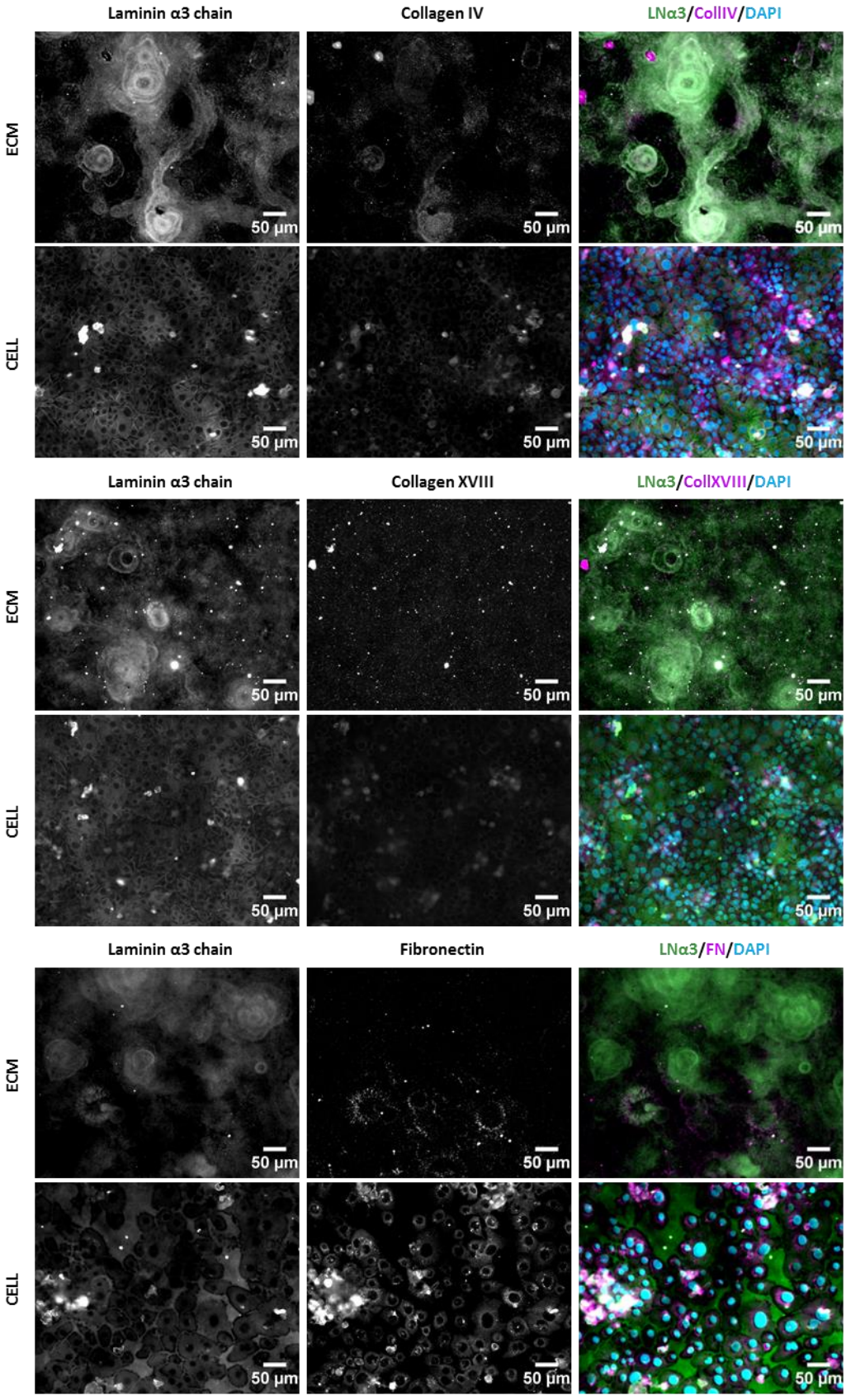

Figure 2.18: Day 28 extracellular matrix; LNα3 - laminin α_3 chain (green), CollIV – type IV collagen (purple), CollXVIII – type XVIII collagen, FN - fibronectin (purple), and DAPI (blue).

Day 42 extracellular matrix

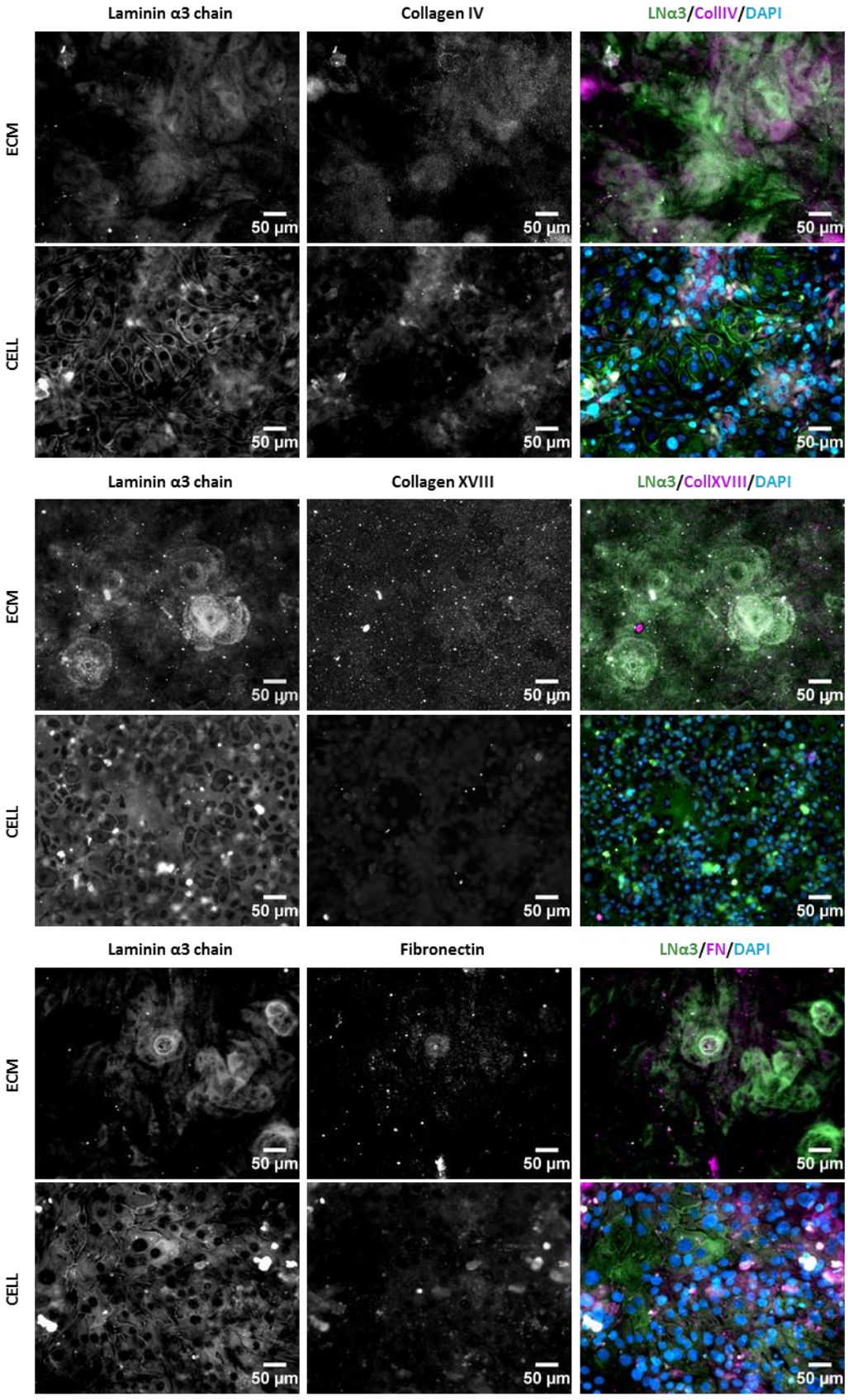

Figure 2.19: Day 42 extracellular matrix; LNα3 - laminin α_3 chain (green), CollIV – type IV collagen (purple), CollXVIII – type XVIII collagen, FN - fibronectin (purple), and DAPI (blue).

Negative controls for immunofluorescence staining

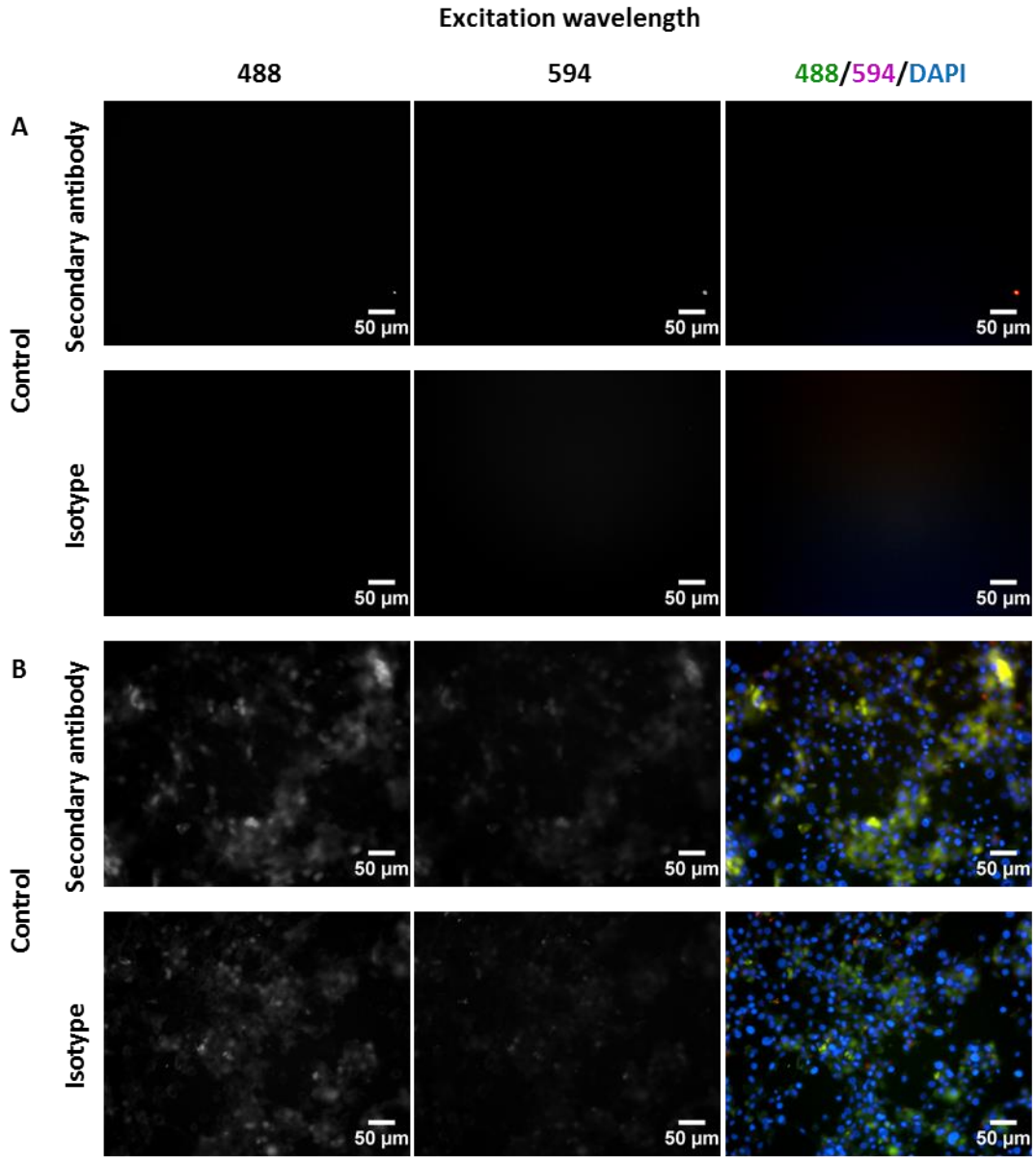

Figure 2.20: Negative controls for immunofluorescence staining used to ensure the specificity of the secondary antibodies and immunoglobulins of the antibodies. This figure is a representative image showing the non-specific staining of the extracellular matrix samples (A) and the cell samples (B) on day forty-two. Qualitatively, there was no significant staining in any of the controls that affected the accurate interpretation of the immunofluorescence staining results.

2.3.4 IDENTIFICATION AND QUANTIFICATION OF HCjE-Gi CELL-SECRETED EXTRACELLULAR MATRIX PROTEINS BY MASS SPECTROMETRY

LC-MS/MS experiments detected peptides of 928 proteins of which only 101 were identified as ECM or ECM-associated proteins using the Uniprot database. The total abundances of ECM and non-ECM peptides followed a similar pattern, where there were statistically significantly lower amount of peptides in the day 1 samples compared to day 7 ($p < 0.001$), similar abundance of peptides from days 7 to 28, and statistically significantly higher abundance of peptides in the day 42 samples compared to day 28 ($p < 0.05$) (figure 2.21). The abundances of the non-ECM peptides were statistically significantly higher than that of the ECM peptides at all the time points ($p < 0.05$). The ECM or ECM-associated proteins were categorised into three major categories: structural (21%), transmembrane (27%) and secreted (52%) proteins (figure 2.22). The structural proteins were sub-categorised into collagens (1%), glycoproteins (16%) and proteoglycans (4%); transmembrane proteins were sub-categorised into integrins (8%) and other (16%); and secreted proteins were sub-categorised into growth factors, binding proteins and cytokines (14%), proteases and inhibitors (17%) and other (24%).

Peptide abundances of extracellular matrix and non-extracellular matrix proteins

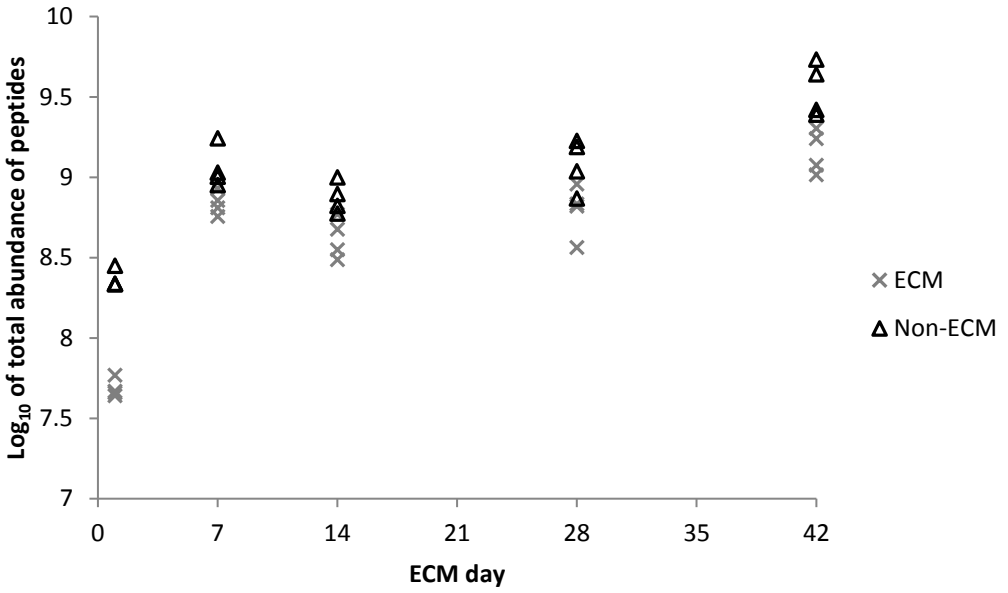

Figure 2.21: Peptide abundances of extracellular matrix and non-extracellular matrix proteins obtained by LC-MS/MS. Data are presented as log_{10} of total abundance of peptides, n = 4. The total abundances of extracellular matrix and non- extracellular matrix peptides followed a similar pattern: there were significantly higher abundance of peptides in the day 7 samples compared to day 1 ($p < 0.001$), similar abundance of peptides from days 7 to 28, and significantly higher abundance of peptides in the day 42 samples compared to day 7 ($p < 0.05$). The total abundance of extracellular matrix peptides was significantly lower compared to the non-extracellular matrix peptides at all the time points ($p < 0.05$). (Two-way ANOVA; Bonferroni post hoc test).

Extracellular matrix proteins secreted by HCjE-Gi cells

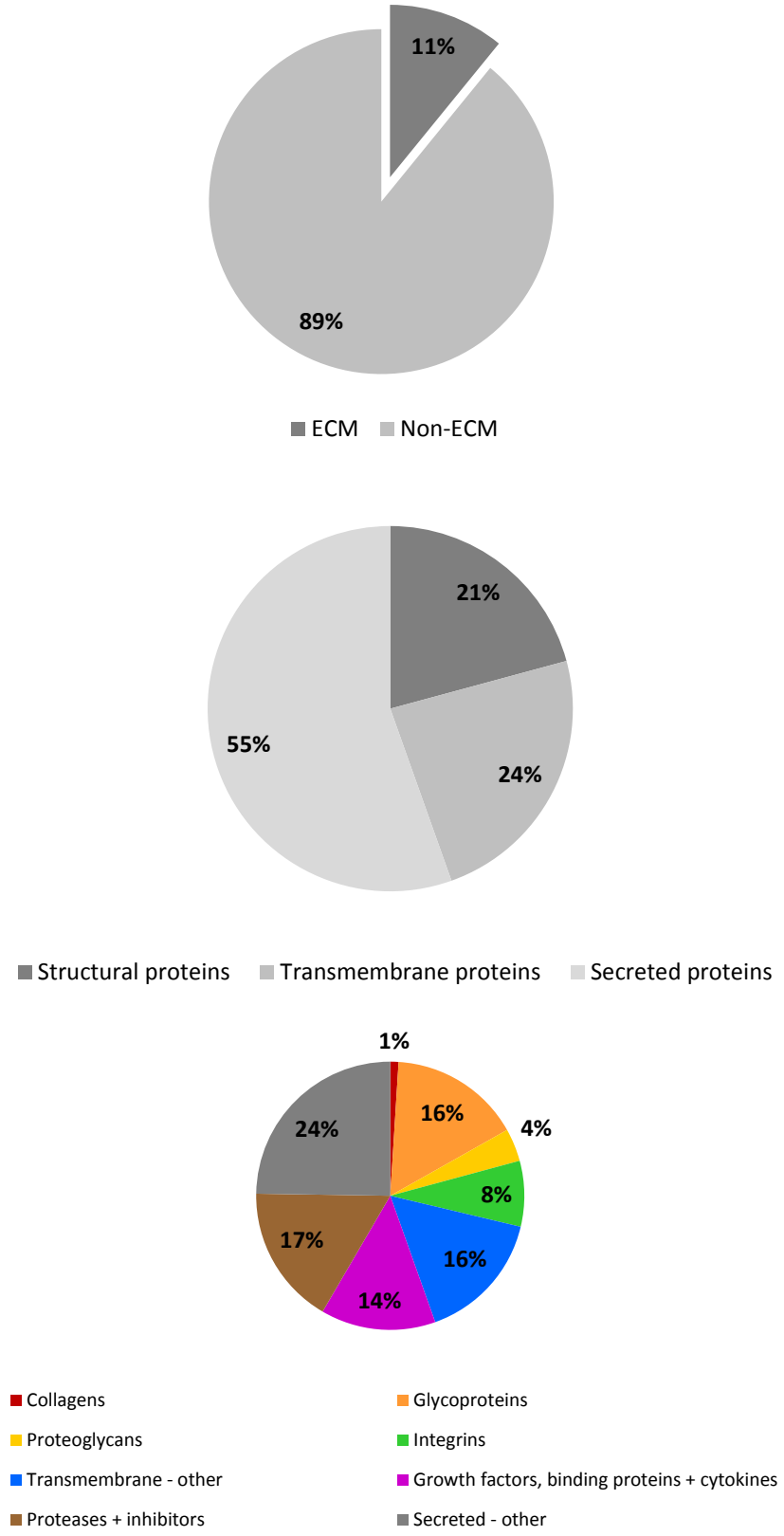

Figure 2.22: Extracellular matrix proteins secreted by HCjE-Gi cells.

Peptide abundances of protein categories

A

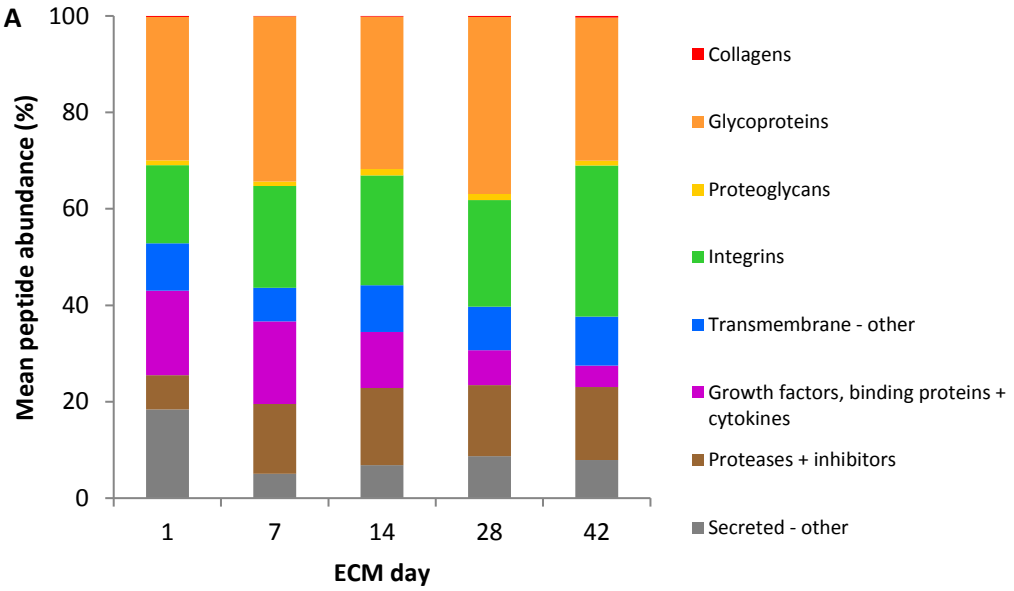

B

	Peptide abundance (%)				
	Day 1	Day 7	Day 14	Day 28	Day 42
Collagens	0.18	0.10	0.13	0.21	0.33
Glycoproteins	29.80	34.25	31.62	36.75	29.69
Proteoglycans	0.95	0.91	1.32	1.23	0.97
Integrins	16.21	21.08	22.76	22.13	31.37
Transmembrane - other	9.85	7.03	9.70	9.00	10.16
GFs, binding proteins + cytokines	17.53	17.08	11.60	7.26	4.44
Proteases + inhibitors	7.10	14.49	16.00	14.74	15.12
Secreted - other	18.40	5.06	6.87	8.68	7.92

Figure 2.23: A. Peptide abundances of protein categories from extracellular matrix days 1 to 42. Data are presented as mean peptide abundance (%), n = 4. There were significantly higher percentage of integrins ($p < 0.001$), and proteases and their inhibitors ($p < 0.001$) in the day 42 extracellular matrix compared to the day 1 extracellular matrix. There were significantly lower percentage of growth factors, their binding proteins and cytokines ($p < 0.001$), and other secreted proteins ($p < 0.001$) in the day 42 extracellular matrix compared to the day 1 extracellular matrix. (Two-way ANOVA; Bonferroni post hoc test). B: Mean peptide abundances (%) of protein categories.

Raw peptide abundances of proteins

	Day 1	Day 7	Day 14	Day 28	Day 42
Collagen α1(XVIII)	85893.78	721109.14	548997.79	1359793.50	5301773.40
α-2-HS-GP	2083234.80	1707513.42	264008.90	360219.21	323144.29
Fibronectin	398540.89	4923114.46	1404979.22	1283281.63	2296536.12
Lactadherin	105634.41	1384108.65	837775.29	1004466.61	2152926.04
Laminin α3	3524280.23	106704413.25	60163700.52	97188944.30	198904909.77
Laminin α5	84341.84	893968.64	1572790.38	1100243.78	1486269.28
Laminin β1	3910.91	123814.24	86096.03	124343.13	362973.58
Laminin β3	2697283.42	46556912.05	27807733.48	48795788.49	80125820.12
Laminin γ1	14565.75	220153.88	144079.98	101942.83	269148.42
Laminin γ2	3550809.41	39394267.90	21342688.32	34070496.40	64471370.42
Matrilin 2	855.88	128598.41	72010.05	108619.42	260938.72
Nephronectin	1258.44	217271.75	52082.65	58918.96	120983.42
Tenascin C	448351.48	2868723.73	2101528.40	6445032.19	9498508.82
Thrombospondin 1	1340194.63	31431773.91	18786972.00	40063227.59	73864516.20
Thrombospondin 2	6266.44	84935.17	119543.94	287767.29	275945.61
TIN Ag-like	76210.64	1578933.02	1825608.31	2588002.50	4268996.55
Vitronectin	36868.03	440663.37	111015.69	206034.18	318013.13
Agrin	179697.00	2817811.30	2577505.53	4291314.22	7832699.26
Perlecan	272727.23	3533524.68	3094285.83	3353530.87	5886213.32
Prolyl 3-hydroxylase 1	62.60	2315.06	4899.88	5050.73	12230.10
Tsukushin	4119.79	51082.66	53026.33	155288.60	208005.38
Integrin α2	60321.01	1091898.98	366551.73	253530.19	2545305.81
Integrin α3	248980.52	1671126.51	1055305.93	1029605.81	4254499.71
Integrin α5	22653.52	408419.57	573475.97	228583.41	723630.82
Integrin α6	3746150.65	70468776.41	49607929.99	63569258.76	184118671.55
Integrin αV	38846.20	557746.34	305230.61	240876.44	1099845.63
Integrin β1	448181.53	5382140.02	2730795.30	2650876.11	11698893.62
Integrin β4	3287507.88	66059716.38	41748179.85	80197640.61	264777156.31
Integrin β6	24515.52	167294.87	78969.46	82379.11	292264.41
BCAM	144019.18	1716180.30	1609268.98	1106506.39	9794177.75
Basigin	439472.30	9948369.82	10593947.67	12511626.42	25843408.54
Cadherin 1	825665.57	6281556.41	6922606.07	7264009.66	7957981.61
CD44	291512.75	3410424.81	2381278.36	2438154.45	7936590.14
CD47	28759.51	240711.73	309211.74	261145.00	665116.23
CD109	664.54	72596.41	29786.18	26096.25	118837.45
CD151	94515.61	979153.54	1239594.90	1400408.10	3581575.91
Collagen α1(XVII)	890007.06	9487028.74	6012916.92	6340464.23	31726583.46
EGF receptor	201782.37	3106415.36	1209196.68	1896117.77	8524097.70
EDDR 1	2316.17	15816.11	1762.85	13467.07	88465.00
Glypican 1	155383.61	2584377.62	897520.14	1924006.86	10055871.68
LYPD 3	61640.26	395969.92	336766.59	581690.88	1064956.41
Putative GGT 3	39594.04	22883.07	17889.66	25938.10	200749.76
Syndecan 1	21064.52	211970.63	294288.23	292987.97	874002.15
Syndecan 4	5787.61	94450.21	89680.16	227238.23	689959.87
TACST 2	1548778.99	10019679.14	8705862.85	22086229.37	40993377.38
CXCL 11	2648.69	163940.53	110773.39	60310.40	61833.52
CXCL 14	7076.60	37983.27	47897.11	118432.86	91111.70
Dermokine	2254.99	37293.89	30790.15	40019.74	185411.77
FGFBP 1	1102579.79	26250731.36	8116908.98	9590750.02	17287884.54
Granulins	6288.74	33173.04	12354.23	36008.75	124618.52
GDF 15	72861.92	781619.04	9945130.49	4990921.14	5723838.05
Insulin	5483128.66	31610906.73	4471388.47	18915734.07	17847672.28
IGFBP 3	423416.89	7370292.75	4950808.23	1248264.76	1570873.65
IGFBP 10	610395.79	25968978.73	10673070.84	6115475.07	8439882.28
LTBP 2	507.79	49520.33	10675.93	4366.10	6883.24
Macrophage MIF	13285.24	56484.04	17208.53	60834.02	177667.63
Midkine	63913.15	2264422.01	2399557.11	618703.76	844572.17
PDGF-A	2004.97	41204.52	54053.07	50677.32	57432.71
TGFβ ig-h3	871889.53	25024450.60	9421466.69	6622215.15	13049269.69
ADAM 10	4400.14	100991.88	47132.95	152447.01	434476.65
ADAM 17	65.25	18308.16	20289.56	44450.32	95838.31
ADAMTS-like protein 6	133623.82	1053013.16	1061674.72	1746619.97	2178424.07
Antileukoproteinase	163020.20	317009.70	359939.68	842259.96	1870278.65
Elafin	2041.20	8246.06	3481.84	14800.23	241272.28
Glia-derived nexin	4625.92	64019.03	55848.01	82838.90	98699.06
HAI 1	18139.24	204655.33	205896.53	223893.73	725640.19
MMP 14	23605.66	345582.11	284781.77	239938.76	1209848.41
MMP 28	12249.49	60763.14	29925.07	149770.06	341202.32
MT-SP 1	122294.06	943738.08	583164.31	884193.00	2699544.94
PAI 1	383335.71	1865190.29	1184975.82	1129833.94	1740556.50
RISC	3818.31	65117.75	77640.61	303199.48	789424.80
Serine protease 23	8113.92	1827281.55	362317.98	1328425.59	4270538.88
Serine protease HTRA1	1067138.80	74675865.99	58395924.74	85108184.15	205083651.57
Serpin B5	471248.28	1380459.78	794684.11	1833961.47	4746042.99
TFPI 2	950445.37	17781684.05	7971086.67	5213198.64	4000204.53
TIMP 3	54559.31	727733.73	357719.14	598162.85	1476544.17
ADM	5982.87	24324.13	56907.16	32285.94	29179.60
Annexin A2	5575283.55	7461760.51	3851580.93	6511081.37	25536113.56
Apolipoprotein E	11685.14	96014.61	117526.29	145278.15	474129.02
Apolipoprotein J	130254.03	2031973.18	2506690.45	3158176.37	4801484.69
β-2-microglobulin	99227.89	1404333.18	842140.55	1128379.26	9130495.94
CCDC 80	47620.96	1851715.83	839781.38	364521.54	592498.54
Dkk 1	5666.27	47485.74	20293.95	6342.90	1263.57
Endothelial lipase	147949.36	960515.72	447637.55	1267494.79	3761050.12
Galectin 1	34640.42	820183.19	525311.90	367348.40	1537384.95
Galectin 3	19219.82	11278.52	6645.57	8335.17	60741.58
Galectin-3-binding protein	896632.53	9585370.14	18006139.82	37198870.04	58783404.85
Hemopexin	9633.78	261667.43	21089.00	198602.20	860584.39
ITI heavy chain H4	11669.33	103092.69	20964.92	62562.34	119735.44
Peroxidasin homolog	68417.69	1571560.75	267089.06	505744.85	1038335.72
Peroxiredoxin 4	60524.11	100529.40	26091.61	75296.52	202159.81
PL transfer protein	268.56	20362.72	7083.00	29721.38	97274.47
Protein Wnt 6	253.96	2099.75	2138.08	8015.51	38756.84
Protein Wnt 7a	21014.41	114697.54	85838.20	200353.82	341230.44
Protein Wnt 7b	1.67	60200.38	58852.73	135148.50	100215.63
Protein Wnt 10a	66816.08	246060.67	207545.45	627695.80	1797005.85
Serotransferrin	919140.97	4254066.31	929921.74	2438528.31	5172906.31
Serum albumin	790076.02	1434003.56	369569.13	474631.16	815332.47
SAA 1	6806.41	96698.72	22099.49	39250.06	209407.66
Tissue factor	9155.29	2646524.67	97670.72	187832.43	4431656.46
AVP-NPII	37487.27	73522.39	23483.88	63927.69	65073.78

Figure 2.24: Raw peptide abundances of proteins from extracellular matrix days 1 to 42.

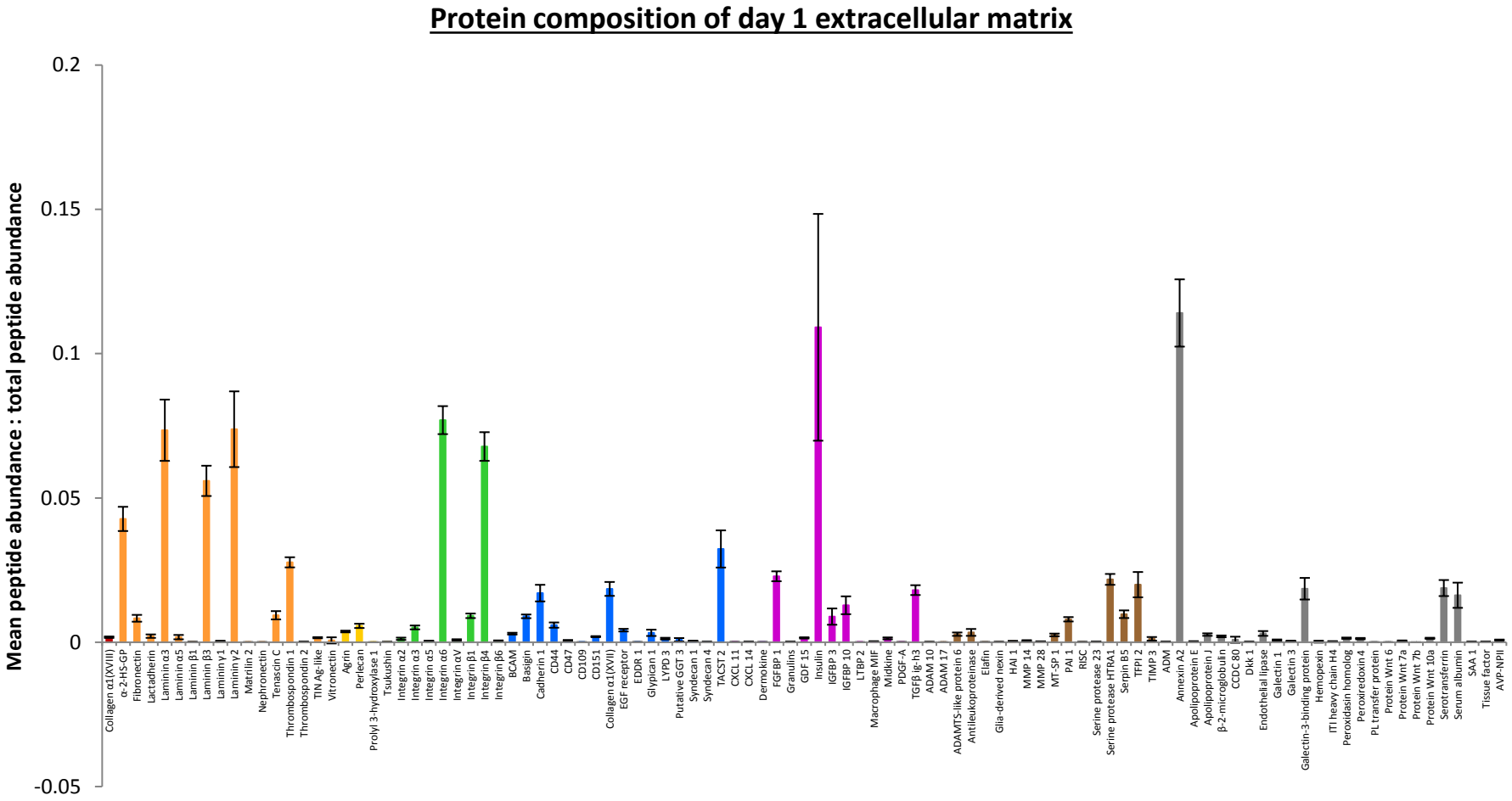

Figure 2.25: Protein composition of day 1 extracellular matrix secreted by HCjE-Gi cells. Data are presented as mean peptide abundance: total peptide abundance ± 1SD, n = 4.

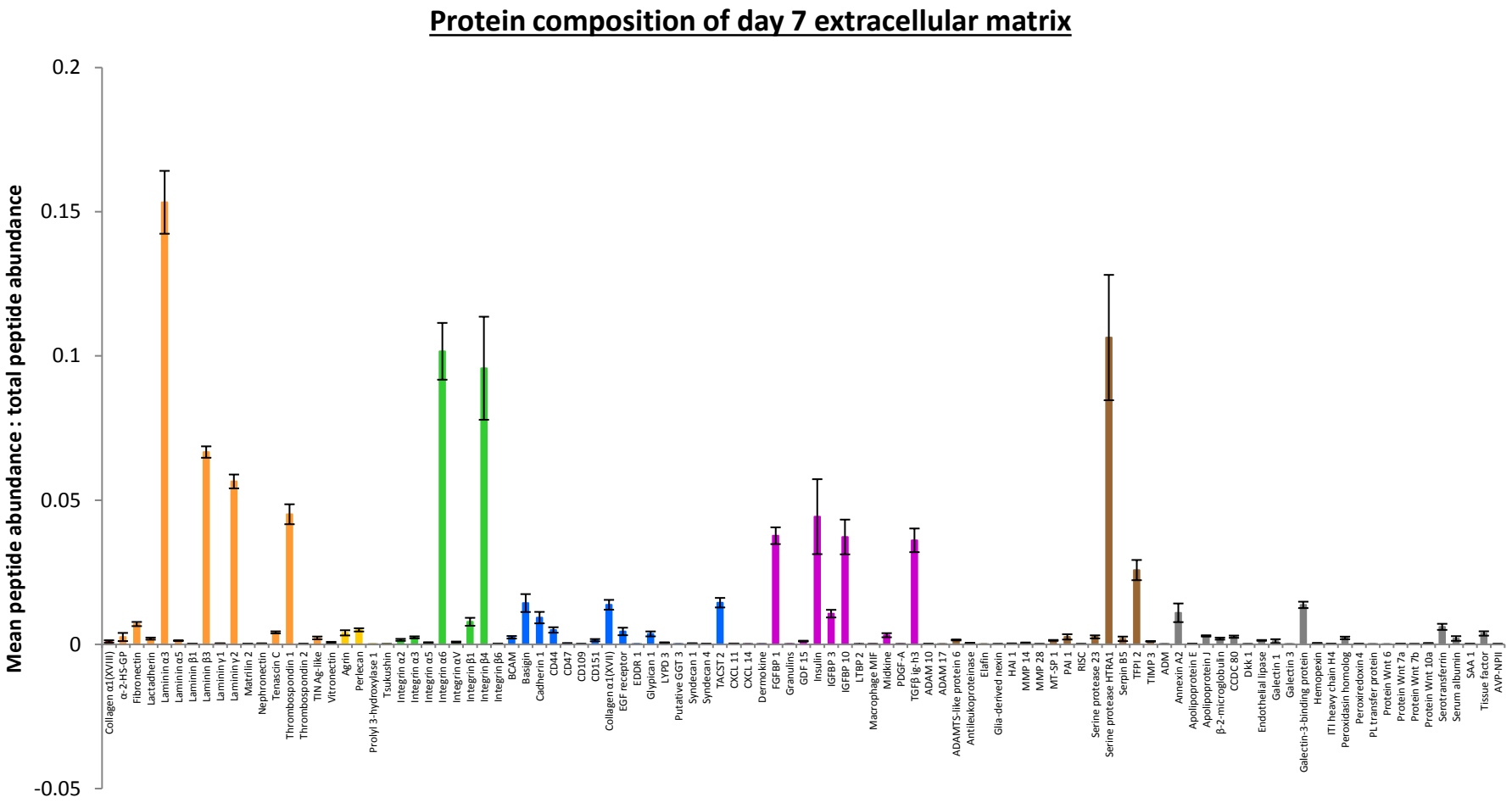

Figure 2.26: Protein composition of day 7 extracellular matrix secreted by HCjE-Gi cells. Data are presented as mean peptide abundance: total peptide abundance ± 1SD, n = 4.

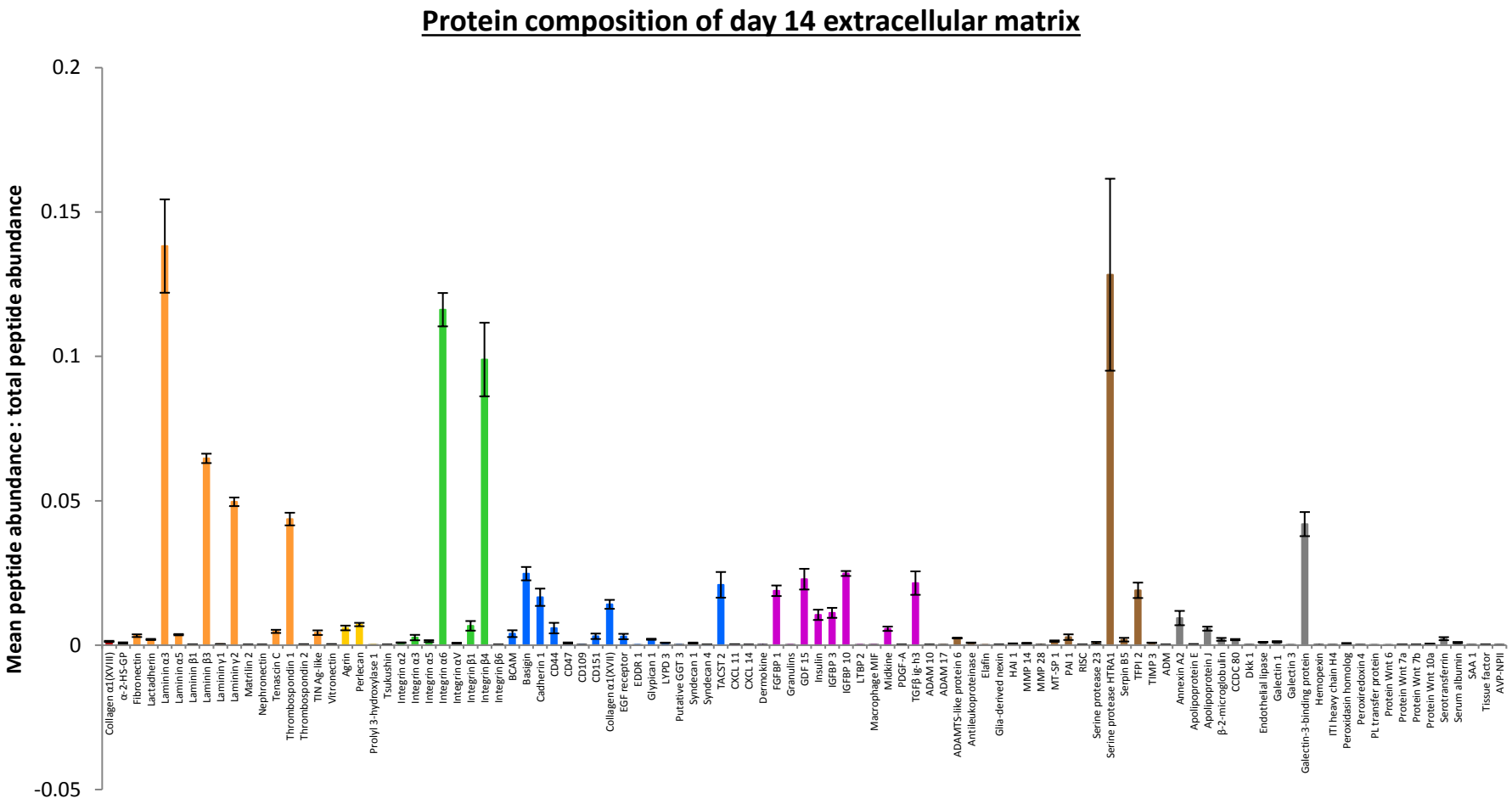

Figure 2.27: Protein composition of day 14 extracellular matrix secreted by HCjE-Gi cells. Data are presented as mean peptide abundance: total peptide abundance ± 1SD, n = 4.

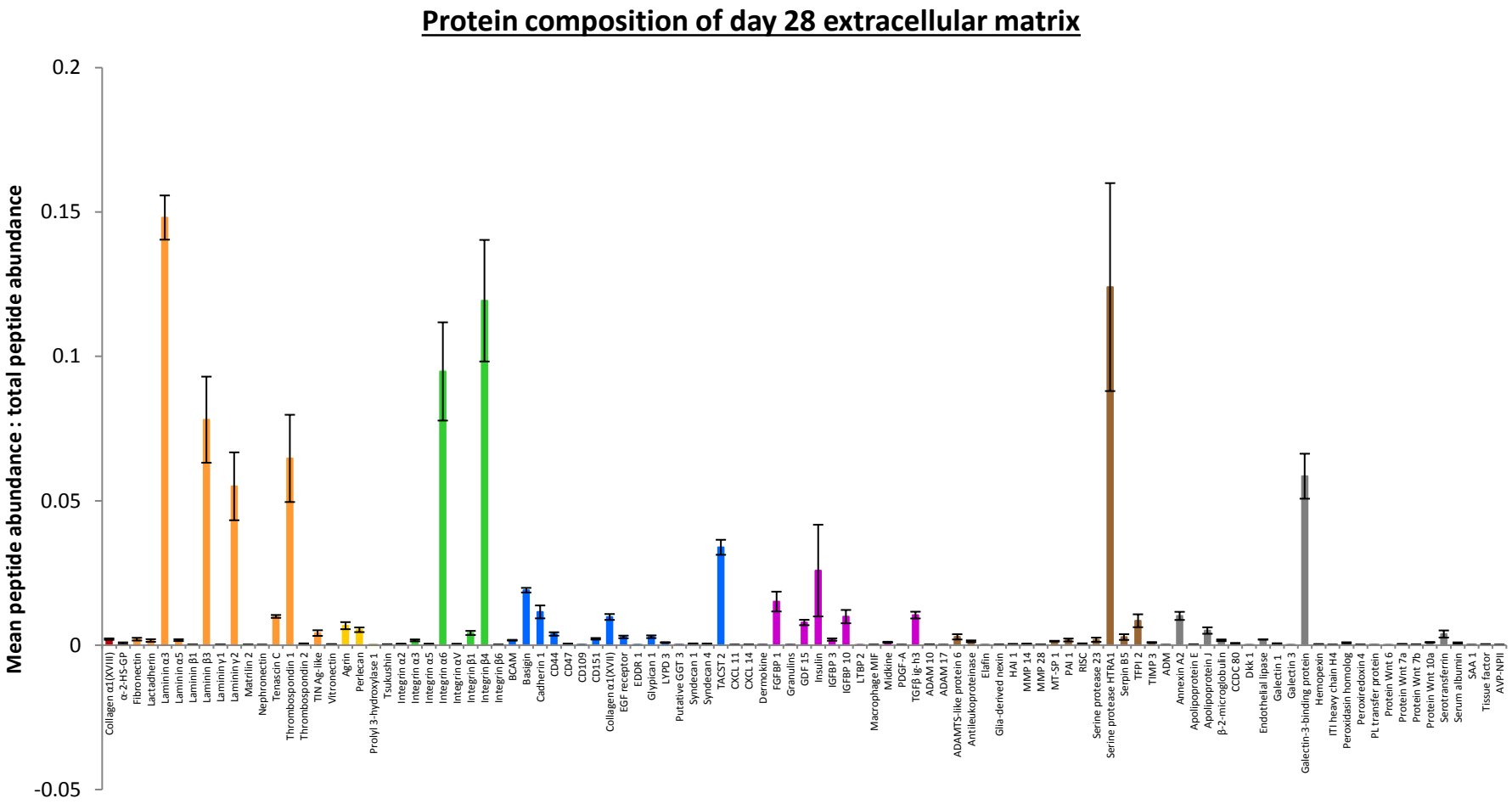

Figure 2.28: Protein composition of day 28 extracellular matrix secreted by HCjE-Gi cells. Data are presented as mean peptide abundance: total peptide abundance ± 1SD, n = 4.

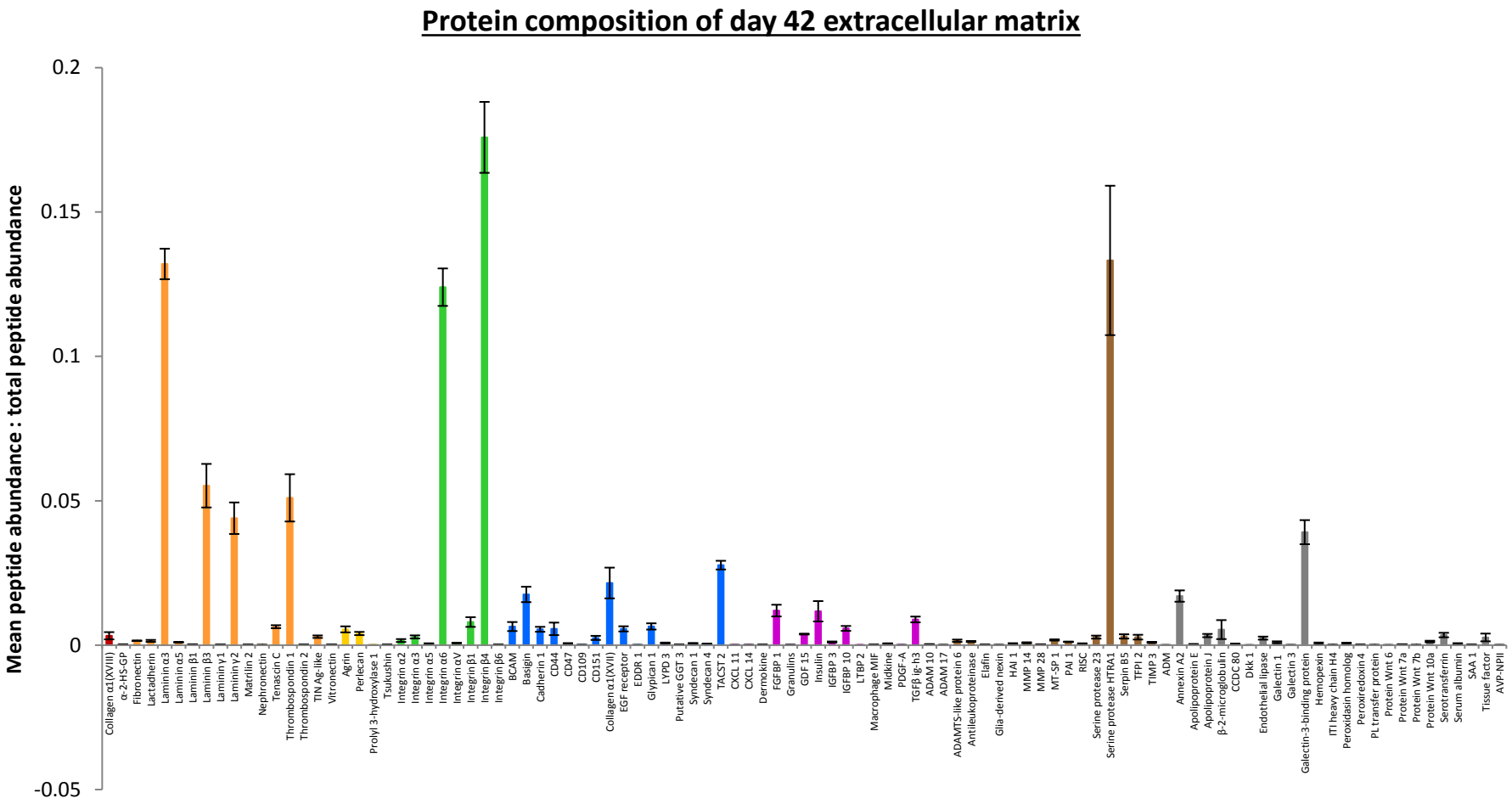

Figure 2.29: Protein composition of day 42 extracellular matrix secreted by HCjE-Gi cells. Data are presented as mean peptide abundance: total peptide abundance ± 1SD, n =4.

2.3.4.1 STRUCTURAL PROTEINS (Figures 2.23-2.30)

Collagens

LC-MS/MS experiments did not show the presence of type IV collagen. However, it did identify the α_1 chain of type XVIII collagen in all the samples at all the time points investigated. The mean raw peptide abundance increased from day 1 to 42, the highest being present in the day 42 ECM sample. The peptides of the structural collagens only contributed 0.18% of the day 1 ECM and 0.33% of the day 42 ECM, which was not found to be statistically significant ($p = 1.000$).

Glycoproteins

Sixteen GPs were identified in the HCjE-Gi cell-secreted ECM, all of which contributed to 29.69-36.75% of the ECM, highest observed on day 28. There was a statistically significantly higher percentage of GPs in the day 7 ECM compared to day 1 ECM ($p = 0.003$), and in the day 28 ECM compared to day 14 ECM ($p < 0.001$). There was a statistically significant reduction to the percentage of GPs in the day 42 ECM compared to day 28 ($p < 0.001$). There was, however, no statistically significant difference to the percentage of GPs between the day 1 and day 42 ECM samples ($p = 1.000$).

Laminin α_3 chain was the most abundant GP throughout all the time points contributing to 7.3% of all peptides in the day 1 ECM and 13.2% of all peptides in the day 42 ECM. The raw peptide abundance of this protein increased statistically significantly on day 7 compared to day 1 ($p = 0.007$) and then continued to increase, highest peptide abundance being observed on day 42. There was no significant difference between the raw peptide abundances in the day 7 and day 42 ECM samples ($p = 0.250$). The raw peptide abundances of laminin β_3 and γ_2 also followed a similar pattern increasing statistically significantly on day 7 compared to day 1 ($p = 0.009$ and $p = 0.009$, respectively) and continued to increase with time, highest being observed on day 42. The proportion of laminin β_3 peptides remained relatively stable throughout the six weeks (approximately 5.5%), whereas that of laminin γ_2 reduced (7.4% in the day 1 ECM and 4.4% in the day 42 ECM). Other laminin chains that were detected by LC-MS/MS were α_5, β_1 and γ_1, all of which increased in abundance and contributed to less than 1% of the ECM at all the time points investigated. There was a statistically significant increase in the raw peptide abundance of laminin α_5 chain from day 1 to 7 ($p = 0.009$), laminin β_1 chain from day 1 to 14 ($p = 0.001$) and laminin γ_1 chain from day 1 to 14 ($p = 0.017$).

Thrombospondins 1 and 2 were present in the ECM secreted by the HCjE-Gi cells throughout the six weeks. The peptide abundance of thrombospondin 1 was higher than that of thrombospondin 2, contributing to 2.8% of the day 1 ECM and 5.1% of the day 42 ECM. The proportion of peptides of thrombospondin 2 in the ECM was negligible, 0.01% in the day 1 ECM and 0.02% in the day 42 ECM. The raw peptide abundance of thrombospondin 1 increased statistically significantly from day 1 to 7 (p= 0.001), from day 14 to 28 (p = 0.014) and from day 28 to 42 (p < 0.001). There was a statistically significant increase in the raw peptide abundance of thrombospondin 2 from day 14 to 28 (p = 0.018) and no significant differences were observed thereafter.

Three adhesive proteins, fibronectin, nephronectin and vitronectin were detected on mass spectrometry, highest raw peptide abundance being observed in the day 7 ECM. The raw peptide abundance of fibronectin was significantly higher on day 7 compared to all the other time points investigated (p < 0.05). It contributed to 0.8% of the day 1 ECM and reduced gradually to contribute 0.2% of the day 42 ECM. Nephronectin and vitronectin contributed in negligible amounts to the ECM of the HCjE-Gi cells. The raw peptide abundance of nephronectin was statistically significantly higher on day 7 compared to that in the day 1 and day 14 ECM samples (p = 0.004 and p = 0.003, respectively). However, the higher raw peptide abundance of vitronectin observed on day 7 was not statistically significant compared to the other time points (p > 0.05).

The raw peptide abundance of α-2-HS-GP was highest on day 1 and statistically significantly reduced from day 14 onwards (p = 0.01). It contributed to 4.3% of the day 1 ECM, 0.3% of the day 7 ECM and continued to reduce thereafter. Other GPs detected were lactadherin, matrillin 2, tenascin C and tubulointerstitial nephritis antigen-like (TIN Ag-like) proteins. The raw peptide abundances of all increased over the six weeks, highest being observed in the day 42 ECM, which was significantly higher than that observed on day 1 (p < 0.05). All these proteins contributed to less than 1% of the ECM at all the time points.

Proteoglycans

There were four PGs that were identified in the ECM of the HCjE-Gi cells. The total peptide abundance contributed by the PGs remained relatively stable over the six weeks in culture (0.91-1.32%), the highest percentage being observed on day 14. There was no statistically significant difference in the percentage of PGs in the day 1 ECM compared to the day 42 ECM (p = 1.000).

The raw peptide abundance of perlecan significantly increased between days 1 and 7 (p = 0.022) and remained relatively constant over the six weeks, highest being on day 42. Similarly, the raw peptide abundance of agrin also increased over the six weeks, highest being on day 42, which was significantly higher than all the other time points. Perlecan was the most abundant PG on day 1 (0.6% of the ECM) and its proportion reduced by day 42 (0.4% of the ECM), highest proportion being observed in the day 14 ECM (0.7%). In contrast, the proportion of agrin in the ECM increased with time, surpassing perlecan on day 28 and was the most abundant PG in the day 42 ECM (0.5%). The raw peptide abundance of tsukushin increased statistically significantly from day 14 to day 28 (p = 0.008) and no significant differences were observed thereafter. Prolyl 3-hydroxylase 1 was only present in one sample of the four day 1 ECM samples. The abundance of this protein statistically significantly increased from day 1 to 7 (p = 0.039) and continued to increase until day 42, although not statistically significant. Tsukushin and prolyl 3-hydroxylase 1 contributed to less than 1% of the ECM at all the time points investigated.

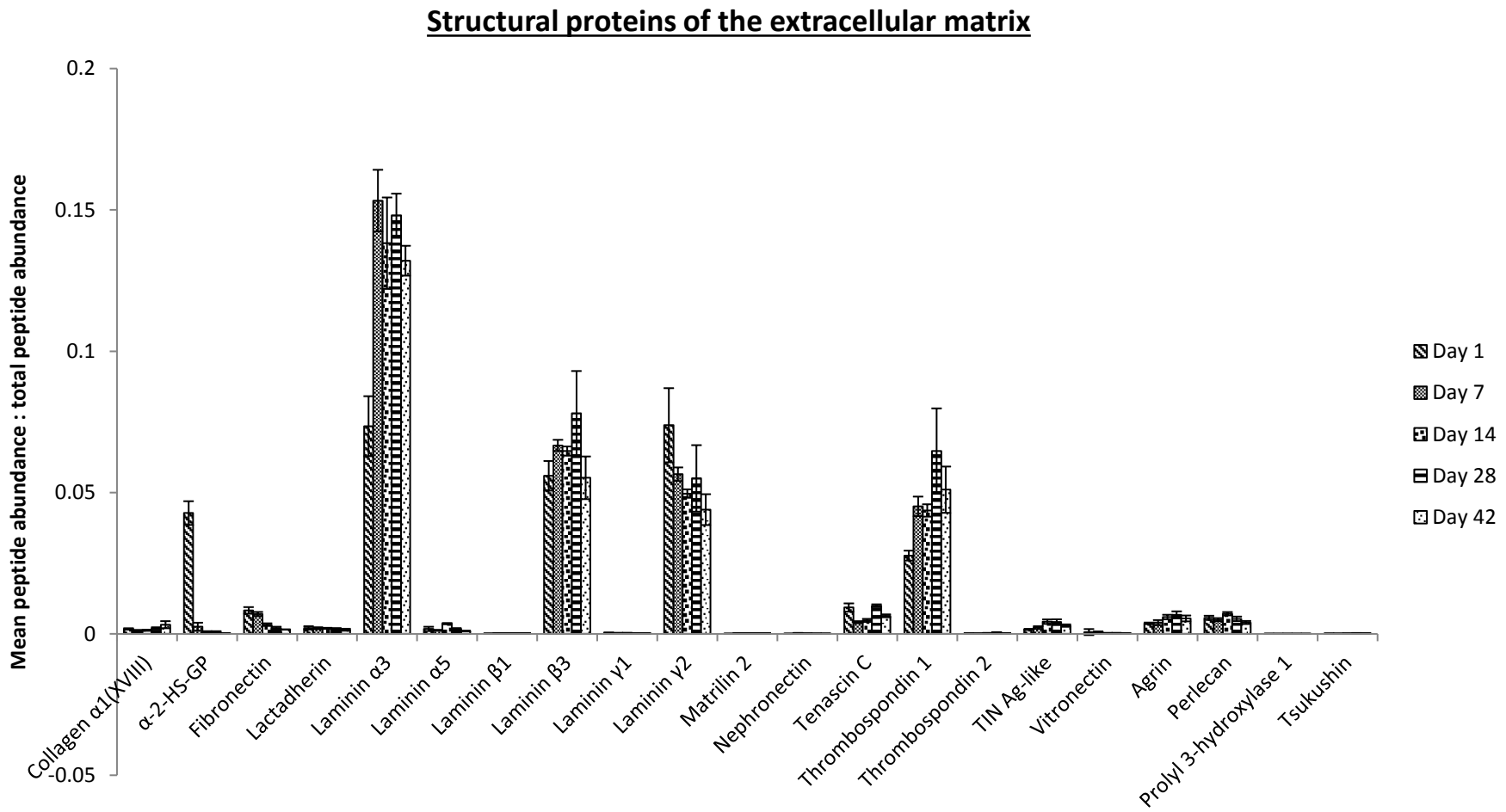

Figure 2.30: Proportions of structural proteins in the extracellular matrix from days 1 to 42. Data are presented as mean peptide abundance: total peptide abundance ± 1SD, n = 4.

2.3.4.2 TRANSMEMBRANE PROTEINS (Figures 2.23-2.29 and 2.31)

Integrins

Integrins α_2, α_3, α_5, α_6, α_V, β_1, β_4 and β_6 were identified in all the ECM samples at all the time points. In the day 1 ECM, integrins contributed to 16.21% of all ECM proteins and increased with time to contribute to 31.37% of all ECM proteins by day 42, which was statistically significant ($p < 0.001$). The percentage of integrins in the ECM between days 7 and 28 was not found to be statistically significant ($p = 1.000$).

In general, all the integrins increased with time and the highest raw peptide abundance was observed on day 42. Only the increase in raw peptide abundances for integrins α_5, α_6, α_v, β_1 and β_4 were statistically significant in the day 42 ECM compared to the day 1 ECM ($p < 0.05$). Integrin α_6 was the most abundant integrin in the day 1 to 14 ECM samples (7.7% and 11.6% of the ECM, respectively), whereas integrin β_4 was the most abundant integrin in day 28 and day 42 ECM samples (11.9% and 17.6%, respectively). All other integrins contributed to less than 1% of the ECM proteins throughout the six weeks in culture, integrin β_1 being the most abundant, next α_3, α_2, α_V, α_5 and β_6 being the least abundant in the day 42 ECM secreted by the HCjE-Gi cells.

Transmembrane - other

LC-MS/MS experiments showed the presence of peptides of sixteen other transmembrane proteins, of which the raw peptide abundances increased over the six weeks, highest being observed in the day 42 ECM. Their proportion relative to the total ECM proteins remained relatively stable (7.03-10.16%), highest observed in the day 42 ECM sample. There was no statistically significant difference between the percentage in the day 1 and day 42 ECM samples ($p = 1.000$)

The hemidesmosome proteins, α_1 chain of type XVII collagen and CD151, contributed to 1-2% and 0.1-0.3% of the ECM, respectively. The raw peptide abundances of these proteins were significantly higher on day 42 compared to that in the day 1 ECM ($p < 0.05$). After the integrins, the next most abundant transmembrane proteins were tumour-associated calcium signal transducer 2 (TACST 2), basigin, glypican 1 and basal cell adhesion molecule (BCAM), which contributed to 2.8%, 1.8%, 0.6% and 0.6% of the day 42 ECM, respectively. Only the increase in raw peptide abundances observed for TACST 2 and basigin in the day 42 ECM compared to day 1 were found to be statistically significant ($p < 0.05$).

Syndecans 1 and 4 were present in all the ECM samples, former being more abundant at all the time points investigated. Although the highest raw peptide abundances were observed on day 42 for both proteins, only that for syndecan 1 was significantly higher compared to that in the day 1 ECM ($p = 0.026$). Other transmembrane proteins identified in the ECM of HCjE-Gi cells were cadherin 1, CD44, CD47, CD109, EGF receptor, epithelial discoidin domain-containing receptor 1 (EDDR 1), Ly6/PLAUR domain-containing protein 3 (LYPD 3) and putative gamma-glutamyltranspeptidase 3 (GGT 3) proteins. All these proteins had the highest raw peptide abundances in the day 42 ECM, however, this was only found to be statistically significant compared to that in the day 1 ECM for cadherin 1, CD44, CD47 and LYPD 3 ($p < 0.05$).

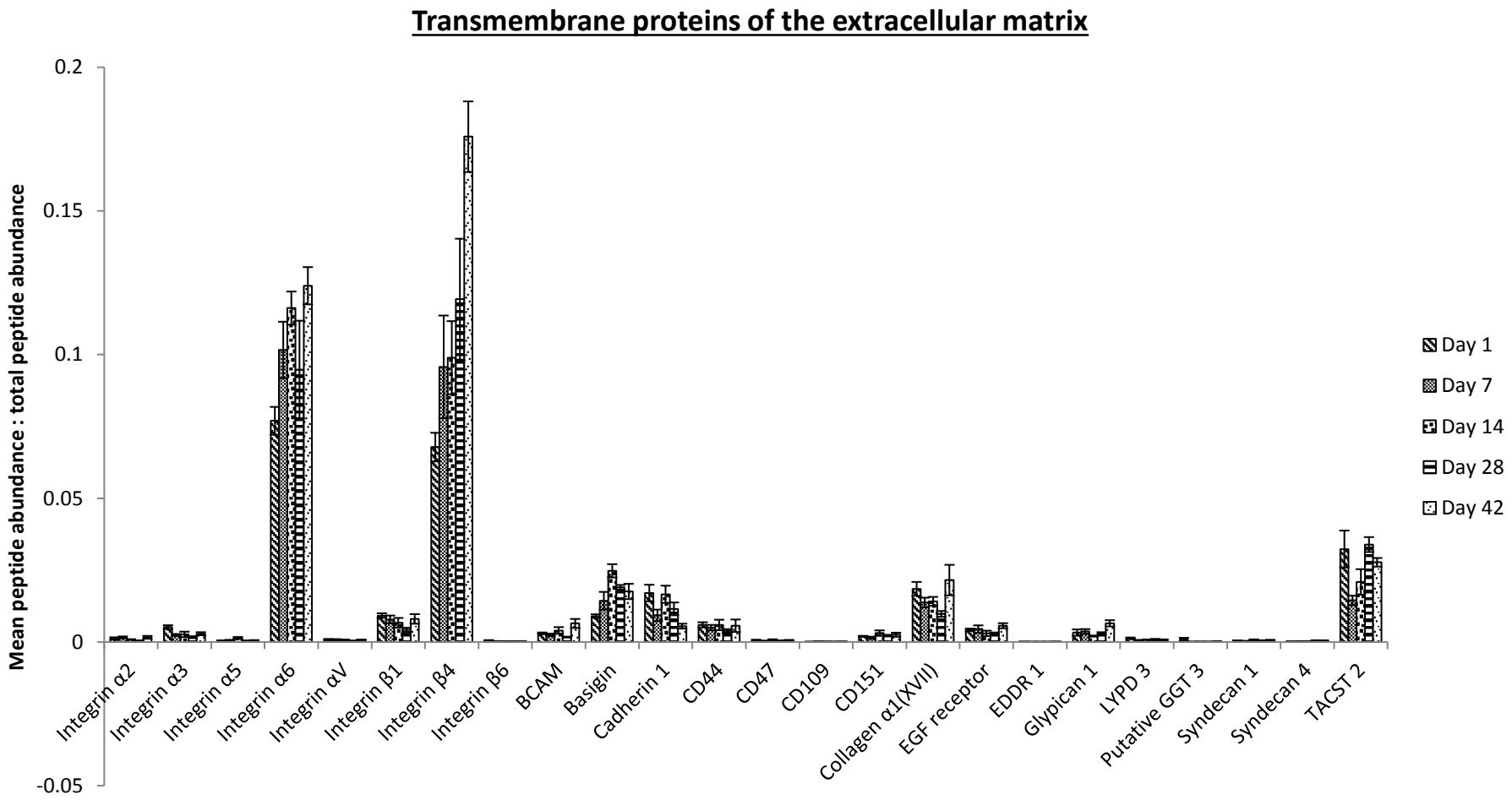

Figure 2.31: Proportions of transmembrane proteins in the extracellular matrix from days 1 to 42. Data are presented as mean peptide abundance: total peptide abundance ± 1SD, n = 4.

2.3.4.3 SECRETED PROTEINS (Figures 2.23-2.29 and 2.32-2.33)

Growth factors, binding proteins and cytokines

There were fourteen proteins identified as GFs, their binding proteins and cytokines that contributed to 17.53% of the day 1 ECM and 17.08% of the day 7 ECM, which was not statistically significant (p = 1.000). However, the percentage reduced statistically significantly from day 7 to day 28 ($p < 0.05$) and no statistically significant difference was observed between the day 28 and day 42 ECM samples (p = 0.213). These proteins contributed to only 4.4% of the day 42 ECM.

C-X-C motif chemokine (CXCL) 11, FGF binding protein 1 (FGFBP 1), insulin, insulin-like GF binding protein (IGFBP) 3, IGFBP 10 (also known as protein CYR61 – cysteine rich angiogenic inducer 61), LTBP 2 and TGFβ-induced protein ig-h3 (TGFβ ig-h3) had the highest raw peptide abundances on day 7 and reduced thereafter. This increase in the day 7 ECM was not found to be statistically significant compared to the other time points in the case of CXCL 11 and insulin ($p > 0.05$). However, insulin was the most abundant protein in this category in the day 1 ECM and day 7 ECM contributing to 10.9% and 4.4% of the total ECM, respectively. CXCL 11 contributed to less than 1% of the total ECM at all the time points. The increase in the raw peptide abundances of FGFBP 1, IGFBP 10 and TGFβ ig-h3 in the day 7 ECM were found to be statistically significant compared to that in the day 1 and day 14 ECM samples ($p < 0.05$). The peptides of these proteins contributed to 3.8%, 3.7% and 3.6% of the day 7 ECM, respectively. A statistically significant increase to the raw peptide abundances of IGFBP 3 and LTBP 2 were observed in the day 7 ECM compared to day 1 ($p < 0.05$), which significantly reduced after day 28 compared to that in the day 7 ECM ($p < 0.05$).

The raw peptide abundance of growth differentiation factor (GDF) 15 was highest on day 14, which was significantly higher than that on day 1 and 7 ($p < 0.05$), however, was not significant compared to that on day 28 and day 42 ($p > 0.05$). The highest raw peptide abundance of midkine was also observed on day 14, which was significantly higher than that on day 1, 28 and 42 ($p < 0.05$). The raw peptide abundance of CXCL 14 was highest in the day 28 ECM, which was significantly higher compared to that in the day 1 and day 7 ECM samples ($p < 0.05$). The raw peptide abundance of platelet derived growth factor A (PDGF-A) increased significantly on day 7 compared to day 1 (p = 0.001) and no significant differences were observed between days 7 and 42. Dermokine, granulins and macrophage migration inhibitory factor (MIF) had the highest raw peptide abundances in the day 42

ECM, which was not significantly different compared to that in the day 1 ECM ($p > 0.05$). All these proteins contributed to less than 1% of the ECM throughout the six weeks.

Proteases and inhibitors

The ECM of the HCjE-Gi cells consisted of seventeen proteases and their inhibitors that contributed to 7.10% of the day 1 ECM, which increased statistically significantly to contribute to 14.49% of the day 7 ECM ($p < 0.001$). There was no statistically significant difference to the percentage between the day 7 and day 42 ECM samples ($p = 1.000$). The proportion of proteases to their inhibitors varied over the six weeks culture period (figure 2.34). The peptide abundance of proteases increased, whereas that of the inhibitors decreased from days 1 to 42 ($p < 0.001$). There were significantly higher proportions of proteases in the ECM of days 7 to 42 compared to their inhibitors ($p < 0.001$).

The most abundant protein in this category at all the time points was serine protease high-temperature requirement A1 (HTRA1), which contributed to 2.2% of the day 1 ECM and 13.3% of the day 42 ECM. Its raw peptide abundance significantly increased in the day 7 ECM compared to day 1 ($p = 0.023$) and no further differences were observed between day 7 and day 42 ($p = 0.198$). The next most abundant protein was tissue factor pathway inhibitor 2 (TFPI 2). The raw peptide abundance was significantly higher in the day 7 ECM ($p < 0.001$) compared to the other points and the abundance gradually reduced with time. It contributed to 2.6% of the day 7 ECM and 0.3% of the day 42 ECM.

All the other proteins contributed to less than 1% of the ECM at all the time points investigated. Proteases that were present in the ECM were ADAM 10, ADAM 17, ADAMTS-like protein 6, MMP 14, MMP 28, membrane type serine protease 1 (MT-SP 1) and serine protease 23. The raw peptides abundances of all these proteins, except that of serine protease 23, increased significantly over the six weeks ($p < 0.05$). The raw peptide abundance of serine protease 23 was significantly higher on day 7 compared to day 1 and 14 ($p = 0.029$ and $p = 0.035$, respectively). Although the highest peptide abundance was observed on day 42, this was not found to be significantly different from that observed on day 7 ($p = 0.235$).

The raw peptide abundances of antileukoproteinase, glia-derived nexin and hepatocyte GF activator inhibitor type 1 (HAI 1) significantly increased in the day 42 ECM compared to the day 1 ECM ($p < 0.05$). Although increases to the raw peptide abundances were also

observed in the day 42 ECM compared to the day 1 ECM for elafin, plasminogen activator inhibitor (PAI), retinoid-inducible serine carboxypeptidase (RISC) and serpin B5, these were not found to be statistically significant ($p < 0.05$). There was a statistically significant increase to the raw peptide abundance of TIMP 3 in the day 7 ECM compared to the day 1 and day 14 ($p = 0.007$ and $p = 0.039$). The raw peptide abundance gradually increased with time, however, this was not found to be significant between the ECM of day 7 and day 42 ($p = 0.323$).

Secreted - other

There were twenty-five other secreted proteins identified as being present in the ECM of the HCjE-Gi cells. There was a statistically significant reduction to the percentage of peptides in this category in the day 7 ECM compared to the day 1 ECM ($p < 0.001$), however, no further significant differences were observed from day 7 to day 42.

In the day 1 ECM, the most abundant protein was annexin A2, the raw peptide abundance of which gradually increased over the six weeks. However, this increase was not statistically significant ($p = 0.079$). It contributed to 11.4% of the day 1 ECM and its proportion relative to the other proteins reduced with time and only contributed to 1.7% of the day 42 ECM. The highest proportion of galectin-3-binding protein was in in the day 14 to day 42 ECM samples. Its raw peptide abundance significantly increased gradually over the six weeks ($p = 0.025$), contributing to 3.9% of the day 42 ECM. The raw peptide abundance of galectin 1 was higher than that of galectin 3 at all the time points. Although, the raw peptide abundance of both increased over the six weeks, this was not found to be statistically significant ($p > 0.05$).

There were four Wnt ligands, Wnt 6, 7a, 7b and 10a that are associated with the Wnt signalling pathway. Wnt 10a was the most abundant out of the four throughout the six weeks. The raw peptide abundances of the four proteins significantly increased over the six weeks ($p < 0.05$), however, their contribution to the ECM was less than 1% at all the time points investigated. Dickkopf-related protein 1 (Dkk 1), a canonical Wnt signalling antagonist, was also present, significantly higher in the day 7 ECM compared to the other time points ($p < 0.001$).

The raw peptide abundance of the coiled-coil domain-containing protein 80 (CCDC 80) was significantly higher on day 7 than the other time points ($p < 0.05$). There was a significantly

higher raw peptide abundance of serotransferrin on day 7 compared to day 1 and 14 (p = 0.003), however, the peptide abundance gradually increased and no significant difference was observed between day 7 and day 42 ECM samples (p = 0.716). Serotransferrin contributed to 1.3% of the day 1 ECM and reduced to 0.4% of the day 42 ECM. Similar pattern of raw peptide abundance was observed for tissue factor as well. Vasopressin-neurophysin 2-copeptin (AVP-NPII) had a significantly lower raw peptide abundance in the day 14 ECM compared to day 7 (p = 0.034), but the peptide abundance gradually increased with time and no significant difference was observed between day 7 and day 42 ECM samples (p= 0.979). The raw peptide abundance of peroxidasin homolog significantly increased on day 7 compared to day 1 (p = 0.041), however, no significant difference was observed between days 7 and 42 (p = 0.431). Serum albumin contributed to 1.6% of the day 1 ECM and reduced with time. Its raw peptide abundance was highest in the day 7 ECM, which was not statistically significant compared to the other time points (p > 0.05). Adrenomedullin (ADM) had significantly higher raw peptide abundance in the day 14 ECM compared to other time points (p < 0.001).

The raw peptide abundances of apolipoprotein E and J (also known as clusterin) and serum amyloid A-1 (SAA 1) protein gradually increased with time and were significantly higher in the day 42 ECM compared to the day 1 ECM (p < 0.05). Proteins that exhibited a gradual increase in the raw peptide abundances but were not found to be statistically significant on day 42 compared to the day 1 ECM were β-2-microglobulin, endothelial lipase, hemopexin, inter-alpha-trypsin inhibitor (ITI) heavy chain H4, peroxiredoxin 4 and phospholipase transfer (PL) protein (p > 0.05).

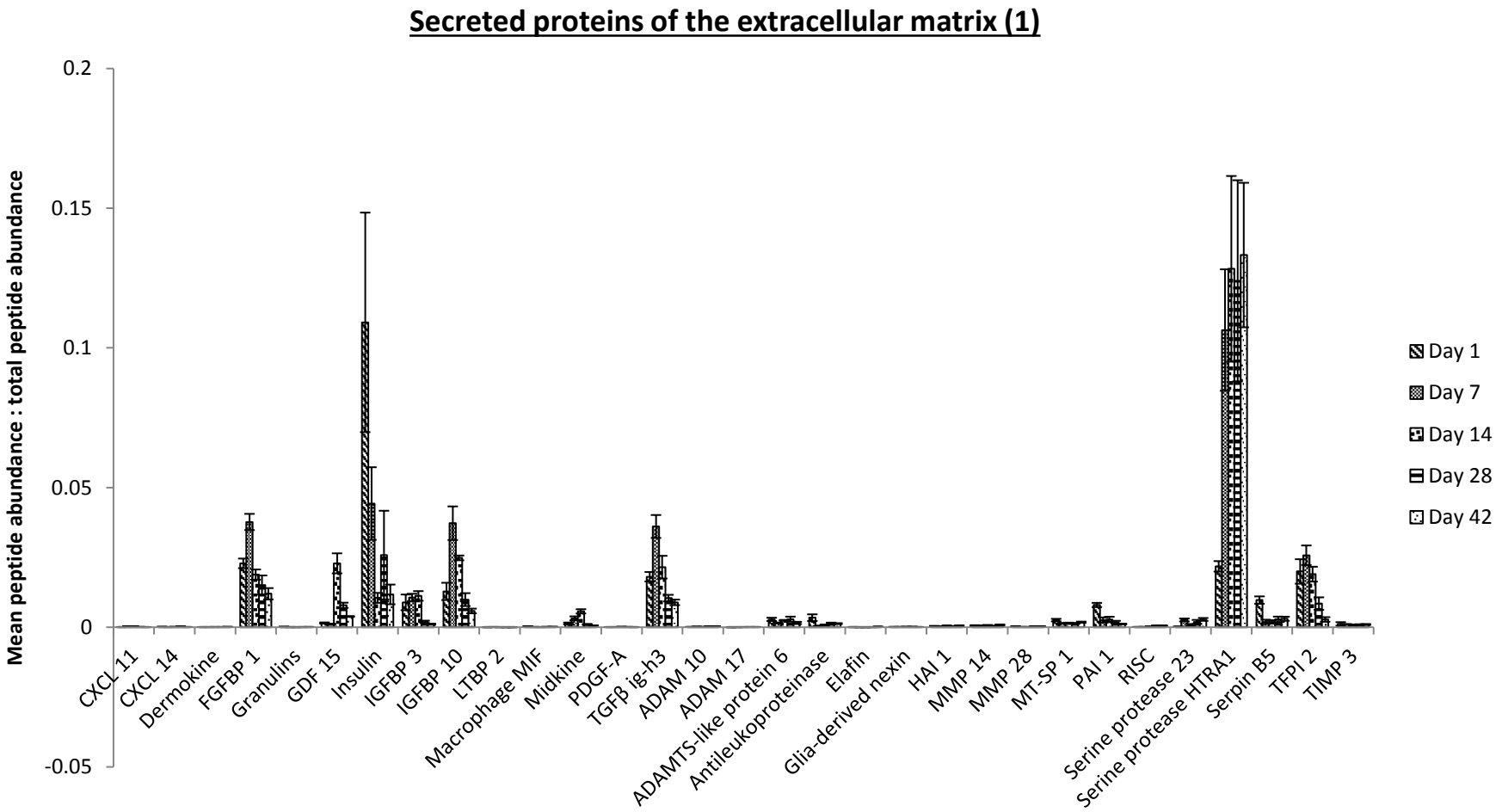

Figure 2.32: Proportions of secreted proteins in the extracellular matrix from days 1 to 42 (1). Data are presented as mean peptide abundance: total peptide abundance ± 1SD, n = 4.

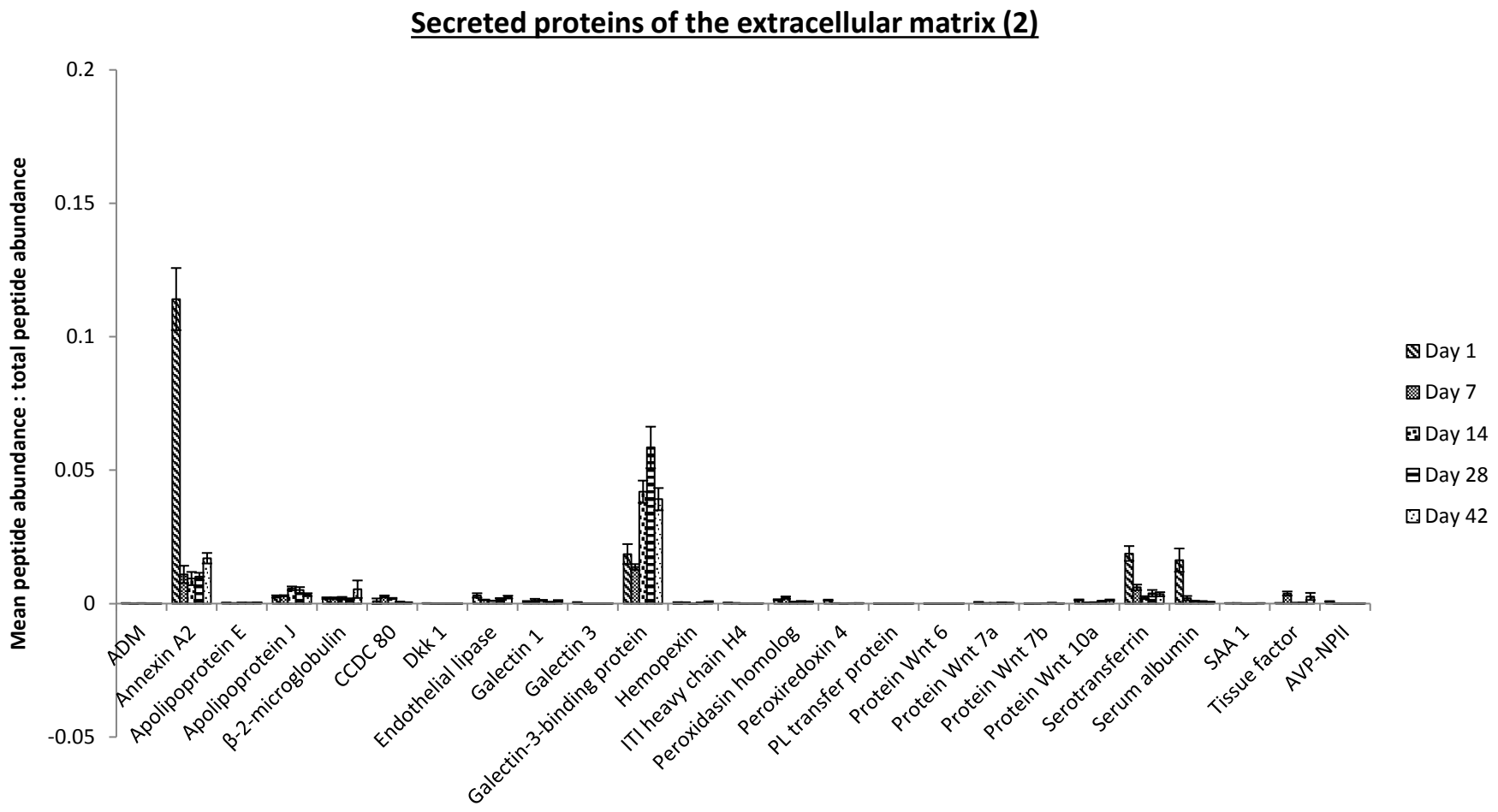

Figure 2.33: Proportions of secreted proteins in the extracellular matrix from days 1 to 42 (2). Data are presented as mean peptide abundance: total peptide abundance ± 1SD, n = 4.

Peptide abundances of proteases and their inhibitors

A

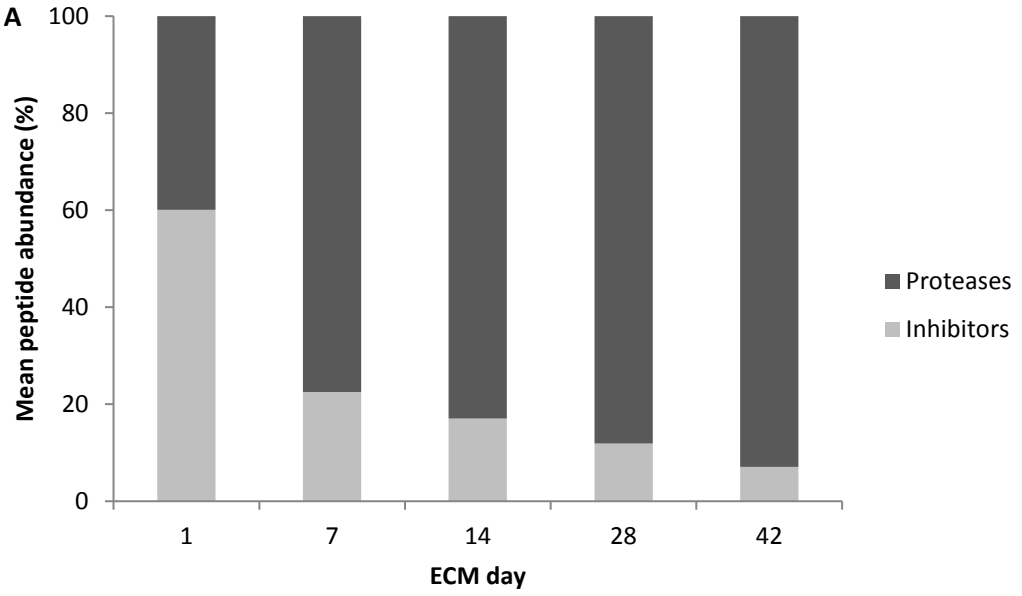

B

	Peptide abundance (%)				
	Day 1	Day 7	Day 14	Day 28	Day 42
Proteases	39.9	77.5	83.0	88.1	92.9
Inhibitors	60.1	22.5	17.0	11.9	7.1

Figure 2.34: A. Peptide abundances of proteases and their inhibitors in the extracellular matrix from days 1 to 42. Data are presented as mean peptide abundance (%), n = 4. The peptide abundances of proteases increased, whereas that of the inhibitors decreased from days 1 to 42 ($p < 0.001$). The proportion of proteases in the extracellular matrix of days 7 to 42 was significantly higher compared to their inhibitors ($p < 0.001$). (Two-way ANOVA; Bonferroni post hoc test). B: Mean peptide abundance (%) in the extracellular matrix from days 1 to 42.

2.3.5 GROWTH OF HCjE-Gi CELLS ON CELL-SECRETED EXTRACELLULAR MATRIX

The ratio of ECM:TCP cell number was highest when HCjE-Gi cells were cultured on the ECM derived from cells that were in culture for three and five days (figure 2.35A). The effects of ECM day and culture day on the ECM:TCP cell number ratio were statistically significant within the model ($p = 0.031$ and $p < 0.001$, respectively). There was a statistically significant increase to the ECM:TCP cell number ratio when HCjE-Gi cells were cultured on the ECM derived from cells that were in culture for three and five days ($p = 0.001$ and $p < 0.001$, respectively). Moreover, the highest ECM:TCP cell number ratio was observed on culture day five, which was found to be statistically significant ($p = 0.011$) (figure 2.35B).

Growth of HCjE-Gi cells on cell-secreted extracellular matrix

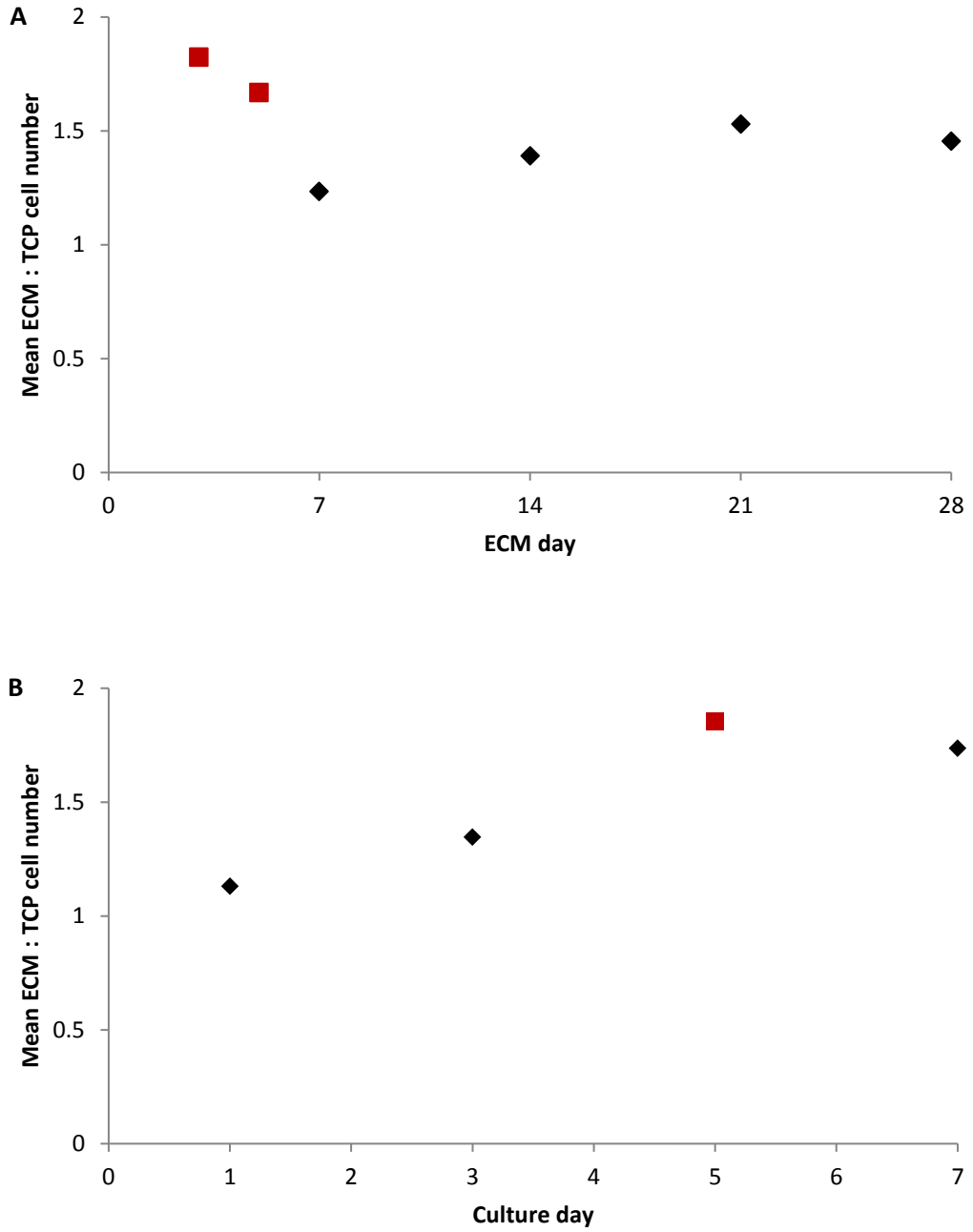

Figure 2.35: Growth of HCjE-Gi cells on cell-secreted extracellular matrix. Data are presented as mean ECM:TCP cell number, n = 9. There was a significant increase to the ECM:TCP cell number ratio when HCjE-Gi cells were cultured on the extracellular matrix derived from cells that were in culture for three and five days (p = 0.001 and p < 0.001, respectively) (A). Moreover, the highest ECM:TCP cell number ratio was observed on culture day five (p = 0.011) (B); ■ p < 0.05. (Generalised linear model).

2.3.6 ADSORPTION OF PROTEINS ONTO TISSUE CULTURE POLYSTYRENE

Adsorption of type IV collagen protein onto TCP was initially investigated by diluting it in either 0.5M acetic acid or PBS to determine any differences in the solubility (figure 2.36). There were twenty-one outliers in the data set and all groups, except the acetic acid - 0µg/mL group, were normally distributed. There was homogeneity of variances. There was a statistically significant interaction effect between the diluent and the concentration of the protein solution on the mean absorbance, $p < 0.001$. There were statistically significant increases to the mean absorbance when type IV collagen was diluted in acetic acid to make 0.5 and 1µg/mL solutions ($p = 0.003$ and $p < 0.001$, respectively) compared to when diluted in PBS. However, there were statistically significant increases to the mean absorbance when type IV collagen was diluted in PBS to make 10 and 20µg/mL solutions ($p = 0.031$ and $p < 0.001$, respectively) compared to when diluted in acetic acid. When the outliers were removed, a statistically significant increase to the mean absorbance was also observed when diluted in acetic acid to make a 2µg/mL solution compared to when diluted in PBS. Since PBS is less toxic to cells, this was used as the diluent for type IV collagen in the subsequent experiments.

Adsorption of type IV collagen protein onto TCP reached a saturation point when pre-adsorbed from a 5µg/mL solution (figure 2.37). There were ten outliers. All data were normally distributed and there was homogeneity of variances. Mean absorbance was statistically significantly different between the different concentration groups, $p < 0.001$. There was a statistically significant increase in the absorbance when type IV collagen was pre-adsorbed from a 0.5µg/mL solution ($p = 0.003$) compared to the control. This continued to increase until a saturation point was reached when type IV collagen was pre-adsorbed from a 5µg/mL solution ($p < 0.001$). There was no change to the overall result when the outliers were removed.

Adsorption of laminin 111 protein onto TCP reached a saturation point when pre-adsorbed from a 0.5µg/mL protein solution (figure 2.38). There were three outliers and all groups were normally distributed, except the control and 5µg/mL groups. There was homogeneity of variances. There was a statistically significant difference in the mean absorbance between the concentration groups, $p < 0.001$. There was an increase to the absorbance when laminin 111 was pre-adsorbed from a 0.5µg/mL solution compared to the control ($p < 0.001$). There were no significant differences in the absorbance when laminin 111 was pre-

adsorbed from 0.5-20µg/mL solutions ($p > 0.05$). No change to the overall result was observed when analysed without the outliers.

Adsorption of fibronectin onto TCP reached a saturation point when pre-adsorbed from a 5µg/mL solution (figure 2.39). There were five outliers and all groups assumed a normal distribution, except the control group. There was homogeneity of variances. The absorbance was statistically significantly different between the concentration groups, $p < 0.001$. There was a statistically significant increase in the mean absorbance when fibronectin was pre-adsorbed from a 0.5µg/mL solution ($p < 0.001$) compared to the control group. This continued to increase until it reached a saturation point when fibronectin was pre-adsorbed from a 5µg/mL solution ($p < 0.001$). There were no significant differences in the mean absorbance values when pre-adsorbed from 5-20µg/mL fibronectin solutions. The overall result was similar when the data were analysed without the outliers.

Adsorption of type IV collagen diluted in acetic acid or PBS

A

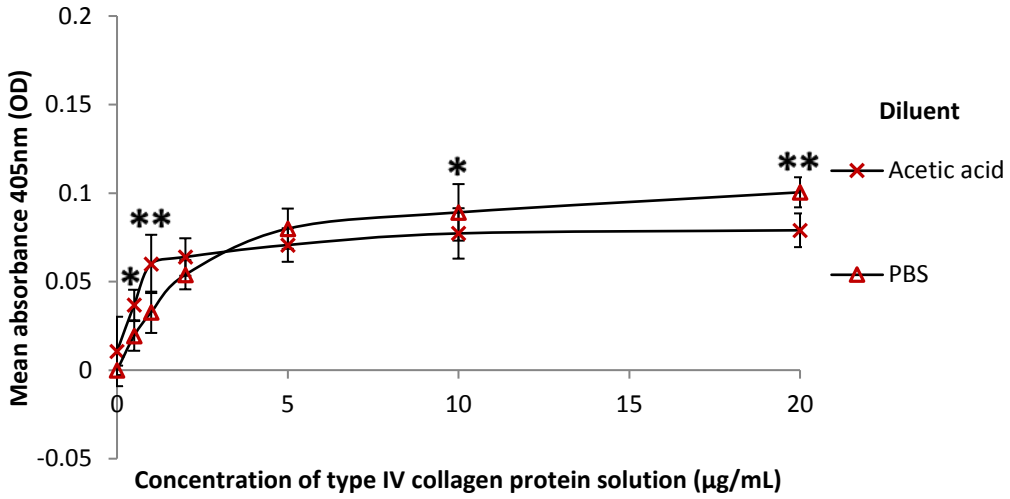

B

	Mean (Acetic acid)	*SD*	Mean (PBS)	*SD*
0	0.011	*0.020*	0.000	*0.003*
0.5	0.037	*0.009*	0.019	*0.008*
1	0.060	*0.016*	0.033	*0.012*
2	0.064	*0.011*	0.054	*0.008*
5	0.071	*0.009*	0.080	*0.011*
10	0.077	*0.014*	0.089	*0.016*
20	0.079	*0.010*	0.100	*0.008*

Figure 2.36: A. Adsorption of type IV collagen when diluted in either 0.5M acetic acid or PBS as determined by indirect ELISA. Data are presented as mean absorbance measured at 405nm ± 1SD, n = 9.There was a significant increase in the mean absorbance when type IV collagen was diluted in 0.5M acetic acid to make 0.5-1µg/mL solutions, whereas a significant increase in the mean absorbance was observed when diluted in PBS to make 10-20µg/mL solutions; *p < 0.05 and **p < 0.001. (Two-way ANOVA; Bonferroni post hoc test). B. Mean absorbance at 405nm (OD – optical density) when diluted in either 0.5M acetic acid or PBS and 1SD.

Adsorption of type IV collagen onto tissue culture polystyrene

A

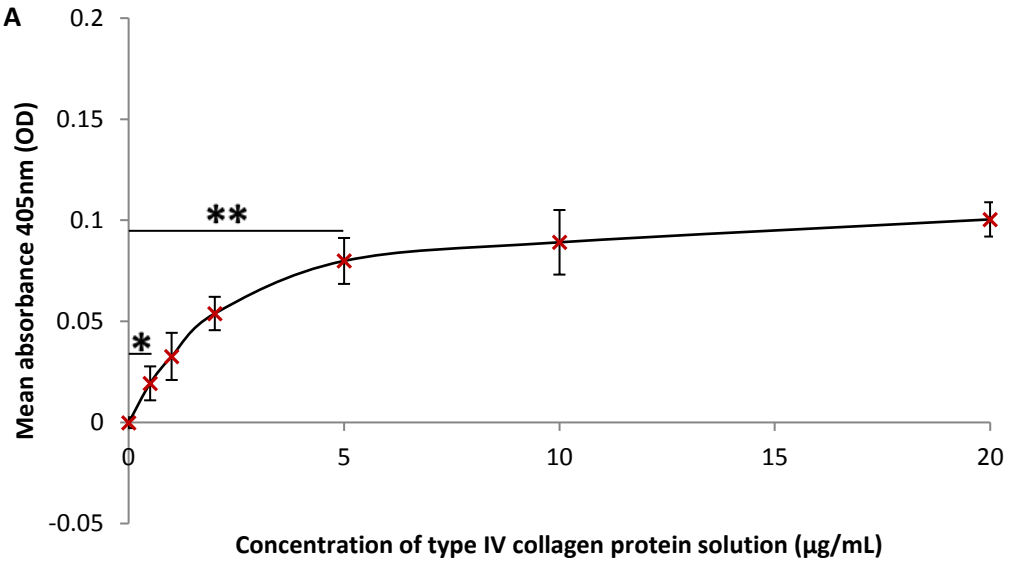

B

	Mean	*SD*
0	0.000	*0.003*
0.5	0.019	*0.008*
1	0.033	*0.012*
2	0.054	*0.008*
5	0.080	*0.011*
10	0.089	*0.016*
20	0.100	*0.008*

Figure 2.37: A. Adsorption of type IV collagen onto tissue culture polystyrene as determined by indirect ELISA. Data are presented as mean absorbance at 405nm ± 1SD, n = 9. There was a significant increase to mean absorbance when type IV collagen was pre-adsorbed from a 0.5µg/mL solution (p = 0.003). The mean absorbance continued to increase to reach a saturation point when type IV collagen was pre-adsorbed from a 5µg/mL solution (p < 0.001); *p < 0.05 and ** p < 0.001. (One-way ANOVA; Tukey post hoc test). B. Mean absorbance at 405nm (OD – optical density) and 1SD.

Adsorption of laminin 111 onto tissue culture polystyrene

A

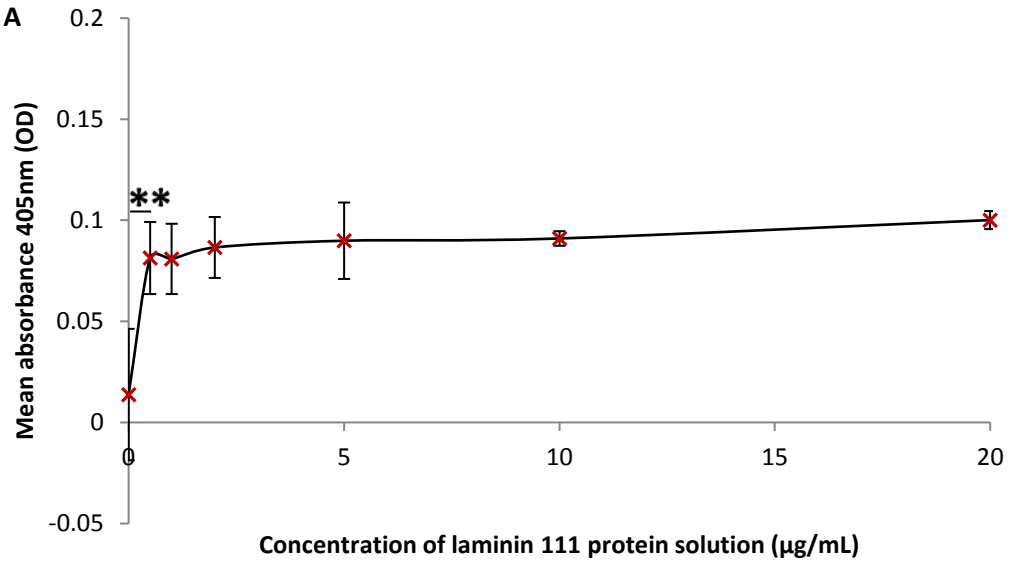

B

	Mean	*SD*
0	0.014	*0.033*
0.5	0.081	*0.018*
1	0.081	*0.017*
2	0.087	*0.015*
5	0.090	*0.019*
10	0.091	*0.004*
20	0.100	*0.004*

Figure 2.38: A. Adsorption of laminin 111 onto tissue culture polystyrene as determined by indirect ELISA. Data are presented as mean absorbance at 405nm ± 1SD, n = 9. There was a significant increase in the mean absorbance when laminin 111 was pre-adsorbed from a 0.5µg/mL solution (p < 0.001). There were no significant differences in the mean absorbance when laminin 111 was pre-adsorbed from 0.5-20µg/mL protein solutions; ** p < 0.001. (One-way ANOVA; Tukey post hoc test). B. Mean absorbance at 405nm (OD – optical density) and 1SD.

Adsorption of fibronectin onto tissue culture polystyrene

A

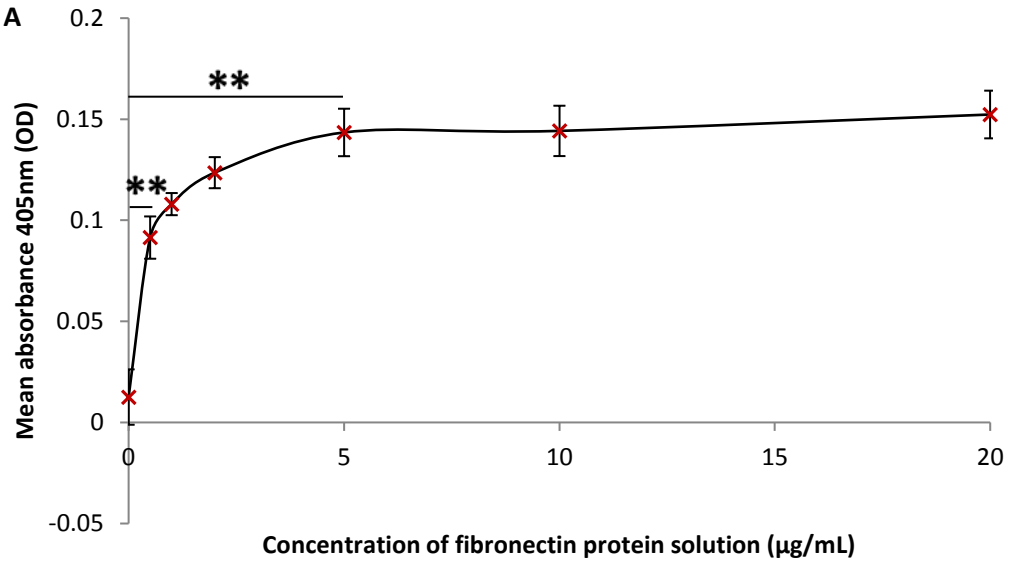

B

	Mean	*SD*
0	0.013	*0.014*
0.5	0.091	*0.010*
1	0.108	*0.005*
2	0.124	*0.008*
5	0.143	*0.012*
10	0.144	*0.012*
20	0.152	*0.012*

Figure 2.39: A. Adsorption of fibronectin onto tissue culture polystyrene as determined by indirect ELISA. Data are presented as mean absorbance at 405nm ± 1SD, n = 9. There was a significant increase in the mean absorbance when fibronectin was pre-adsorbed from a 0.5µg/mL solution ($p < 0.001$). The mean absorbance continued to increase to reach a saturation point when fibronectin was pre-adsorbed from a 5µg/mL solution ($p < 0.001$); ** $p < 0.001$. (One-way ANOVA; Tukey post hoc test). B. Mean absorbance at 405nm (OD – optical density) and 1SD.

2.3.7 ADHESION OF HCjE-Gi CELLS ON PRE-ADSORBED PROTEINS

Pre-adsorption of type IV collagen from a 2µg/mL solution increased the adhesion of HCjE-Gi cells (figure 2.40). The adhesion of cells increased as the concentration of type IV collagen solution increased. There were six outliers and homogeneity of variances was violated (p = 0.036). All groups were normally distributed, except the 1µg/mL group. There was a statistically significant difference to the mean number of cells between the concentration groups, $p < 0.001$. There was a statistically significant increase to the number of cells when cultured on type IV collagen pre-adsorbed from a 2µg/mL solution ($p < 0.001$) compared to that on TCP. There were no statistically significant differences to the number of cells when cultured on pre-adsorbed type IV collagen from 2-10µg/mL solutions. The results were similar when analysed without the outliers.

Pre-adsorption of laminin 111 did not affect the adhesion of the HCjE-Gi cells (figure 2.41). There were four outliers, however, all groups assumed normal distribution and there was homogeneity of variances. There was no statistically significant change to the adhesion of cells on laminin 111 pre-adsorbed from 0.1-1µg/mL solutions compared to the control, $p > 0.05$. The results were similar when analysed without the outliers.

Pre-adsorption of fibronectin from a 0.5µg/mL solution increased the adhesion of HCjE-Gi cells (figure 2.42). The adhesion of cells increased as the concentration of fibronectin solution increased. There were no outliers and all groups were normally distributed, except the 0.5µg/mL group. There was heterogeneity of variances (p = 0.026). There was a statistically significant difference to the mean number of cells between the groups, $p < 0.001$. There was a statistically significant increase to the cell number when cultured on fibronectin pre-adsorbed from a 0.5µg/mL solution compared to that on TCP (p = 0.001). The cell adhesion continued to increase with increasing concentrations of fibronectin solutions up to 5µg/mL ($p < 0.001$). There was no difference to the cell number when cultured on fibronectin pre-adsorbed from 5-10µg/mL solutions.

Pre-adsorption of α-2-HS-GP did not affect the adhesion of the HCjE-Gi cells (figure 2.43). There were six outliers, however, all groups assumed normal distribution and there was homogeneity of variances. There was no statistically significant change to the adhesion of cells on α-2-HS-GP pre-adsorbed from 0.5-20µg/mL solutions compared to the control, $p > 0.05$. There was no change to the overall result when analysed without the outliers.

Adhesion of HCjE-Gi cells on type IV collagen

A

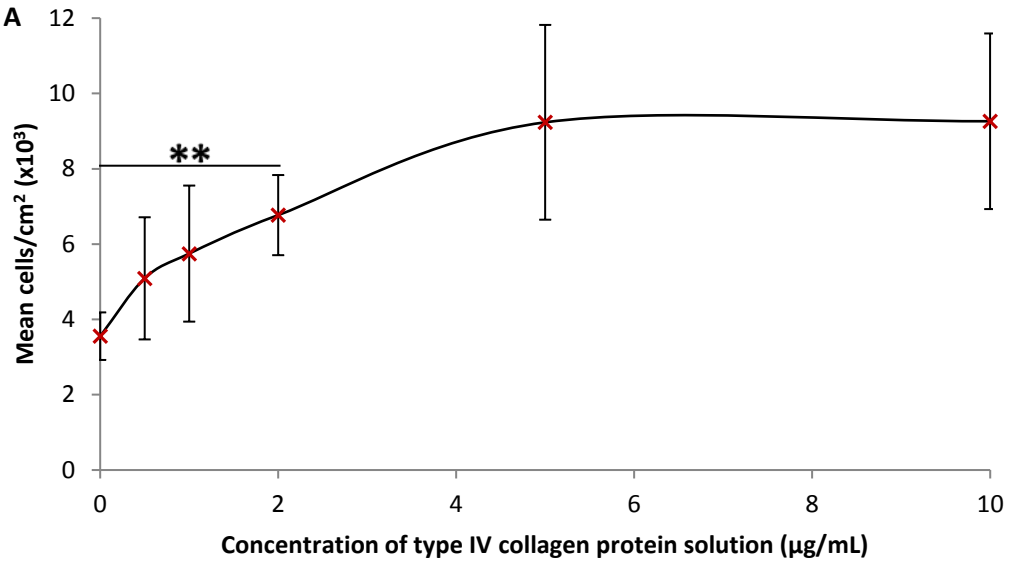

B

	Mean	*SD*
0	3554.5	*631.8*
0.5	5090.1	*1622.1*
1	5747.1	*1806.6*
2	6769.5	*1064.0*
5	9233.6	*2586.0*
10	9261.6	*2331.8*

Figure 2.40: A. Adhesion of HCjE-Gi cells on pre-adsorbed type IV collagen. Data are presented as mean cells/cm² (x10³) ± 1SD, n = 9. The adhesion of cells increased with increasing concentrations of type IV collagen solutions. There was a significant increase to the mean number of cells adhered on type IV collagen pre-adsorbed from a 2µg/mL solution compared to the control (p < 0.001). There were no significant differences to the adhesion of cells on type IV collagen pre-adsorbed from 2-10µg/mL solutions; **p < 0.001. (One-way ANOVA; Games-Howell post hoc test). B. Mean number of cells/cm² and 1SD.

Adhesion of HCjE-Gi cells on laminin 111

A

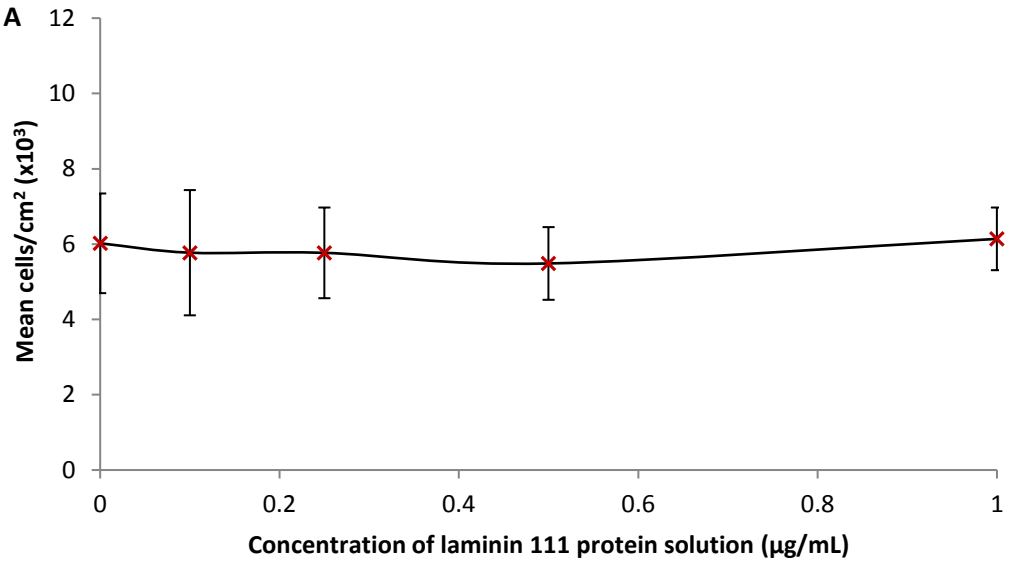

B

	Mean	*SD*
0	6020.6	*1323.4*
0.1	5771.0	*1662.9*
0.25	5767.0	*1204.0*
0.5	5485.5	*965.1*
1	6138.5	*832.0*

Figure 2.41: A. Adhesion of HCjE-Gi cells on pre-adsorbed laminin 111. Data are presented as mean number of cells/cm² (x10³) ± 1SD, n = 9. There was no significant difference to the cell adhesion on laminin 111 pre-adsorbed from 0.1-1µg/mL solutions compared the control (p > 0.05). (One-way ANOVA; Tukey post hoc test). B. Mean number of cells/cm² and 1SD.

A

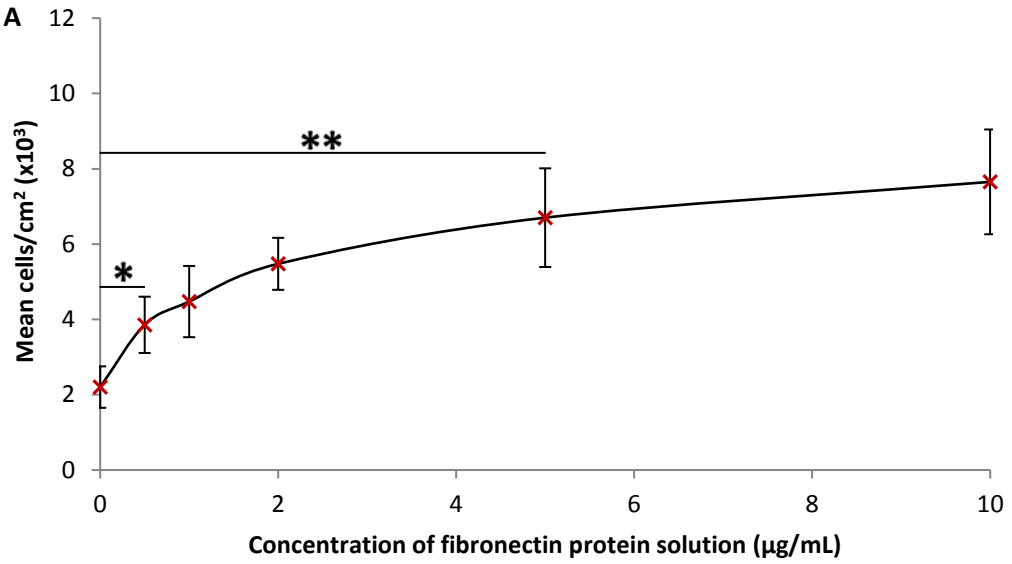

B

	Mean	*SD*
0	2202.6	*550.5*
0.5	3856.0	*747.5*
1	4473.0	*946.3*
2	5475.5	*690.6*
5	6701.6	*1310.1*
10	7652.1	*1391.5*

Figure 2.42: A. Adhesion of HCjE-Gi cells on pre-adsorbed fibronectin. Data are presented as mean cells/cm² (x10³) ± 1SD, n = 9. There was a significant increase to the mean number of cells adhered on fibronectin pre-adsorbed from a 0.5µg/mL solution compared to the control (p = 0.001). The mean number of cells continued to increase with increasing concentrations of fibronectin solutions up to 5µg/mL (p < 0.001). There was no difference to the cell number when cultured on fibronectin pre-adsorbed from 5-10µg/mL solutions; *p < 0.05 and **p < 0.001. (One-way ANOVA; Games-Howell post hoc test). B. Mean number of cells/cm² and 1SD.

Adhesion of HCjE-Gi cells on α-2-HS-glycoprotein

A

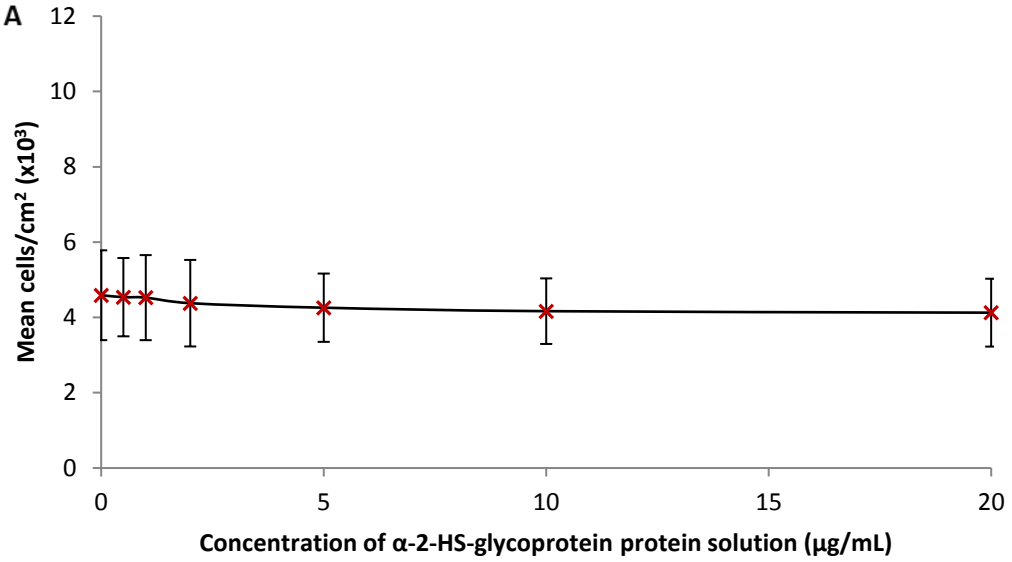

B

	Mean	*SD*
0	4588.9	*1192.5*
0.5	4536.9	*1039.9*
1	4525.0	*1129.6*
2	4377.2	*1149.3*
5	4257.4	*906.9*
10	4165.5	*870.5*
20	4125.6	*901.3*

Figure 2.43: A. Adhesion of HCjE-Gi cells on pre-adsorbed α-2-HS-glycoprotein. Data are presented as mean cells/cm² (x10³) ± 1SD, n = 9. There was no statistically significant differences to the mean number of cells adhered on α-2-HS-glycoprotein pre-adsorbed from 0.5-20µg/mL solutions compared to the control (p > 0.05). (One-way ANOVA; Tukey post hoc test). B. Mean number of cells/cm² and 1SD.

2.3.8 GROWTH AND DIFFERENTIATION OF HCjE-Gi CELLS ON PRE-ADSORBED PROTEINS

There were significant increases to the cell number on days five and seven when cultured on pre-adsorbed type IV collagen compared to TCP (figure 2.44). There were ten outliers and three groups (day 1 - 10µg/mL, day 7 – TCP and day 7 - 10µg/mL) were not normally distributed. Homogeneity of variances was violated ($p < 0.001$). There was a statistically significant interaction effect between the protein concentration and culture day on the mean cell number, $p < 0.001$. As expected, there were statistically significant increases to the mean cell number over the seven day culture period for all the protein concentrations investigated ($p < 0.05$). There was a statistically significant difference to mean cell number between the concentrations on day five ($p < 0.001$) and day seven ($p < 0.001$). On culture day five, statistically significant increases to the cell number were observed when cultured on type IV collagen pre-adsorbed from 5 and 10µg/mL solutions compared to TCP ($p < 0.001$ and $p = 0.011$, respectively). There were statistically significant increases to the cell number when cultured on type IV collagen pre-adsorbed from 5µg/mL solution compared to when pre-adsorbed from 0.5µg/mL ($p = 0.002$) and 1µg/mL ($p = 0.013$) solutions. On culture day seven, statistically significant increases to the cell number were observed when cultured on type IV collagen pre-adsorbed from 0.5-10µg/mL solutions compared to TCP ($p < 0.001$). There was also a statistically significant increase to the cell number on type IV collagen pre-adsorbed from a 5µg/mL solution compared to when pre-adsorbed from a 1µg/mL solution ($p = 0.031$). When analysed without the outliers, a significant increase to the cell number was seen on type IV collagen pre-adsorbed from a 5µg/mL solution compared to when pre-adsorbed from a 2µg/mL solution on day five. On day seven, significant increases were also observed on type IV collagen pre-adsorbed from a 10µg/mL solution compared to when pre-adsorbed from 0.5-2µg/mL solutions, and when pre-adsorbed from a 5µg/mL solution compared to when pre-adsorbed from a 0.5µg/mL solution.

Pre-adsorption of laminin 111 did not affect the growth curve of HCjE-Gi cells over a culture period of seven days (figure 2.45). There were eleven outliers and three groups were not normally distributed (day 1 – TCP, day 3 – TCP and day 7 – TCP). There was heterogeneity of variances ($p < 0.001$). There was no statistically significant interaction effect between the protein concentration and culture day on the cell number, $p = 0.073$. Analysis of main effect between the protein concentrations showed no statistically significant difference ($p = 0.127$), whereas a significant difference was observed between the culture days ($p < 0.001$). When the outliers were removed, an interaction effect was observed between the protein

concentration and culture day on the cell number (p = 0.002). There were significant reductions to the cell number on laminin 111 pre-adsorbed from 0.25 and 1μg/mL solutions compared to that on TCP (p < 0.05) on culture day seven. Moreover, significant reductions to the cell number were also observed on laminin 111 pre-adsorbed from 0.25-1μg/mL solutions compared to that on laminin 111 pre-adsorbed from a 0.1μg/mL solution (p < 0.05) on culture day seven.

The growth of HCjE-Gi cells on pre-adsorbed fibronectin was comparable to that on TCP (figure 2.46). There were fourteen outliers and three groups were not normally distributed (day 1 - 5μg/mL, day 5 - 2μg/mL and day 7 - 10μg/mL). There was heterogeneity of variances (p < 0.001). There was no significant interaction effect between protein concentration and culture day on the mean cell number, p = 0.364. Analysis of the main effect between protein concentrations showed a statistically significant difference (p = 0.04). Further analysis showed a statistically significant increase to the cell number on fibronectin pre-adsorbed from a 5μg/mL compared to TCP (p = 0.037). There were statistically significant increases to the cell number over the culture period of seven days in all protein concentration groups investigated. When analysed without the outliers, a statistically significant interaction was observed between the protein concentration and culture day on the mean cell number (p = 0.003). There were significant increases to the cell number on day seven when cultured on fibronectin pre-adsorbed from 0.5, 5 and 10μg/mL solutions compared to TCP (p < 0.05). Additionally, significant increases to the cell number were observed on fibronectin pre-adsorbed from a 10μg/mL solution compared to 0.5-2μg/mL solutions (p < 0.05), and on fibronectin pre-adsorbed from a 5μg/mL solution compared to that pre-adsorbed from a 1μg/mL solution (p < 0.05).

There were significant increases to the cell number when cultured on pre-adsorbed α-2-HS-GP for five to seven days (figure 2.47). There were eleven outliers and two groups were not normally distributed (day 1 - 5μg/mL and day 5 - 2μg/mL). There was heterogeneity of variances (p < 0.001). There was a statistically significant interaction effect between the protein concentration and culture day on the mean cell number, p < 0.001. There were statistically significant increases to the mean cell number over the seven day culture period for all the protein concentrations investigated. There was a statistically significant difference to the mean cell number between the concentrations on day five (p < 0.001) and day seven (p < 0.001). On culture day five, statistically significant increases to the cell number were observed when cultured on α-2-HS-GP pre-adsorbed from 10-20μg/mL

solutions compared to TCP and α-2-HS-GP pre-adsorbed from 0.5-5μg/mL solutions (p < 0.05). On culture day seven, there were statistically significant increases to the cell number when cultured on α-2-HS-GP pre-adsorbed from a 20μg/mL solution compared to TCP and α-2-HS-GP pre-adsorbed from 0.5μg/mL and 5μg/mL solutions (p < 0.05). When analysed without the outliers, significant increases to the cell numbers were observed on culture day five on α-2-HS-GP pre-adsorbed from 10-20μg/mL solutions compared to TCP and α-2-HS-GP pre-adsorbed from 0.5-2μg/mL solutions (p < 0.001). Further significant increases were observed on α-2-HS-GP pre-adsorbed from a 5μg/mL solution compared to TCP and α-2-HS-GP pre-adsorbed from 0.5-1μg/mL solutions (p < 0.05), and on α-2-HS-GP pre-adsorbed from a 2μg/mL solution compared to that on α-2-HS-GP pre-adsorbed from 0.5-1μg/mL solutions (p < 0.05). On culture day seven, significant increases to the cell number were observed on α-2-HS-GP pre-adsorbed from a 20μg/mL solution compared to TCP and α-2-HS-GP pre-adsorbed from 0.5-1μg/mL and 5μg/mL solutions (p < 0.05). There were significant increases to the cell number observed on α-2-HS-GP pre-adsorbed from a 10μg/mL solution compared to TCP, and α-2-HS-GP pre-adsorbed from 0.5μg/mL and 5μg/mL solutions (p < 0.05). A further significant increase to the cell number was also observed on α-2-HS-GP pre-adsorbed from a 2μg/mL solution compared to α-2-HS-GP pre-adsorbed from a 5μg/mL solution (p = 0.046).

The HCjE-Gi cells formed a monolayer by day seven when cultured on pre-adsorbed type IV collagen, laminin 111, fibronectin and α-2-HS-GP. There was positive staining for keratin 19, a simple epithelial cell marker, on culture day seven on all the substrates investigated (figures 2.48-2.51). There was no evidence, however, of expression of keratin 4, a marker of non-keratinised stratified epithelial cells, on culture day seven on any of the substrates.

Growth curve of HCjE-Gi cells on type IV collagen

A

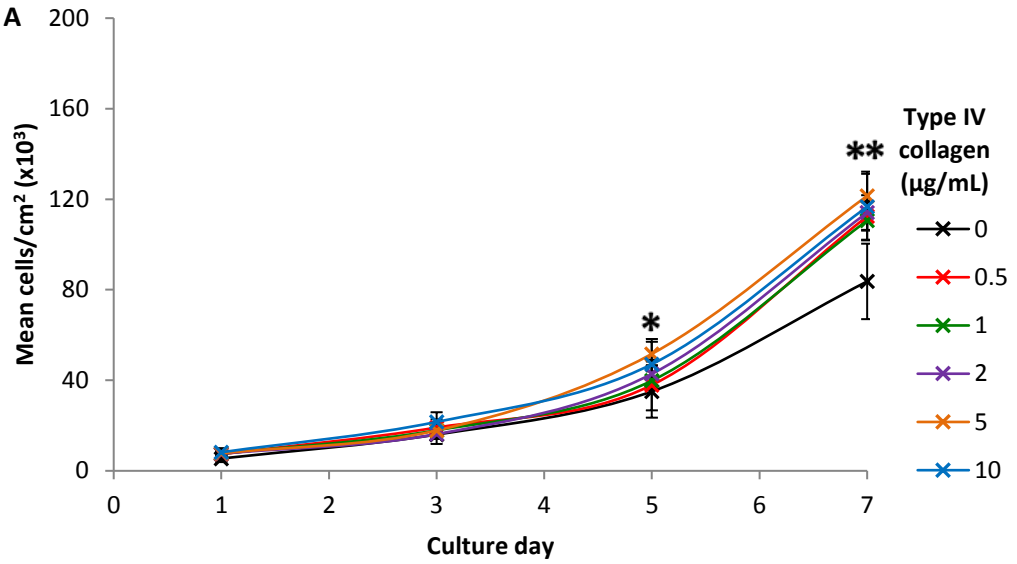

B

	Day 1		Day 3		Day 5		Day 7	
	Mean	*SD*	Mean	*SD*	Mean	*SD*	Mean	*SD*
0	5437.5	*1579.3*	16 025.1	*1934.1*	35 079.4	*11 594.8*	83 681.8	*16 671.2*
0.5	7348.6	*1208.9*	19 100.3	*3657.7*	37 905.0	*11 192.2*	112 441.1	*6318.7*
1	7504.3	*1282.4*	17 898.2	*2508.6*	39 832.0	*4107.8*	110 570.0	*8748.4*
2	7568.2	*1766.6*	16 214.8	*4345.4*	42 841.4	*5454.8*	114 112.5	*7664.3*
5	7722.0	*966.5*	17 838.3	*3594.9*	51 675.6	*5339.9*	121 495.0	*10 687.4*
10	8195.3	*1831.9*	21 616.4	*4267.5*	47 120.7	*11 118.9*	116 668.5	*14 561.3*

Figure 2.44: A. Growth curve of HCjE-Gi cells cultured on pre-adsorbed type IV collagen. Data are presented as mean number of cells/cm² (x10³) ± 1SD, n = 9. There was a significant interaction effect between the protein concentration and culture day on the mean cell number (p < 0.001). The cell number significantly increased during the culture period on all protein concentrations. On day five, there were significant increases to the cell number when cultured on type IV collagen pre-adsorbed from 5 and 10µg/mL solutions compared to tissue culture polystyrene (p < 0.001 and p = 0.011, respectively). On day seven, there were significant increases to the cell number when cultured on type IV collagen pre-adsorbed from 0.5-10µg/mL solutions compared to tissue culture polystyrene (p < 0.001); *p = 0.05 and ** p < 0.001. (Two-way ANOVA; Bonferroni post hoc test). B. Mean number of cells/cm² and 1SD.

Growth curve of HCjE-Gi cells on laminin 111

A

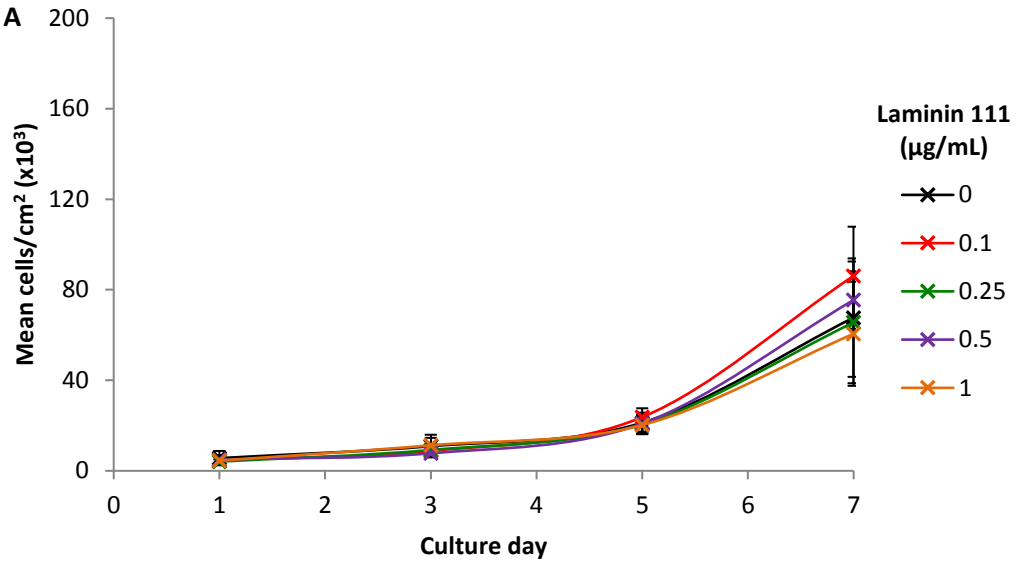

B

	Day 1		Day 3		Day 5		Day 7	
	Mean	*SD*	Mean	*SD*	Mean	*SD*	Mean	*SD*
0	5605.3	*3172.7*	10885.1	*3676.8*	21 235.0	*4455.0*	67 682.7	*26 178.6*
0.1	4710.7	*1657.9*	8786.3	*1603.0*	23 723.1	*3918.8*	86 156.0	*21 694.7*
0.25	4091.6	*955.9*	9203.7	*2778.5*	20 582.0	*4069.4*	65 582.0	*26 888.7*
0.5	4986.2	*1956.4*	7751.9	*1823.7*	20 915.5	*3573.3*	75 480.6	*12 698.9*
1	4501.0	*1458.1*	11 280.5	*4667.3*	20 238.5	*4056.8*	60 551.8	*22 988.7*

Figure 2.45: A. Growth curve of HCjE-Gi cells cultured on pre-adsorbed laminin 111. Data are presented as mean number of cells/cm² (x10³) ± 1SD, n = 9. There was no significant interaction effect observed between protein concentration and culture day on the mean cell number (p = 0.073). The cell number significantly increased during the culture period on all protein concentrations. There was no significant change to the cell number when cultured on laminin 111 protein pre-adsorbed from 0.1-1µg/mL solutions (p > 0.05). (Two-way ANOVA; Bonferroni post hoc test). B. Mean number of cells/cm² and 1SD.

Growth curve of HCjE-Gi cells on fibronectin

A

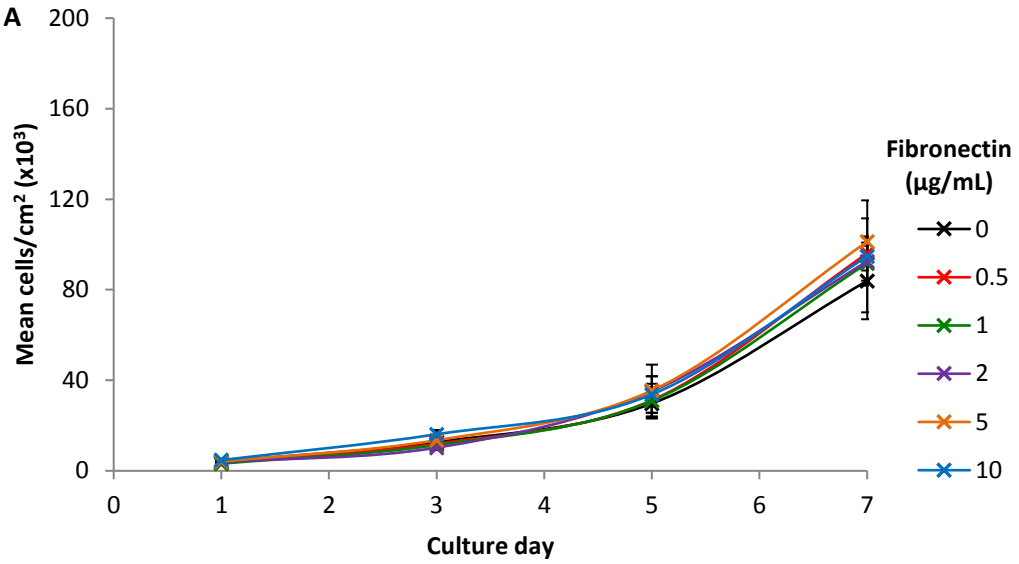

B

	Day 1		Day 3		Day 5		Day 7	
	Mean	*SD*	Mean	*SD*	Mean	*SD*	Mean	*SD*
0	4067.7	*473.8*	12 720.2	*2837.2*	29 753.7	*6650.6*	83 901.5	*16 932.5*
0.5	3756.2	*764.2*	11 951.4	*2354.5*	31 179.5	*5606.7*	96 040.6	*7524.4*
1	3159.1	*623.6*	11 380.3	*2032.6*	30 963.8	*7504.8*	91 653.4	*7673.2*
2	3834.0	*575.3*	10 256.0	*1081.6*	35 121.4	*6652.7*	92 530.1	*10 713.6*
5	4085.6	*1100.6*	13 525.0	*2446.3*	35 490.8	*11 429.3*	101 218.6	*10 323.3*
10	4752.6	*577.8*	16 150.9	*1872.6*	33 731.5	*8035.6*	94 748.6	*24 733.6*

Figure 2.46: A. Growth curve of HCjE-Gi cells cultured on pre-adsorbed fibronectin. Data are presented as mean number of cells/cm² (x10³) ± 1SD, n = 9. There was no significant interaction effect between protein concentration and culture day on the mean cell number (p = 0.364). The cell number significantly increased during the culture period on all protein concentrations. Analysis of main effect for protein concentration showed a significant increase to the cell number when cultured on fibronectin pre-adsorbed from a 5µg/mL solution compared to TCP (p = 0.037). (Two-way ANOVA; Bonferroni post hoc test). B. Mean number of cells/cm² and 1SD.

Growth curve of HCjE-Gi cells on α-2-HS-glycoprotein

A

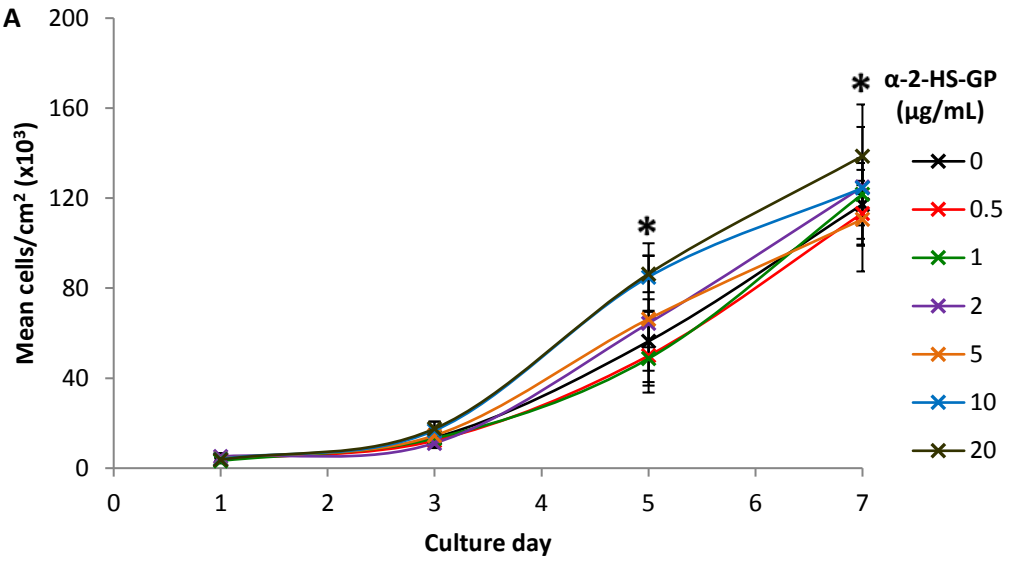

B

	Day 1		Day 3		Day 5		Day 7	
	Mean	*SD*	Mean	*SD*	Mean	*SD*	Mean	*SD*
0	3872.0	*874.3*	13 560.9	*2032.7*	56 374.3	*13 072.9*	117 239.6	*15 317.2*
0.5	3840.0	*711.9*	12 252.9	*2785.1*	49 998.2	*13 302.4*	113 267.8	*14 444.1*
1	3258.9	*1151.3*	13 209.5	*2942.7*	48 702.2	*15 119.1*	121 754.6	*13 857.3*
2	5174.0	*1548.9*	11 116.7	*2207.1*	64 385.9	*10 670.5*	124 967.6	*12 755.6*
5	4271.4	*1861.6*	14 533.4	*3000.6*	66 286.9	*28 024.7*	110 606.0	*11 225.7*
10	4113.6	*1520.8*	16 757.9	*3898.7*	84 955.9	*14 983.4*	124 532.3	*37 109.1*
20	3764.1	*847.5*	17 562.7	*3171.8*	86 371.7	*8172.1*	138 708.3	*12 932.7*

Figure 2.47: A. Growth curve of HCjE-Gi cells cultured on pre-adsorbed α-2-HS-glycoprotein. Data are presented as mean number of cells/cm² (x10³) ± SD, n = 9. There was a significant interaction effect between the protein concentration and culture day on the mean cell number (p < 0.001). On culture day five, significant increases to the cell number were observed when cultured on α-2-HS- glycoprotein pre-adsorbed from 10-20µg/mL solutions compared to tissue culture polystyrene and α-2-HS- glycoprotein pre-adsorbed from 0.5-5µg/mL solutions (p < 0.05). On culture day seven, there were statistically significant increases to the cell number when cultured on α-2-HS- glycoprotein pre-adsorbed from a 20µg/mL solution compared to tissue culture polystyrene and α-2-HS- glycoprotein pre-adsorbed from 0.5µg/mL and 5µg/mL solutions (p < 0.05); *p < 0.05. (Two-way ANOVA; Bonferroni post hoc test). B. Mean number of cells/cm² and 1SD.

Expression of conjunctival cell differentiation markers by HCjE-Gi cells cultured on pre-adsorbed type IV collagen

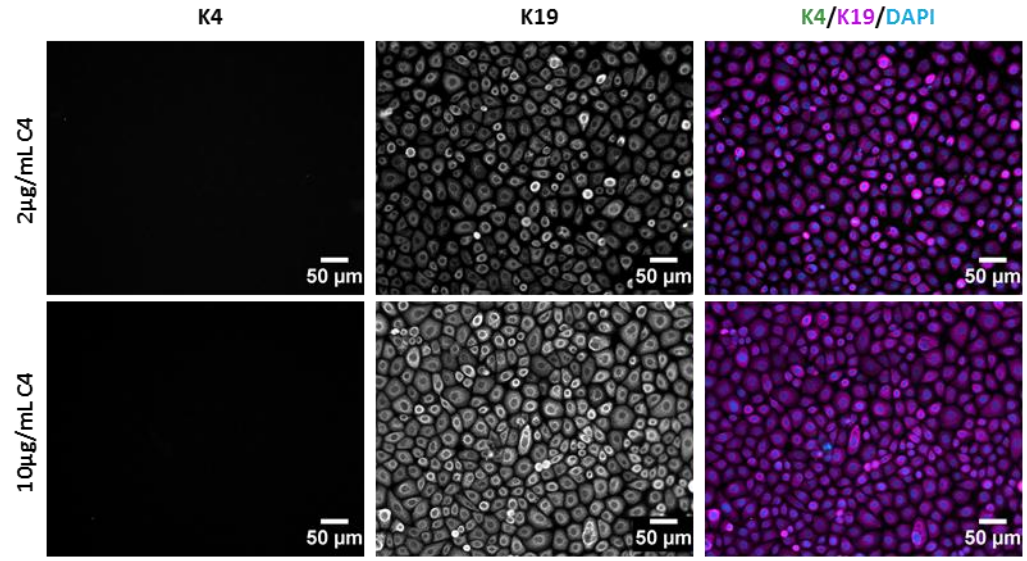

Figure 2.48: Expression of conjunctival cell differentiation markers by HCjE-Gi cells cultured on pre-adsorbed type IV collagen (C4) for seven days; K4 – keratin 4 (green), K19-keratin 19 (purple) and DAPI (blue).

Expression of conjunctival cell differentiation markers by HCjE-Gi cells cultured on pre-adsorbed laminin 111

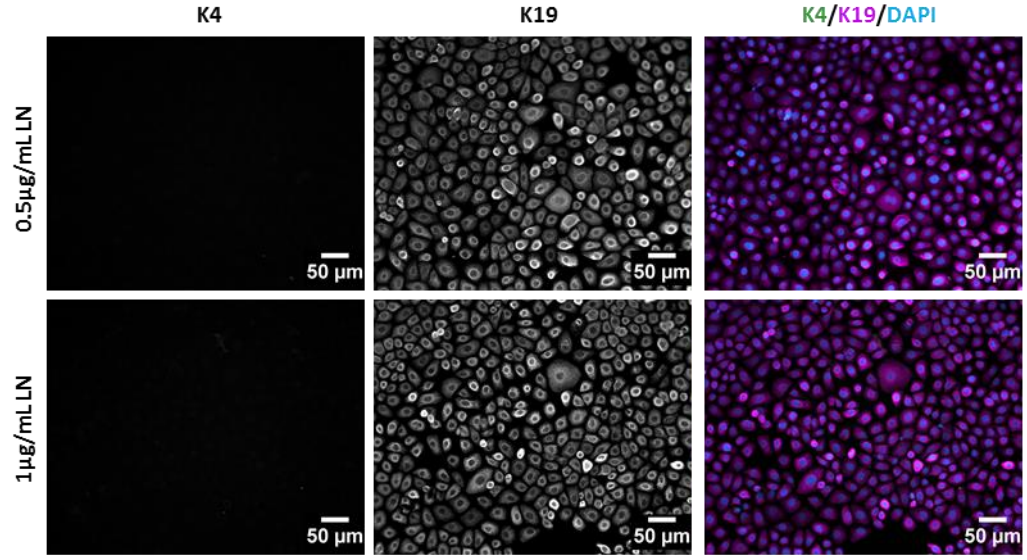

Figure 2.49: Expression of conjunctival cell differentiation markers by HCjE-Gi cells cultured on pre-adsorbed laminin 111 (LN) for seven days; K4 – keratin 4 (green), K19-keratin 19 (purple) and DAPI (blue).

Expression of conjunctival cell differentiation markers by HCjE-Gi cells cultured on pre-adsorbed fibronectin

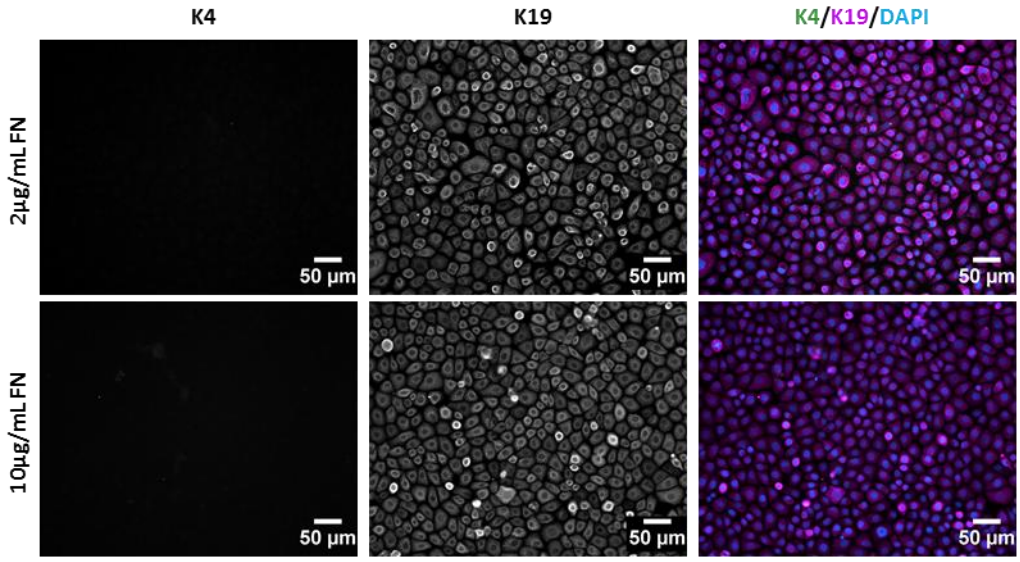

Figure 2.50: Expression of conjunctival cell differentiation markers by HCjE-Gi cells cultured on pre-adsorbed fibronectin (FN) for seven days; K4 – keratin 4 (green), K19- keratin 19 (purple) and DAPI (blue).

Expression of conjunctival cell differentiation markers by HCjE-Gi cells cultured on pre-adsorbed α-2-HS-glycoprotein

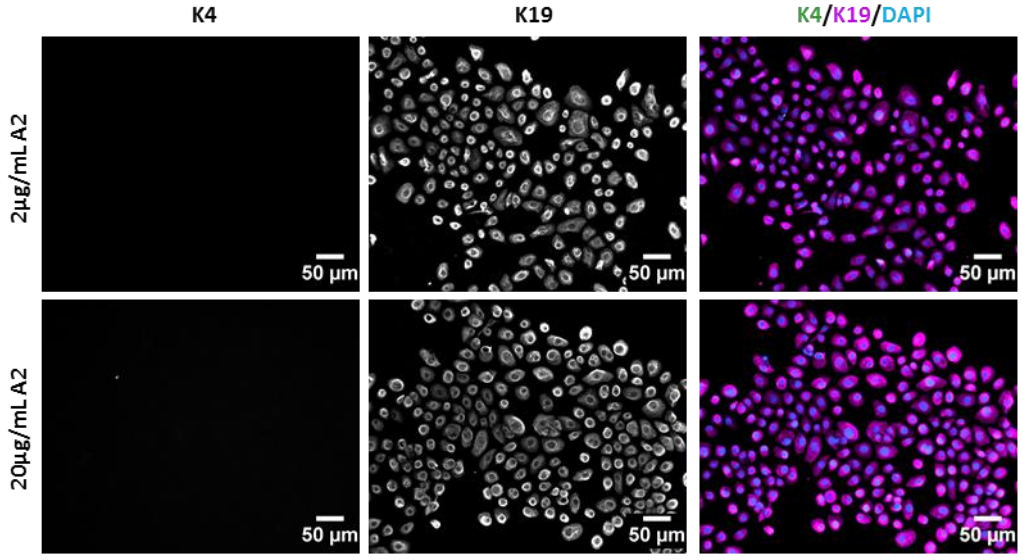

Figure 2.51: Expression of conjunctival cell differentiation markers by HCjE-Gi cells cultured on pre-adsorbed α-2-HS-glycoprotein (A2) for seven days; K4 – keratin 4 (green), K19- keratin 19 (purple) and DAPI (blue).

2.3.9 EXPRESSION OF STEM CELL MARKERS BY HCjE-Gi CELLS ON PRE-ADSORBED PROTEINS

ΔNp63

On culture day one, there was strong staining for ΔNp63 around the nuclei, however, by culture days seven and fourteen, the staining was weaker and co-localised with the DAPI staining in the nucleus (figure 2.52).

Pre-adsorption of proteins did not affect the expression of ΔNp63 compared to TCP over a culture period of fourteen days (figure 2.53). There were seven outliers and three groups did not exhibit normal distribution (day 7 – laminin 111 0.5μg/mL, day 14 – TCP, and day 14 – type IV collagen 10μg/mL). There was heterogeneity of variances ($p < 0.001$). There was a statistically significant interaction effect between substrate and culture day on the expression ΔNp63 protein, $p = 0.015$. There were statistically significant differences between the culture days for each substrate ($p < 0.001$), where there were significant reductions to the percentage of stained cells on days seven and fourteen compared to day one. There were no statistically significant differences between the substrates pre-adsorbed with proteins and TCP ($p < 0.05$). On culture day fourteen, there were statistically significant increases to the percentage of stained cells on substrates pre-adsorbed with fibronectin from 2 and 10μg/mL solutions compared to those pre-adsorbed with type IV collagen from a 10μg/mL solution ($p = 0.008$ and $p = 0.047$, respectively). Additionally, there was a significant increase to the percentage of stained cells on substrates pre-adosrbed with fibronectin from a 2μg/mL solution compared to those pre-adsorbed with laminin 111 from a 0.5μg/mL solution ($p = 0.048$). When the data were analysed without the outliers, further significant differences were observed on day one, where there were significant reductions to the percentage of stained cells on substrates pre-adsorbed with fibronectin from a 10μg/mL solution compared to those pre-adsorbed with fibronectin from a 2μg/mL solution and laminin 111 pre-adsorbed from 0.5 and 1μg/mL solutions ($p < 0.05$).

Expression of ΔNp63 by HCjE-Gi cells

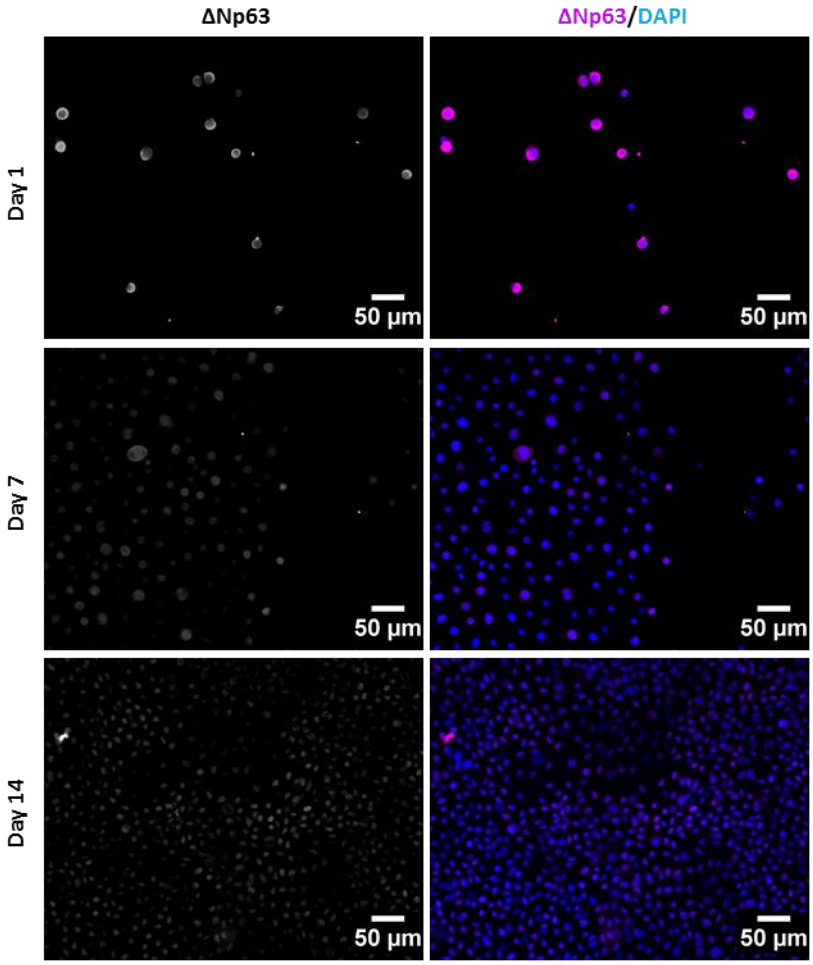

Figure 2.52: Expression of ΔNp63 by HCjE-Gi cells; ΔNp63 (purple) and DAPI (blue). On culture day one, there was strong staining for ΔNp63 around the nuclei; however, by culture days seven and fourteen, the staining was weaker and co-localised with the DAPI staining in the nucleus.

Expression of ΔNp63 by HCjE-Gi cells on pre-adsorbed proteins

A

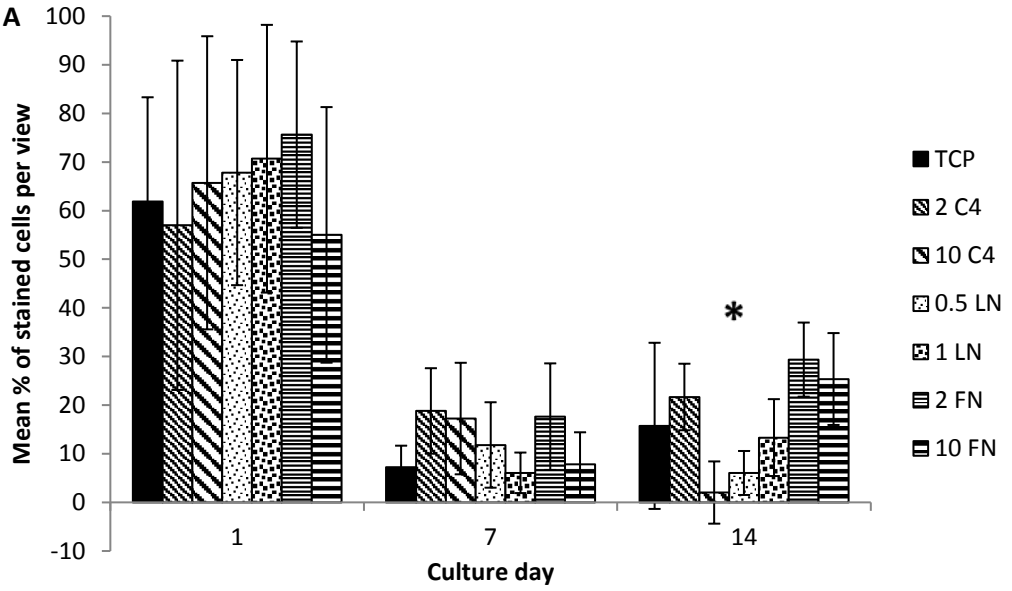

B

	Day 1		Day 7		Day 14	
	Mean	***SD***	**Mean**	***SD***	**Mean**	***SD***
TCP	61.9	*21.5*	7.2	*4.4*	15.7	*17.1*
2 C4	57.0	*33.9*	18.8	*8.8*	21.7	*6.8*
10 C4	65.7	*30.1*	17.2	*11.5*	2.0	*6.4*
0.5 LN	67.8	*23.2*	11.8	*8.8*	6.0	*4.5*
1 LN	70.7	*27.5*	6.1	*4.2*	13.3	*7.9*
2 FN	75.6	*19.2*	17.6	*11.0*	29.4	*7.6*
10 FN	55.0	*26.3*	7.8	*6.6*	25.4	*9.4*

Figure 2.53: A. Expression of ΔNp63 by HCjE-Gi cells on pre-adsorbed proteins. Data are presented as mean percentage (%) of stained cells per view ± 1SD, n = 2. There were significant reductions to the percentage of stained cells on days seven and fourteen compared to day one (p < 0.001). There were no significant differences between the substrates pre-adsorbed with proteins and tissue culture polystyrene. On day fourteen, there were significant increases to the percentage of stained cells on fibronectin pre-adsorbed from 2 and 10µg/mL solutions compared to that on type IV collagen pre-adsorbed from a 10µg/mL solution, and on fibronectin pre-adsorbed from a 2µg/mL solution compared to that on laminin 111 pre-adsorbed from a 0.5µg/mL solution (p < 0.05); *p < 0.05. (Two-way ANOVA; Bonferroni post hoc test). B. Mean percentage of stained cells per view on culture days 1, 7 and 14, and 1SD; C4 - type IV collagen 2 and 10µg/mL, LN - laminin 111 0.5 and 1µg/mL and FN – fibronectin 2 and 10µg/mL.

ABCG2

On culture days one and seven, there was positive staining for ABCG2 in the nucleus, cytoplasm and cell membranes (figure 2.54). A granular staining pattern was observed in the cytoplasm. By culture day fourteen, the staining was mostly transmembrane and no evidence of nuclear staining was present.

Pre-adsorption of type IV collagen from a 10µg/mL solution increased the expression of ABCG2 protein in HCjE-Gi cells compared to TCP on culture day one (figure 2.55). There were seven outliers and six groups were not normally distributed (day 1 – fibronectin 10µg/mL, day 7 – laminin 111 1µg/mL, day 14 – TCP, day 14 – laminin 111 0.5µg/mL, day 14 – laminin 111 1µg/mL, and day 14 – fibronectin 2µg/mL). There was heterogeneity of variances ($p < 0.001$). There was a statistically significant interaction effect between substrate and culture day on the expression of ABCG2 protein, $p = 0.018$. There were statistically significant differences between the culture days for each substrate ($p < 0.001$), where there were significant reductions to the percentage of stained cells on days seven and fourteen compared to day one. There were statistically significant differences to the percentage of stained cells between the substrates on culture day one ($p < 0.001$). There were significant increases to the percentage of stained cells on substrates pre-adsorbed with type IV collagen from a 10µg/mL solution compared to TCP ($p = 0.028$). In addition, there were significant reductions to the percentage of stained cells on substrates pre-adsorbed with laminin 111 from 0.5 and 1µg/mL solutions compared to those pre-adsorbed with type IV collagen from 2 and 10 µg/mL solutions ($p < 0.05$). The percentage of stained cells on substrates pre-adsorbed with laminin 111 from a 0.5µg/mL solution was significantly lower compared to the substrates pre-adsorbed with fibronectin from a 2µg/mL solution ($p = 0.011$). When the outliers were removed, all the substrates pre-adsorbed with fibronectin and type IV collagen had significantly higher percentage of stained cells compared to TCP and substrates pre-adsorbed with laminin 111 on culture day one ($p < 0.05$).

Expression of ABCG2 by HCjE-Gi cells

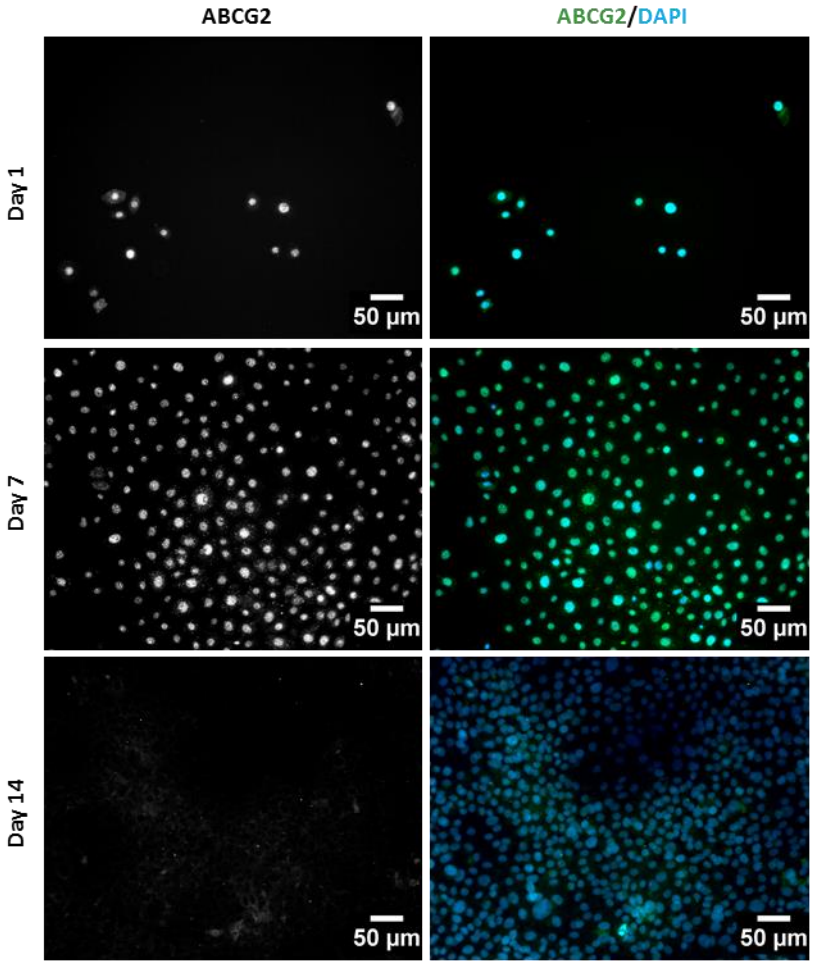

Figure 2.54: Expression of ABCG2 by HCjE-Gi cells; ABCG2 (green) and DAPI (blue). On culture days one and seven, there was positive staining for ABCG2 in the nucleus, cytoplasm and cell membranes. A granular staining pattern was observed in the cytoplasm. By culture day fourteen, the staining was mostly transmembrane and no evidence of nuclear staining was present.

Expression of ABCG2 by HCjE-Gi cells on pre-adsorbed proteins

A

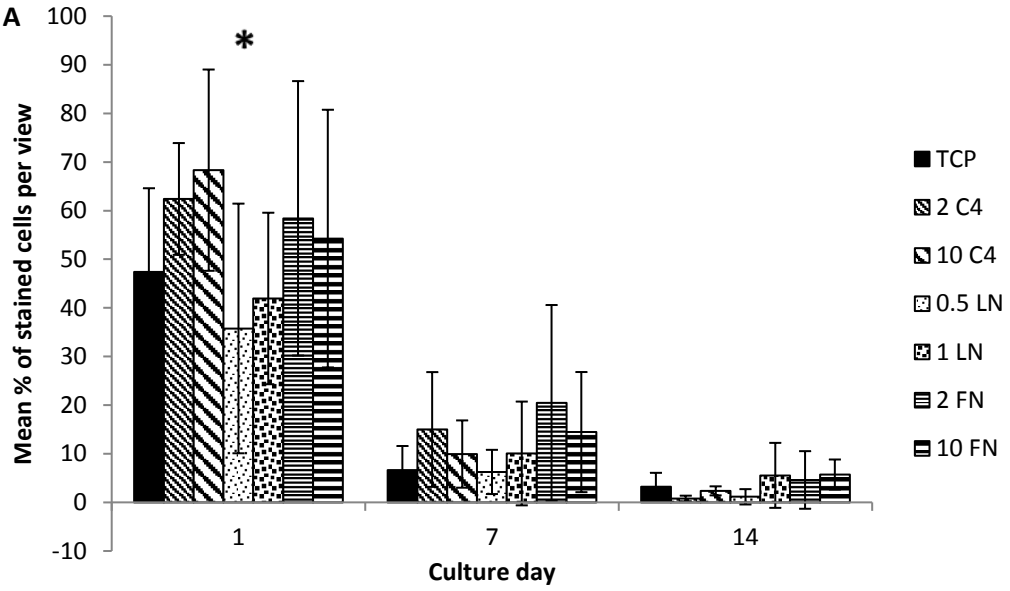

B

	Day 1		Day 7		Day 14	
	Mean	*SD*	Mean	*SD*	Mean	*SD*
TCP	47.4	*17.2*	6.6	*5.0*	3.2	*2.9*
2 C4	62.4	*11.5*	15.0	*11.8*	0.8	*0.6*
10 C4	68.3	*20.7*	9.9	*6.9*	2.4	*0.9*
0.5 LN	35.8	*25.7*	6.3	*4.5*	1.1	*1.6*
1 LN	41.9	*17.6*	10.1	*10.7*	5.6	*6.7*
2 FN	58.4	*28.2*	20.5	*20.1*	4.6	*5.9*
10 FN	54.2	*26.5*	14.5	*12.4*	5.7	*3.1*

Figure 2.55: A. Expression of ABCG2 by HCjE-Gi cells on pre-adsorbed proteins. Data are presented as mean percentage (%) of stained cells per view ± 1SD, n = 2. There were significantly lower percentages of stained cells on days seven and fourteen compared to day one ($p < 0.001$). There was a significantly higher percentage of stained cells on type IV collagen pre-adsorbed from a 10µg/mL solution compared to tissue culture polystyrene on culture day one ($p = 0.028$). Moreover, there were significantly higher percentages of stained cells on type IV collagen pre-adsorbed from 2 and 10 µg/mL solutions compared to laminin 111 pre-adsorbed from 0.5-1µg/mL solutions, and on fibronectin pre-adsorbed from a 2µg/mL solution compared to laminin 111 pre-adsorbed from a 0.5µg/mL solution on day one ($p = 0.011$); *$p < 0.05$. (Two-way ANOVA; Bonferroni post hoc test). B. Mean percentage of stained per view on culture days 1, 7 and 14, and 1SD; C4 - type IV collagen 2 and 10µg/mL, LN - laminin 111 0.5 and 1µg/mL and FN – fibronectin 2 and 10µg/mL.

2.3.10 EXPRESSION OF GOBLET CELL MARKERS BY HCjE-Gi CELLS ON PRE-ADSORBED PROTEINS

MUC5AC

There was positive staining for MUC5AC in the cytoplasm of HCjE-Gi cells (figure 2.56). The staining was mostly observed in colonies of cells.

Pre-adsorption of proteins did not affect the expression of MUC5AC by HCjE-Gi cells over a culture period of fourteen days (figure 2.57). There were eight outliers in the data set and nine groups were not normally distributed (day 1 – type IV collagen 10µg/mL, day 1 - laminin 111 1µg/mL, day 7 – TCP, day 7 – type IV collagen 2µg/mL, day 7 - laminin 111 0.5µg/mL, day 7 - laminin 111 1µg/mL, day 7 - fibronectin 10µg/mL, day 14 – TCP, and day 14 – laminin 111 1µg/mL). There was heterogeneity of variances ($p < 0.001$). The interaction effect between substrate and culture day on the expression of MUC5AC protein was not statistically significant ($p = 0.234$). Analysis of the main effect between the substrates showed no statistically significant difference, $p = 0.543$. However, there was a significant difference between the culture days, specifically; there were higher percentages of stained cells on days seven and fourteen compared to day one ($p < 0.001$). When the outliers were removed, there was no change to the overall result.

Expression of MUC5AC by HCjE-Gi cells

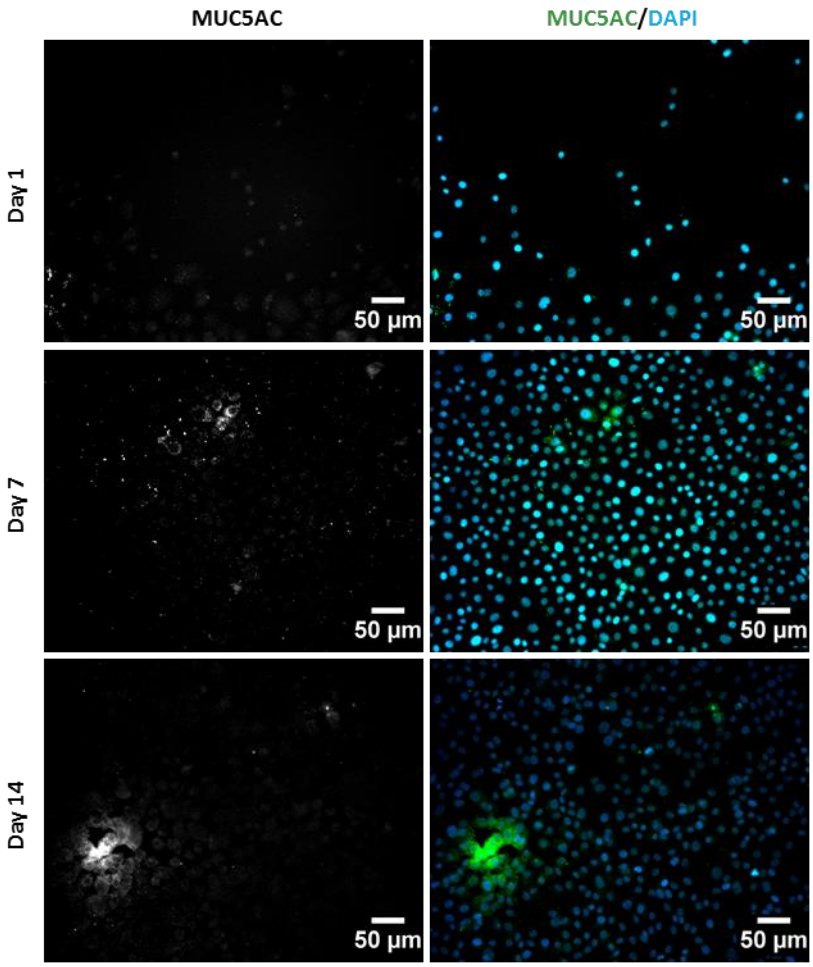

Figure 2.56: Expression of MUC5AC by HCjE-Gi cells; MUC5AC (green) and DAPI (blue). There was positive staining for MUC5AC in the cytoplasm of HCjE-Gi cells, mostly in colonies of cells.

Expression of MUC5AC by HCjE-Gi cells on pre-adsorbed proteins

A

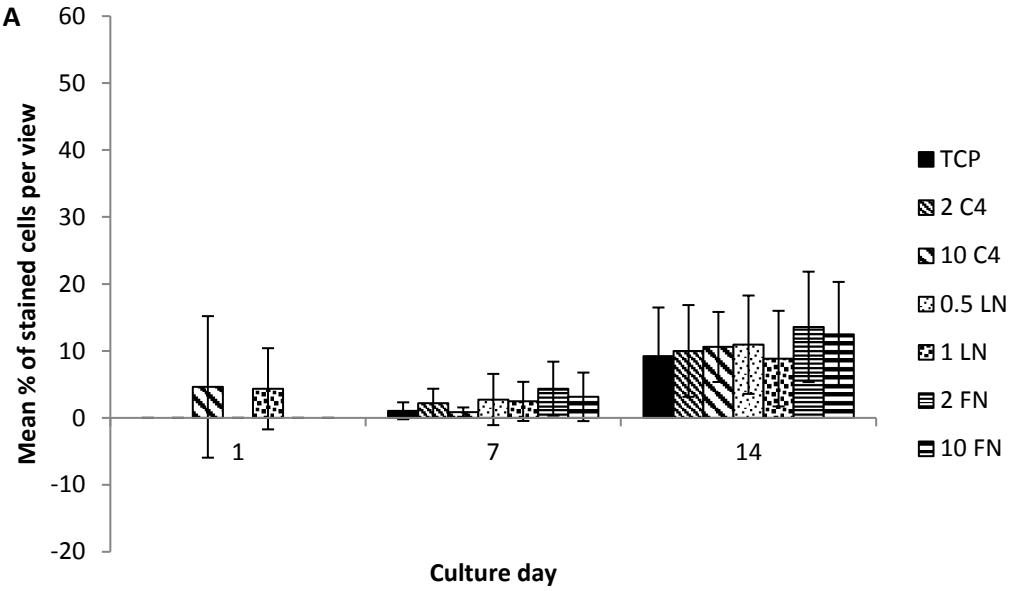

B

	Day 1		Day 7		Day 14	
	Mean	*SD*	Mean	*SD*	Mean	*SD*
TCP	0	*0*	1.1	*1.3*	9.2	*7.2*
2 C4	0	*0*	2.2	*2.2*	10.0	*6.9*
10 C4	4.6	*10.6*	0.9	*0.7*	10.6	*5.2*
0.5 LN	0	*0*	2.7	*3.8*	10.9	*7.3*
1 LN	4.3	*6.1*	2.5	*2.9*	8.9	*7.1*
2 FN	0	*0*	4.4	*4.0*	13.6	*8.2*
10 FN	0	*0*	3.1	*3.6*	12.5	*7.8*

Figure 2.57: A. Expression of MUC5AC by HCjE-Gi cells on pre-adsorbed proteins. Data are presented as mean percentage (%) of stained cells per view ± 1SD, n = 2. The interaction effect between substrate and culture day on the mean percentage of stained cells was not significant (p = 0.234). There was no significant difference to the percentage of stained cells between the substrates (p = 0.543). However, there were significant increases to the percentage of stained cells on culture days seven and fourteen compared to culture day one (p < 0.001). (Two-way ANOVA; Bonferroni post hoc test). B Mean percentage of stained per view on culture days 1, 7 and 14, and 1SD; C4 - type IV collagen 2 and 10µg/mL, LN - laminin 111 0.5 and 1µg/mL and FN – fibronectin 2 and 10µg/mL.

UEAI and keratin 7

There was positive staining for keratin 7 in all the cells from culture days one to fourteen on ICC (figure 2.58). The staining for UEAI was peri-nuclear on day one with some weak staining of the cytoplasm. By day seven, there was stronger cytoplasmic staining and granular staining pattern in some cells. On culture day fourteen, there was strong staining of the cell membranes with some granular staining pattern in the cytoplasm of cells.

Pre-adsorption of proteins did not affect the co-expression of keratin 7 and UEAI by HCjE-Gi cells over a culture period of fourteen days (figure 2.59). There were seven outliers in the data set and seven groups were not normally distributed (day 1 – TCP, day 1 – type IV collagen 2µg/mL, day 1 - type IV collagen 10µg/mL, day 1 - laminin 111 1µg/mL, day 1 - fibronectin 10µg/mL, day 14 – laminin 111 1µg/mL, and day 14 – fibronectin 2µg/mL). There was heterogeneity of variances ($p < 0.001$). The interaction effect between substrate and culture day on the co-expression of keratin 7 and UEAI was not statistically significant ($p = 0.072$). Analysis of the main effect between the substrates and between the culture days showed no statistically significant differences, $p = 0.226$ and $p = 0.900$, respectively. When the outliers were removed, there was a statistically significant interaction effect observed between substrate and culture day on the co-expression of keratin 7 and UEAI ($p = 0.005$). There were significant reductions to the percentage of stained cells on day one when cultured on fibronectin pre-adsorbed from a 10µg/mL solution compared to that when cultured on fibronectin from a 2µg/mL solution and laminin 111 pre-adsorbed from a 1µg/mL solution ($p = 0.003$ and $p = 0.001$, respectively). There were also significant increases to the percentage of stained cells on day one when cultured on laminin 111 pre-adsorbed from a 1µg/mL solution compared to that when cultured on type IV collagen pre-adsorbed from a 10µg/mL solution ($p = 0.016$), and when cultured on fibronectin pre-adsorbed from a 2µg/mL solution compared to that when cultured on type IV collagen pre-adsorbed from a 10µg/mL solution ($p = 0.006$). Additionally, a statistically significant increase to the percentage of stained cells was observed on type IV collagen pre-adsorbed from a 10µg/mL solution on culture day seven compared to day one ($p = 0.002$). Lastly, statistically significant increases to the percentage of stained cells were observed on fibronectin pre-adsorbed from a 10µg/mL solution on culture days seven and fourteen compared to day one ($p = 0.001$ and $p = 0.043$, respectively).

Co-expression of UEAI and keratin 7 by HCjE-Gi cells

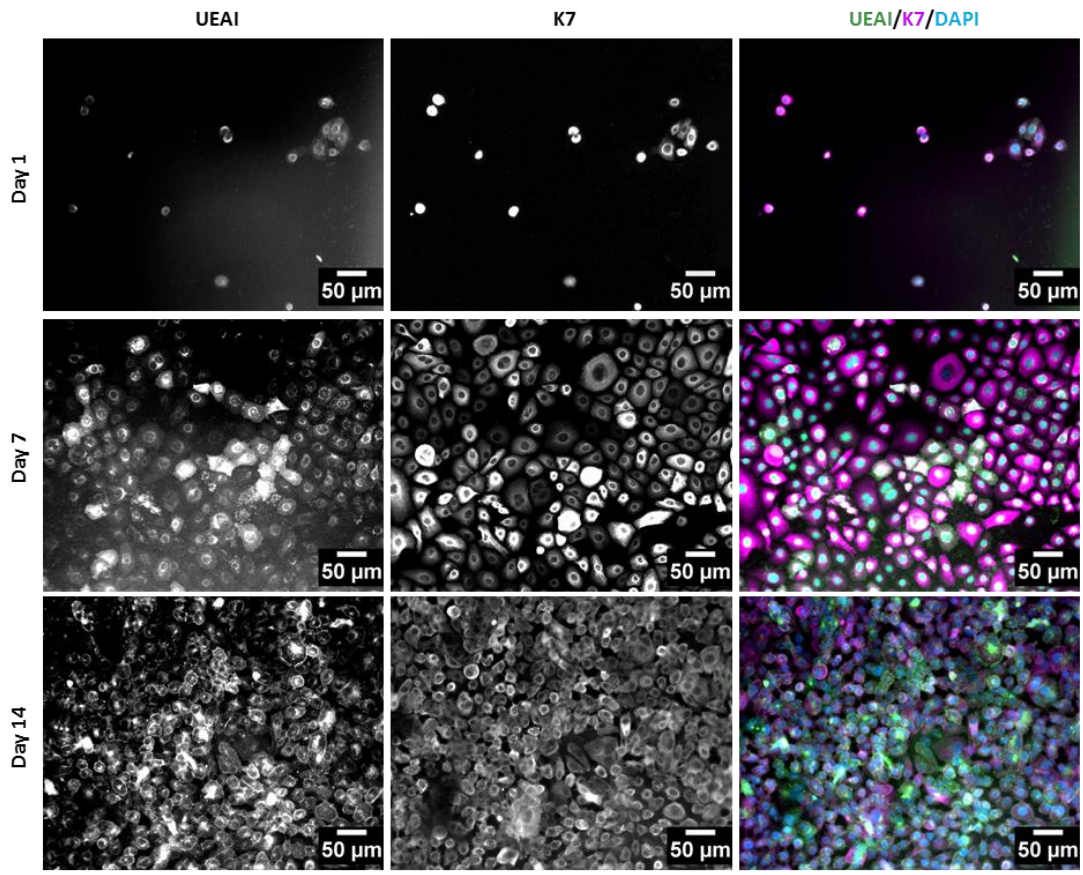

Figure 2.58: Co-expression of UEAI and keratin 7 by HCjE-Gi cells; UEAI (green), keratin 7 (K7, purple) and DAPI (blue). There was positive staining for keratin 7 in all the cells from culture days one to fourteen. The staining for UEAI was peri-nuclear on day one with some weak staining of the cytoplasm. By day seven, there was stronger cytoplasmic staining and granular staining pattern in some cells. On culture day fourteen, there was strong staining of the cell membranes with some granular staining pattern in the cytoplasm of cells.

Co-expression of UEAI and keratin 7 by HCjE-Gi cells on pre-adsorbed proteins

A

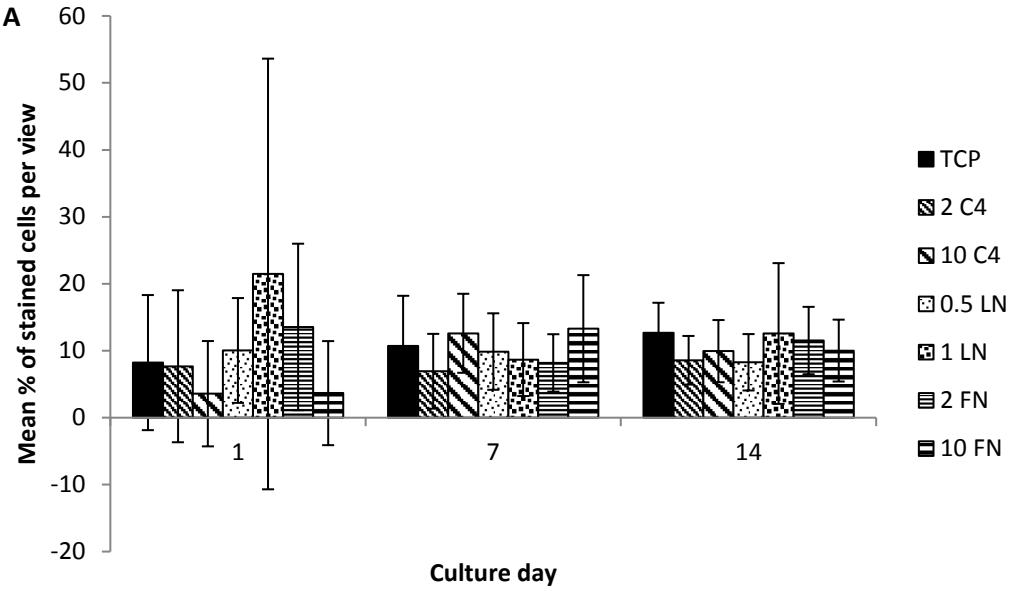

B

	Day 1		Day 7		Day 14	
	Mean	*SD*	Mean	*SD*	Mean	*SD*
TCP	8.2	*10.1*	10.7	*7.5*	12.7	*4.5*
2 C4	7.7	*11.4*	6.9	*5.6*	8.6	*3.6*
10 C4	3.6	*7.9*	12.6	*5.9*	9.9	*4.6*
0.5 LN	10.0	*7.8*	9.9	*5.7*	8.3	*4.2*
1 LN	21.5	*32.2*	8.7	*5.4*	12.6	*10.5*
2 FN	13.6	*12.4*	8.2	*4.3*	11.5	*5.0*
10 FN	3.7	*7.8*	13.3	*8.0*	10.0	*4.6*

Figure 2.59: A. Co-expression of UEAI and keratin 7 by HCjE-Gi cells on pre-adsorbed proteins. Data are presented as mean percentage (%) of stained cells per view ± 1SD, n = 2. The interaction effect between substrate and culture day on the mean percentage of stained cells was not significant (p = 0.072). There was no significant difference in the percentage of stained cells between the substrates or between the culture days (p = 0.226 and p = 0.900, respectively). (Two-way ANOVA; Bonferroni post hoc test). B. Mean percentage of stained per view on culture days 1, 7 and 14, and 1SD; C4 - type IV collagen 2 and 10µg/mL, LN - laminin 111 0.5 and 1µg/mL and FN – fibronectin 2 and 10µg/mL.

2.4 DISCUSSION

2.4.1 Ammonium hydroxide successfully isolated the proteins of the extracellular matrix of HCjE-Gi cells

The choice of decellularisation method varies for each cell or tissue type. The aim of the decellularisation method is to remove all the cellular material without disrupting the composition, biological activity or the mechanical properties of the ECM. A typical decellularisation protocol involves cell lysis using physical methods or ionic treatments, then separation of the cells from the underlying ECM using enzymes, solubilising the cellular organelles using detergents, and lastly removing the cellular debris.(130) In the present study, we showed that 1% NH_4OH was sufficient to successfully isolate the ECM of the HCjE-Gi cells (figures 2.10-2.11). Thorough washes with PBS were required to ensure that all the cell debris was removed from the isolated ECM. It is imperative that the cell debris is adequately washed off to ensure that they do not adsorb onto the remaining matrix, which could give rise to sources of immunogenicity when the ECM scaffolds are subsequently transplanted *in vivo*.(130) Additionally, thorough washes remove the chemicals used in the decellularisation process that could potentially be toxic to the cells.(130, 131) The NH_4OH protocol is also known to isolate the transmembrane proteins that are associated with the ECM proteins.(123) Studies will be required to investigate the immunogenicity of these proteins when undertaking *in vivo* studies.

NH_4OH is a hypertonic solution that disrupts the cells by osmotic shock.(130) Additionally, alkaline solutions denature proteins, solubilise cell organelles and remove nucleic acids.(130) However, they may remove GAGs from collagenous tissues.(131) Most physical methods are known to maintain the architecture and collagen content in the ECM.(132) Sodium dodecyl sulfate is an ionic detergent, whose negative charge leads to increased water content and swelling of cells thereby disrupting the cell membranes.(56) Studies on porcine conjunctival tissue have shown that more than 92% of the DNA was removed and that more than 90% of GAGs and hydroxyproline were intact following decellularisation using sodium dodecyl sulfate.(56) However, it may disrupt the architecture of collagens due to the swelling.(131) Triton X-100 is a non-ionic detergent, which disrupts lipid-lipid and lipid-protein interactions but maintains protein-protein interactions.(131) It has been shown to reduce the contents of GAGs, laminin and fibronectin.(130) Long-term exposure to enzymes is known to damage the ultrastructure of the ECM by removing the contents of collagen, elastin, laminin, fibronectin and GAGs. (130)

2.4.2 Immunofluorescence staining and mass spectrometry experiments were undertaken to identify and quantify the protein composition of the extracellular matrix of HCjE-Gi cells

IF staining of ECM samples is a qualitative measure of assessing the presence and the distribution of individual proteins. This method relies on the interactions between a target protein antigen and an antibody (primary antibody), that is visualised via a fluorescence tag (secondary antibody) that is targeted to bind the primary antibody.(42) Accuracy of results obtained from IF staining depends on the specificity of antibodies and prevention of non-specific binding to proteins in the samples, which is a major limitation of this method.

The ECM is a dynamic protein structure in which the composition of proteins and their quantities may vary with age. As well as identifying the proteins present in the ECM, mass spectrometry allows quantification of individual proteins. Thus, mass spectrometry can be employed as a complementary quantitative method to IF staining to determine the protein profile of the ECM of the HCjE-Gi cells. As described in section 2.2.4, trypsin cleaves proteins by targeting the C-termini of lysine and arginine to produce a mixture of peptides. Mass spectrometry involves analysis of the individual peptides that are present in a sample to produce a protein profile with their relative abundances.(42) First, the mass spectrometer ionises the peptides to produce a stream of positive ions.(133) These are then accelerated to produce a stream of ions that have equal kinetic energies. The positive ions enter a magnetic field and are deflected according to their mass/charge ratios. These are then detected as an electric current that is amplified and recorded. The electric current increases proportionately to the number of ions arriving at the detector. The output from the mass spectrometer shows the relative abundance, as determined by the electric current, for each mass/charge ratio.(133) Data-dependent LC-MS/MS undertaken in the present study involves two mass spectrometers that increase the accuracy of the results. The first spectrometer separates the ions according to their mass/charge ratios.(42) Then ions with a selected mass/charge ratio (precursor ions) undergo collisional activation to produce fragment ions (product ions).The second spectrometer separates these product ions according to their masses. The number of peptides formed from each protein during sample preparation depends on the number of lysine and arginine present in the parent protein and the size of the parent protein. Although this is not a problem when investigating the change to the abundances of individual proteins with time, it may be a limitation when determining protein ratios relative to each other at each time point.

2.4.3 The protein composition of the extracellular matrix of HCjE-Gi cells varied over six weeks in culture *in vitro*

2.4.3.1 There was no change to the proportion of structural collagens in the extracellular matrix of the HCjE-Gi cells over six weeks in culture

Type XVIII collagen was the only structural collagen detected by mass spectrometry from ECM days 1 to 42 (figure 2.24). IF staining using an antibody targeting the non-collagenous domains of type XVIII collagen showed a granular staining pattern in the ECM of HCjE-Gi cells that were in culture for 21 to 42 days (figures 2.12-2.19). Positive staining for type IV collagen that co-localised with the staining for the laminin α_3 chain was observed during IF staining (figures 2.12-2.19). However, type IV collagen was not detected by mass spectrometry. The raw abundance and the proportion of type XVIII collagen in the ECM increased over the six weeks culture period (0.18% in the day 1 ECM to 0.33% in the day 42 ECM), although this was not found to be statistically significant.

Type XVIII collagen is a non-fibrillar collagen-HSPG. There are three isoforms of type XVIII collagen: the short isoform is expressed in vascular and epithelial BMs, the medium isoform in liver and glomerular BMs and, the long isoform in glomerular BMs and a small amount in most tissues.(89) It plays a role in maintaining the structural integrity of BMs and has also been implicated in the regulation of cell survival and maintenance of stem and progenitor cells.(89) Genes regulating the production of type XVIII collagen have been shown to be up-regulated in the haematopoietic SCs of the bone marrow and epidermal SCs of the hair follicle budge. The endostatin domain at the C-terminal has anti-angiogenic properties when cleaved from the parent protein.(134) The mass spectrometry experiments of the present study only detected peptides of the α_1 chain of type XVIII collagen and no evidence of peptides of endostatin. This suggests that this peptide sequence may not be cleaved from the parent protein in the ECM secreted by the HCjE-Gi cells. Immunohistochemistry staining has shown the presence of type XVIII collagen in the BM of the OS (table 1.2). In contrast, moderate expression of endostatin was observed throughout corneal and limbal BMs, however, there was only focal expression or no expression of this protein in the conjunctival BM.(11) It is important that the cornea remains avascular to ensure its transparency, whereas conjunctival and limbal tissues are vascular tissues with a rich blood supply. Endostatin has also been found to be expressed in structures that border the anterior chamber (lens, iris, ciliary body and trabecular meshwork) and the vitreous (internal limiting membrane of the retina), suggesting a role in forming a “barrier” to

neovascularisation and thus allowing light rays to pass through ocular structures undisturbed.(135, 136)

Type XVIII has been shown to co-localise with type IV collagen in the BM of the cornea.(137) A polarised orientation of type XVIII collagen within BMs has been demonstrated with the C-terminal endostatin facing the cells and N-terminal facing the connective tissue stroma.(89) This is similar to the orientation suggested for type IV collagen within the BMs. The endostatin domain has been shown to interact with integrin $\alpha_5\beta_1$, glypican, laminin complex, nidogen, perlecan, fibulin, SPARC and type I, IV and VI collagens.(88, 89) It inhibits endothelial cell migration and proliferation and induces cell apoptosis by binding to integrin $\alpha_5\beta_1$ and glypican.(88) In contrast to the monomeric endostatin molecule that has anti-migratory effects, the trimerised non-collagenous domains at the C-terminal of type XVIII collagen has been shown to bind to laminin 111 to induce cell migration.(138)

Interestingly, mass spectrometry experiments of the present study failed to detect peptides of type IV collagen that is known to be one of the major proteins of all the BMs. However, staining for this protein was observed by IF experiments that co-localised with the staining for laminin α_3 chain in the ECM of days 21 to 42. The target antigen for the antibody was the α_1 chain of type IV collagen, which is known to be expressed in the limbal and conjunctival BMs and not in the corneal BM. Studies have shown that the non-collagenous domains at the C-termini of type IV collagen also have anti-angiogenic fragments, such as arrestin (α_1 chain), canstatin (α_2 chain) and tumstatin (α_3 chain). The antibody used in the present study may have interacted with the C-terminal of the α_1 chain of type IV collagen that may have similarities to that of the type XVIII collagen. However, the staining pattern for type IV and type XVIII collagens were different, which questions the specificity of the type IV collagen antibody used in IF experiments.

The absence of type IV collagen observed in the present study may have been due to the culture substrate and the *in vitro* conditions. It may be that this protein is not deposited by the cultured HCjE-Gi cells on TCP and instead, type XVIII collagen is deposited as a structural collagen to provide adequate stability to the BM. Pöschl et al. showed that type IV collagen is important for the stability of BMs and maintenance of their structural integrity, especially in conditions of increasing mechanical demands, however, indispensable for the initial assembly of the BM *in vivo*.(139) They showed that mutant mice with inactivated *Col4a1/a2*

genes had normal embryonic development during the early stages with no changes to the mRNA expression of laminin α_1 chain or nidogen 1. They also showed that these mice did not have compensatory expression of other type IV collagen isomers. However, by E10.5-11.5 there were discontinuities and ruptures in the BM. In the present study, mass spectrometry experiments did not detect nidogen, a bridging protein between the laminin and type IV collagen networks. The lack of nidogen in the ECM show that this protein is not required as type IV collagen is not deposited by the HCjE-Gi cells cultured on TCP. Nidogen is not required for type XVIII collagen to bind to the laminin network.

In the present study, mass spectrometry experiments detected integrins α_5 and β_1 in the ECM of the HCjE-Gi cells, although both accounted for less than 1% of the total peptides in the ECM at all the time points (figure 2.31). Both α_5 and β_1 increased significantly with time and this accounts for the increase in type XVIII collagen observed over the six weeks culture period (figure 2.24). The proportion of integrin β_1 was always higher than that of integrin α_5, which is expected as integrin β_1 is known to associate with other α subunits. Integrins that are thought to be associated with type IV collagen are $\alpha_1\beta_1$ and $\alpha_2\beta_1$. Only integrin α_2 was present in the ECM of the HCjE-Gi cells, which accounted for less than 1% of the total peptides in the ECM at all the time points (figure 2.31). The increase in peptide abundance for this integrin on day 42 was not found to be statistically significant compared to that on day 1.

2.4.3.2 Laminin chains that give rise to trimers 332, 311 and 511 were present in the extracellular matrix of the HCjE-Gi cells

There were six laminin chains that were expressed in the ECM of the HCjE-Gi cells, α_3, α_5, β_1, β_3, γ_1 and γ_2 chains (figure 2.24). All these chains have previously been shown to be present in conjunctival tissue by immunohistochemistry (table 1.2). Combinations of these laminin chains can give rise to laminin trimers 332, 311 ($\alpha_3\beta_1\gamma_1$, also known as laminin 6) and 511. Previous studies have shown that laminins 111, 332, 311 and 511 are found in the BM of the cornea and additional trimers incorporating the α_2 and β_2 chains are found in the BM of the conjunctiva (laminin 211, 221 ($\alpha_2\beta_2\gamma_1$, also known as laminin 4) and 521 ($\alpha_5\beta_2\gamma_1$, also known as laminin 11)).(119) In the present study, there was no evidence of α_2 and β_2 laminin chains in the ECM, which may explain the lack of expression of keratin 4 by the HCjE-Gi cells.

The most abundant structural protein in the ECM of HCjE-Gi cells was laminin α_3 chain throughout the six weeks culture period, the raw abundance of which increased significantly on day 7 compared to day 1 (figures 2.24 and 2.30). Although the highest raw peptide abundance was observed in the day 42 ECM this was not found to be statistically significant compared to that on day 7. The next most abundant chains were laminin β_3 and γ_2 chains, whose raw peptide abundance followed a similar pattern to that observed for the laminin α_3 chain. The proportion of laminin β_3 in the ECM remained relatively stable, whereas that of γ_2 chain reduced over the six weeks (figure 2.30). This may suggest that with time there is an increase in the formation of laminin 311 that contains the α_3 chain. Nevertheless, the results of the present study indicated that the ECM secreted by the HCjE-Gi cells is predominantly made up of laminin 332. The present study also showed the presence of the α_3 chain of laminin using IF experiments. This protein was present in the day 1 ECM and continued to be deposited abundantly throughout the six weeks culture period (figures 2.12-2.19). Laminin 332 has been shown to be deposited into the provisional ECM within eight hours of epithelial wounding.(140)

Laminins are deposited in various patterns by cultured cells that may suggest differences in the function of the laminin matrix or represent various stages of the matrix formation.(129) Human keratinocytes have been shown to deposit laminin 332 in a rosette-like pattern when stationary.(129) This is in contrast to that deposited by the migrating cells, which deposit laminin 332 in a trail-like pattern. Similar results were observed in the present study by IF staining for the laminin α_3 chain (figures 2.12-2.19). Syndecan 1 has been implicated in the deposition of laminin 332, where a lack of syndecan 1 has been shown to deposit laminin 332 in arrowhead-like arrays by keratinocytes.(129) This was in contrast to the wild-type cells that deposited laminin 332 as cloud-like trails. The peptides of syndecan 1 were present in the ECM secreted by the HCjE-Gi cells, which increased significantly over the six weeks (figure 2.24). Laminins 211 and 221 has been shown to be deposited as a mesh by Schwann cells and laminin 311 as fibrils by alveolar cells, where it plays a role in transmitting stretch signals to the cells.(129) The possibility of increased deposition of laminin 311 by HCjE-Gi cells with time may suggest a similar role in being able to transmit mechanical signals from a maturing ECM to the cells.

Laminin 332 is secreted as a 460kDa molecule that is processed to form a 440kDa molecule by keratinocytes in the presence of low calcium (0.035mM) and a smaller mature molecule (400kDa) in the presence of high calcium (1mM).(140) This is due to the processing of the γ_2

chain and the globular domains IV and V of the α_3 chain. The α_3 chain of laminin 332 has been shown to support the adhesion and migration of cells *in vitro* via integrins $\alpha_6\beta_4$ and $\alpha_3\beta_1$, respectively.(140) The processed mature laminin α_3 chain has been shown to be involved in the formation of stable adhesions via hemidesmosomes, whereas the unprocessed chain is deposited by the migrating keratinocytes.(140) The proteolytic cleavage of the γ_2 chain by MMPs 2 and 14 has been shown to enhance the migration of cells.(141) These studies show that the main cell binding site on the laminin α_3 chain is located in the globular domains I-III.(141) However, studies have shown that globular domain IV has a strong affinity to heparin and has been shown to promote cell adhesion by binding to syndecans on the cell membranes.

Laminin 332 is an important constituent of hemidesmosomes connecting epithelial cells to their BM and the underlying connective tissue stroma. The α_3 chain of laminin interacts with integrin $\alpha_6\beta_4$ on the cell membrane and the β_4 integrin interacts with the keratin cytoskeleton via plectin.(140) These structures are strengthened by type XVII collagen that interact with laminin 332 and bullous pemphigoid antigen 230 that interacts with integrin β_4.(140) Focal adhesions connect the laminin α_3 chain to the actin cytoskeleton via integrin $\alpha_3\beta_1$.(140) Integrin α_6 was the most abundant integrin in the ECM of the HCjE-Gi cells from days 1 to 14 (7.7% and 11.6% of the total ECM peptides, respectively), whereas integrin β_4 was the most abundant integrin from days 28 to 42 (11.9 and 17.6%, respectively) (figure 2.31). Integrins α_3 and β_1 were also present, although they only contributed to less than 1% of the ECM throughout the six weeks (figure 2.31). The raw peptide abundances of these integrins were significantly higher on day 42 than day 1, except for that of integrin α_3. The ECM of the HCjE-Gi cells consisted of the transmembrane proteins type XVII collagen and CD151 (figure 2.24). The raw peptide abundances of both these proteins increased significantly by day 42. Plectin and bullous pemphigoid antigen 230 were also shown to be present in the samples by mass spectrometry, however, these were classified as intracellular proteins. These results demonstrate that the HCjE-Gi cells were able to form stable attachments to the underlying ECM via hemidesmosomes as the epithelium matured during the culture period.

Another laminin trimer that may be present in the ECM of the HCjE-Gi cells is laminin 311. Although laminin 311 shares the same α_3 chain as that in laminin 332, its cell adhesive and migratory properties have been found to be significantly less than that of laminin 332.(140) Hirosaki et al. showed that unprocessed laminin 311, laminin 311 without the IV-V globular

domains on the α_3 chain and mature laminin 332 with processed α_3 and γ_2 chains supported cell adhesion via integrins $\alpha_3\beta_1$ and $\alpha_6\beta_1$ in human fibrosarcoma cells.(141) However, unprocessed laminin 311 did not support spreading or migration of the cells compared to the processed laminins 311 and 332. The authors suggested that the reduced cell spreading and migration in human fibrosarcoma cells may be due to steric hindrance of the cell binding globular domains I-III by the globular domain V of the unprocessed α_3 chain. Hirosaki et al. also showed that mature laminin 332 supported cell migration more effectively than the processed laminin 311 lacking the IV-V globular domains of the α_3 chain. Thus, cell migration not only depends on the lack of the globular domains IV-V of the α_3 chain, but also on the proteolytic processing of the γ_2 chain of laminin 332 in these cells.(141) Additionally, studies on amniotic and skin tissues have shown that approximately half of the laminin 332 is covalently linked to either laminin 311 or 321 ($\alpha_3\beta_2\gamma_1$, also known as laminin 7).(141) These laminin complexes together with laminin 332-type VII collagen complexes synergistically are responsible for forming strong interactions between the epidermis and dermis.(141, 142)

The peptides of laminin chains α_5, β_1 and γ_1 contributed to less than 1% of the total ECM from day 1 to 42 (figure 2.30). Although the raw peptide abundances of all the chains increased with time, significant increases were only observed from day 1 to 7 for the α_5 chain, and from day 1 to 14 for β_1 and γ_1 chains. Laminin 511 together with laminin 521 are known as placental laminins.(119) The lack of the α_5 chain has been shown to lead to death during late embryogenesis and has been shown to be present in fetal and adult tissues.(143) Hasenson et al. showed that the α_5 chain mediates cell adhesion and spreading via integrins $\alpha_3\beta_1$ and BCAM on the membranes of corneal epithelial cells.(143) In addition to integrin $\alpha_3\beta_1$, BCAM was also present in the ECM of the HCjE-Gi cells (figure 2.24), although there was no significant difference to its peptide abundance between culture days 1 and 42. It only contributed to 0.6% of the total peptide abundance in the day 42 sample (figure 2.31). Additionally, Hasenson et al. suggested that these transmembrane proteins bind to the globular domains I-III of the laminin α_5 chain independently of each other to mediate intracellular signalling.(143) Lin et al. showed that the conjunctival epithelial cells interacted with the globular domain IV of the α_5 chain via syndecan 4. Blocking this specific domain on the laminin α_5 chain only reduced cell adhesion by 16% suggesting the presence of alternative binding sites on laminin 511.(144) Syndecan 4 was present in the ECM of the HCjE-Gi cells (figure 2.24), although its raw peptide abundance was less than that observed for syndecan 1. It contributed to less than 1% of the total

peptide abundance throughout the six weeks (figure 2.31) and there was no significant difference in the peptide abundances between the day 1 and day 42 samples. Nakashima et al. showed that the short arm of the β_3 chain of laminin 332 stimulates human embryonic kidney cells to deposit laminin 511 to enhance laminin 511-dependent adhesion and spreading.(142) It is likely that the laminin 332, 311 and 511 interact with each other in a synergistic manner to enhance adhesion, spreading and migration of HCjE-Gi cells *in vitro*.

2.4.3.3 Thrombospondins 1 and 2 were present but thrombospondin 4 was absent in the extracellular matrix of HCjE-Gi cells

Thrombospondin 1 was the next most abundant GP in the ECM of the HCjE-Gi cells after laminin 332 chains. It contributed to 4.4-6.5% of the ECM from days 7 to 42 (figure 2.30). Thrombospondin 2 was also present in the ECM of the HCjE-Gi cells, however, contributed to less than 1% of the ECM throughout the six weeks (figure 2.30). Thrombospondins 1 and 2 are anti-angiogenic, whereas thrombospondin 4 is pro-angiogenic, which has been shown to have a focal distribution in conjunctival tissues by immunohistochemistry.(145) The conjunctiva is a vascular tissue, however, thrombospondin 4 was not present in the ECM secreted by the HCjE-Gi cells. These findings suggest that thrombospondins 1 and 2 may play a role different to an anti-angiogenic role in the conjunctival tissues. Contreras-Ruiz et al. showed the presence of conjunctival inflammation and associated loss of GC function in thrombospondin 1-null mice.(94) Soriano-Romani et al. showed the expression of small amounts of thrombospondin 1 by conjunctival epithelial cells *in vitro*.(106) Thrombospondin 1 is thought to mediate its effects via CD36 and CD47 (also known as platelet glycoprotein 4 and leukocyte surface antigen CD47, respectively). The present study did not show the expression of CD36, however, the raw peptide abundance of CD47 increased significantly on day 42 compared to that on day 1 (figure 2.24). Soriano-Romani et al. showed that the conjunctival epithelial cells predominantly exerted its anti-inflammatory effects via CD47 rather than CD36.(106) Thus, thrombospondin 1, and maybe 2, may play an immunomodulatory role via CD47 in the HCjE-Gi cells to maintain the normal tissue homeostasis.

2.4.3.4 The highest peptide abundance of adhesive glycoproteins were in the extracellular matrix of the HCjE-Gi cells that has been in culture for seven days

The adhesive GPs found to be expressed in the ECM of the HCjE-Gi cells were fibronectin, nephronectin and vitronectin (figure 2.24). The peptide abundances of all these proteins

were highest in the day 7 ECM, however, only that of fibronectin and nephronectin were statistically significant compared to the other time points.

The proportion of fibronectin was highest in the day 1 and 7 ECM samples (0.8% and 0.7%, respectively) (figure 2.30). Fibronectin only contributed to 0.2% of the total peptide abundance in the day 42 ECM. This was confirmed by IF staining that showed a 'spike-like' staining pattern around the staining for the laminin α_3 chain, the expression of which reduced after day 7 (figures 2.12-2.19). In wound healing, cells secrete and migrate over a provisional matrix made up of laminin 332 and fibronectin.(103, 146) This provisional matrix is degraded and remodelled by the cells by secreting new matrix proteins.(103) As cultured cells migrate the focal complexes at the edge of cell mature into focal contacts, which together with the actin cytoskeleton produce the tractional forces required to pull the cell forward.(103) At the opposite end of the cell, the focal contacts disassemble allowing the cell to detach from the underlying matrix, again allowing the movement of cell forward.(103) Kligys et al. showed that laminin 332 enhanced bronchial epithelial cell migration, whereas fibronectin reduced cell migration by enhancing cell adhesion.(146) The main integrin that fibronectin is thought to be associated with is $\alpha_5\beta_1$. The highest proportion of fibronectin in the present study was found in the ECM secreted by the cells that have been in culture for 1 to 7 days. However, the proportions of laminin α_3 and γ_2 chains, thought to enhance cell migration, in the day 1 ECM were approximately nine-folds higher than that of fibronectin. It may be that the provisional matrix of the HCjE-Gi cells provides a balanced matrix that supports initial cell adhesion as well as cell migration.

Vitronectin was present in the ECM of the HCjE-Gi cells, which has not been shown to be present in conjunctival tissue previously using immunohistochemistry (table 1.2). In contrast, weak staining for this protein has been observed in the cornea and as a sub-BM layer in the limbus. Like fibronectin, it is thought to play an adhesive role in the provisional matrix. In the present study, although there was no significant change to the raw peptide abundance over the six weeks, the highest proportion of this protein was observed in the day 1 and day 7 ECM samples (approximately 0.06%) (figure 2.30). Moreover, vitronectin has also been shown to enhance cell migration and rate of wound closure in corneal epithelial cells.(92) Vitronectin is thought to mediate its effects by binding to integrins $\alpha_v\beta_3$ and $\alpha_v\beta_5$.(92) The ECM of the HCjE-Gi cells did not express these β subunits. However, Huang et al. showed that β_6-null mouse keratinocytes exhibited reduced cell migration when cultured on vitronectin and fibronectin *in vitro*, suggesting that these proteins

interacted with integrin $\alpha_v\beta_6$ to mediate their effects on the cells.(147) Similarly, the HCjE-Gi cells may interact with vitronectin via integrin $\alpha_v\beta_6$. The peptide abundance of the α_v subunit increased significantly over the six weeks, whereas that of the β_6 subunit did not (figure 2.24).

Gildner et al. showed that fibronectin-null mouse embryonic fibroblasts when cultured on vitronectin deposited fibronectin fibrils that were less extended than when cultured on type I collagen, although the amount of fibronectin deposited was similar on both substrates.(91) Moreover, they showed that the cells cultured on vitronectin had a lower proliferation rate than when cultured on type I collagen, which they suggested was due to the altered conformation of the fibronectin fibril and therefore the exposure of its growth promoting domains. The altered functionality of the cells may also be due to independent effects of the two substrates alone, where type I collagen may induce a higher proliferative effect on fibroblasts than vitronectin. In the present study, the peptide abundances of both proteins followed a similar pattern in the ECM of the HCjE-Gi cells, although the peptide abundance of fibronectin was approximately ten times higher than that of vitronectin on days 1 and 7. This may be due to differences in the sizes of the two proteins. A future study would be to look at the functional effects on HCjE-Gi cells in the presence of these two proteins alone and together.

To our knowledge to date, nephronectin has not been shown to be present in the ECM of the conjunctiva. We showed that it is present in the ECM of HCjE-Gi cells cultured *in vitro*, the highest raw peptide abundance and proportion (0.03%) being observed in the day 7 ECM (figure 2.30). It has been shown to support the adhesion and migration of rat cardiomyocytes via its RGD domain by interacting with integrin $\alpha_8\beta_1$ on cell membranes.(148) However, the present study failed to show the presence of the integrin subunit α_8 in the ECM of the HCjE-Gi cells. This suggests the presence of another binding site for nephronectin. Sato et al. showed that nephronectin binds to HSPG in the ECM, such as perlecan and agrin, via its MAM (meprin, A5 protein, protein-tyrosine phosphatase mu) domain.(149) However, the physiological relevance of this interaction remains unknown. Further studies are required to investigate the importance of nephronectin on conjunctival cells.

2.4.3.5 The highest proportion of α-2-HS-glycoportein and annexin A2 was in the extracellular matrix of the HCjE-Gi cells that has been in culture for one day

The highest raw peptide abundance and proportion (4.3%) of α-2-HS-GP was in the day 1 ECM (figures 2.24 and 2.30). Although there was no significant difference to the peptide abundance of annexin A2 in the ECM over the six weeks, its highest proportion was found in the day 1 ECM (11.4%) (figure 2.33). To our knowledge to date, α-2-HS-GP has not been shown to be expressed in the ECM of the normal conjunctiva or the ocular surface. Fetuin-A, its bovine homologue, was first detected in fetal and new born calf serum. It is one of the major components of fetal calf serum that is thought to mediate cell adhesion and migration when used in the culture medium *in vitro*. In humans, it is predominantly found in fetal tissue compared to adult tissue. α-2-HS-GP has been shown to have cell adhesive properties that are mediated via annexins A2 and A6 in intestinal epithelial cells and breast carcinoma cells, respectively.(98) In breast carcinoma cells, adhesion has also shown to be mediated via integrin β_1 in the presence of magnesium ions.(96) Studies involving primary keratinocytes have shown significant increases to rates of cell migration and wound closure when cultured in serum-free media in the presence of α-2-HS-GP.(96) Additionally, α-2-HS-GP has been shown to promote scarless healing in an ovine burn model.(97) It is an antagonist of TGFβ and bone morphogenetic proteins (TGFβ related proteins), thus improving the outcome of burns by reducing the inflammatory responses and myofibroblast formation.

2.4.3.6 Perlecan was the most abundant proteoglycan from days one to fourteen, whereas agrin was the most abundant proteoglycan from days twenty-eight to forty-two in the extracellular matrix of the HCjE-Gi cells

Perlecan was the most abundant PG in the ECM of HCjE-Gi cells on culture day 1 (5.7% of the total peptides), the highest proportion being observed on day 14 (7.1%) (figure 2.30). Its raw peptide abundance significantly increased on day 7 compared to day 1 and, no further significant differences were observed thereafter. By day 28, the proportion of agrin surpassed that of perlecan contributing to 5.8% of the total ECM on day 42 (figure2.30).

Perlecan is a large multi-domain HSPG found throughout the OS. It has been associated with various cellular functions, including wound healing, cell proliferation, survival and terminal differentiation.(150) Inomata et al. showed that mice that lacked perlecan in ocular tissues had microphthalmos and small palpebral fissures.(150) Although, these mice

had structurally normal corneal BMs on transmission electron microscopy, the overlying epithelium was thin consisting of an undifferentiated wing cell layer compared to that in the wild-type mice.(150) These findings were thought to be due to the lack of perlecan important for cell proliferation and terminal differentiation.(150) To our knowledge to date, although the presence of perlecan has been shown in the BM of the conjunctiva (table 1.2), functional studies in the conjunctiva have not been undertaken. It is likely that perlecan supports cell proliferation and differentiation of HCjE-Gi cells, similar to that observed with corneal cells.

Miosge et al. showed that approximately half of the endostatin domains of type XVIII collagen co-localised with perlecan and not nidogen 1 in adult mouse kidney BMs *in vivo*.(134) This explains the results observed in the present study, which showed the presence of type XVIII collagen and perlecan and not nidogen in the ECM secreted by the HCjE-Gi cells. This demonstrates one mechanism by which the type XVIII collagen network may interact with the rest of the ECM laid down by the cells. The interaction with endostatin is thought to be mediated via domain V of perlecan that has three globular domains, homologous to the globular domains of laminin, separated by two EGF-like domains.(88) This domain on perlecan has also been shown to bind to the laminin-nidogen complex and integrin $\alpha_2\beta_1$ of cells. Domain I of perlecan consists of heparan sulphate side chains that interact with type IV collagen, laminin 111, thrombospondin, fibronectin and GFs. Binding of perlecan to GFs modulate their functions and plays a role in the maintenance of homeostasis of BMs in tissues.(88)

Agrin is a modular HSPG that has been shown to be present throughout the OS, however, has a specialised role in the development of neuromuscular junctions.(88) It has been shown to be associated with limbal SCs of the OS. It is possible that agrin plays a similar role in the BM of the conjunctiva. In the present study, its proportion increased more than that of perlecan from days 28 to 42 (figure 2.30). This increase in the proportion of agrin in the late ECM of the HCjE-Gi cells may support the maintenance of SCs during long term culture *in vitro*. However, other roles in the conjunctiva, possibly related to the heparan sulphate side chains, cannot be excluded. Therefore, further studies are required to elicit the functional roles of agrin in the BM of conjunctiva.

2.4.3.7 The highest proportions of growth factors and their binding proteins were in the extracellular matrix of the HCjE-Gi cells that have been in culture for one to seven days

GFs are soluble proteins produced by cells that bind to other ECM proteins, especially the PGs. The proteases in the ECM ensure the controlled release of bound GFs into the ECM. GFs modulate cellular functions, including the production of ECM proteins, via autocrine, juxtacrine or paracrine mechanisms. In the present study, the highest proportion of GFs and their binding proteins were in the day 1 and 7 ECM samples (approximately 17% of the total peptides) (figure 2.23). This proportion reduced from day 14 to day 42. One reason for this reduction in GFs may be due to the simultaneous increase in proteases observed from day 7 (figure 2.34). The proteases may cleave the GFs from the other ECM proteins and due to their soluble nature, could have been washed during sample preparation. However, a true reduction in the synthesis of GFs and their binding proteins by the HCjE-Gi cells cannot be excluded.

Insulin was the most abundant protein in this category in the day 1 ECM (figure 2.32). Its raw peptide abundance was highest in the day 7 ECM (figure 2.24), although this was not found to be statistically significant compared to the other time points. Insulin and insulin-like GFs has been shown to promote migration, growth, glucose metabolism and hydration of corneal epithelial cells *in vitro*.(151) In the present study, we did not observe insulin-like GFs, however, there were IGFBPs 3 and 10 in the ECM of the HCjE-Gi cells (figure 2.24). IGFBP bind to insulin-like GFs and regulate their biological actions by prolonging their half-lives.(152) High expression of IGFBP 3 has been shown to be protective against carcinomas, whereas low levels have been associated with increased risk of carcinomas.(153) Down-regulation of IGFBP 3 has been shown to be associated with uncontrolled cell proliferation in conjunctival tissue obtained from patients with pterygia.(153)

IGFBP 10, also known as protein CYR61 due to its cysteine-rich structure, belongs to the family of CCN (CYR61, Connective tissue GF and Neuroblastoma overexpressed) proteins.(154) All the proteins in this family are thought to interact with various proteins due to their modular structure consisting of IGFBP, von Willebrand factor type C repeat and thrombospondin 1 repeat modules. This class of proteins are thought to be involved in angiogenesis. IGFBP 10 in particular has been shown to promote adhesion, migration and proliferation of endothelial cells by interacting with integrins $\alpha_V\beta_3$, $\alpha_V\beta_5$ and $\alpha_6\beta_1$ *in vitro*. Studies have also shown that the presence of this protein in the cornea can induce

neovascularisation *in vivo*. Since conjunctiva is a vascular tissue, the presence of this protein is likely to be physiological. Moreover, IGFBP 10 has also been shown to bind to HSPGs in the ECM, displacing other GFs, and subsequently promoting their roles within the ECM.(154)

In the present study, there was no evidence of TGFβ, however, TGFβ ig-h3 and LTBP 2 proteins were present (figure 2.24). The raw peptide abundance of TGFβ ig-h3 was significantly higher on day 7 compared to the other time points, contributing to 3.7% of the day 7 ECM (figure 2.32). However, LTBP 2 increased significantly on day 7 compared to day 1 and reduced on day 28 compared to day 7. It contributed to less than 1% of the ECM at all the time points (figure 2.32). TGFβ promotes differentiation of epithelial cells and inhibits their proliferation and production of inflammatory proteins.(151) In contrast, it stimulates the proliferation of myofibroblasts and the production of ECM proteins. The expression of TGFβ ig-h3 is thought be stimulated by a complex mixture of proteins including TGFβ.(155) TGFβ ig-h3 has been shown to bind to fibrillar collagens, type IV collagens, laminins, fibronectin and small leucine-rice PGs in the ECM.(155) Maeng et al. showed that TGFβ ig-h3 promoted the adhesion, migration and proliferation of corneal epithelial cells in a dose dependent-manner.(156) This is thought to be mediated via the binding of this protein to integrin $\alpha_3\beta_1$.(155) Moreover, they showed that this protein plays a role in the differentiation of cells and increased the mRNA levels of membrane-type and gel-forming mucins in corneal and conjunctival epithelial cells.(156) Further studies are required to investigate the functional roles of this protein on HCjE-Gi cells cultured *in vitro*, in particular the expression of MUC5AC producing GCs.

LTBPs are known to bind predominantly to fibrillins, however, have been shown to bind to fibronectin, fibulins, HSPGs and ADAMTS-like proteins.(157) LTBP 2 is the only protein in this family that does not bind to any TGFβ isoforms. Instead, it has been shown to interact with other GFs, such as GDF 8. Although this specific GF was not present in the ECM of the HCjE-Gi cells, GDF 15 was present, which might be interacting with LTBP 2. The highest proportion of growth differentiation factor 15 was observed in the day 14 ECM, in which it contributed to 2.3% of the ECM (figure 2.32). However, the functional significant of this on the HCjE-Gi cells is unknown. It may be that interaction of GFs with LTBP 2 promotes increased production of ECM proteins by binding to other ECM proteins, such as fibronectin.

FGFBP 1 was another protein in this category, whose highest proportion and raw peptide abundance were observed in the day 7 ECM (figures 2.24 and 2.32). FGFBP 1 is thought to enhance the activity of FGF.(158) FGF induces migration and proliferation of endothelial cells and is therefore important for angiogenesis. Moreover, FGF inhibits differentiation of smooth muscle cells. Briones et al. showed that the presence of TGFβ can down-regulate the expression of FGFBP 1 mRNA during smooth muscle differentiation *in vitro*.(158) The present study did not show evidence of presence of FGF, thus, further studies are required to investigate the functional significance of FGFBP 1 on HCjE-Gi cells.

2.4.3.8 The expression of proteases and their inhibitors increased and decreased, respectively, in the extracellular matrix of HCjE-Gi cells over six weeks in culture

The proportion of proteases in the day 1 ECM of HCjE-Gi cells was 40.1%, whereas that of protease inhibitors was 59.9% (figure 2.34). By day 7, there were more proteases than there were protease inhibitors (77.9% and 22.1%, respectively). The proportion of proteases in the ECM continued to increase, whereas that of protease inhibitors decreased from day 7 to day 42. The balance between the proteases and their inhibitors is important for normal tissue homeostasis and prevention of pathological states.

Serine protease HTRA1 was the most abundant protein in this category throughout the six weeks culture period, its peptide abundance significantly increased on day 7 compared to day 1 (figures 2.24 and 2.32). This protein may account for the significant reduction in fibronectin, vitronectin, LTBP 2 and TGFβ ig-h3 observed after day 7. It has been shown to be expressed in various tissues, highest expression being found in the mature epidermis and placenta, where it has been shown to have non-specific protease activity, including degradation of fibronectin, aggrecan and IGFBP 5.(159) An et al. showed that serine protease HTRA1 breaks down proteins that are associated with the complement pathway (vitronectin, apolipoprotein J and fibromodulin) and with deposition of amyloid (α-2-macroglobulin, apolipoprotein J and ADAM 9) in retinal pigment epithelial cells *in vitro*, linking it to the pathogenesis of age-related macular degeneration.(159) In this study, fibronectin was not shown to be degraded by serine protease HTRA1. Moreover, Karring et al. showed that serine protease HTRA1 breaks down a mutant form of TGFβ ig-h3, a protein that is found abundantly in amyloid deposits of the cornea in lattice corneal dystrophy.(160) They also suggested that the glia derived nexin inhibits the activity of serine proteases, thus regulating the proteolytic processing of amyloid deposits. Oka et al.

showed that serine protease HTRA1 protein binds to a range of TGFβ family proteins, including TGFβ 1 and 2, bone morphogenetic protein 4 and GDF 5, to inhibit their functions in a mouse myoblast cell line.(161) This suggests that serine protease HTRA1 may be responsible for the reduction of GFs and their binding proteins observed in the ECM of HCjE-Gi cells from day 7 onwards.

Studies on human conjunctival tissue have shown the expression of MMPs 1, 2, 3 and 9 in the epithelium and stroma, as well as the expression of TIMPs 1, 2, and 3.(162) A study by Girolamo et al. however, failed to show the presence of MMPs 1 and 2 and TIMPs 1 and 2, whereas TIMP 3 was observed only in approximately 27% of the normal conjunctival tissues.(163) They showed that these proteins are up-regulated in tissues of patients with pterygia suggesting roles in tissue inflammation, remodelling and angiogenesis. A study by Liu et al. showed expression of mRNA of MMPs 1, 2, and 14 and TIMP 1 in rabbit conjunctival tissue but failed to demonstrate the expression of MMPs 3 and 9.(164) In the present study, mass spectrometry experiments showed the expression of MMPs 14 and 28 in the ECM secreted by the HCjE-Gi cells *in vitro* (figure 2.24). The peptide abundance of MMP 14 was higher than that of MMP 28 throughout the six week culture period and the raw peptide abundance of both proteins increased significantly with time. The HCjE-Gi cells also secreted TIMP 3 (figure 2.24), which had a significantly higher raw peptide abundance on day 7 compared to days 1 and 14, however, the peptide abundance at day 42 was similar to that observed on day 7. MMP 1 is thought degrade fibrillar collagens, MMPs 2 and 9 degrade type IV collagen, and MMP 3 degrade laminins, fibronectin and PGs.(163) The lack of fibrillar and BM-associated type IV collagen in the ECM of the HCjE-Gi cells may explain the lack of MMPs 1, 2 and 9 in the present study. Endostatin, the biologically active domain of type XVIII collagen, was not observed in the ECM secreted by the HCjE-Gi cells. This is likely to be due to the lack of the MMPs 3, 7, 9, 13 and 20 that has been shown to cleave this domain from the parent protein in previous studies.(137, 165)

MMP 14 is a transmembrane protease found in the cornea, lens, choroid, retina, retinal pigment epithelium and the sclera in human tissues.(166) To date, MMPs 2 and 14 are the only MMPs known to cleave laminin 332 *in vitro*.(167) Koshikawa et al. showed that migration of epithelial cells was mediated by the presence of MMP 14 to cleave the γ_2 chain of laminin 332.(168) They suggested that MMP 2 may be acting as an adjunct that enhances the effects of MMP 14. Moreover, it has been suggested that cell lines that secrete MMP 14 degrade laminin 332 into its migratory form, whereas those that do not secrete MMP 14

allow laminin 332 to be employed to form hemidesmosomes that are present in non-migratory cells.(168) This is in contrast to the theories that have been suggested for MMP 28. Heiskanen et al. showed that MMP 28 is deposited into the ECM of cultured epithelial cells lines, such as A549 (human lung adenocarnicoma), MDCK (Madin-Darby canine kidney epithelial cells) and HeLa (human cervix carcinoma cells).(169) Saarialho-Kere et al. showed that MMPs 3 and 28 were produced by non-migrating proliferating keratinocytes.(167) They showed that MMP 28 positive areas of tissue consisted of highly proliferative cells with a BM composed of type IV collagen. This was in contrast to that observed around migrating cells, which consisted of a BM predominantly made up of laminin 332. MMPs 14 and 28 may play roles in migration and adhesion, respectively, in HCjE-Gi cells cultured *in vitro*.

2.4.3.9 The highest proportions of galectin-3-binding protein was in the extracellular matrix of the HCjE-Gi cells that have been in culture for fourteen to forty-two days

The highest proportion of galectin-3-binding protein was in the day 14 to day 42 ECM samples, contributing to 4.2-5.9% of the peptides (figure 2.33). The ECM of HCjE-Gi cells also expressed peptides of galectins 1 and 3 (figure 2.24). The peptide abundance of galectin 1 was higher than that of galectin 3 at all the time points investigated. Argueso et al. presented a model where galectin 3 was shown to bind to MUCs 1 and 16 on the OS, to form an epithelial barrier.(170) Moreover, Cao et al. showed that there was a significant reduction in re-epithelialisation of corneal wounds in the absence of galectin 3, whereas absence of galectin 1 did not affect the rates of wound closure.(171) They also showed that addition of exogenous galectin 3 did not have a rescue effect on the corneal wounds and suggested that endogenous galectin 3 production must influence the expression of other proteins that promote cell migration. Previous studies have shown that breast carcinoma cells overexpressing galectin 3 consists of high expression of integrins $\alpha_4\beta_7$ and $\alpha_6\beta_1$, and increased adhesion to laminin, fibronectin and vitronectin compared to cells that did not express galectin 3.(171) Tinara et al. showed that galectins 1 and 3 bound to different sites on galectin-3-binding protein.(172) All three proteins have been found to be over-expressed in carcinoma cells where they may play a role in their progression.

2.4.3.10 The proportions of serotransferrin and serum albumin were highest in the day one extracellular matrix of the HCjE-Gi cells

Serotransferrin contributed 1.3% of the day 1 ECM and 0.4% of the day 42 ECM (figure 2.33). Its raw abundance was highest on day 7, which was significantly higher compared to that on day 1 and 14, however, not day 42. Serotransferrin is a protein that is responsible for maintaining physiological levels of iron in serum.(152) Tears on the OS have also been shown to contain transferrin. Weinzimer et al. showed that serotransferrin increased the growth of sheep bladder smooth muscle cells and reduced apoptosis of prostate carcinoma cells compared to the controls.(152) Moreover, they showed that serotransferrin is a ligand for IGFBP 3 and culturing cells with serotransferrin-IGFBP 3 together inhibited the growth of cells. Interestingly, this combination also reduced cell apoptosis induced by IGFBP 3 alone. It may be possible that serotransferrin plays multiple functions in the ECM of the HCjE-Gi cells, including maintaining physiological levels of iron that may be toxic to cells if present at too higher levels, and modulate cell proliferation and their viability.

Serum albumin contributed to 1.6% of the day 1 ECM and reduced with time (figure 2.33). Its raw peptide abundance was highest in the day 7 ECM, although this was not found to be statistically significant. Koblinski et al. showed that BSA, SPARC and cytochrome C 'activate' adhesive proteins, such as laminin, fibronectin and vitronectin when present in concentrations too low to exert a biological activity.(173) The authors showed that the increase in cell adhesion was only observed when these proteins are added prior to or together with the adhesive proteins, whereas no increase to the cell adhesion was observed when added after the adhesive proteins. They suggested that these proteins activate the adhesive proteins by affecting the conformation by which the adhesive proteins are pre-adsorbed onto a substrate and therefore exposing important integrin binding sites.(173) In the present study, fibronectin and vitronectin had the highest raw peptide abundances on day 7 and the highest proportions of these proteins were in the day 1 and day 7 ECM samples. Peptides of fibronectin and vitronectin contributed to 0.8% and 0.06% of the total ECM on day 1, respectively, which gradually reduced over the six weeks (figure 2.30). It may be that serum albumin plays a role in activating fibronectin and vitronectin, which appear to be present in low concentrations in the ECM of the HCjE-Gi cells, thereby enhancing their cell-adhesive properties.

Apolipoprotein J, also known as clusterin, is an extracellular chaperone protein that regulates the clearance of partially unfolded proteins by promoting endocytosis and

lysosomal degradation that may aggregate to cause pathology.(174) Serum albumin has been shown to bind to apolipoprotein J to serve as a vehicle for the transportation of the abnormal proteins. This suggests another possible role for serum albumin in the ECM of the HCjE-Gi cells. As expected, the raw abundance of apolipoprotein J increased significantly over the six weeks, which is likely to be due to the presence of increased amount of abnormal proteins associated with increased oxidative stress during the ageing process of the ECM.

2.4.4 Type IV collagen and fibronectin increased the adhesion, and type IV collagen, α-2-HS-GP and the extracellular matrix derived from cells that were in culture for three and five days increased the growth of HCjE-Gi cells *in vitro*

In the present study, we showed that the cell-secreted ECM derived from cells that were in culture for three and five days enhanced the growth of HCjE-Gi cells compared to that on TCP (figure 2.35). This could be explained by the various changes to the composition and quantity of proteins that occurred in the ECM of HCjE-Gi cells during this time. The raw abundances of most proteins increased significantly from day 7 onwards. However, there were few proteins that were most abundant in the day 1 ECM compared to the other time points investigated. It is likely that synergistic effects of a combination of proteins that were present in the early cell-secreted ECM contributed to the enhanced cell growth observed in the present study (table 2.9). Moreover, we also investigated the individual effects of pre-adsorbed type IV collagen, laminin 111, fibronectin and α-2-HS-GP on the adhesion and growth of HCjE-Gi cells.

Pre-adsorbing laminin 111 from 0.1-1μg/mL protein solutions did not affect the adhesion or the growth of HCjE-Gi cells over seven days in culture (figures 2.41 and 2.45). Laminin 111, a developmental protein, is the most abundant laminin in all BMs. Although the ECM of the HCjE-Gi cells expressed the β_1 and the γ_1 chains, there was no evidence of expression of the α_1 chain *in vitro*. This together with the functional studies suggests that laminin 111 does not play an important role in the growth of HCjE-Gi cells *in vitro*. Koblinski et al. suggested that laminin 111 when pre-adsorbed from a 2μg/mL solution was too low to enhance cell adhesion and requires non-adhesive proteins, such as SPARC or serum albumin.(173) They suggested that these non-adhesive proteins ensure that laminin 111 is pre-adsorbed in such a conformation that the integrin binding sites are exposed. Further studies could be

undertaken to investigate if adding non-adhesive proteins enhanced the cellular functions of HCjE-Gi cells when cultured on pre-adsorbed laminin 111.

The functions of each laminin chain depend on the domains exposed and other laminin chains they interact with to form specific laminin trimers.(140) The present study showed that the HCjE-Gi cells secrete laminin chains that form trimers 332, 311 and 511 (figure 2.24). Thus, further studies are required to investigate the effects on adhesion and growth of HCjE-Gi cells when cultured on pre-adsorbed laminin 332, 311 or 511 *in vitro*. Laminin 332 and fibronectin are known to be present in the provisional matrix during wound healing that promote adhesion and migration of epithelial cells. The proportion of peptides of laminin α_3 chain increased on day 7 compared to day 1 (figure 2.30). However, that of laminin γ_2 chain was highest in the day 1 ECM compared to the other time points. It is likely that the laminin γ_2 chain enhances the migration of HCjE-Gi cells via integrin $\alpha_3\gamma_1$ in the early ECM. As discussed previously, although laminin chains β_1 and γ_1 contributed to less than 1% of the total peptides in the ECM of HCjE-Gi cells, laminin 332 is likely to act synergistically with laminins 311 and 511 to enhance cell adhesion and migration.

Fibronectin, a well-known cell adhesive protein, increased the adhesion of HCjE-Gi cells when pre-adsorbed from 0.5-10µg/mL solutions in a dose dependent manner (figure 2.42). However, no change to the growth of cells was observed when cultured on fibronectin pre-adsorbed from 0.5-10µg/mL solutions compared to that on TCP over a culture period of seven days (figure 2.46). Sottile et al. showed that the presence of the RGD peptide of fibronectin promoted clustering of integrin $\alpha_5\beta_1$ and therefore the adhesion of fibronectin-null mouse embryonic cells, but there was no change to the growth of cells.(175) However, culturing these cells in the presence of exogenously added fibronectin enhanced the growth of the cells in an adhesion-dependent manner. Moreover, the authors showed that this growth was only observed in the presence of fibronectin matrix assembly possibly by exposing cryptic binding sites on the protein.(175) In the present study, we showed that the highest proportion of fibronectin was present in the day 1 ECM of HCjE-Gi cells and reduced with time (figure 2.30). This suggests lack of fibronectin matrix assembly at the later time points and that fibronectin is employed by the HCjE-Gi cells for the initial adhesion, however, is not required for the subsequent growth of cells. Moreover, serum albumin is known to have a synergistic effect with the adhesive proteins, which together are likely to be enhancing cell adhesion on the early ECM compared to the ECM secreted by the cells after seven days in culture.

Moreover, the higher proportion of α-2-HS-GP and annexin A2 may also be responsible for the increased growth observed on the early ECM by promoting cell adhesion and migration. There was no change to the adhesion of HCjE-Gi cells when cultured on α-2-HS-GP pre-adsorbed from 0.5-20μg/mL solutions compared to TCP (figure 2.43). However, there was a significantly higher cell number on day five when cultured on α-2-HS-GP pre-adsorbed from 10-20μg/mL solutions, and on day seven when cultured on α-2-HS-GP pre-adsorbed from a 20μg/mL solution compared to that on TCP (figure 2.47). α-2-HS-GP is the human homologue of fetuin A found in fetal calf serum that is thought to be one of the many cell-adhesive proteins present in serum used in tissue culture. Although we did not observe a change to the adhesion of HCjE-Gi cells in the present study, there was an increase to the cell number on culture days five and seven when cultured on α-2-HS-GP pre-adsorbed from 10-20μg/mL solutions. Studies involving primary keratinocytes have shown significant increases to rates of cell migration and wound closure when cultured in serum-free media in the presence of α-2-HS-GP.(95) However, the wound closure rates when cultured in complete KSF media containing bovine pituitary extract and EGF was similar to that when cultured in KSF media alone containing 0.5-1mg/mL α-2-HS-GP.(100) The KSF media used in the present study contained 25μg/mL bovine pituitary extract and 0.2ng/mL EGF (table 2.1). Bovine pituitary extract and EGF at these concentrations may be inducing a similar effect on the adhesion of HCjE-Gi cells as when cultured on α-2-HS-GP pre-adsorbed from 0.5-20μg/mL solutions. Similarly, these proteins may be inducing a similar effect on the growth of cells as that observed when cultured on α-2-HS-GP pre-adsorbed from 0.5-5μg/mL solutions. Higher concentrations of α-2-HS-GP, similar to that used by Wang et al, may show an effect on the adhesion and a larger effect on the growth of HCjE-Gi cells. The interaction between α-2-HS-GP and annexin A2 is thought to be mediated via calcium, which was present in the KSF culture media used in the present study (table 2.1).(96)

The present study showed that type IV collagen as a substrate enhanced the adhesion of HCjE-Gi cells when pre-adsorbed from a 2μg/mL solution and the growth of cells on day seven when pre-adsorbed from 0.5-10μg/mL solutions (figures 2.40 and 2.44). He et al. showed that primary human corneal epithelial cells attached and formed a stratified epithelium when cultured on collagen shields pre-adsorbed with type IV collagen.(176) This was in contrast to collagen shields pre-adsorbed with matrigel, a mixture of ECM proteins derived from the mouse EHS sarcoma, on which the cells failed to reach confluence. Iwashita et al. showed that pre-adsorbing substrates with type IV collagen from a 10μg/mL significantly increased the adhesion of lung carcinoma cells, however, did not affect the cell

number at thirty hours.(177) In the present study, significant increases to the cell number was only observed from culture day five onwards. Type IV collagen is known to bind to integrins via the CB3-region on the collagenous domains. It has a higher affinity for integrin $\alpha_1\beta_1$ than for integrin $\alpha_2\beta_1$.(178) Öhlund et al. showed that the growth of pancreatic cancer cells on culture day two increased as the pre-adsorbed concentration of type IV collagen increased from 0.01 to 0.5µg/cm^2.(178) Moreover the authors showed that the cell migration was significantly higher and cell apoptosis after two days is significantly lower when cultured on type IV collagen (0.5µg/cm^2) than when cultured on BSA. Blocking the integrins that are known to associate with type IV collagen reduced the cell growth. This reduction was dose-dependent when integrins α_1 and β_1 were blocked. Blocking the CB3-region of type IV collagen also led to a reduction in cell growth, however, blocking the non-collagenous region at the C-terminal, also known to bind to integrins, did not affect the cell growth. Down-regulation of synthesis of the α_1 chain of type IV collagen reduced the cell growth by 20% at forty hours compared to the control, which could be rescued by culturing the cell on pre-adsorbed type IV collagen.(178) Although, type IV collagen was not present in the ECM of the HCjE-Gi cells cultured *in vitro*, this protein may be employed in future studies to modify the surface of substrates to enhance the growth of conjunctival cells.

Moreover, the present study showed that the day 1 and day 7 ECM samples had the highest proportion of GFs and their binding proteins (figure 2.23). In particular, the peptides of insulin contributed to 10.9% of the day 1 ECM (figure 2.32). Insulin is a growth promoting GF. Lastly, the ratio of proteases and their inhibitors changed between the day 1 and day 7 ECM samples (figure 2.34). The increase in the proportion of proteases observed in the day 7 ECM may be responsible for remodelling the proteins of the ECM that expose cryptic domains on the ECM that modulate the growth of HCjE-Gi cells.

The major differences observed between the early and late stages of the extracellular matrix secreted by HCjE-Gi cells

PROTEIN CATEGORY	EARLY ECM (Day 1 ECM)	LATE ECM (Day 7 to day 42 ECM)
GLYCOPROTEINS	Highest proportions of α-2-HS-GP and annexin A2 Highest proportion of fibronectin Highest proportion of laminin γ_2 chain Highest proportion of tenascin C	Proportion of laminin α_3 chain increased Proportion of thrombospondin 1 increased
INTEGRINS		Proportions of integrins α_6 and β_4 subunits increased Proportion of basigin increased
GROWTH FACTORS	Highest proportion of insulin	
PROTEASES AND INHIBITORS	Highest proportions of PAI 1 and serpin B5	Proportion of serine protease HTRA1 increased
OTHER SECRETED PROTEINS	Highest proportion of serotransferrin Highest proportion of serum albumin	

Table 2.9: The major differences observed between the early and late stages of the extracellular matrix secreted by HCjE-Gi cells.

2.4.5 The expression of stem cell markers by HCjE-Gi cells reduced over fourteen days in culture *in vitro*

Studies investigating the expression of conjunctival SCs on exogenous proteins are limited in comparison to those investigating the expression of limbal SCs. In the present study, the positive staining for ΔNp63 and ABCG2 proteins reduced significantly from culture day seven onwards on all the substrates investigated (figures 2.53 and 2.55). The mean number of cells expressing ΔNp63 protein reduced from 64.8% to 16.2%, whereas those expressing ABCG2 reduced from 52.6% to 3.3% from culture days one to fourteen. Further experiments that are more quantitative than the method used in the present study are required to support these findings. Rama et al. showed that limbal epithelial tissue used for transplantation must consist of 3% or more ΔNp63 positive cells to ensure a better prognosis.(179) ΔNp63 is formed by truncation of the N-terminus of the p63 proteins. This truncated transcript has three isoforms, of which the α isoform has been shown to identify epithelial SCs, whereas isoforms β and γ are thought to promote epithelial cell differentiation.(180) ΔNp63 positive cells are thought to represent a pool of SCs that have the ability to form holoclones.(179) ABCG2 protein has also been shown to be a marker of limbal SCs, however, there is a possibility that TACs may also be stained during ICC. (180)

In general, the expression of ΔNp63 and ABCG2 proteins was higher in HCjE-Gi cells cultured on pre-adsorbed type IV collagen and fibronectin compared to TCP and laminin 111 (figures 2.53 and 2.55). To date, no studies have been undertaken to show associations between ECM proteins and the expression of conjunctival SCs. Li et al. showed that primary limbal epithelial cells that adhered within twenty minutes onto type IV collagen pre-adsorbed from a 20µg/mL solution were label-retaining cells that had the highest proliferative capacity compared to the cells that took a longer time to adhere onto type IV collagen. (181) They also showed that these cells expressed the highest mRNA levels of integrin β_1, p63 and ABCG2, and consisted of the highest population of cells expressing integrin β_1 and p63 proteins. In addition, they also showed that the cells that adhered within twenty minutes had a low expression of corneal differentiation markers. Igarashi et al. showed that oral epithelial progenitor cells that adhered onto type IV collagen within ten minutes were label-retaining cells that had a higher proliferative capacity compared to the cells that took a longer time to adhere onto type IV collagen.(182) They also showed that these rapidly attached cells had higher expression of integrins α_6 and β_1 compared to the cells that took a longer time to adhere onto type IV collagen. These results show that

type IV collagen is important for isolating epithelial SCs and that integrins β_1 and α_6 may play a role in the interaction between the SCs and type IV collagen.

Laminins 111 and 511 are important for early mouse embryogenesis and have been shown to be deposited by human embryonic SCs *in vitro*.(183) Vuoristo et al. showed that human embryonic SCs expressed integrins α_3, α_5, α_6 α_v, β_1 and β_3, as well as BCAM on their cell membranes.(183) The authors showed that these cells adhered to laminin 511 via integrin $\alpha_3\beta_1$ and BCAM. They also showed that laminin 511 supported the proliferation and maintenance of embryonic SCs in an undifferentiated state. Although laminin 111 supported the adhesion of cells, it stimulated the differentiation of embryonic SCs down a neural lineage. These studies suggest that laminin 511 expressed by the HCjE-Gi cells may play a role in the self-renewal of conjunctival SCs. Therefore, a future study would be to investigate the role of laminin 511 in the maintenance of SCs via integrin $\alpha_3\beta_1$ and BCAM *in vitro*. Embryonic SCs were shown to have a higher growth rate on recombinant laminin 332 than laminin 511 and laminin 111, and the cells maintained the undifferentiated state on all laminin trimers.(184) The authors showed that the laminins interacted with cells via integrin $\alpha_6\beta_1$. In contrast, other studies have shown that culture of embryonic SCs on laminin 332 stimulates the differentiation of cells down an osteogenic lineage.(185)

Previous studies have shown that fibronectin supports the long-term maintenance of human embryonic SCs.(186) Moreover, various media that are used commercially for culture of SCs is known to contain fibronectin.(187) Kalaskar et al. showed that only one-quarter of a surface needed to be saturated with fibronectin to promote adhesion, growth and maintenance of human embryonic SCs.(186) They showed that this saturation level can be achieved by pre-adsorbing a surface from a solution of approximately 10µg/mL of fibronectin. In contrast, other studies have shown that culture of human embryonic SCs on fibronectin for a long period of time stimulate cells to lose their undifferentiated state.(184)

There are numerous proteins in the ECM of HCjE-Gi cells that may influence the maintenance of SCs (figure 2.60). Further studies are required to investigate the effects of these proteins on the expression of conjunctival SC markers. In addition, studies may be undertaken to investigate the expression of SC markers on cell-secreted ECM. The sample number in the present study was too low to determine accurate conclusions regarding the effect of pre-adsorbed proteins on the expression of SC markers, thus requiring further experiments with larger sample sizes.

Proteins in the extracellular matrix of HCjE-Gi cells that may influence the maintenance of stem cells

COLLAGENS	Type XVIII collagen (89)
GLYCOPROTEINS	α-2-HS-GP (188) Laminin chains α_3, α_5, β_2 and γ_2 Nephronectin (189) Tenascin C (11) Vitronectin (190)
PROTEOGLYCANS	Agrin (11) Perlecan (191) Tsukushin (192)
INTEGRINS AND TRANSMEMBRANE PROTEINS	Integrins α_6 (182), α_V (193), β_1 (185) Basigin (194) EGF receptor (195) CD44 (196) and CD109 (197)
MATRIX METALLOPROTEINASES AND INHIBITORS	ADAMs 10 and 17 (198) PAI 1 (187)
OTHER SECRETED PROTEINS	Galectins 1 (199) and 3 (200) Wnt proteins (inhibited by Dkk1) (201)

Figure 2.60: Proteins in the extracellular matrix of HCjE-Gi cells that may influence the maintenance of stem cells. Previous studies have shown these proteins to be associated with stem cell niches or support the maintenance of stem cells in vitro.

2.4.6 The expression of goblet cell markers by HCjE-Gi cells increased over fourteen days in culture *in vitro*

In the present study, we investigated the expression of MUC5AC and co-expression of keratin 7 and UEAI by HCjE-Gi cells cultured on pre-adsorbed type IV collagen, fibronectin and laminin 111. MUC5AC is a gel-forming secreted mucin produced by the GCs. Keratin 7 is expressed by glandular epithelia, and the clone OV-TL 12/30 has been shown to be expressed in conjunctival tissue.(202) Mucins are GPs that have a carbohydrate side chain. UEAI is a lectin that binds to fucose. Although we observed positive staining in HCjE-Gi cells when probed with UEAI, Kawano et al. showed that this lectin did not bind to most GCs in the human conjunctiva indicating that there is only very little or no fucose in the mucins produced by the GCs.(203) In contrast, the authors showed that most GCs stained positive when probed with wheat germ agglutinin and soybean agglutinin that bind to N-acetyl-glucosamine and N-acetyl-galactosamine on the mucins, respectively.(203)

In the present study, we did not observe any significant differences to the percentage of cells that stained positive for GC markers when cultured on pre-adsorbed proteins compared to TCP (figures 2.57 and 2.59). However, further experiments are required with larger sample sizes to determine the effect of pre-adsorbed proteins on the expression of GC markers more accurately. There was a significant increase to the percentage of cells that stained positive for protein MUC5AC on culture day seven and fourteen compared to culture day one. In contrast, there were no significant differences to the percentage of cells that stained positive for keratin 7 and UEAI between culture days one, seven and fourteen. Studies on human tissue have shown that the amount of GCs vary between the bulbar, forniceal and palpebral conjunctiva. LSCM studies on human conjunctival tissue have shown that approximately 4.8% and 50.7% of the bulbar and palpebral conjunctiva consist of GCs, respectively. Impression cytology studies have shown that there are approximately one GC for every eight epithelial cells in the superior bulbar conjunctiva of healthy individuals.(13) MUC5AC is produced by GCs, however, can be extracellular when secreted. Therefore, it is difficult to accurately determine the percentage of GCs by ICC. The cells that stained positive for MUC5AC in the present study could be true GCs or non-secretory epithelial cells that the secreted mucins bound to. On the other hand, the cells that co-expressed keratin 7 and UEA1 could be the true GCs. However, it is not possible to ascertain if these cells are immature GCs or actively secreting mature GCs.

Iwashita et al. showed that MUC5AC production was down-regulated when human lung carcinoma cells were cultured on type IV collagen pre-adsorbed from a 33µg/mL solution, whereas no change was observed when cultured on type IV collagen pre-adsorbed from a 10µg/mL solution, which was independent of cell density.(177) No change to the MUC5AC production was observed when cells were cultured on fibronectin, however, the production increased in a dose-dependent manner when cultured on laminin and Matrigel. Ito et al. showed that MUC5B, another gel-forming secreted mucin, is up-regulated when these cells were cultured on fibronectin and laminin in a dose-dependent manner, however, was unaffected when cultured on type IV collagen.(204) Blocking integrin β_1 down-regulated the production of both MUCs 5AC and 5B. The down-regulation of MUC5AC on type IV collagen was shown to be due to the activation of the Akt pathway, which was suppressed when the cells were cultured on laminin.(205) Studies have shown that the up-regulation of MUCs 5AC and 5B are mediated via the action of EGF receptors that activate intracellular pathways, such as the ERK pathway, that increases the production of NF-κB transcription factor.(177, 204) These results showed that these mucins are regulated differentially in cells cultured on type IV collagen and fibronectin, whereas both are up-regulated when cultured on laminin. Although the authors did not specify the laminin trimer, the cells appear to be studied on pre-adsorbed laminin 111. Thus, it would be interesting to investigate the effect of laminins found to be present in the ECM of the HCjE-Gi cells on the differentiation of GCs.

In the present study we showed that the addition of fetal calf serum and a higher concentration of calcium increased the expression of MUC5AC, although the difference between culture days seven and fourteen was not statistically significant. The presence of GCs on culture day seven indicates that fetal calf serum is not essential for the differentiation process. Thus, a future study would be to investigate the presence of GCs in serum-free media over a longer culture period. In addition to the above mentioned extracellular proteins, other proteins that were found to be present in the ECM of the HCjE-Gi cells could influence the differentiation of GCs and the production of gel-forming mucins (figure 2.61). Further studies are required to investigate the effects of these proteins individually or in combination on the differentiation of GCs. Moreover, it would be interesting to study the ECM proteins present in an isolated culture of GCs. Lastly, another further study would be to investigate the variations in the protein composition of the ECM secreted by the conjunctival cells of the bulbar, forniceal and palpebral regions that could explain the variations in the quantities of GCs observed in these regions of the native tissue.

Proteins in the extracellular matrix of HCjE-Gi cells that may influence the differentiation of goblet cells and the production of MUC5AC

COLLAGENS	Type IV collagen (down-regulates production)
GLYCOPROTEINS	Laminin Thrombospondin 1 (206)
INTEGRINS AND TRANSMEMBRANE PROTEINS	Integrin β_1 CD44 (via hyaluronan) (207) EGF receptor (208)
GROWTH FACTORS AND BINDING PROTEINS	GDF 15 (209) TGFβ ig-h3 (155)
MATRIX METALLOPROTEINASES AND INHIBITORS	ADAM 17 (may be inhibited by TIMP 3) (210) Elafin (down-regulates production) (211) MMP 14 (212)
OTHER SECRETED PROTEINS	Annexin A2 (up-regulates secretion) (213)

Figure 2.61: Proteins in the extracellular matrix of HCjE-Gi cells that may influence the differentiation of goblet cells and the production of MUC5AC. Previous studies, predominantly using lung carcinoma cells, have shown that these proteins either up-regulate or down-regulate the production and/or the secretion of MUC5AC protein by goblet cells.

Summary of key findings

- Ammonium hydroxide successfully isolated the ECM proteins and the transmembrane proteins associated with the ECM of the HCjE-Gi cells cultured *in vitro*.
- The protein composition of the ECM of the HCjE-Gi cells cultured *in vitro* varied over six weeks (figure 2.62).
    - Type IV collagen was absent; however, type XVIII collagen was deposited as a structural collagen.
    - Laminin 332 was the most abundant glycoprotein in the ECM. Other possible laminin trimers that may be present in the ECM were laminins 311 and 511.
    - The highest peptide abundances of fibronectin, nephronectin and vitronectin were in the day seven ECM.
    - α-2-HS-GP was present in the ECM, which has not been shown to be present in the conjunctival ECM previously, the highest proportion being observed in the day one ECM.
    - Perlecan and agrin were the most abundant proteoglycans in the early and late ECMs, respectively.
    - Integrins α_6 and β_4 subunits were the most abundant transmembrane proteins in the ECM.
    - The highest proportion of growth factors, their binding proteins and cytokines were in the day one and seven ECM samples.
    - The expression of proteases and their inhibitors in the ECM increased and decreased, respectively, with time.
- The adsorption of type IV collagen and fibronectin onto TCP reached a saturation point when pre-adsorbed from a 5μg/mL solution, whereas the adsorption of laminin 111 onto TCP reached a saturation point when pre-adsorbed from a 0.5μg/mL solution.
- Type IV collagen pre-adsorbed from 2-10μg/mL solutions and fibronectin pre-adsorbed from 0.5-10μg/mL solutions increased cell adhesion compared to TCP.
- Type IV collagen pre-adsorbed from 0.5-10μg/mL solutions and α-2-HS-HP pre-adsorbed from a 20μg/mL solution increased the growth of HCjE-Gi cells on culture day seven. Moreover, ECM derived from cells that were in culture for three and five days increased the growth of HCjE-Gi cells *in vitro*.
- Preliminary data show that the expression of stem cell markers by HCjE-Gi cells decreased, whereas the expression of goblet cell markers by HCjE-Gi cells increased over fourteen days in culture *in vitro*.

The protein composition of the ECM of the HCjE-Gi cells

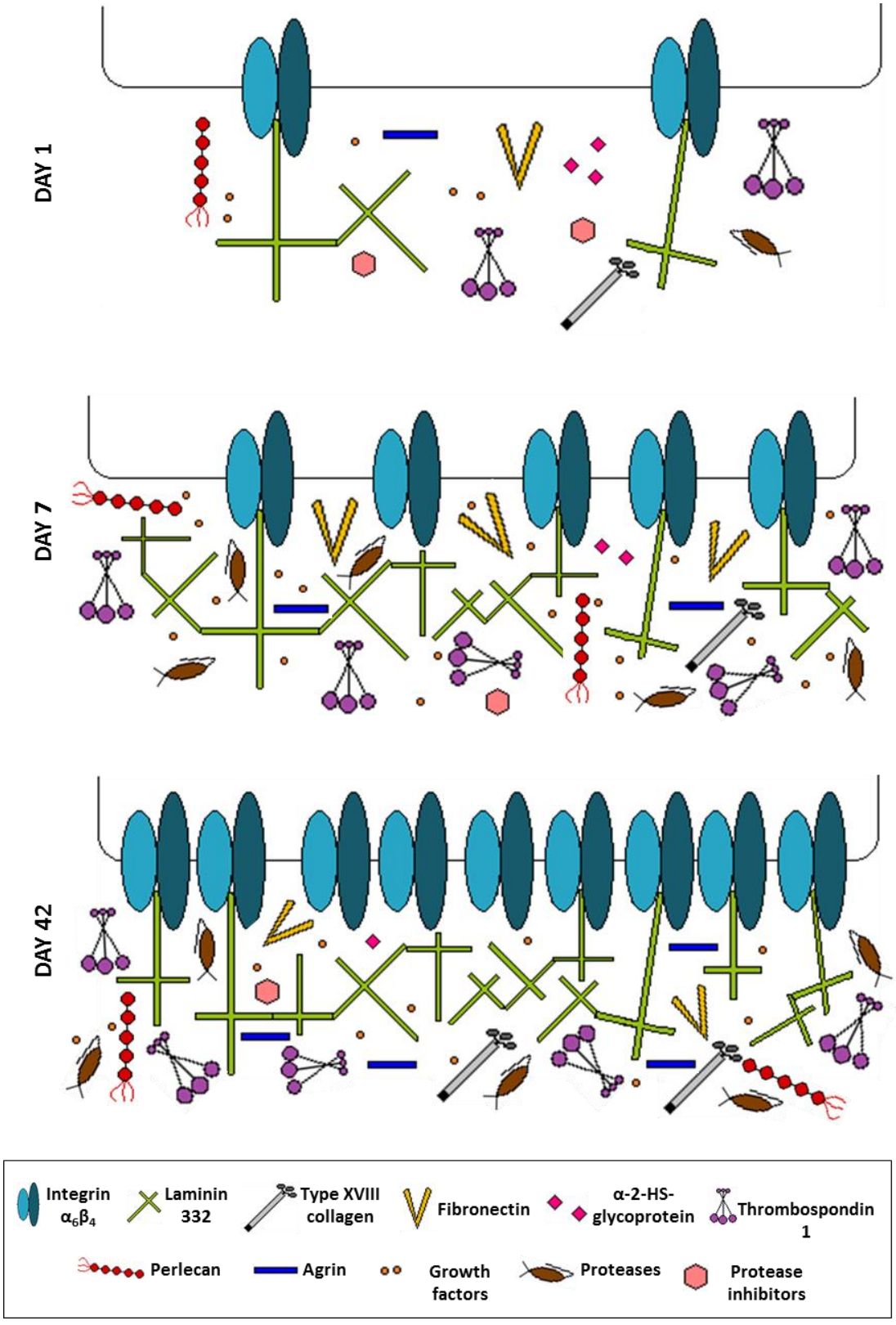

Figure 2.62: The protein composition of the ECM of HCjE-Gi cells. A schematic diagram summarising the protein composition of the ECM of HCjE-Gi cell line cultured in vitro over six weeks in keratinocyte serum-free media.

3 CELLULAR RESPONSE OF HCjE-Gi CELLS ON SURFACE MOFIDIED PεK HYDROGELS

3.1 AIMS AND OBJECTIVES

To establish the cellular response of HCjE-Gi cells cultured on surface modified PεK hydrogels.

1. To determine the adhesion of HCjE-Gi cells on PεK hydrogels with and without pre-adsorbed proteins.

2. To determine the growth and differentiation of HCjE-Gi cells on PεK hydrogels with and without pre-adsorbed proteins over a culture period of fourteen days.

3.2 METHODS

3.2.1 SYNTHESIS OF PεK HYDROGELS

PεK hydrogels consisting of homopolymers of PεK chemically cross-linked with dicarboxylic acids were synthesised according to the protocol given by SpheriTech Ltd. The quantities of reagents were taken from an Excel spreadsheet provided by the company (appendix 2). By taking into account the data from previous research, it was decided to synthesise gels with a PεK density of 0.1g/mL and a cross-linking density of 60% (60:10 PεK gels) for the following experiments. Two dicarboxylic acids, azelaic acid (AA) and suberic acid (SA), were investigated in this study.

The appropriate quantities of PεK (*Zhengzhou Bainafo Bioengineering Co.,Ltd*) to make AA and SA cross-linked PεK gels were weighed out into two separate tubes and were dissolved in dH_2O with Tween 80 (*Fisher Scientific T/4203/60*). The volume of Tween 80 was calculated as 1% of the final volume of the PεK gel solution that was to be made. The PεK solutions were mixed on a tube roller mixer (*Denley Spiramix 5*). The dicarboxylic acids, AA (*TCI A1318*) and SA (*Sigma Aldrich 60930*) were dissolved in dH_2O and 4-Methylmorpholine (NMM) (*Alfa Aesar A12158*) in two separate tubes. NMM was added as a solvent to aid the solubility of the dicarboxylic acids in water. These solutions were left in a sonicator bath (*Grant* XUBA3) until fully dissolved. Just prior to the initiation of the polymerisation reaction, N-Hydroxysuccinimide (NHS) (*Sigma-Aldrich 130672*) and 1-(3-Dimethylaminopropyl)-3-ethylcarbodiimide HCl (EDCI) (*Carbosynth FD05800*) were dissolved in dH_2O in two separate tubes for each type of PεK gel. The NHS and EDCI activate the carboxyl groups on the dicarboxylic acids that are used to form peptide bonds with the amine groups on the PεK homopolymer. Each dicarboxylic acid solution was mixed with the corresponding PεK solution on a tube roller mixer. The NHS and EDCI solutions were added together and mixed on a tube roller mixer. Each PεK-dicarboxylic acid solution and the corresponding NHS-EDCI solution were mixed together and the tubes were inverted five times. Lastly, the PεK gel solutions were filtered using 0.2µm syringe filters (*Sartorius 16534K*) and the appropriate volumes of gel solution was pipetted into petri dishes (*Greiner bio-one 633185*). The gel solutions were left exposed to air at RT to be polymerised overnight.

The next day, the polymerised gels were washed in dH_2O. Circular gels with an area of $1cm^2$ were cut using a 11.5mm trephine (figure 3.1A) and were stored in dH_2O until the day of

the experiment. The gels were washed in 70% ethanol (*Department of Chemistry, University of Liverpool*) for two hours and then washed three times in PBS inside a class II biosafety cabinet prior to cell culture. The gels were handled with a non-toothed and non-serrated forceps (figure 3.1B).

3.2.2 THICKNESS OF PεK HYDROGELS

To determine the thickness of the hydrogels, 2mL, 3mL, 4mL and 5mL of 60:10 PεK gel solutions were pipetted into 94mm wide petri dishes (*Greiner bio-one 633185*).The polymerised gels were cut into $1cm^2$ circular gels as described previously. The circular gels were placed on the lids of the petri dishes and the thickness of each gel was measured using a dial thickness gauge (figure 3.2). The thickness of the lid of the petri dish alone, and the thickness of the gel and the lid together were measured. The former measurement was subtracted from the total thickness of the gel and the lid to obtain the thickness of the PεK hydrogel. The dial thickness gauge was used instead of a vernier caliper to ensure a uniform load was used to press the gel and therefore avoid potential human errors. The thickness of both AA and SA cross-linked PεK gels were measured in three sets of triplicates.

Instruments used to prepare and handle PεK gels

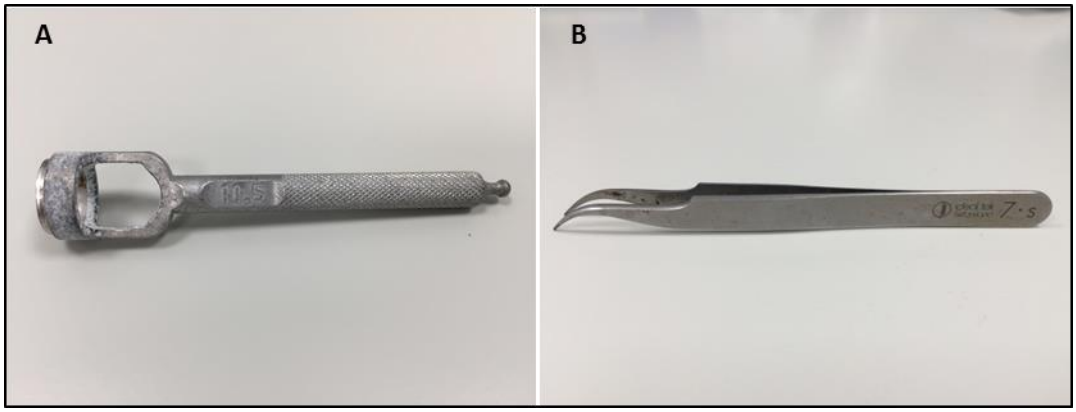

Figure 3.1: Instruments used to prepare and handle PεK hydrogels. The 11.5mm trephine used to cut 1cm^2 circular gels (A) and the non-toothed and non-serrated forceps used to handle gels (B).

Dial thickness gauge

Figure 3.2: Dial thickness gauge used to measure the thickness of PεK hydrogels.

3.2.3 ADHESION OF HCjE-Gi CELLS ON PεK HYDROGELS

Type IV collagen (2 and 10μg/mL), laminin 111 (0.5 and 1μg/mL), fibronectin (2 and 10μg/mL) and α-2-HS-GP (2 and 10μg/mL) protein solutions were prepared in PBS. The 60:10 PεK gels were placed in wells of forty-eight well plates on the day of the experiment and incubated with 200μL of protein solution for one hour at 37°C. PεK gels and TCP incubated with PBS alone were used as controls. All the gels were washed three times in PBS, and due to the highly hydrophilic nature of the gels, these were air-dried briefly while cells were sub-cultured. This is to ensure that the aliquots of cells remained beaded until the cells attached onto the gels without spreading outside it. HCjE-Gi cells were seeded at a density of $3x10^4$ cells/cm^2 in a volume of KSF media not exceeding 15μL. No additional media was added into wells to prevent the cells from being washed off the gel before attachment. The cells were incubated in a humidifying incubator set at 37°C with 5% CO_2 for three hours, following which the wells were gently washed once in PBS. Then the cells were fixed in 100% methanol for two minutes and the nuclei were stained with DAPI. Five images from each well were taken with a 10X objective of a Nikon Eclipse Ti-E microscope. The cell nuclei were counted using the Image-based Tool for Counting Nuclei plugin on Image J software, as described in chapter 2. The mean number of nuclei per view ($0.011cm^2$) was calculated to determine the number of cells per cm^2 on all the substrates investigated. These experiments were done in one set of triplicates.

3.2.4 GROWTH OF HCjE-Gi CELLS ON PεK HYDROGELS

As before, the 60:10 PεK gels were placed in wells of forty-eight well plates on the day of the experiment and incubated with protein solutions for one hour at 37°C. The PεK gels and TCP incubated with PBS were used as controls. The gels were washed in PBS and briefly air-dried while cells were sub-cultured. HCjE-Gi cells were seeded at a density of $1x10^4$ cells/cm^2 in a volume of media not exceeding 15μL. The cells were allowed to adhere for three hours prior to adding more media (400μL per well). The cells were cultured for seven days in KSF medium and then switched to the differentiation and stratification medium for a further seven days. On culture days one, four, seven, eleven and fourteen, the cells were fixed in 100% methanol and nuclei were stained with DAPI. Five images from each well were taken with a 10X objective of a Nikon Eclipse Ti-E microscope. The mean number of nuclei per view was calculated to determine the number of cells per cm^2 on all the substrates for each culture day investigated. These experiments were done in one set of triplicates.

3.2.5 DIFFERENTIATION OF HCjE-Gi CELLS ON PεK HYDROGELS

On culture days seven and fourteen, the PεK gels with and without pre-adsorbed proteins were stained for conjunctival cell differentiation markers and GC markers. The PεK gels pre-adsorbed with type IV collagen from a 10µg/mL solution, fibronectin from a 10µg/mL solution and laminin 111 from a 1µg/mL solution were used in this study. The same protocols and reagents as described in chapter 2 for ICC staining for keratin 4, keratin 19 and MUC5AC were used. The cells were fixed in 10% NBF for ten minutes and were permeabilised with 0.2% Triton X-100 for fifteen minutes at RT. Next, the cells were blocked with 10% goat serum for one hour and probed with antibodies against keratin 4, keratin 19 and MUC5AC overnight at 4°C. The next day, the cells were incubated with appropriate secondary antibodies for one hour at 37°C and the nuclei were stained with DAPI. Cells cultured on PεK gels that were probed with secondary antibodies only were used as negative controls. Images were taken with a 20X objective of a Nikon Eclipse Ti-E microscope.

3.2.6 STATISTICS

All the data were analysed using the SPSS Statistics 22 software. Significance level of 0.05 was set for all the experiments.

<u>One-way ANOVA</u>

- The adhesion of HCjE-Gi cells on AA and SA cross-linked PεK gels with and without pre-adsorbed proteins.

One-way ANOVA was undertaken as described in chapter 2.

<u>Two-way ANOVA</u>

- The thickness measurements between the volumes of gel solution used in the polymerisation reaction for AA and SA cross-linked PεK gels.
- The growth of HCjE-Gi cells on AA and SA cross-linked PεK gels with and without pre-adsorbed proteins.

Two-way ANOVA was undertaken as described in chapter 2. All the data that were analysed in this chapter did not show an interaction effect between the two independent variables, thus analysis of the main effect for each independent variable was performed.

3.3 RESULTS

3.3.1 PHYSICAL PROPERTIES OF PεK HYDROGELS

The 60:10 PεK gels had excellent transparency, although the SA cross-linked gels had a slight yellow tinge compared to the AA cross-linked gels (figure 3.3). Both types of PεK hydrogels were easy to handle with the non-toothed and non-serrated forceps. However, the SA cross-linked hydrogels were more brittle than those cross-linked with AA and had a tendency to crack when folded. This is a limitation in conjunctival reconstruction, where the substrate needs to be able to conform to the surface, especially the fornices.

Two-way ANOVA was conducted to examine the effects of gel type and the volume of gel solution used in the polymerisation reaction on the thickness of the gels. There was one outlier in the AA - 5mL group as assessed by box plot diagrams, however, excluding this did not affect the overall result. The residuals were normally distributed and there was homogeneity of variances. The interaction effect between the gel type and the volume of gel solution on the thickness of gels was not statistically significant ($p = 0.123$). In general, the PεK hydrogels cross-linked with AA were thinner than those cross-linked with SA (figure 3.4). Analysis of the main effect between gel types showed that this difference was statistically significant, $p = 0.012$. As expected, the thicknesses of AA and SA cross-linked PεK hydrogels increased with increasing volumes of PεK gel solution used in the polymerisation reaction. Analysis of the main effect between volumes of gel solution showed that this difference was statistically significant, $p < 0.001$. Statistically significant differences were observed between 2mL and 4mL, 2mL and 5mL, 3mL and 4mL, and 3mL and 5mL groups ($p < 0.001$). The gels that were made with 2mL and 3mL gel solutions were sufficiently thin to be folded easily compared to the thicker gels. Due to easier handling during *in vitro* studies, gels synthesised with a volume of 3mL of PεK gel solution were used in the subsequent experiments. These hydrogels had a mean thickness of 0.17mm and 0.24mm when cross-linked with AA and SA, respectively.

Transparency of the 60:10 PεK gels

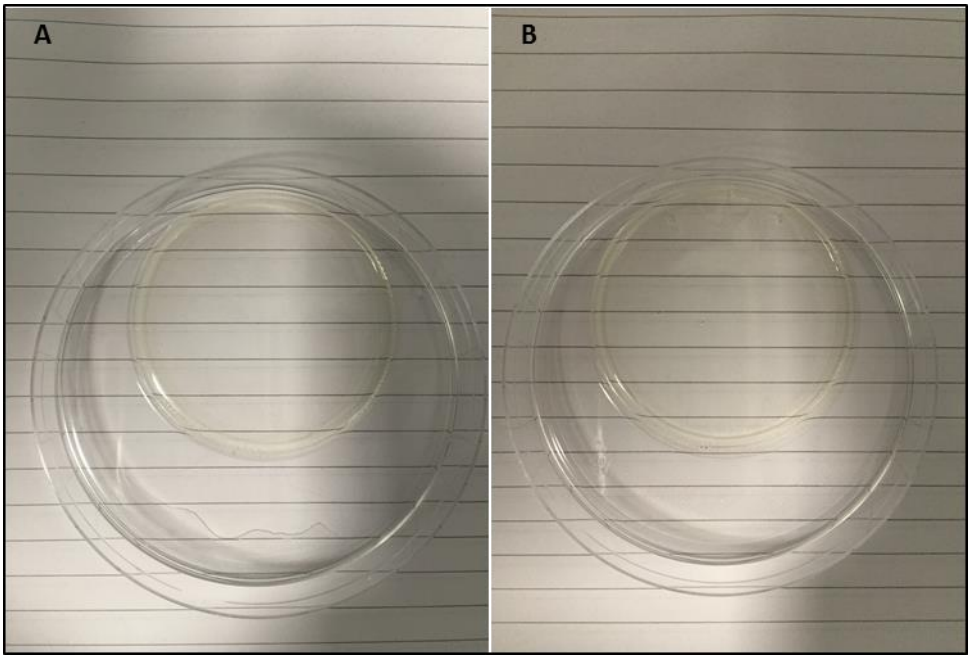

Figure 3.3: Transparency of the 60:10 PεK hydrogels. The gels were synthesised with a PεK density of 0.1g/mL and a cross-linking density of 60% with either azelaic acid (A) or suberic acid (B). Both types of PεK hydrogels exhibited excellent transparency, although gels cross-linked with suberic acid had a slight yellow tinge compared to those cross-linked with azelaic acid.

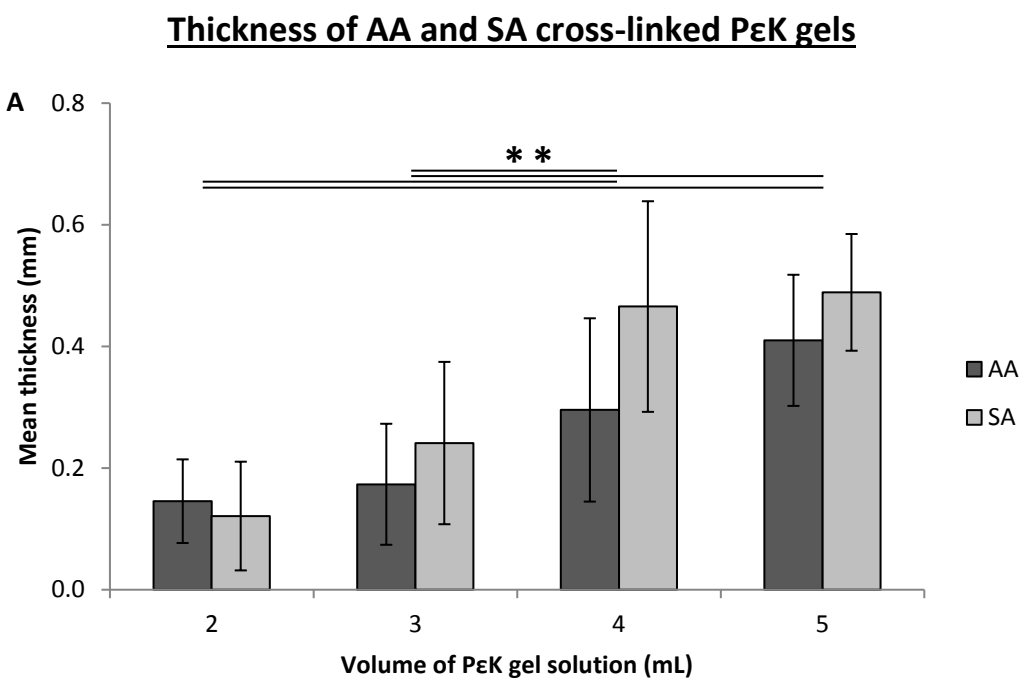

B

		Mean	*SD*
AA	**2**	0.15	*0.07*
	3	0.17	*0.10*
	4	0.30	*0.15*
	5	0.41	*0.11*
SA	**2**	0.12	*0.09*
	3	0.24	*0.13*
	4	0.47	*0.17*
	5	0.49	*0.10*

Figure 3.4: A. Thickness of AA and SA cross-linked PεK hydrogels. Data are presented as mean thickness (mm) ± 1SD, n = 9. There was no significant interaction effect between the gel type and the volume of PεK gel solution on the thickness of gels. Analysis of the main effect between gel types showed that the thicknesses of SA cross-linked gels were significantly higher than those cross-linked with AA (p = 0.012). There was also a significant difference in the main effect between the volumes of gel solution (p < 0.001), where significant increases were seen between 2mL and 4mL, 2mL and 5mL, 3mL and 4mL, and 3mL and 5mL groups; **p < 0.001. (Two-way ANOVA; Bonferroni post hoc test). B. Mean thickness of PεK hydrogels (mm) and 1SD.

3.3.2 ADHESION OF HCjE-Gi CELLS ON PεK HYDROGELS

The HCjE-Gi cell adhesion on AA cross-linked PεK gels three hours post seeding were comparable to that on TCP without pre-adsorbed proteins (figure 3.5). All data within all groups were normally distributed, except the laminin 111 1µg/mL and α-2-HS-GP 10µg/mL groups. There were no outliers and there was heterogeneity of variances (p = 0.003). There was a statistically significant difference in the cell adhesion between the substrate groups, p = 0.001. There was no difference in the cell adhesion on AA cross-linked PεK gels with and without pre-adsorbed proteins compared to that on TCP (p > 0.05). Moreover, there were no differences to the cell number on gels with pre-adsorbed proteins compared to those without pre-adsorbed proteins (p > 0.05). The highest mean cell number was observed on PεK gels with fibronectin pre-adsorbed from a 10µg/mL solution. Although the cell number was two-fold higher than that observed on PεK gels without pre-adsorbed proteins, this was not found to be statistically significant (p = 0.803). However, there was a significant reduction to the cell number observed when cultured on gels with laminin 111 pre-adsorbed from a 1µg/mL solution (p = 0.033) and gels with α-2-HS-GP pre-adsorbed from a 2µg/mL solution (p = 0.007) compared to that on gels with type IV collagen pre-adsorbed from a 10µg/mL solution.

The adhesion of HCjE-Gi cells on SA cross-linked gels was comparable to that on TCP without pre-adsorbed proteins (figure 3.6). Data within all groups were normally distributed, except the α-2-HS-GP 10µg/mL group. There were no outliers within the data set and there was homogeneity of variances. One-way ANOVA did not show any statistically significant differences between the substrate groups, p = 0.068. Although there was a 3.5-fold reduction in the cell number on SA cross-linked PεK gels without pre-adsorbed proteins compared to that on TCP, this was not found to be statistically significant (p = 0.456). Similarly, there were no statistically significant differences to the cell number on gels with pre-adsorbed proteins and TCP (p > 0.05). However, a significant five-fold increase in the cell adhesion was observed on the SA cross-linked PεK gels with type IV collagen pre-adsorbed from a 2µg/mL solution compared to that on gels without pre-adsorbed proteins (p = 0.036). There were no differences to the cell adhesion between the gels pre-adsorbed with other proteins and those without pre-adsorbed proteins (p > 0.05).

Adhesion of HCjE-Gi cells on AA cross-linked PεK gels

A

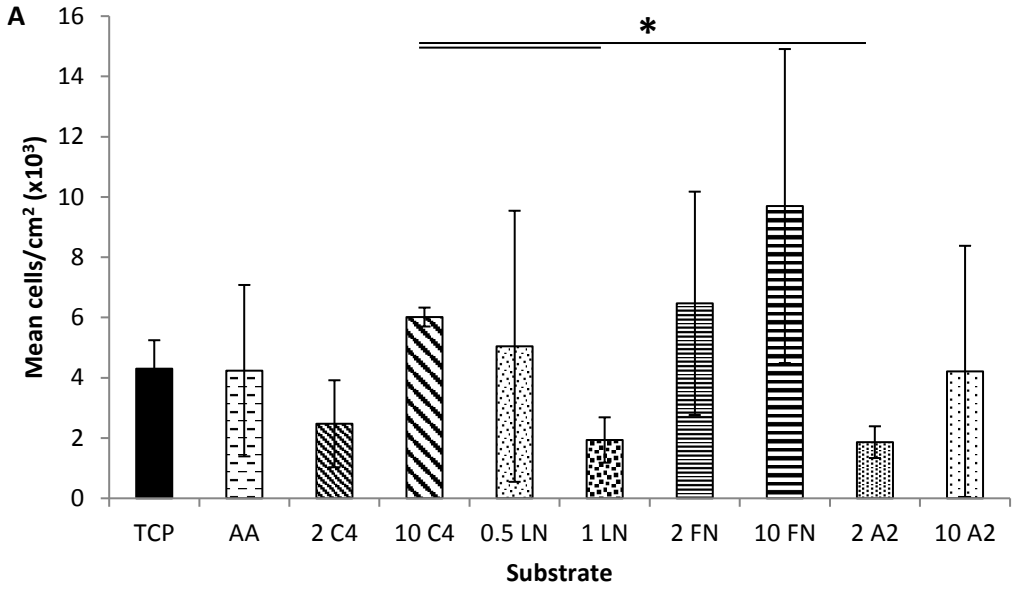

B

	Mean	*SD*
TCP	4301.3	*944.2*
AA	4235.4	*2843.9*
2 C4	2474.2	*1443.3*
10 C4	6014.6	*314.0*
0.5 LN	5044.2	*4497.5*
1 LN	1935.0	*752.3*
2 FN	6469.9	*3705.5*
10 FN	9698.9	*5209.2*
2 A2	1863.1	*526.5*
10 A2	4211.4	*4167.2*

Figure 3.5: A. Adhesion of HCjE-Gi cells on AA cross-linked PεK hydrogels. Data are presented as mean number of cells/cm² (x10³) ± 1SD, n = 3. There was a significant increase in the number of cells adhered on AA cross-linked PεK gels with type IV collagen pre-adsorbed from a 10µg/mL solution compared to those with laminin 111 and α-2-HS-GP pre-adsorbed from 1µg/mL (p = 0.033) and 2µg/mL (p = 0.007) solutions, respectively; *p < 0.05. (One-way ANOVA; Games-Howell post hoc test). B. Mean number of cells/cm² and 1SD; C4 - type IV collagen 2 and 10µg/mL, LN - laminin 111 0.5 and 1µg/mL, FN – fibronectin 2 and 10µg/mL and A2 – 2 and 10µg/mL.

Adhesion of HCjE-Gi cells on SA cross-linked PεK gels

A

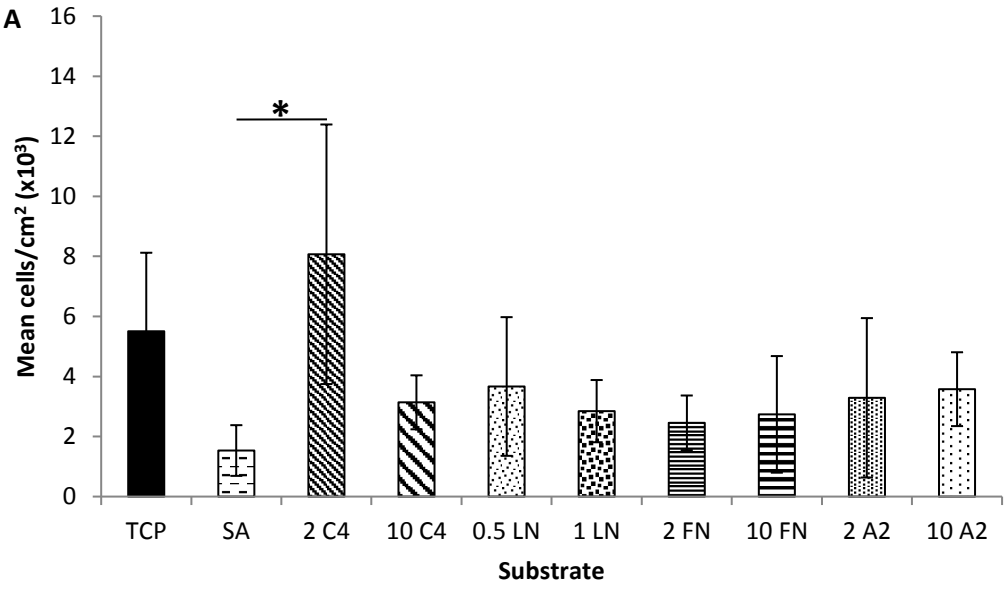

B

	Mean	*SD*
TCP	5505.4	*2614.9*
SA	1533.6	*844.7*
2 C4	8069.4	*4322.5*
10 C4	3139.1	*898.7*
0.5 LN	3666.3	*2309.5*
1 LN	2845.6	*1036.2*
2 FN	2456.2	*909.7*
10 FN	2737.7	*1941.8*
2 A2	3288.9	*2654.7*
10 A2	3576.4	*1229.6*

Figure 3.6: A. Adhesion of HCjE-Gi cells on SA cross-linked PεK hydrogels. Data are presented as mean number of cells/cm² (x10³) ± 1SD, n = 3. There was a significant increase in the number of cells adhered on the SA cross-linked PεK gels with type IV collagen pre-adsorbed from a 2µg/mL solution compared to the gels without pre-adsorbed proteins (p = 0.036); *p < 0.05. (One-way ANOVA; Tukey post hoc test). B. Mean number of cells/cm² and 1SD; C4 - type IV collagen 2 and 10µg/mL, LN - laminin 111 0.5 and 1µg/mL, FN – fibronectin 2 and 10µg/mL and A2 – 2 and 10µg/mL.

3.3.3 GROWTH OF HCjE-Gi CELLS ON PεK HYDROGELS

In general, all substrate groups supported the growth of HCjE-Gi cells over fourteen days. By culture day fourteen, nuclear staining of cells showed evidence of more than one layer of cells as there were two levels of focus during microscopy (figures 3.7-3.9).

The growth of HCjE-Gi cells on AA cross-linked PεK gels with and without pre-adsorbed proteins over fourteen days in culture was comparable to that on TCP without pre-adsorbed proteins (figure 3.10). The residuals were not normally distributed in four groups (day 4 - fibronectin 2µg/mL, day 7 - TCP, day 7 – type IV collagen 2µg/mL, and day 14 – α-2-HS-GP 10µg/mL groups). There was heterogeneity of data ($p < 0.001$) and there were no outliers present. The interaction effect between substrate and culture day on the cell number was not statistically significant ($p = 0.218$). Analysis of the main effect between substrates showed that the differences were not statistically significant, $p = 0.508$. However, analysis of the main effect between culture days showed a statistically significant difference, $p < 0.001$. Statistically significant increases in the cell number were observed on culture days 7 to 14 compared to culture days 1 to 4, and culture days 11 to 14 compared to culture day 7 ($p < 0.05$). These results show that the HCjE-Gi cells were in the lag phase during culture days 1 to 4, log phase during days 4 to 11 and plateau phase during days 11 to 14 when cultured on AA cross-linked PεK gels.

The growth of HCjE-Gi cells on SA cross-linked PεK gels with and without pre-adsorbed proteins over fourteen days in culture was comparable to that on TCP without pre-adsorbed proteins (figure 3.11). The residuals were not normally distributed in three groups (day 7 – α-2-HS-GP 2µg/mL, day 11 – laminin 111 0.5µg/mL, and day 11 – fibronectin 10µg/mL groups). There was heterogeneity of variances ($p < 0.001$) and there were no outliers. There was no statistically significant interaction effect between substrate and culture day on the cell number ($p = 0.466$). Analysis of the main effect between substrates showed that the differences were not statistically significant, $p = 0.111$. However, analysis of the main effect between culture days showed a statistically significant difference, $p < 0.001$. Statistically significant increases in the cell number were observed on culture days 7 to 14 compared to culture days 1 to 4, culture days 11 to 14 compared to culture day 7, and culture day 14 compared to culture day 11 ($p < 0.001$). The HCjE-Gi cells were in the lag phase from days 1 to 4, following which they entered the log phase. In contrast to the cells cultured on AA cross-linked PεK gels, HCjE-Gi cells cultured on SA cross-linked PεK gels have not yet entered the plateau phase by day 14.

Nuclear staining of HCjE-Gi cells cultured on PεK gels

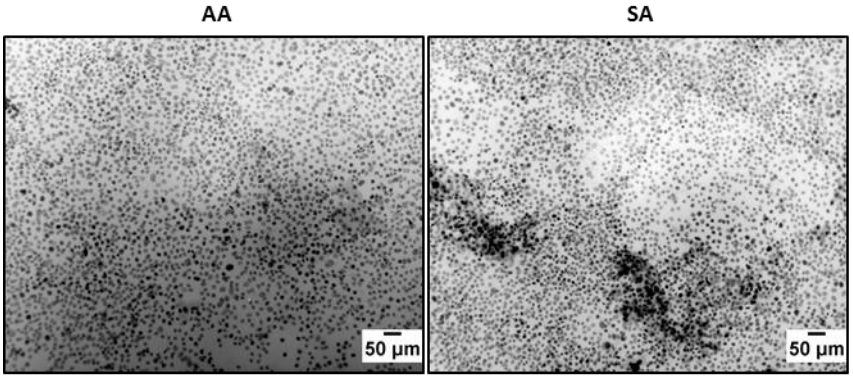

Figure 3.7: Nuclear staining of HCjE-Gi cells cultured on azelaic acid and suberic acid cross-linked PεK gels for fourteen days (8-bit images inverted on Image J software).

Nuclear staining of HCjE-Gi cells cultured on AA cross-linked PεK gels with pre-adsorbed proteins

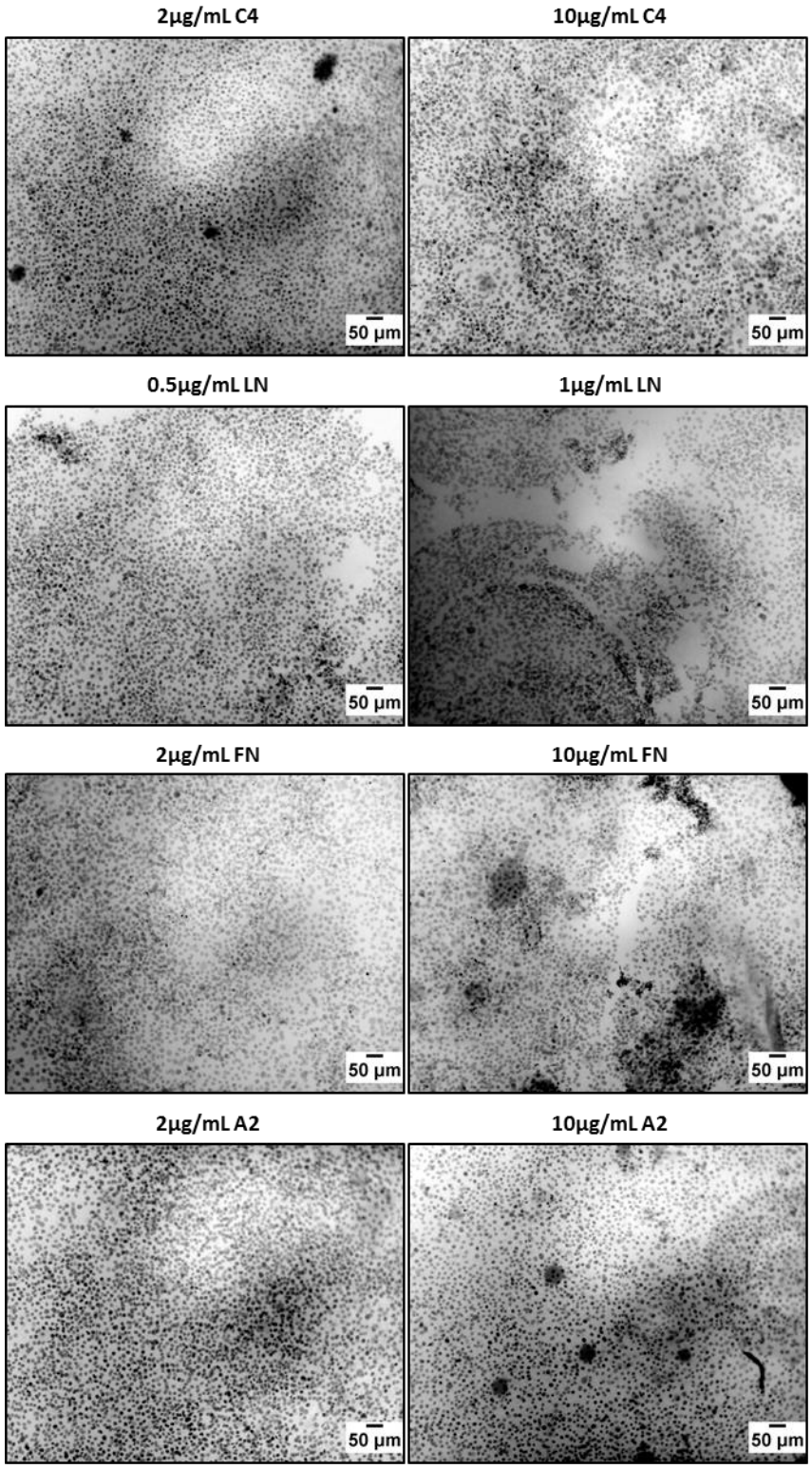

Figure 3.8: Nuclear staining of HCjE-Gi cells cultured on AA cross-linked PεK gels with pre-adsorbed proteins for fourteen days (8-bit images inverted on Image J software); C4 - type IV collagen, LN - laminin 111, FN – fibronectin and A2 - α-2-HS-GP.

Nuclear staining of HCjE-Gi cells cultured on SA cross-linked PεK gels with pre-adsorbed proteins

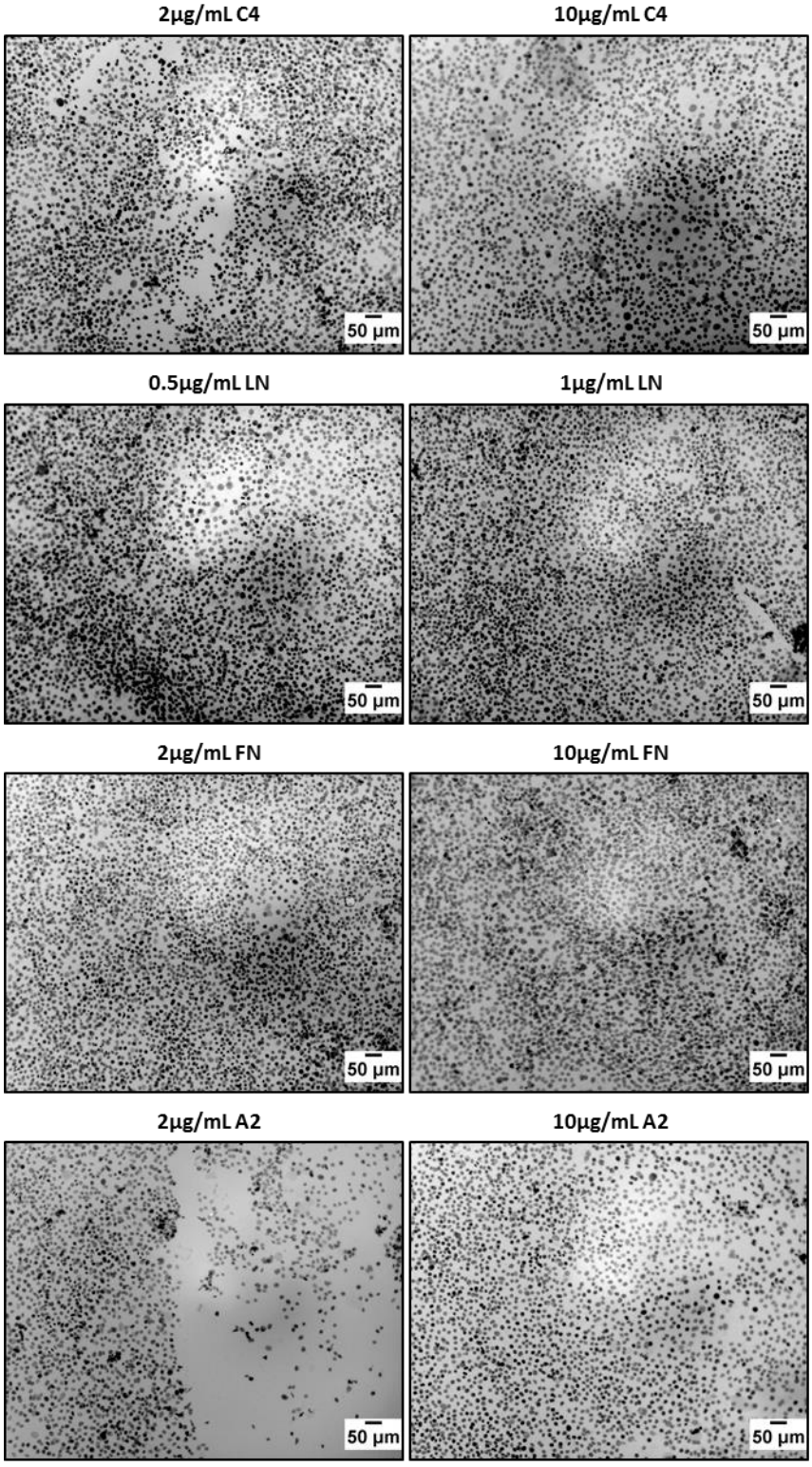

Figure 3.9: Nuclear staining of HCjE-Gi cells cultured on SA cross-linked PεK gels with pre-adsorbed proteins for fourteen days (8-bit images inverted on Image J software); C4 - type IV collagen, LN - laminin 111, FN – fibronectin and A2 - α-2-HS-GP.

Growth of HCjE-Gi cells on AA cross-linked PεK gels

A

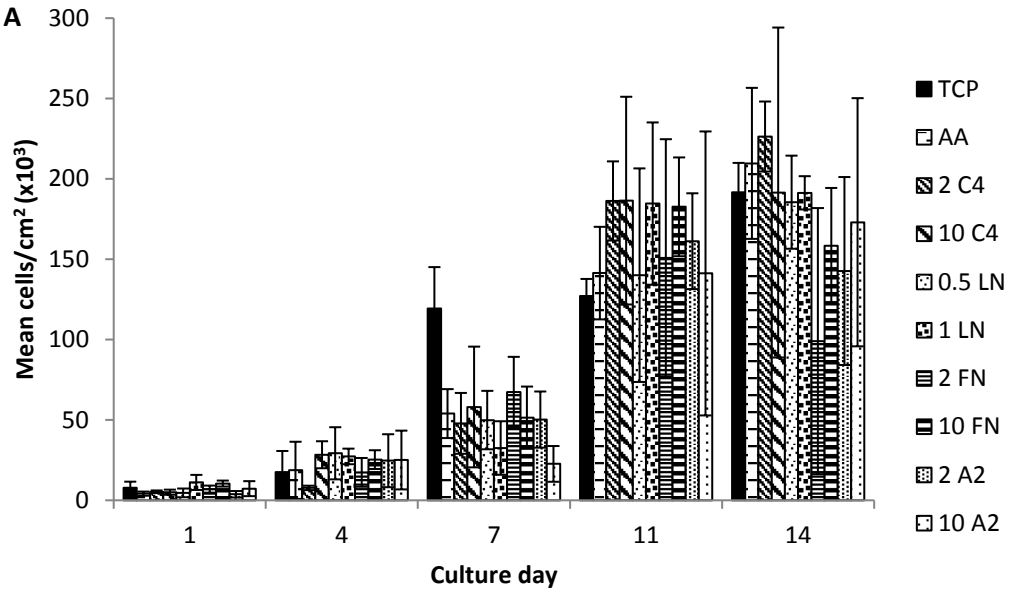

B

	Day 1		Day 7		Day 14	
	Mean	*SD*	Mean	*SD*	Mean	*SD*
TCP	7895.7	*3699.7*	119 310.4	*25 796.2*	191 719.8	*18 212.2*
AA	4157.5	*1290.8*	53 946.1	*15 227.4*	209 643.9	*46 978.0*
2 C4	5307.7	*834.9*	47 877.5	*18 931.9*	226 339.9	*21 777.3*
10 C4	5050.1	*1578.7*	58 061.7	*37 561.4*	191 504.1	*102 647.3*
0.5 LN	4630.8	*2705.6*	49 920.4	*18 173.1*	185 483.5	*28 964.6*
1 LN	11 130.7	*4688.6*	32 541.4	*16 655.9*	191 324.4	*10 348.9*
2 FN	6955.1	*2201.2*	67 443.1	*21 818.1*	99 055.9	*82 771.6*
10 FN	10 417.8	*1857.5*	51 460.0	*19 307.0*	158 417.6	*35 930.9*
2 A2	3768.1	*2002.0*	50 225.9	*17 469.5*	142 662.1	*58 465.7*
10 A2	7248.7	*4667.8*	22 650.8	*11 122.1*	173 004.9	*77 203.9*

Figure 3.10: A. Growth of HCjE-Gi cells on AA cross-linked PεK hydrogels. Data are presented as mean number of cells/cm² (x10³) ± 1SD, n = 3. HCjE-Gi cells were cultured in KSF medium for seven days and in the differentiation and stratification medium for a further seven days. There was no significant interaction effect between substrate and culture day on the cell number (p = 0.218). Analysis of the main effect between the substrates showed no significant difference (p = 0.058). However, there was a significant difference to the main effect between the culture days (p < 0.001). (Two-way ANOVA; Bonferroni post hoc test). B. Mean number of cells/cm² on culture days 1, 7 and 14, and 1SD; C4 - type IV collagen 2 and 10µg/mL, LN - laminin 111 0.5 and 1µg/mL, FN – fibronectin 2 and 10µg/mL and A2 – 2 and 10µg/mL.

Growth of HCjE-Gi cells on SA cross-linked PεK gels

A

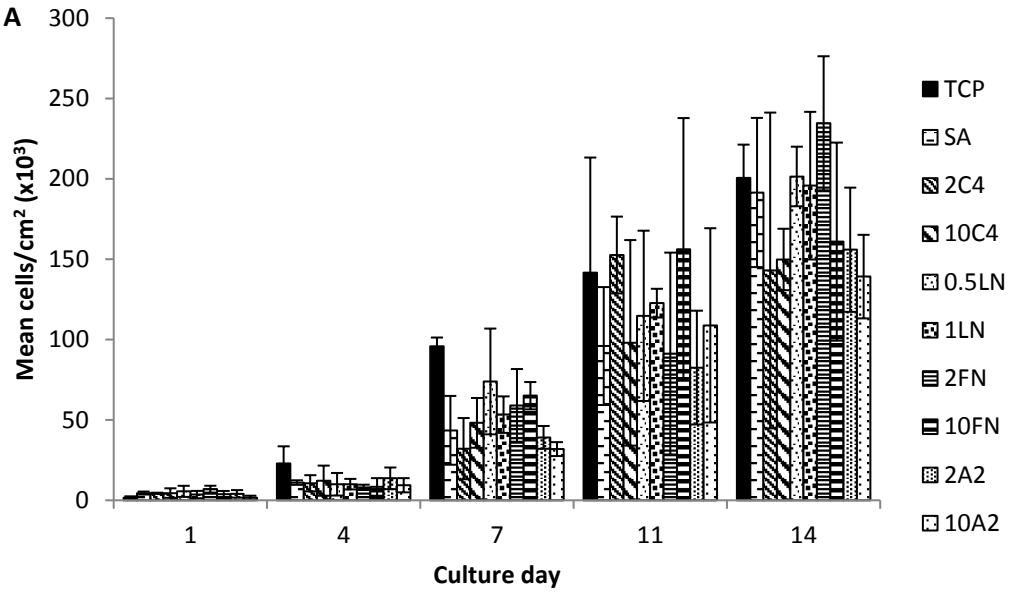

B

	Day 1		Day 7		Day 14	
	Mean	*SD*	Mean	*SD*	Mean	*SD*
TCP	1701.4	*760.9*	95 874.9	*5411.5*	200 538.1	*20 758.4*
SA	4511.0	*921.8*	43 546.3	*21 401.3*	191 516.1	*46 421.3*
2 C4	4361.2	*381.0*	32 140.0	*19 046.2*	143 009.6	*98 223.2*
10 C4	4505.0	*2966.3*	48 183.1	*15 488.6*	149 844.9	*19 103.4*
0.5 LN	5577.3	*3454.2*	73 949.0	*32 900.3*	201 478.6	*18 537.6*
1 LN	3564.5	*2289.8*	53 311.1	*11 359.7*	195 775.5	*45 927.5*
2 FN	6925.2	*2129.8*	59 056.1	*22 618.1*	234 565.1	*41 735.7*
10 FN	3822.1	*1983.3*	65 076.8	*8495.9*	160 933.7	*61 631.0*
2 A2	4007.8	*2343.0*	39 155.1	*7104.5*	155 895.5	*38 651.4*
10 A2	1631.0	*1235.4*	31 864.4	*4325.4*	139 181.5	*25 996.8*

Figure 3.11: A. Growth of HCjE-Gi cells on SA cross-linked PεK hydrogels. Data are presented as mean number of cells/cm² (x10³) ± 1SD, n = 3. HCjE-Gi cells were cultured in KSF medium for seven days and in the differentiation and stratification medium for a further seven days. There was no significant interaction effect between substrate and culture day on the cell number (p = 0.466). Analysis of the main effect between the substrates showed no significant difference (p = 0.111). However, there was a significant difference to the main effect between the culture days (p < 0.001). (Two-way ANOVA; Bonferroni post hoc test). B: Mean number of cells/cm² on culture days 1, 7 and 14, and 1SD; C4 - type IV collagen 2 and 10µg/mL, LN - laminin 111 0.5 and 1µg/mL, FN – fibronectin 2 and 10µg/mL and A2 – 2 and 10µg/mL.

3.3.4 DIFFERENTIATION OF HCjE-Gi CELLS ON PεK HYDROGELS

Keratin 19, a marker of simple epithelial cells, was expressed by all cells cultured for seven and fourteen days on AA and SA cross-linked PεK gels with and without pre-adsorbed proteins (figures 3.12-3.14). The morphology of the cells on culture day seven was similar on all substrates investigated. However, by culture day fourteen, the cells cultured on AA cross-linked PεK gels with and without pre-adsorbed proteins were larger and more flattened than those observed on culture day seven. The cells imaged are likely to be the cells of the superficial layer of the epithelium. Similar morphology was seen when cells were cultured on SA cross-linked PεK gels with pre-adsorbed fibronectin. In contrast, cells cultured on SA cross-linked PεK gels without pre-adsorbed proteins and those with pre-adsorbed type IV collagen and laminin 111, consisted of a mixture of large flattened cells and smaller cells similar to those observed on culture day seven. This may be due to a lesser degree of differentiation and stratification of HCjE-Gi cells cultured on these substrates compared to those on AA cross-linked PεK gels and SA cross-linked PεK gels with pre-adsorbed fibronectin. This is further supported by staining for keratin 4, a marker of non-keratinised stratified epithelial cells, where a few cells stained positive when cultured on AA cross-linked PεK gels, whereas none stained positive when cultured on SA cross-linked PεK gels.

No positive staining for the GC marker, MUC5AC, was evident on culture day seven on any of the substrates investigated (figures 3.15-3.17). By culture day fourteen, after seven days in the differentiation and stratification medium, there was positive staining for MUC5AC in cells cultured on AA cross-linked PεK gels with and without pre-adsorbed proteins. In contrast, positive staining for MUC5AC was only observed in cells cultured on SA cross-linked PεK gels with pre-adsorbed fibronectin, although qualitatively this appeared to be less than that seen on AA cross-linked gels. The staining pattern observed on imaging indicate that the MUC5AC protein is found intra- and extracellularly. There was no positive staining in cells cultured on SA cross-linked PεK gels without pre-adsorbed proteins and those pre-adsorbed with type IV collagen and laminin 111.

Expression of conjunctival cell differentiation markers by HCjE-Gi cells cultured on PεK gels

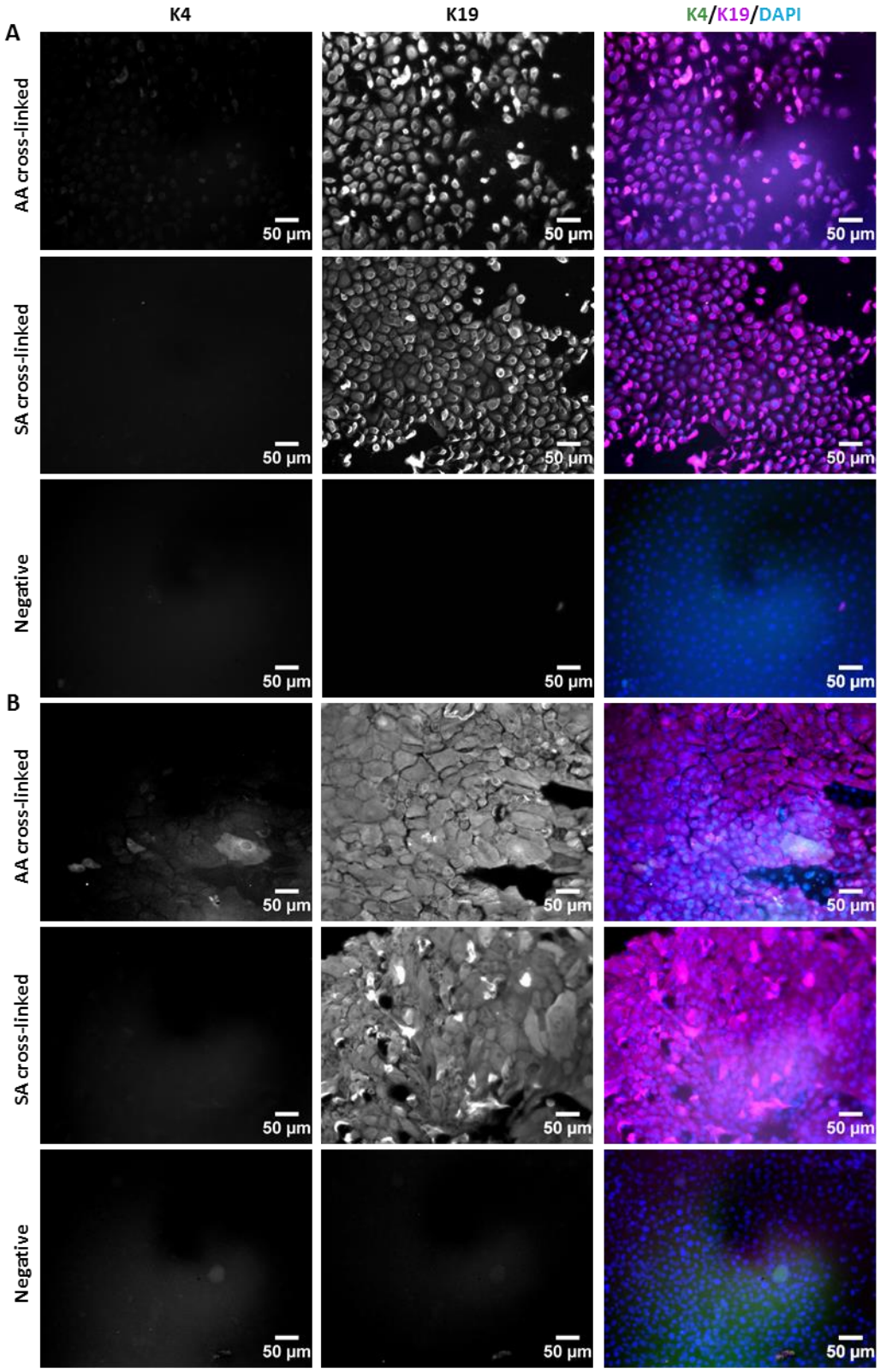

Figure 3.12: Expression of conjunctival cell differentiation markers by HCjE-Gi cells cultured on PεK hydrogels for seven (A) and fourteen (B) days; K4 – keratin 4 (green), K19 – keratin 19 (purple) and DAPI (blue).

Expression of conjunctival cell differentiation markers by HCjE-Gi cells cultured on AA cross-linked PεK gels with pre-adsorbed proteins

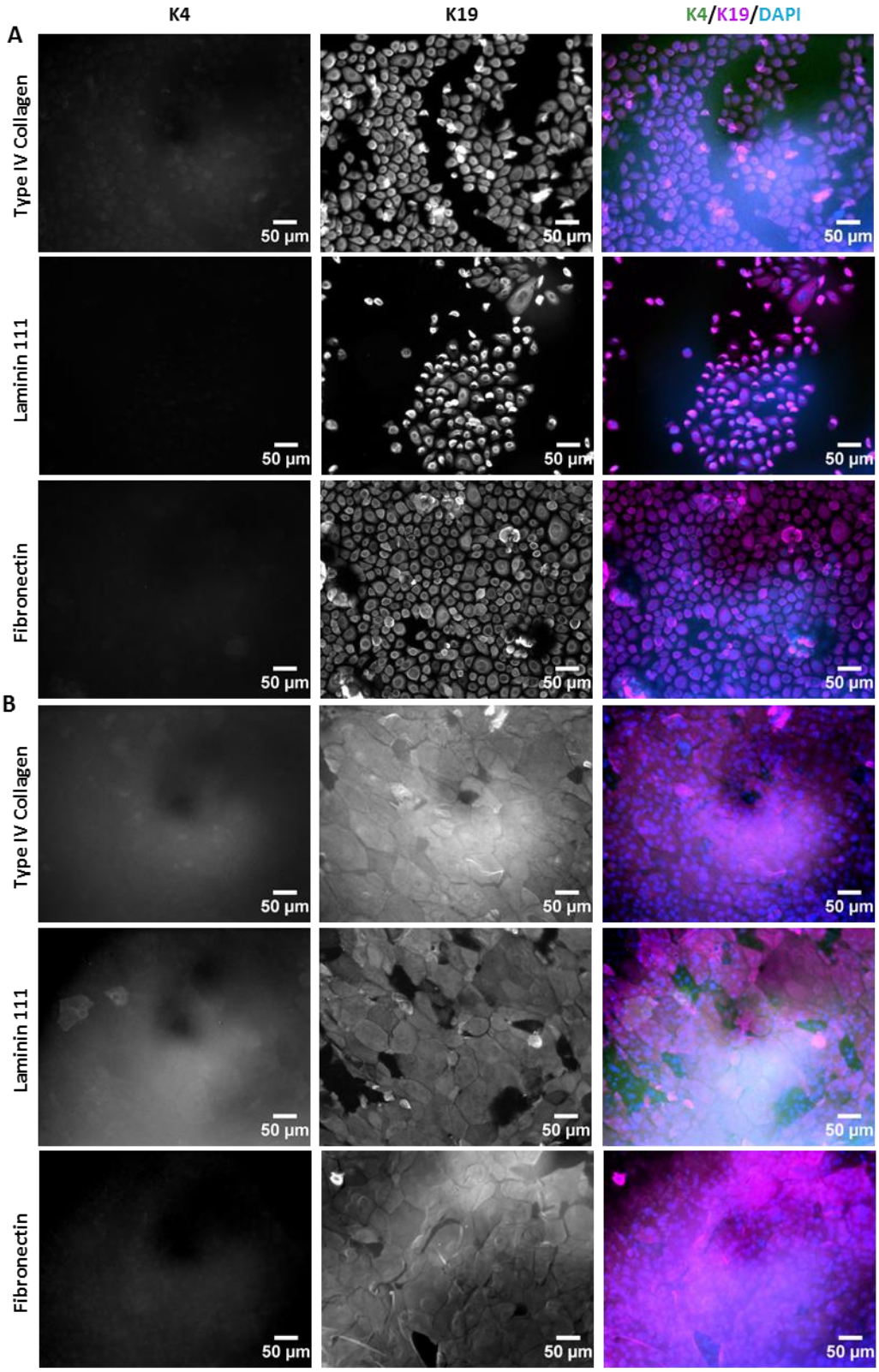

Figure 3.13: Expression of conjunctival cell differentiation markers by HCjE-Gi cells cultured on AA cross-linked PεK hydrogels with pre-adsorbed proteins for seven (A) and fourteen (B) days; K4 – keratin 4 (green), K19 – keratin 19 (purple) and DAPI (blue).

Expression of conjunctival cell differentiation markers by HCjE-Gi cells cultured on SA cross-linked PεK gels with pre-adsorbed proteins

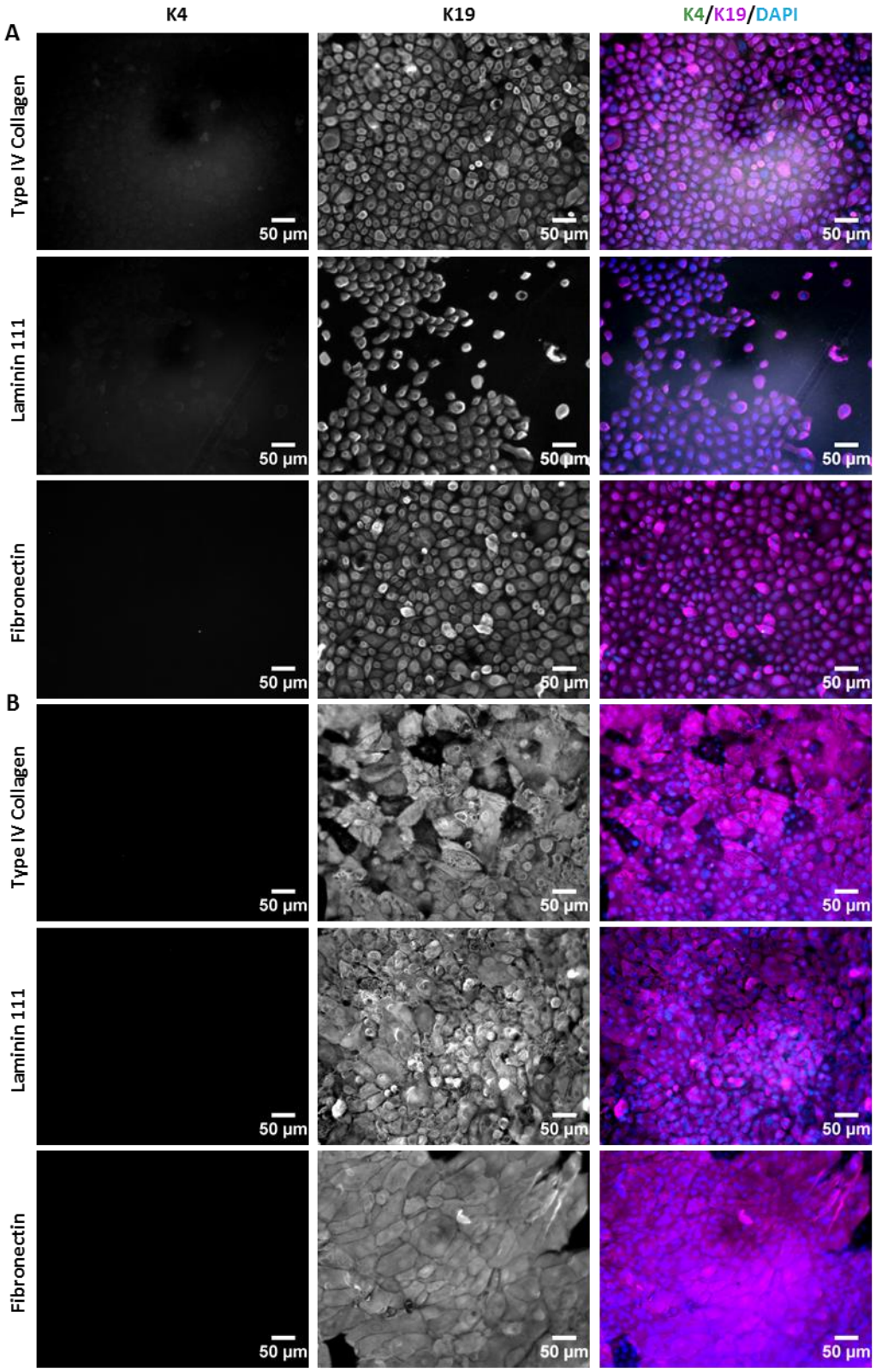

Figure 3.14: Expression of conjunctival cell differentiation markers by HCjE-Gi cells cultured on SA cross-linked PεK hydrogels with pre-adsorbed proteins for seven (A) and fourteen (B) days; K4 – keratin 4 (green), K19 – keratin 19 (purple) and DAPI (blue).

Expression of MUC5AC by HCjE-Gi cells cultured on PεK gels

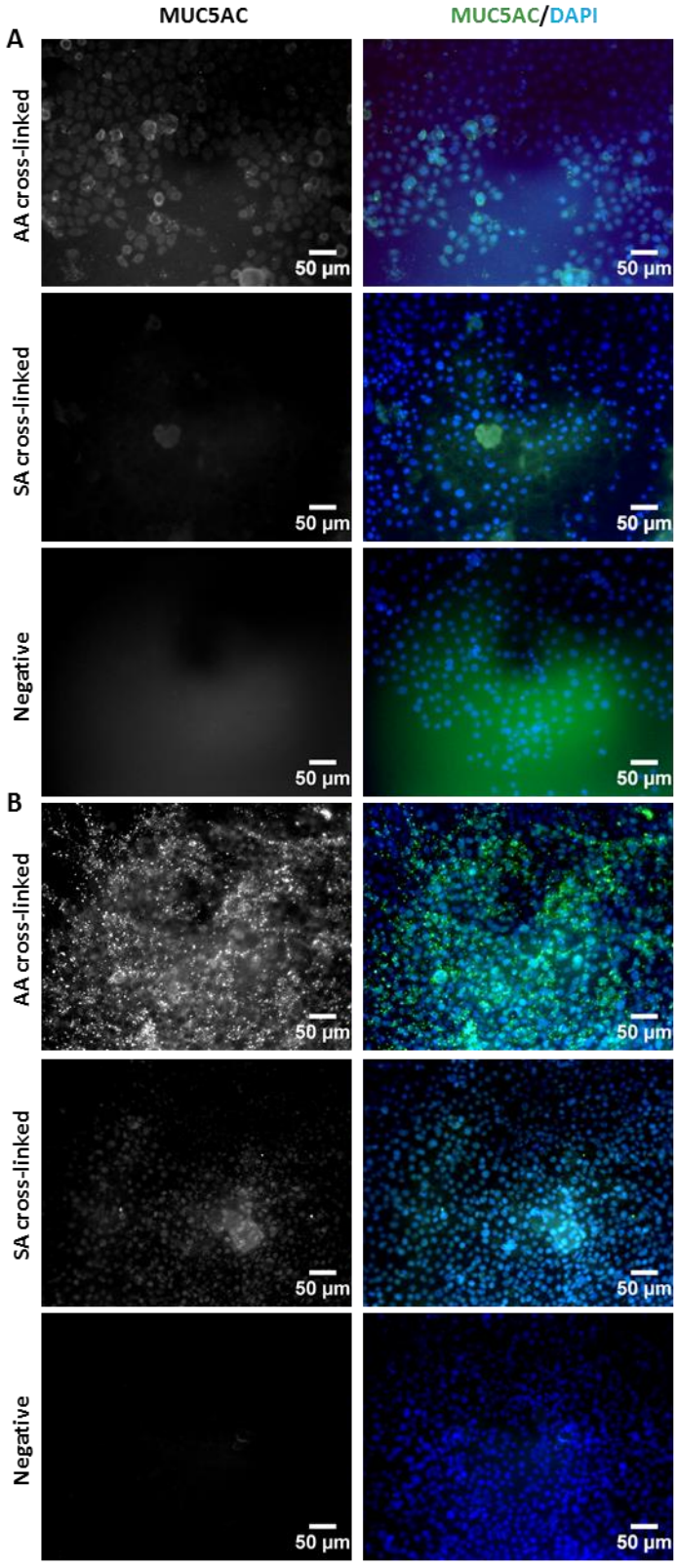

Figure 3.15: Expression of MUC5AC by HCjE-Gi cells cultured on PεK hydrogels for seven (A) and fourteen (B) days; MUC5AC (green) and DAPI (blue).

Expression of MUC5AC by HCjE-Gi cells cultured on AA cross-linked PεK gels with pre-adsorbed proteins

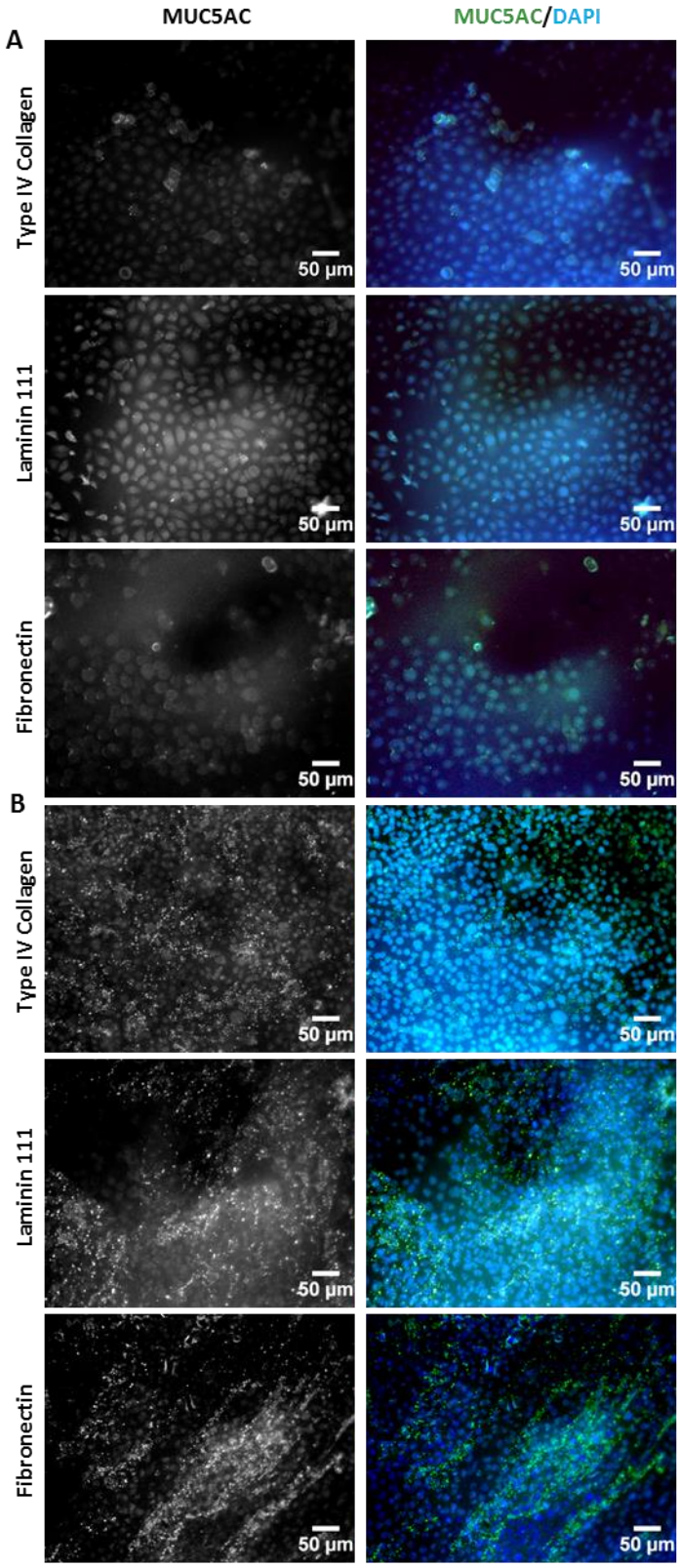

Figure 3.16: Expression of MUC5AC by HCjE-Gi cells cultured on AA cross-linked PεK hydrogels with pre-adsorbed proteins for seven (A) and fourteen (B) days; MUC5AC (green) and DAPI (blue).

Expression of MUC5AC by HCjE-Gi cells cultured on SA cross-linked PεK gels with pre-adsorbed proteins

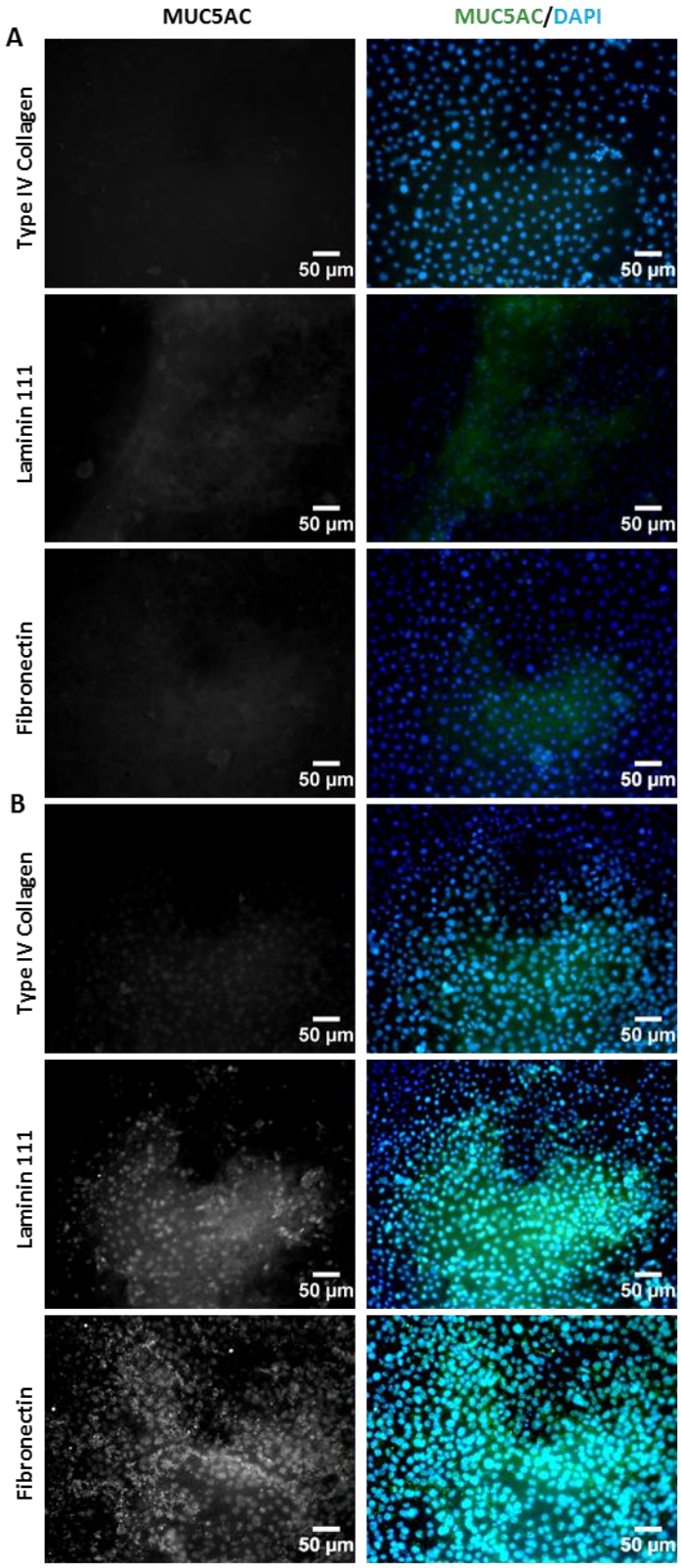

Figure 3.17: Expression of MUC5AC by HCjE-Gi cells cultured on SA cross-linked PεK hydrogels with pre-adsorbed proteins for seven (A) and fourteen (B) days; MUC5AC (green) and DAPI (blue).

3.4 DISCUSSION

3.4.1 PεK hydrogels were thin, transparent and easy to handle

We investigated a peptide-based hydrogel as a substrate for the *ex vivo* expansion of HCjE-Gi cells. PεK hydrogels that were chemically cross-linked with either AA or SA to form three-dimensional structures were investigated in the present study. Both the AA (nine carbon atoms long) and SA (eight carbon atoms long) cross-linked PεK hydrogels were transparent (figure 3.3). Gallagher et al. reported that qualitatively the transparency of these hydrogels decreased with increasing length of the carbon chain of the dicarboxylic acid used for cross-linking the polymer.(112) Quantitative studies are required to accurately assess any significant differences in transparency between AA and SA cross-linked hydrogels. Although transparency of the substrate is not essential for conjunctival transplantation purposes, it is desirable as the conjunctiva *in vivo* is actually an almost transparent mucous membrane.

In the present study, there was a slight yellow tinge to the hydrogels cross-linked with SA compared to those cross-linked with AA (figure 3.3). These hydrogels are known to be yellow in colour and this may be more apparent in the SA cross-linked hydrogels due to the larger thickness compared to those cross-linked with AA. The yellow tinge to the PεK hydrogels is an advantageous property when being considered for corneal transplantation, since it filters out the ultraviolet light. The intraocular lenses currently being employed to replace the natural crystalline lens in patients with cataracts is yellow in colour, which has been shown to filter out light of wavelengths of up to approximately 400nm.(214) This yellow colour mimics the physiological discolouration observed in ageing lenses of the human and does not affect the visual acuity or the contrast sensitivity.(214)

All the PεK hydrogels were easy to handle with the non-toothed and non-serrated forceps. The surgical handle-ability of these hydrogels was verified by a consultant ophthalmologist (Professor S. B. Kaye), who demonstrated the ability of the thin gels to fold and unfold as required similar to the AM used clinically. This is useful in TE of the conjunctiva where the substrates need to be able to conform to the surface of the fornices. Gallagher et al. showed that the tensile strength of these gels can be manipulated by altering the density of PεK, carbon chain length of the dicarboxylic acids and the cross-linking density of the polymer.(112) They showed that the tensile strength generally increased as the carbon chain length increased from six carbon atoms to nine carbon atoms. Although they did not show the change to the elastic modulus with varying carbon chain lengths of the

dicarboxylic acids, it was evident in the present study that the SA cross-linked hydrogels were more brittle than those cross-linked with AA, especially when folded. This suggests that, similar to the tensile strength, the elasticity of these hydrogels also increase as the carbon chain length of the dicarboxylic acid increases. The hydrogels need to be mechanically strong but flexible to be employed to reconstruct the conjunctival fornices. Additionally, Gallagher et al. showed that the greatest effect on the tensile strength is the density of PεK, where approximately a two-fold increase was observed when the PεK density was increased from 0.066g/mL to 0.1g/mL.(112) Moreover, the authors showed that the tensile strength also increased by increasing the cross-linking density from 60% to 80%.(112) The hydrogels synthesised for the current study had a PεK density of 0.1g/mL and a cross-linking density of 60%. The ability to vary the mechanical properties to suit tissue requirements is an appealing characteristic of these hydrogels for TE purposes.

The conjunctival stroma has a rich blood supply from the anterior ciliary and palpebral vessels that supply the epithelium. Thin substrates are ideal for TE to ensure adequate interaction between the graft and the underlying stroma to allow rapid exchange of nutrients and waste products in and out of the cells when transplanted *in vivo*. Hydrogels that were synthesised with 2mL and 3mL of hydrogel solution had a mean thickness of 100-250µm, which was comparable to that of the AM (figure 3.4). The reported thickness of AM varies between 20-500µm.(50) However, the hydrogels investigated in the present study were much thicker than the stretched PCL membranes developed by Ang et al., which were 6µm thick.(35) In the present study, the PεK hydrogels cross-linked with AA were thinner than those cross-linked with SA (figure 3.4). This was an interesting finding since the carbon chain of AA is longer than that of SA. This may be due to the hydrophobicity of the longer chains and therefore the lower water content within the polymer, thus giving rise to a thinner hydrogel. Further studies are required to measure the water content of these hydrogels to investigate this hypothesis.

3.4.2 PεK hydrogels were able to support the adhesion, growth and differentiation of conjunctival cells *ex vivo*

Next, we investigated the adhesion, growth and differentiation of HCjE-Gi cells on the AA and SA cross-linked PεK hydrogels. PεK is a naturally occurring, non-toxic polymer that is approved as a food preservative by the Food and Drug Administration. AA and SA are also naturally occurring products produced from oxidation of longer chain fatty acids in animals and plants. NHS and EDCI were used to activate the carboxyl groups on the dicarboxylic acids to form peptide bonds with the amine groups on the PεK homopolymer. The excess NHS and EDCI should be adequately washed off due to the toxic nature of these reagents. In the present study, the hydrogels were sterilised in 70% ethanol and thoroughly washed in dH_2O prior to cell culture. Gallagher et al. demonstrated the cytocompatibility of the PεK hydrogels by monitoring the cell number of a corneal cell line over a culture period of eight days.(112) Moreover, Griffith et al. showed successful culture of primary human limbal epithelial cells on type III collagen scaffolds that were cross-linked with NHS and EDCI.(176)

Both AA and SA cross-linked PεK hydrogels were able to support the adhesion and growth of HCjE-Gi cells comparable to that on TCP without pre-adsorbed proteins over a culture period of fourteen days (figures 3.5-3.6 and 3.10-3.11). The cells generally followed the lag and log phases of cultured cells in KSF media over the first seven days. Then the cells exhibited a gradual reduction in the rate of growth in the differentiation and stratification media in the next seven days, with some evidence of stratification by culture day fourteen. In chapter 2, I showed that TCP pre-adsorbed with type IV collagen and fibronectin increased the adhesion of cells and that pre-adsorbed with type IV collagen and α-2-HS-GP increased the growth of cells over seven days (figures 2.40, 2.42, 2.44 and 2.47). However, these experiments showed that PεK hydrogels pre-adsorbed with proteins did not affect the adhesion or the growth of HCjE-Gi cells. Chen et al. cultured rat islet tumour cells on TCP coated with ECM proteins, including type IV collagen, laminin, fibronectin and vitronectin, and poly(ι-lysine).(215) They showed that the adhesion and growth of these cells on poly (ι-lysine) over two days is comparable to that on TCP with pre-adsorbed ECM proteins. The surfaces of substrates may be optimised for cell attachment by adding cell adhesive peptides, adding chemical groups to alter the wettability of the surface or by having a cationic surface to allow negatively charged cell membranes to attach to the surface by electrostatic interactions.(216) We have shown that peptide-based hydrogels that carry positive charges on their amino groups are able to support the attachment and growth of HCjE-Gi cells without the need for surface modification by other biomolecules.

The sample size of the adhesion and growth experiments on PεK hydrogels in the present study was three. Thus, further experiments are required with larger sample size to draw accurate conclusions regarding the adhesion and growth of cells on PεK hydrogels with and without pre-adsorbed proteins. Another limitation of the present study is that we did not investigate the protein adsorption onto the hydrogels. Both surface charge and wettability of the substrates determine the balance between hydrophobicity and hydrophilicity that affects the adsorption of proteins.(217) Thus, a future study would be to investigate the protein adsorption onto PεK hydrogels by ELISA, as undertaken in chapter 2 to determine the protein adsorption onto TCP. Another future study would be to determine if the ECM proteins secreted by the HCjE-Gi cells when cultured on PεK hydrogels are similar to that observed when cultured on TCP. This may explain the results observed in the present study by showing that the biological and physical cues provided by the two ECMs are similar.

All the cells cultured on AA and SA cross-linked PεK hydrogels with and without pre-adsorbed proteins expressed keratin 19, a marker of simple epithelial cells, on culture days seven and fourteen (figures 3.12-3.14). After seven days in the differentiation and stratification medium containing 10% fetal bovine serum and higher concentrations of EGF and calcium, the cells on AA cross-linked PεK hydrogels exhibited a flattened morphology. The cells on SA cross-linked PεK hydrogels had a mixture of flattened cells and smaller cells observed on day seven, except those cultured on hydrogels with pre-adsorbed fibronectin that consisted of flattened cells only. These flattened cells could be the superficial cells of a stratified epithelium, although the morphology is different to the cells observed on TCP without pre-adsorbed proteins after seven days in the differentiation and stratification medium (figure 2.8). This difference in morphology observed on culture day fourteen between TCP and PεK hydrogels could be due to the absence and presence of serum in the culture media, respectively. The presence of positive staining for MUC5AC provided further evidence of possible higher degree of differentiation of cells cultured on AA cross-linked hydrogels and SA cross-linked hydrogels with pre-adsorbed fibronectin (figures 3.15-3.17). It is known that expression of this protein requires a higher degree of differentiation and stratification of conjunctival cells. However, further studies are required to assess the differentiation and stratification of conjunctival cells on the PεK hydrogels. In the present study, we have not looked at the presence of SCs following culture on these hydrogels. This is important as substrates employed for TE purposes must be able to support and maintain SCs, which will ensure the long-term survival of the transplant *in vivo*.

Lastly, further studies are required to investigate the biocompatibility of these hydrogels, as well as the growth and differentiation of conjunctival cells *in vivo*. Although, biodegradation is not essential, it is important to assess the fate of the substrate *in vivo* as this may be affected by the activity of local proteases, as well as activity of inflammatory cells, such as in the presence of chronic inflammation due to diseases.

Summary of key findings

- The PεK hydrogels were transparent and easy to handle.
- The PεK hydrogels cross-linked with AA were thinner than those cross-linked with SA.
- Both AA and SA cross-linked PεK hydrogels supported the adhesion and the growth of HCjE-Gi cells over fourteen days.
- Pre-adsorption of type IV collagen, laminin 111, fibronectin and α-2-HS-GP onto PεK hydrogels did not enhance the adhesion or the growth of HCjE-Gi cells compared to those without pre-adsorbed proteins.
- HCjE-Gi cells cultured for fourteen days on AA cross-linked PεK hydrogels with and without pre-adsorbed proteins and on SA cross-linked PεK hydrogels with pre-adsorbed fibronectin differentiated into MUC5AC producing GCs. However, this was not evident on SA cross-linked PεK hydrogels without pre-adsorbed proteins and those pre-adsorbed with type IV collagen and laminin 111.

Comparison of physical, mechanical and biological properties of azelaic and suberic acid cross-linked PεK hydrogels

Azelaic acid cross-linked hydrogels	Suberic acid cross-linked hydrogels
Azelaic acid structure nine carbon atoms long	Suberic acid structure eight carbon atoms long
Light transmission approximately 95% that is reduced at lower wavelengths (485nm) than at higher wavelengths of light (600nm) (unpublished data)	Similar data to azelaic acid (unpublished data)
Thinner (mean thickness 0.17mm)	Thicker (mean thickness 0.24mm)
Theoretically more hydrophobic than suberic acid	Theoretically more hydrophilic than azelaic acid but no significant difference in contact angle measurements, 11-12° (unpublished data)
Higher tensile strength	Lower tensile strength
Stiffness (Young's modulus) approximately 0.25MPa (unpublished data)	Stiffness (Young's modulus) approximately 0.50MPa (unpublished data)
More flattened and larger cells by culture day fourteen (with and without pre-adsorbed proteins)	A mixture of smaller cells and larger and flattened cells on hydrogels without pre-adsorbed proteins and those pre-adsorbed with type IV collagen and laminin 111 by culture day fourteen. Hydrogels with pre-adsorbed fibronectin had larger and flattened cells only.
Positive staining for MUC5AC protein by culture day fourteen (with and without pre-adsorbed proteins)	Positive staining for MUC5AC proteins only on hydrogels with pre-adsorbed fibronectin by culture day fourteen, although qualitatively this was less than that observed on AA cross-linked hydrogels.

Table 3.1: Comparison of physical, mechanical and biological properties of azelaic and suberic acid cross-linked PεK hydrogels.

4 DISCUSSION

The conjunctiva is a thin translucent mucous membrane that extends from the limbus to cover the majority of the OS; covering the posterior surfaces of the eyelids and ending at the muco-cutaneous junctions. It is an integral component of the OS system protecting the eyes from external insults by acting as a physical barrier against injury and entry of foreign bodies including pathogens. It also provides an immunological barrier against pathogens. The epithelial and goblet cells produce mucins, which in addition to acting as a barrier to pathogens, prevent desiccation of the epithelium. Despite the existence of multiple defence mechanisms of the OS, due to its exposure to the environment, the conjunctiva is prone to injury and entry of pathogens. Damage to the conjunctiva may also be caused by systemic autoimmune diseases. Subsequent scarring may lead to anatomical and functional impairment. In severe cases, the limbus and cornea may be impaired that will eventually lead to impairment of vision. Without restoration of function of the conjunctiva in such cases, surgical procedures such as limbal and corneal transplantation will fail. Thus, it is imperative that the health of the conjunctiva is restored prior to repair of the limbus and cornea. Therefore, when considering management of OS disorders, it is essential that the OS system as a whole is taken into account in preference to targeting a single component of the system.

Initial management in most patients with OS disease is removal or control of the inciting agent if identifiable and prevention of disease progression. Unfortunately, there may be extensive tissue loss and scarring leading to a disturbance and loss of homeostasis of the OS. Therefore replacement of the damaged tissue with a suitable substrate containing healthy functional tissue is needed. The ideal graft is an autograft, however, the disease may involve both eyes and there is often insufficient uninvolved tissue in the fellow eye. Although allogenic grafts may be an option, this carries a risk of graft rejection and microbial disease transmission. Other limitations of autografts and allogenic grafts are lack of sufficient tissue to cover large defects and the risk of damage to the donor site with potential scar tissue formation. An alternative to a graft is the development of a functional tissue construct *ex vivo* that can be transplanted to restore the anatomical structure and functions of the original tissue. This could involve the *ex vivo* culture of cells from a small tissue biopsy on an appropriate substrate. The success of an *ex vivo* expanded tissue construct depends on three factors: the source of cells and the presence of SCs, the carrier substrate and the presence of GFs. The substrate provides the initial support for the

cultured cells and the appropriate physical and biological cues for growth of cells. Moreover, it facilitates the delivery of cultured cells to the site of interest and provides a three-dimensional scaffold for the formation of new tissue. A large number of studies have been carried out to investigate various biological and synthetic substrates in the search for an optimal substrate for the *ex vivo* culture of conjunctival epithelial cells.

AM is widely used in the field of ophthalmology as a graft and as a substrate for the *ex vivo* expansion of conjunctival cells to replace damaged OS tissue.(50, 51) As discussed in chapter 1, although there are numerous advantages to using AM in the management of OS disease, there are limitations to its use. Despite precautions taken to collect the AM aseptically, process and store the samples in sterile conditions and testing of the donors for infectious agents, there is still a risk of potential microbial disease transmission. This is especially the case for diseases such as Creutzfeld-Jacob disease that do not have a screening test at present. Moreover, AM is prone to early degradation, *in vivo* shrinkage and lack SCs and adequate GCs. It is also not a standardised product and its composition may vary between donors. Lastly, it is an expensive product that may limit its availability to all patients. Other substrates that have been investigated for TE purposes include biological substrates, such as nasal and oral mucous membranes, and synthetic substrates, such as PCL and PLGA.(27, 31, 46, 70) Although synthetic substrates may have superior mechanical properties to biological substrates, they lack tissue-specific extracellular environments that are present in biological substrates. Thus, there is much scope for the development of a better substrate for conjunctival cell and tissue transplantation.

The aim of the present study was to develop a synthetic substrate for conjunctival cell transplantation by establishing the role of ECM proteins on the functionality of conjunctival epithelial cells and using this information to modify the surfaces of PεK hydrogels. The working hypothesis was that the growth and differentiation of conjunctival epithelial cells on PεK hydrogels is optimal when the surfaces of these substrates are modified with ECM proteins to mimic that of the native tissue. The rationale for this hypothesis is the well-known principle that the protein composition in the ECM regulates the growth and differentiation of the native cells by providing specific biological and physical cues. Therefore, gaining knowledge about the composition and structure of the native ECM of a given tissue and its role in cellular functions will benefit in developing an improved synthetic substrate for cell and tissue transplantation purposes.

In the present study, I was able to identify and quantify the protein composition of the ECM secreted by the HCjE-Gi cells over a culture period of six weeks *in vitro*. I found that the ECM secreted by cells between days three and five in culture, enhanced the growth of HCjE-Gi cells compared to the ECM secreted by cells during long-term culture *in vitro*. Specifically, pre-adsorbed type IV collagen and fibronectin increased the adhesion and pre-adsorbed type IV collagen and α-2-HS-GP increased the growth of HCjE-Gi cells. I have shown that the PεK hydrogels that were cross-linked with AA and SA supported the adhesion and growth of HCjE-Gi cells. However, AA and SA cross-linked PεK hydrogels pre-adsorbed with type IV collagen, laminin 111, fibronectin and α-2-HS-GP did not affect the adhesion or the growth of the HCjE-Gi cells compared to that on PεK hydrogels without pre-adsorbed proteins. This rejects our hypothesis that the growth of conjunctival epithelial cells on PεK hydrogels is optimal when the surfaces of these substrates are modified with ECM proteins of the native tissue. It is possible that these peptide-based hydrogels already provide the necessary cues for the adhesion and the growth of the HCjE-Gi cells. Alternatively, the cationic charges on the surfaces of these hydrogels may support the pre-adsorption of the cell-secreted ECM proteins and thereby support the growth of the cells.

The above finding is in contrast to previous studies undertaken to investigate other synthetic substrates. These studies showed that surface modification of synthetic substrates by increasing the surface hydrophilicity or pre-adsorbing with biomolecules, such as ECM proteins, is required to optimise the adhesion and growth of cells.(35, 75) PCL and PLGA investigated as substrates for the growth of conjunctival epithelial cells are polyesters, unlike the PεK hydrogels that are homopolymers PεK. The knowledge about the composition of the native ECM and its role in cellular functions may be a benefit in developing peptides, such as the RGD peptide of fibronectin, which could be bound to the PεK hydrogels to enhance and optimise the growth and differentiation of cells on these substrates under some conditions.

In the present study, we also showed that the AA and SA cross-linked PεK hydrogels supported the conjunctival cell differentiation and maybe the stratification of cells *ex vivo*. Moreover, we showed that the hydrogels that were cross-linked with AA supported the culture of mucin producing GCs. It is important to develop tissue constructs that replace the function of the original tissue that was damaged, in this case the ability of the conjunctiva to contribute to the tear film and prevent desiccation of the OS. Further studies are required to determine the ECM proteins that are important for GC differentiation. This

information could be used to modify the surfaces of the PεK hydrogels to enhance the differentiation of conjunctival progenitor cells into mucus-producing GCs, especially on the SA cross-linked PεK hydrogels that did not show evidence of GC differentiation. Moreover, the substrate must be able to maintain a pool of SCs for epithelial renewal, especially when used to replace tissue with SC deficiency. In the present study, we have not investigated the ability of PεK hydrogels to support SCs in long-term culture. The ability of a substrate to maintain SCs will ensure the long-term survival of the transplant *in vivo.* Although, the PεK hydrogels were able to support the adhesion and growth of conjunctival cells without surface modification, it may be that it is required for the maintenance of SCs. Therefore, further studies could be undertaken to determine the ECM proteins that govern the maintenance of conjunctival SCs. This information may be employed to modify the surfaces of the PεK hydrogels to ensure its ability to support and maintain SCs in long-term culture *ex vivo* and *in vivo*.

In chapter 1, I described the characteristics of an ideal substrate for conjunctival cell and tissue transplantation. In the present study, I have shown that the PεK hydrogels are a promising substrate for the *ex vivo* culture of conjunctival cells that could potentially be used to replace damaged conjunctival tissue (table 4.1). In the present study we cultured HCjE-Gi cells in serum-free media that contained 25µg/mL bovine pituitary extract. Future studies involving the culture of primary human conjunctival cells on PεK hydrogels will require the maintenance of these cells in similar serum- and BPE-free conditions to meet the standards of good manufacturing practice to be employed as a transplant substrate in humans.

PεK hydrogels as a substrate for conjunctival cell and tissue transplantation

SUBSTRATE CHARACTERISTIC	EVIDENCE FROM THE PRESENT STUDY	FURTHER STUDIES REQUIRED
1. Thin	Yes, comparable to AM	
2. Porous allowing interaction between the graft and the underlying host tissue		Require *in vivo* studies
3. Flexibility and surgical handle-ability	Yes	Require studies to investigate the ability of the hydrogel to be sutured onto the host
4. Biocompatible	Substrate was not toxic to cells *in vitro*	Require *in vivo* studies
5. Supports adhesion, migration and proliferation of epithelial cells	Yes	
6. Supports mucus-producing goblet cells	Yes	
7. Supports maintenance of SCs		Require further studies
8. Biodegradability		Require further studies, especially in the presence of active inflammation
9. Low *in vivo* shrinkage		Require *in vivo* studies

Table 4.1: PεK hydrogels as a substrate for conjunctival cell and tissue transplantation.

5 CONCLUSIONS

- Ammonium hydroxide successfully isolated the extracellular proteins and the transmembrane proteins associated with the extracellular matrix of the HCjE-Gi cells *in vitro*.

- The protein composition and their quantities in the extracellular matrix of the HCjE-Gi cells varied over six weeks in culture *in vitro*.

- TCP pre-adsorbed with type IV collagen and fibronectin increased the adhesion of HCjE-Gi cells compared to TCP without pre-adsorbed proteins.

- TCP pre-adsorbed with type IV collagen, α-2-HS-GP and the extracellular matrix derived from the cells that were in culture for three and five days increased the growth of HCjE-Gi cells compared to TCP without pre-adsorbed proteins.

- Preliminary data showed that the expression of stem cell and goblet cell protein markers by HCjE-Gi cells decreased and increased, respectively, over fourteen days in culture *in vitro*.

- PεK hydrogels were thin, transparent and easy to handle.

- PεK hydrogels that were cross-linked with AA and SA supported the adhesion and growth of HCjE-Gi cells.

- Pre-adsorption of PεK hydrogels with type IV collagen, laminin 111, fibronectin and α-2-HS-GP did not enhance the adhesion or the growth of HCjE-Gi cells compared to PεK hydrogels without pre-adsorbed proteins.

- HCjE-Gi cells cultured for fourteen days on AA cross-linked PεK hydrogels with and without pre-adsorbed proteins and on SA cross-linked PεK hydrogels with pre-adsorbed fibronectin differentiated into MUC5AC producing goblet cells. However, this was not evident on SA cross-linked PεK hydrogels without pre-adsorbed proteins and those pre-adsorbed with type IV collagen and laminin 111.

Current literature

- The ideal grafts to replace damaged conjunctival tissue are conjunctival autografts.
- An alternative to conjunctival autografts and allografts are amniotic membranes that are used as a graft and as a substrate for the *ex vivo* expansion of conjunctival cells.
- Other biological and synthetic substrates investigated as grafts or substrates for the *ex vivo* expansion of conjunctival cells have advantages and disadvantages peculiar to the material.
- Immunohistochemistry studies have shown the differential expression of a selected array of proteins throughout the ocular surface.

Contribution to the literature made by the present study

- The change to the composition and the quantities of proteins in the extracellular matrix of a conjunctival epithelial cell line cultured over six weeks *in vitro*.
- The extracellular matrix derived from cells that were in culture for three and five days increased the growth of conjunctival epithelial cells compared to tissue culture polystyrene.
- Pre-adsorption of tissue culture polystyrene with type IV collagen and fibronectin increased the adhesion of cells and pre-adsorption of tissue culture polystyrene with type IV collagen and α-2-Heremans Schmid-glycoprotein increased the growth of conjunctival epithelial cells compared to tissue culture polystyrene without pre-adsorbed proteins over seven days in culture.
- PεK hydrogels cross-linked with azelaic acid and suberic acid supported the adhesion and growth of conjunctival cells over fourteen days *ex vivo*. Surface modification PεK hydrogels with pre-adsorbed proteins did not affect the adhesion or the growth of cells compared to those without pre-adsorbed proteins.
- Azelaic acid cross-linked PεK hydrogels with and without pre-adsorbed proteins supported the differentiation of MUC5AC-producing goblet cells. However, only suberic acid cross-linked PεK hydrogels pre-adsorbed with fibronectin supported the differentiation of MUC5AC-producing goblet cells compared to those without pre-adsorbed proteins.

6 FUTURE STUDIES

1. Investigate the composition of the extracellular matrix of HCjE-Gi cells when cultured on PεK hydrogels. This may explain the results observed in the present study where the growth of HCjE-Gi cells cultured on tissue culture polystyrene were comparable to that on the PεK hydrogels.

2. Investigate the ability of the PεK hydrogels to support the adhesion, growth and differentiation of primary human conjunctival cells. Functional peptides of extracellular matrix proteins identified to enhance the growth and differentiation of conjunctival cells may be employed to optimise the growth and differentiation of primary human conjunctival cells if required.

3. Investigate the ability of the PεK hydrogels to maintain a population of stem cells *ex vivo* and *in vivo*.

4. Investigate the biocompatibility of the PεK hydrogels when transplanted *in vivo*.

5. Investigate the ability of the PεK hydrogels with *ex vivo* expanded conjunctival cells to integrate into the host tissue and repair the anatomical and functional deficiencies.

7 APPENDICES

Appendix 1: LC-MS/MS Instrumentation and software

Data-dependent LC-MS/MS analyses were conducted on a QExactiveHF quadrupole-Orbitrap mass spectrometer coupled to a Dionex Ultimate 3000 RSLC nano-liquid chromatograph (Hemel Hempstead, UK). Sample digests (15µL) was loaded onto a trapping column (Acclaim PepMap 100 C18, 75µm x 2cm, 3µm packing material, 100Å) using a loading buffer of 0.1% TFA (*v/v*) and 2% acetonitrile (*v/v*) (*Fluka 34668*) in water for seven minutes at a flow rate of 12µL/minute. The trapping column was then set in-line with an analytical column (EASY-Spray PepMap RSLC C18, 75µm x 50cm, 2µm packing material, 100Å) and the peptides eluted using a linear gradient of 96.2% A (0.1% formic acid (*v/v*) (*Biosolve 0006914143BS*)), 3.8% B (0.1% formic acid (*v/v*) in water:acetonitrile [80:20] (*v/v*)) to 50% A:50% B over thirty minutes at a flow rate of 300nL/minute, followed by washing with 1% A:99% B for five minutes and re-equilibration of the column to starting conditions. The column was maintained at 40°C, and the effluent introduced directly into the integrated nano-electrospray ionisation source operating in positive ion mode. The mass spectrometer was operated in data dependent acquisition mode with survey scans between mass/charge ratios 350-2000 acquired at a mass resolution of 60,000 (full width half maximum) at mass/charge ratio 200. The maximum injection time was 100 milliseconds, and the automatic gain control was set to $3x10^6$. The eighteen most intense precursor ions with charge states of between 2+ and 5+ were selected for MS/MS with an isolation window of 1.2 m/z units. The maximum injection time was 45 milliseconds, and the automatic gain control was set to $1x10^5$. Fragmentation of the peptides was by higher-energy collisional dissociation using a stepped normalised collision energy of 28-30%. Dynamic exclusion of mass/charge ratio values to prevent repeated fragmentation of the same peptide was used with an exclusion time of 20 seconds.

Raw mass spectral data files were processed using Progenesis-QI (version 2; Nonlinear Dynamics) to determine the total protein abundances. Protein quantification was based on averaging the individual abundances for every unique peptide for each protein and comparing them relatively across sample runs and between sample groups. The raw data file was imported into Progenesis QI for Proteomics (version 3.0.5995.47167 Nonlinear Dynamics, Newcastle upon Tyne UK; Waters Company). Samples were aligned according to retention time using a combination of manual and automatic alignment. Peak picking parameters were applied with sensitivity set to maximum and features with charges of 2+

to 7+ were retained. A Mascot Generic File, created by Progenesis, was searched against the human reviewed database from Uniprot (20 187 sequences). Trypsin was specified as the protease with one missed cleavage allowed and with fixed carbamidomethyl modification for cysteine and variable oxidation modification for methionine. A precursor mass tolerance of 10 parts per million and a fragment ion mass tolerance of 0.01Da were applied. The results were then filtered to obtain a peptide false discovery rate of 1%.

Appendix 2: Quantities of reagents used to synthesise 60:10 PεK hydrogels

(1) AA cross-linked 60:10 PεK hydrogels

No. residues	28.000	
M.Wt parent	3602.000	
Amount of poly-Lys	4.051	g (gross)
Strength of poly-Lys	72.200	%
Amount of poly-Lys	2.925	g (net)
Amount of poly-Lys	0.812	mmole
Amount of amino groups	23.547	mmole
Degree of neutralisation	100.000	% total amino groups
Amount of NMM required	23.547	mmole
Amount of NMM required	2.585	ml
% cross linking required	60.000	mole %
Amount of dicarboxylic acid	7.064	mmole
M.Wt	188.220	
Amount of dicarboxylic acid	1.330	g
Degree of acidification	50.000	% total amino groups
M.Wt NHS	115.090	
Amount of NHS	1.355	g
Equivalents of WSC to dicarboxylic acid	2.500	times
M.Wt WSC	191.700	
Amount of WSC	6.771	g
Amount of polymer	4.000	g
Swell	10.000	ml/g (poly-Lys)
Total volume	40.000	ml
Volume of buffer required	23.909	ml
Capacity	2.355	mmoles/g

(2) SA cross-linked 60:10 PεK hydrogels

No. residues	28.000	
M.Wt parent	3602.000	
Amount of poly-Lys	4.154	g (gross)
Strength of poly-Lys	72.200	%
Amount of poly-Lys	2.999	g (net)
Amount of poly-Lys	0.833	mmole
Amount of amino groups	24.145	mmole
Degree of neutralisation	100.000	% total amino groups
Amount of NMM required	24.145	mmole
Amount of NMM required	2.651	ml
% cross linking required	60.000	mole %
Amount of dicarboxylic acid	7.243	mmole
M.Wt	174.200	
Amount of dicarboxylic acid	1.262	g
Degree of acidification	50.000	% total amino groups
M.Wt NHS	115.090	
Amount of NHS	1.389	g
Equivalents of WSC to dicarboxylic acid	2.500	times
M.Wt WSC	191.700	
Amount of WSC	6.943	g
Amount of polymer	4.000	g
Swell	10.000	ml/g (poly-Lys)
Total volume	40.000	ml
Volume of buffer required	23.602	ml
Capacity	2.414	mmoles/g

8 REFERENCES

1. Forrester JV, Dick AD, McMenamin PG, Roberts F, Pearlman E. The Eye: Basic Sciences in Practice. 4th ed. UK: Elsevier; 2016.
2. Fundamentals and Principles of Ophthalmology. Basic and Clinical Science Course. San Francisco: American Academy of Ophthalmology; 2011-2012.
3. Riordan-Eva P. Anatomy & Embryology of the Eye. In: Riordan-Eva P, Whitcher JP, editors. Vaughan & Ashbury's General Ophthalmology. 17th ed. New York: McGraw-Hill; 2008.
4. DelMonte DW, Kim T. Anatomy and physiology of the cornea. J Cataract Refract Surg. 2011;37(3):588-98.
5. Tong L, Lan W, Petznick A. Definition of the ocular surface. In: Herranz RM, Herran RM, editors. Ocular Surface: Anatomy and Physiology, Disorders and Therapeutic Care: CRC Press; 2012.
6. Gipson IK. The ocular surface: the challenge to enable and protect vision: the Friedenwald lecture. Invest Ophthalmol Vis Sci. 2007;48(10):4390-8.
7. Bolaños-Jiménez R, Navas A, López-Lizárraga EP, Ribot FMd, Peña A, Graue-Hernández EO, et al. Ocular surface as barrier of innate immunity. Open Ophthalmol J. 2015;9:49-55.
8. Zhou H, Lu Q, Guo Q, Chae J, Fan X, Elisseeff JH, et al. Vitrified collagen-based conjunctival equivalent for ocular surface reconstruction. Biomaterials. 2014;35(26):7398-406.
9. Lavker RM, Sun T-T. Epithelial stem cells: the eye provides a vision. Eye. 2003;17(8):937-42.
10. Merjava S, Neuwirth A, Tanzerova M, Jirsova K. The spectrum of cytokeratins expressed in the adult human cornea, limbus and perilimbal conjunctiva. Histol Histopathol. 2011;26(3):323-31.
11. Schlötzer-Schrehardt U, Dietrich T, Saito K, Sorokin L, Sasaki T, Paulsson M, et al. Characterization of extracellular matrix components in the limbal epithelial stem cell compartment. Exp Eye Res. 2007 85(6):845-60.
12. Qi H, Zheng X, Yuan X, Pflugfelder SC, Li D-Q. Potential localization of putative stem/progenitor cells in human bulbar conjunctival epithelium. J Cell Physiol. 2010;225(1):180-5.
13. Rivas L, Blázquez A, Muñoz-Negrete FJ, López S, Rebolleda G, Domínguez F, et al. Characterization of epithelial primary culture from human conjunctiva. Arch Soc Esp Oftalmol. 2014;89(1):10-6.
14. Stewart RM, Sheridan CM, Hiscott PS, Czanner G, Kaye SB. Human Conjunctival Stem Cells are Predominantly Located in the Medial Canthal and Inferior Forniceal Areas. Invest Ophthalmol Vis Sci. 2015;56(3):2021-30.
15. Efron N, Al-Dossari M, Pritchard N. In vivo confocal microscopy of the bulbar conjunctiva. Clin Exp Ophthalmol. 2009;37(4):335-44.
16. Wei A, Hong J, Sun X, Xu J. Evaluation of age-related changes in human palpebral conjunctiva and meibomian glands by in vivo confocal microscopy. Cornea. 2011;30(9):1007-12.
17. Kessing SV. Mucous gland system of the conjunctiva. A quantitative normal anatomical study. Acta Ophthalmol (Copenh). 1968;Suppl 95:1+.
18. Johnson ME, Murphy PJ. Changes in the tear film and ocular surface from dry eye syndrome. Prog Retin Eye Res. 2004;23(4):449-74.
19. Yañez-Soto B, Mannis MJ, Schwab IR, Li JY, Leonard BC, Abbott NL, et al. Interfacial phenomena and the ocular surface. Ocul Surf. 2014;12(3):178-201.

20. Peters E, Colby K. The tear film. In: Tasman W, Jaeger EA, editors. Duane's Ophthalmology. Philadelphia: Lippincott Williams & Wilkin; 2009.
21. Schrader S, Notara M, Beaconsfield M, Tuft SJ, Daniels JT, Geerling G. Tissue Engineering for Conjunctival Reconstruction: Established Methods and Future Outlooks. Curr Eye Res. 2009;34(11):913-24.
22. Revoltella RP, Papini S, Rosellini A, Michelini M. Epithelial stem cells of the eye surface. Cell Prolif. 2007;40(4):445-61.
23. Li W, Hayashida Y, Chen Y-T, Tseng SCG. Niche regulation of corneal epithelial stem cells at the limbus. Cell Res. 2007;17(1):26-36.
24. Dietrich-Ntoukas T, Hofmann-Rummelt C, Kruse FE, Schlotzer-Schrehardt U. Comparative analysis of the basement membrane composition of the human limbus epithelium and amniotic membrane epithelium. Cornea. 2012;31:564-69.
25. Wolosin JM, Budak MT, Akinci MAM. Ocular surface epithelial and stem cell development. Int J Dev Biol. 2004;48:981-91.
26. Chiou AG, Florakis GJ, Kazim M. Management of conjunctival cicatrizing diseases and severe ocular surface dysfunction. Surv Ophthalmol. 1998;43(1):19-46.
27. Hatton MP, Rubin PAD. Conjunctival regeneration. Adv Biochem Eng Biotechnol. 2005;94:125-40.
28. Mai C, Bertelmann E. Oral mucosal grafts: old technique in new light. Ophthalmic Res. 2013;50(2):91-8.
29. Queisi MM, Zein M, Lamba N, Meese H, Foster CS. Update on ocular cicatricial pemphigoid and emerging treatments. Surv Ophthalmol. 2016 61(3):314-7.
30. Ciralsky JB, Sippel KC, Gregory DG. Current ophthalmologic treatment strategies for acute and chronic Stevens-Johnson syndrome and toxic epidermal necrolysis. Curr Opin Ophthalmol. 2013;24(4):321-8.
31. Lu Q, Al-Sheikh O, Elisseeff JH, Grant MP. Biomaterials and Tissue Engineering Strategies for Conjunctival Reconstruction and Dry Eye Treatment. Middle East Afr J Ophthalmol. 2015;22(4):428-34.
32. Tan D. Conjunctival grafting for ocular surface disease. Curr Opin Ophthalmol. 1999;10(4):277-81.
33. Nakamura T, Inatomi T, Sotozono C, Koizumi N, Kinoshita S. Ocular surface reconstruction using stem cell and tissue engineering. Prog Retin Eye Res. 2016;51:187-207.
34. Kuckelkorn R, Schrage N, Redbrake C, Kottek A, Reim M. Autologous transplantation of nasal mucosa after severe chemical and thermal eye burns. Acta Ophthalmol Scand. 1996;74(5):442-8.
35. Ang LP, Cheng ZY, Beuerman RW, Teoh SH, Zhu X, Tan DT. The development of a serum-free derived bioengineered conjunctival epithelial equivalent using an ultrathin poly(epsilon-caprolactone) membrane substrate. Invest Ophthalmol Vis Sci. 2006;47(1):105-12.
36. Kwitko S, Marinho D, Barcaro S, Bocaccio F, Rymer S, Fernandes S, et al. Allograft conjunctival transplantation for bilateral ocular surface disorders. Ophthalmology. 1995;102(7):1020-5.
37. Daya SM, Ilari L. Living related conjunctival limbal allograft for the treatment of stem cell deficiency. Ophthalmology. 2001;108(1):126-34.
38. Fayez MFA. Limbal-conjunctival vs conjunctival autograft transplant for recurrent pterygia: a prospective randomized controlled trial. JAMA Ophthalmol. 2013;131(1):11-6.
39. Janson BJ, Sikder S. Surgical management of pterygium. Ocul Surf. 2014;12(2):112-9.
40. Xu F, Li M, Yan Y, Lu K, Cui L, Chen Q. A novel technique of sutureless and glueless conjunctival autografting in pterygium surgery by electrocautery pen. Cornea. 2013;32(3):290-5.

41. Prabhasawat P, Tesavibul N. Preserved Amniotic Membrane Transplantation for Conjunctival Surface Reconstruction. Cell Tissue Bank. 2001;2(1):31-9.
42. Kular JK, Basu S, Sharma RI. The extracellular matrix: Structure, composition, age-related differences, tools for analysis and applications for tissue engineering. J Tissue Eng. 2014;20(5):1-17.
43. Pradhan S F-CM. Mining the extracellular matrix for tissue engineering applications. Regen Med. 2010;5(6):961-70.
44. Malhotra C, Jain AK. Human amniotic membrane transplantation: Different modalities of its use in ophthalmology. World J Transplant. 2014;4(2):111-21.
45. Safinaz MK, Norzana AG, Nizam MHH, Ropilah AR, Faridah HA, Chua KH, et al. The use of autologous fibrin as a scaffold for cultivating autologous conjunctiva in the treatment of conjunctival defect. Cell Tissue Bank. 2014;15(4):619-26.
46. Inatomi T, Nakamura T, Koizumi N, Sotozono C, Yokoi N, Kinoshita S. Midterm results on ocular surface reconstruction using cultivated autologous oral mucosal epithelial transplantation. Am J Ophthalmol. 2006;141(2):267-75.
47. Hoshiba T, Lu H, Kawazoe N, Chen G. Decellularized matrices for tissue engineering. Expert Opin Biol Ther. 2010;10(12):1717-28.
48. Rosso F, Giordano A, Barbarisi M, Barbarisi A. From cell-ECM interactions to tissue engineering. J Cell Physiol. 2004;199(2):174-80.
49. Zhu J, Marchant RE. Design properties of hydrogel tissue-engineering scaffolds. Expert Rev Med Devices. 2011;8(5):607-26.
50. Meller D, Pauklin M, Thomasen H, Westekemper H, Steuhl K-P. Amniotic membrane transplantation in the human eye. Dtsch Arztebl Int. 2011;108(14):243-8.
51. Mamede AC, Carvalho MJ, Abrantes AM, Laranjo M, Maia CJ, Botelho MF. Amniotic membrane: from structure and functions to clinical applications. Cell Tissue Res. 2012;349(2):447-58.
52. Rahman I, Said DG, Maharajan VS, Dua HS. Amniotic membrane in ophthalmology: indications and limitations. Eye. 2009;23(10):1954-61.
53. Fernandes M, Sridhar MS, Sangwan VS, Rao GN. Amniotic membrane transplantation for ocular surface reconstruction. Cornea. 2005;24(6):643-53.
54. Endo K-i, Nakamura T, Kawasaki S, Kinoshita S. Human amniotic membrane, like corneal epithelial basement membrane, manifests the α5 chain of type IV collagen. Invest Ophthalmol Vis Sci. 2004;45(6):1771-4.
55. Celik T, Katircioglu YA, Singar E, Kosker M, Budak K, Kasim R, et al. Clinical outcomes of amniotıc membrane transplantatıon in patients with corneal and conjunctival disorders. Semin Ophthalmol. 2013;28(1):41-5.
56. Zhao H, Qu M, Wang Y, Wang Z, Shi W. Xenogeneic acellular conjunctiva matrix as a scaffold of tissue-engineered corneal epithelium. PLoS One. 2014;9(11):e111846.
57. Wenkel H, Rummelt V, Naumann G. Long term results after autologous nasal mucosal transplantation in severe mucus deficiency syndromes. Br J Ophthalmol. 2000 84(3):279-84.
58. Weinberg DA, Tham V, Hardin N, Antley C, Cohen AJ, Hunt K, et al. Eyelid mucous membrane grafts: a histologic study of hard palate, nasal turbinate, and buccal mucosal grafts. Ophthal Plast Reconstr Surg. 2007;23(3):211-6.
59. Morgan PV, Suh JD, Hwang CJ. Nasal Floor Mucosa: New Donor Site for Mucous Membrane Grafts. Ophthal Plast Reconstr Surg. 2016;32(3):174-7.
60. Kheirkhah A, Ghaffari R, Kaghazkanani R, Hashemi H, Behrouz MJ, Raju VK. A Combined Approach of Amniotic Membrane and Oral Mucosa Transplantation for Fornix Reconstruction in Severe Symblepharon. Cornea. 2013;32:155-60.
61. Fu Y, Liu J, Tseng SCG. Oral mucosal graft to correct lid margin pathologic features in cicatricial ocular surface diseases. Am J Ophthalmol. 2011;152(4):600-8.

62. Kobayashi M, Nakamura T, Yasuda M, Hata Y, Okura S, Iwamoto M, et al. Ocular surface reconstruction with a tissue-engineered nasal mucosal epithelial cell sheet for the treatment of severe ocular surface diseases. Stem Cells Transl Med. 2015;4(1):99-109.
63. Madhira SL, Vemuganti G, Bhaduri A, Gaddipati S, Sangwan VS, Ghanekar Y. Culture and characterization of oral mucosal epithelial cells on human amniotic membrane for ocular surface reconstruction. Mol Vis. 2008;14:189-96.
64. Nakamura T, Inatomi T, Sotozono C, Amemiya T, Kanamura N, Kinoshita S. Transplantation of cultivated autologous oral mucosal epithelial cells in patients with severe ocular surface disorders. Br J Ophthalmol. 2004;88(10):1280-4.
65. Hori Y, Sugiyama H, Soma T, Nishida K. Expression of membrane-associated mucins in cultivated human oral mucosal epithelial cells. Cornea. 2007;26(9 Suppl 1):S65-9.
66. Satake Y, Dogru M, Yamane G-Y, Kinoshita S, Tsubota K, Shimazaki J. Barrier function and cytologic features of the ocular surface epithelium after autologous cultivated oral mucosal epithelial transplantation. Arch Ophthalmol. 2008;126(1):23-8.
67. Prabhasawat P, Ekpo P, Uiprasertkul M, Chotikavanich S, Tesavibul N, Pornpanich K, et al. Long-term result of autologous cultivated oral mucosal epithelial transplantation for severe ocular surface disease. Cell Tissue Bank. 2016;17(3):491-503.
68. Martínez-Osorio H, Juárez-Campo M, Diebold Y, Girotti A, Alonso M, Arias FJ, et al. Genetically engineered elastin-like polymer as a substratum to culture cells from the ocular surface. Curr Eye Res. 2009;34(1):48-56.
69. Borrelli M, Joepen N, Reichl S, Finis D, Schoppe M, Geerling G, et al. Keratin films for ocular surface reconstruction: evaluation of biocompatibility in an in-vivo model. Biomaterials. 2015;42:112-20.
70. Eidet JR, Dartt DA, Utheim TP. Concise Review: Comparison of Culture Membranes Used for Tissue Engineered Conjunctival Epithelial Equivalents. J Funct Biomater. 2015;6(4):1064-84.
71. Song JJ, Ott HC. Organ engineering based on decellularized matrix scaffolds. Trends Mol Med. 2011;17(8):424-32.
72. Dhandayuthapani B, Yoshida Y, Maekawa T, Kumar DS. Polymeric scaffolds in tissue engineering application: A review. Int J Polym Sci. 2011;2011:290602.
73. Sharma S, Gupta D, Mohanty S, Jassal M, Agrawal AK, Tandon R. Surface-modified electrospun poly(epsilon-caprolactone) scaffold with improved optical transparency and bioactivity for damaged ocular surface reconstruction. Invest Ophthalmol Vis Sci. 2014;55(2):899-907.
74. Shin YJ, Lee HI, Kim MK, Wee WR, Lee JH, Koh JH, et al. Biocompatibility of nanocomposites used for artificial conjunctiva: in vivo experiments. Curr Eye Res. 2007;32(1):1-10.
75. Lee SY, Hwan J, Kim JC, Kim YH, Kim SH, Choi JW. In vivo conjunctival reconstruction using modified PLGA grafts for decreased scar formation and contraction. Biomaterials. 2003;24(27):5049-59.
76. Huhtala A, Pohjonen T, Salminen L, Salminen A, Kaarniranta K, Uusitalo H. In vitro biocompatibility of degradable biopolymers in cell line cultures from various ocular tissues: direct contact studies. J Biomed Mater Res A. 2007;83(2):407-13.
77. Kalluri R. Basement membranes: structure, assembly and role in tumour angiogenesis. Nat Rev Cancer. 2003;3:422-33.
78. LeBleu VS, MacDonald B, Kalluri R. Structure and function of basement membranes. Exp Biol Med. 2007;232:1121-9.
79. Halfter W, Oertle P, Monnier CA, Camenzind L, Reyes-Lua M, Hu H, et al. New concepts in basement membrane biology. FEBS J. 2015;282(23):4466-79.
80. Mouw JK, Ou G, Weaver VM. Extracellular matrix assembly: a multiscale deconstruction. Nat Rev Mol Cell Biol. 2014;15(12):771-85.

81. Torricelli AA, Singh V, Santhiago MR, Wilson SE. The corneal epithelial basement membrane: structure, function, and disease. Invest Ophthalmol Vis Sci. 2013 54(9):6390-400.
82. Yue B. Biology of the extracellular matrix: an overview. J Glaucoma. 2014;23(8 Suppl 1):S20-3.
83. Fukuda K, Chikama T-i, Nakamura M, Nishida T. Differential distribution of subchains of the basement membrane components type IV collagen and laminin among the amniotic membrane, cornea, and conjunctiva. Cornea. 1999;18(1):73-9.
84. Hynes RO, Naba A. Overview of the matrisome - An inventory of extracellular matrix constituents and functions. Cold Spring Harb Perspect Biol. 2012;4(1):a004903.
85. Messmer EM, Valet VM, Kampik A. Differences in basement membrane zone components of normal conjunctiva, conjunctiva in glaucoma and normal skin. Acta Ophthalmol. 2012;90(6):e476-81.
86. Michelacci YM. Collagens and proteoglycans of the corneal extracellular matrix. Braz J Med Biol Res. 2003;36(8):1037-46.
87. Yurchenco PD. Basement membranes: cell scaffoldings and signaling platforms. Cold Spring Harb Perspect Biol. 2011;3(2):a004911.
88. Iozzo RV. Basement membrane proteoglycans: from cellar to ceiling. Nat Rev Mol Cell Biol. 2005;6(8):646-56.
89. Heljasvaara R, Aikio M, Ruotsalainen H, Pihlajaniemi T. Collagen XVIII in tissue homeostasis and dysregulation - Lessons learned from model organisms and human patients. Matrix Biol. 2016
90. Singh P, Carraher C, Schwarzbauer JE. Assembly of fibronectin extracellular matrix. Annu Rev Cell Dev Biol. 2010;26:397-419.
91. Gildner CD, Roy DC, Farrar CS, Hocking DC. Opposing effects of collagen I and vitronectin on fibronectin fibril structure and function. Matrix Biol. 2014;34:33-45.
92. Chow S, Girolamo ND. Vitronectin: a migration and wound healing factor for human corneal epithelial cells. Invest Ophthalmol Vis Sci. 2014;55(10):6590-600.
93. Hiscott P, Paraoan L, Choudhary A, Ordonez JL, Al-Khaier A, Armstrong DJ. Thrombospondin 1, thrombospondin 2 and the eye. Prog Retin Eye Res. 2006;25(1):1-18.
94. Contreras-Ruiz L, Regenfuss B, Mir FA, Kearns J, Masli S. Conjunctival inflammation in thrombospondin-1 deficient mouse model of Sjögren's syndrome. PLoS One. 2013;8(9):e75937.
95. Bosman FT, Stamenkovic I. Functional structure and composition of the extracellular matrix. J Pathol. 2003;200(4):423-8.
96. Kundranda MN, Ray S, Saria M, Friedman D, Matrisian LM, Lukyanov P, et al. Annexins expressed on the cell surface serve as receptors for adhesion to immobilized fetuin-A. Biochim Biophys Acta. 2004;1693(2):111-23.
97. Wang X-Q, Hung BS, Kempf M, Liu P-Y, Dalley AJ, Saunders NA, et al. Fetuin-A promotes primary keratinocyte migration: independent of epidermal growth factor receptor signalling. Exp Dermatol. 2010;19(8):e289-92.
98. Sakwe AM, Koumangoye R, Goodwin SJ, Ochieng J. Fetuin-A (α_2HS-Glycoprotein) is a major serum adhesive protein that mediates growth signaling in breast tumor cells. J Biol Chem. 2010;285(53):41827-35.
99. Wang H, Sama AE. Anti-inflammatory role of fetuin-A in injury and infection. Curr Mol Med. 2012;12(5):625-33.
100. Wang X-Q, Hayes MT, Kempf M, Fraser JF, Liu P-Y, Cuttle L, et al. Fetuin-A: a major fetal serum protein that promotes "wound closure" and scarless healing. J Invest Dermatol. 2008;128(3):753-7.
101. Tuori A, Uusitalo H, Burgeson RE, Terttunen J, Virtanen I. The immunohistochemical composition of the human corneal basement membrane. Cornea. 1996;15(3):286-94.

102. Tsuruta D, Hashimoto T, Hamill KJ, Jones JCR. Hemidesmosomes and focal contact proteins: Functions and cross-talk in keratinocytes, bullous diseases and wound healing. J Dermatol Sci. 2011;62(1):1-7.
103. Hopkinson SB, Hamill KJ, Wu Y, Eisenberg JL, Hiroyasu S, Jones JCR. Focal contact and hemidesmosomal proteins in keratinocyte migration and wound repair. Adv Wound Care (New Rochelle). 2014;3(3):247-63.
104. Määttä M, Heljasvaara R, Sormunen R, Pihlajaniemi T, Autio-Harmainen H, Tervo T. Differential expression of collagen types XVIII/endostatin and XV in normal, keratoconus, and scarred human corneas. Cornea. 2006;25(3):341-9.
105. Ljubimov AV, Burgeson RE, Butkowski RJ, Michael AF, Sun T-T, Kenney MC. Human corneal basement membrane heterogeneity: topographical differences in the expression of type IV collagen and laminin isoforms. Lab Invest. 1995;72(4):461-73.
106. Soriano-Romaní L, García-Posadas L, López-García A, Paraoan L, Diebold Y. Thrombospondin-1 induces differential response in human corneal and conjunctival epithelial cells lines under in vitro inflammatory and apoptotic conditions. Exp Eye Res. 2015;134:1-14.
107. Sekiyama E, Nakamura T, Cooper LJ, Kawasaki S, Hamuro J, Fullwood NJ, et al. Unique distribution of thrombospondin-1 in human ocular surface epithelium. Invest Ophthalmol Vis Sci. 2006;47(4):1352-8.
108. Wen D, Wang H, Liu H. Transplantation of the allogeneic conjunctiva and conjunctival extracellular matrix. Bratisl Lek Listy. 2014;115(3):136-9.
109. Lu H, Hoshiba T, Kawazoe N, Koda I, Song M, Chen G. Cultured cell-derived extracellular matrix scaffolds for tissue engineering. Biomaterials 2011;32(36):9658-66.
110. Zhu X, Beuerman RW, Chan-Park MBE, Cheng Z, Ang LPK, Tan DTH. Enhancement of the mechanical and biological properties of a biomembrane for tissue engineering the ocular surface. Ann Acad Med Singapore. 2006;35(3):210-4.
111. Bankar SB, Singhal RS. Optimization of poly-epsilon-lysine production by Streptomyces noursei NRRL 5126. Bioresour Technol. 2010;101(21):8370-5.
112. Gallagher AG, Alorabi JA, Wellings DA, Lace R, Horsburgh MJ, Williams RL. A novel peptide hydrogel for an antimicrobial bandage contact lens. Adv Healthc Mater. 2016;5(16):2013-8.
113. Yoshida T, Nagasawa T. epsilon-Poly-L-lysine: microbial production, biodegradation and application potential. Appl Microbiol Biotechnol. 2003;62(1):21-6.
114. Gipson IK, Spurr-Michaud S, Argüeso P, Tisdale A, Ng TF, Russo CL. Mucin gene expression in immortalized human corneal-limbal and conjunctival epithelial cell lines. Invest Ophthalmol Vis Sci. 2003;44(6):2496-506.
115. Toouli CD, Huschtscha LI, Neumann AA, Noble JR, Colgin LM, Hukku B, et al. Comparison of human mammary epithelial cells immortalized by simian virus 40 T-Antigen or by the telomerase catalytic subunit. Oncogene. 2002;21(1):128-39.
116. Spurr-Michaud SJ, Gipson IK. Methods for culture of human corneal and conjunctival epithelia. Methods Mol Biol. 2013;945:31-43.
117. Krenzer KL, Freddo TF. Cytokeratin expression in normal human bulbar conjunctiva obtained by impression cytology. Invest Ophthalmol Vis Sci. 1997;38:142-52.
118. Ramirez-Miranda A, Nakatsu MN, Zarei-Ghanavati S, Nguyen CV, Deng SX. Keratin 13 is a more specific marker of conjunctival epithelium than keratin 19. Mol Vis. 2011;17:1652-61.
119. Lin L, Daneshvar C, Kurpakus-Wheater M. Evidence for differential signaling in human conjunctival epithelial cells adherent to laminin isoforms. Exp Eye Res. 2000;70(4):537-46.
120. Dowgiert J, Sosne G, Kurpakus-Wheater M. Laminin-2 stimulates the proliferation of epithelial cells in a conjunctival epithelial cell line. Cell Prolif. 2004;37(2):161-75.

121. Cell culture protocols. ThermoFisher Scientific; [cited 2017]; Available from: https://www.thermofisher.com/uk/en/home/references/gibco-cell-culture-basics/cell-culture-protocols.html.
122. Javois LC, editor. Immunocytochemical Methods and Protocols. Totowa, NJ: Humana Press Inc.
123. Todorovic V, Desai BV, Eigenheer RA, Yin T, Amargo EV, Mrksich M, et al. Detection of differentially expressed basal cell proteins by mass spectrometry. Mol Cell Proteomics. 2010;9(2):351-61.
124. RapiGest SF protein digestion surfactant. Waters [cited 2017]; Available from: https://www.waters.com/webassets/cms/library/docs/720000468en.pdf.
125. Gundry RL, White MY, Murray CI, Kane LA, Fu Q, Stanley BA, et al. Preparation of proteins and peptides for mass spectrometry analysis in a bottom-up proteomics workflow. Curr Protoc Mol Biol. 2009;Chapter 10:Unit 10.25.
126. Iloki Assanga SB G-SA, Lewis Luj&an LM, Rosas-Durazo A, Acosta-Silva AL, Rivera-Castañeda EG, Rubio-Pino JL. Cell growth curves for different cell lines and their relationship with biological activities. Int J Biotechnol Mol Biol Res. 2013;4(4):60-70.
127. Freshney RI. Culture of Animal Cells: A Manual of Basic Technique and Specialized Applications: John Wiley & Sons; 2010.
128. Freshney RI. Culture of Cells for Tissue Engineering. John Wiley & Sons; 2006. p. 2-22.
129. Hamill KJ, Kligys K, Hopkinson SB, Jones JCR. Laminin deposition in the extracellular matrix: a complex picture emerges. J Cell Sci. 2009;122(24):4409 - 17.
130. Fu R-H, Wang Y-C, Liu S-P, Shih T-R, Lin H-L, Chen Y-M, et al. Decellularization and recellularization technologies in tissue engineering. Cell Transplant. 2014;23:621-30.
131. Gilbert TW, Sellaro TL, Badylak SF. Decellularization of tissues and organs. Biomaterials. 2006;27(19):3675-83.
132. Lynch AP, Ahearne M. Strategies for developing decellularized corneal scaffolds. Exp Eye Res. 2013;108:42-7.
133. Clark J. The mass spectrometer. 2015 [cited 2017]; Available from: http://www.chemguide.co.uk/analysis/masspec/howitworks.html.
134. Miosge N, Simniok T, Sprysch P, Herken R. The collagen type XVIII endostatin domain is co-localized with perlecan in basement membranes in vivo. J Histochem Cytochem. 2003;51(3):285-96.
135. Ohlmann AV, Ohlmann A, Welge-Lüssen U, May CA. Localization of collagen XVIII and endostatin in the human eye. Curr Eye Reseach. 2005;30(1):27-34.
136. Määttä M, Heljasvaara R, Pihlajaniemi T, Uusitalo M. Collagen XVIII/endostatin shows a ubiquitous distribution in human ocular tissues and endostatin-containing fragments accumulate in ocular fluid samples. Graefes Arch Clin Exp Ophthalmol. 2007;245(1):74-81.
137. Lin H-C, Chang J-H, Jain S, Gabison EE, Kure T, Kato T, et al. Matrilysin cleavage of corneal collagen type XVIII NC1 domain and generation of a 28-kDa fragment. Invest Ophthalmol Vis Sci. 2001;42(11):2517-24.
138. Seppinen L, Pihlajaniemi T. The multiple functions of collagen XVIII in development and disease. Matrix Biol. 2011;30(2):83-92.
139. Pöschl E, Schlötzer-Schrehardt U, Brachvogel B, Saito K, Ninomiya Y, Mayer U. Collagen IV is essential for basement membrane stability but dispensable for initiation of its assembly during early development. Development. 2004;131(7):1619-28.
140. Hamill KJ, Paller AS, Jones JCR. Adhesion and migration, the diverse functions of the laminin α3 subunit. Dermatol Clin. 2010;28(1):79-87.
141. Hirosaki T, Tsubota Y, Kariya Y, Moriyama K, Mizushima H, Miyazaki K. Laminin-6 is activated by proteolytic processing and regulates cellular adhesion and migration differently from laminin-5. J Biol Chem. 2002;277(51):49287-95.

142. Nakashima Y, Kariya Y, Miyazaki K. The beta3 chain short arm of laminin-332 (laminin-5) induces matrix assembly and cell adhesion activity of laminin-511 (laminin-10). J Cell Biochem. 2007;100(3):545-56.
143. Hasenson S, Määttä M, Rousselle P, Kikkawa Y, Miner JH, Tervo T, et al. The immortalized human corneal epithelial cells adhere to laminin-10 by using Lutheran glycoproteins and integrin alpha3beta1. Exp Eye Res. 2005;81(4):415-21.
144. Lin L, Kurpakus-Wheater M. Laminin α5 chain adhesion and signaling in conjunctival epithelial cells. Invest Ophthalmol Vis Sci. 2002;43(8):2615-21.
145. Muppala S, Frolova E, Xiao R, Krukovets I, Yoon S, Hoppe G, et al. Proangiogenic Properties of Thrombospondin-4. Arterioscler Thromb Vasc Biol. 2015;35(9):1975-86.
146. Kligys K, Wu Y, Hamill KJ, Lewandowski KT, Hopkinson SB, Budinger GR, et al. Laminin-332 and α3β1 integrin-supported migration of bronchial epithelial cells is modulated by fibronectin. Am J Respir Cell Mol Biol. 2013;49(5):731-40.
147. Huang X, Wu J, Spong S, Sheppard D. The integrin alphavbeta6 is critical for keratinocyte migration on both its known ligand, fibronectin, and on vitronectin. J Cell Sci. 1998;111(Pt 15):2189-95.
148. Patra C, Ricciardi F, Engel FB. The functional properties of nephronectin: an adhesion molecule for cardiac tissue engineering. Biomaterials. 2012;33(17):4327-35.
149. Sato Y, Shimono C, Li S, Nakano I, Norioka N, Sugiura N, et al. Nephronectin binds to heparan sulfate proteoglycans via its MAM domain. Matrix Biol. 2013;32(3-4):188-95.
150. Inomata T, Ebihara N, Funaki T, Matsuda A, Watanabe Y, Ning L, et al. Perlecan-deficient mutation impairs corneal epithelial structure. Invest Ophthalmol Vis Sci. 2012;53(3):1277-84.
151. Klenkler B, Sheardown H, Jones L. Growth factors in the tear film: role in tissue maintenance, wound healing, and ocular pathology. Ocul Surf. 2007;5(3):228-39.
152. Weinzimer SA, Gibson TB, Collett-Solberg PF, Khare A, Liu B, Cohen P. Transferrin is an insulin-like growth factor-binding protein-3 binding protein. J Clin Endocrinol Metab. 2001;86(4):1806-13.
153. Wong YW, Chew J, Yang H, Tan DT, Beuerman R. Expression of insulin-like growth factor binding protein-3 in pterygium tissue. Br J Ophthalmol. 2006;90(6):769-72.
154. Kubota S, Takigawa M. CCN family proteins and angiogenesis: from embryo to adulthood. Angiogenesis. 2007;10(1):1-11.
155. Thapa N, Lee B-H, Kim I-S. TGFBIp/betaig-h3 protein: a versatile matrix molecule induced by TGF-beta. Int J Biochem Cell Biol. 2007;39(12).
156. Maeng Y-S, Lee G-H, Lee B, Choi S-I, Kim T-i, Kim EK. Role of TGFBIp in wound healing and mucin expression in corneal epithelial cells. Yonsei Med J. 2017;58(2):423-31.
157. Robertson IB, Horiguchi M, Zilberberg L, Dabovic B, Hadjiolova K, Rifkin DB. Latent TGF-β-binding proteins. Matrix Biol. 2015;47:44-53.
158. Briones VR, Chen S, Riegel AT, Lechleider RJ. Mechanism of fibroblast growth factor-binding protein 1 repression by TGF-beta. Biochem Biophys Res Commun. 2006;345(2):595-601.
159. An E, Sen S, Park SK, Gordish-Dressman H, Hathout Y. Identification of novel substrates for the serine protease HTRA1 in the human RPE secretome. Invest Ophthalmol Vis Sci. 2010;51(7):3379-86.
160. Karring H, Poulsen ET, Runager K, Thøgersen IB, Klintworth GK, Højrup P, et al. Serine protease HtrA1 accumulates in corneal transforming growth factor beta induced protein (TGFBIp) amyloid deposits. Mol Vis. 2013;19:861-76.
161. Oka C, Tsujimoto R, Kajikawa M, Koshiba-Takeuchi K, Ina J, Yano M, et al. HtrA1 serine protease inhibits signaling mediated by Tgfbeta family proteins. Development. 2004;131(5):1041-53.

162. Helin-Toiviainen M, Rönkkö S, Puustjärvi T, Rekonen P, Ollikainen M, Uusitalo H. Conjunctival matrix metalloproteinases and their inhibitors in glaucoma patients. Acta Ophthalmol. 2015;93(2):165-71.
163. Girolamo ND, McCluskey P, Lloyd A, Coroneo MT, Wakefield D. Expression of MMPs and TIMPs in human pterygia and cultured pterygium epithelial cells. Invest Ophthalmol Vis Sci. 2000;41(3):671-9.
164. Liu CJ-l, Huang Y-L, Chiu AW, Ju J-P. Transcript expression of matrix metalloproteinases in the conjunctiva following glaucoma filtration surgery in rabbits. Ophthalmic Res. 2004;36(2):114-9.
165. Heljasvaara R, Nyberg P, Luostarinen J, Parikka M, Heikkilä P, Rehn M, et al. Generation of biologically active endostatin fragments from human collagen XVIII by distinct matrix metalloproteases. Exp Cell Res. 2005;307(2):292-304.
166. Smine A, Plantner JJ. Membrane type-1 matrix metalloproteinase in human ocular tissues. Curr Eye Res. 1997 16(9):925-9.
167. Saarialho-Kere U, Kerkelä E, Jahkola T, Suomela S, Keski-Oja J, Lohi J. Epilysin (MMP-28) expression is associated with cell proliferation during epithelial repair. J Invest Dermatol. 2002;119(1):14-21.
168. Koshikawa N, Giannelli G, Cirulli V, Miyazaki K, Quaranta V. Role of cell surface metalloprotease MT1-MMP in epithelial cell migration over laminin-5. J Cell Biol. 2000;148(3):615-24.
169. Heiskanen TJ, Illman SA, Lohi J, Keski-Oja J. Epilysin (MMP-28) is deposited to the basolateral extracellular matrix of epithelial cells. Matrix Biol. 2009;28(2):74-83.
170. Argüeso P, Guzman-Aranguez A, Mantelli F, Cao Z, Ricciuto J, Panjwani N. Association of cell surface mucins with galectin-3 contributes to the ocular surface epithelial barrier. J Biol Chem. 2009;284(34):23037-45.
171. Cao Z, Said N, Amin S, Wu HK, Bruce A, Garate M, et al. Galectins-3 and -7, but not galectin-1, play a role in re-epithelialization of wounds. J Biol Chem. 2002;277(44):42299-305.
172. Tinari N, Kuwabara I, Huflejt ME, Shen PF, Iacobelli S, Liu F-T. Glycoprotein 90K/MAC-2BP interacts with galectin-1 and mediates galectin-1-induced cell aggregation. Int J Cancer. 2001;91(2):167-72.
173. Koblinski JE, Wu M, Demeler B, Jacob K, Kleinman HK. Matrix cell adhesion activation by non-adhesion proteins. J Cell Sci. 2005 118(Pt 13):2965-74.
174. Wyatt AR, Wilson MR. Identification of human plasma proteins as major clients for the extracellular chaperone clusterin. J Biol Chem. 2010;285(6):3532-9.
175. Sottile J, Hocking DC, Swiatek PJ. Fibronectin matrix assembly enhances adhesion-dependent cell growth. J Cell Sci. 1998;111 (Pt 19):2933-43.
176. Feng Y, Borrelli M, Reichl S, Schrader S, Geerling G. Review of alternative carrier materials for ocular surface reconstruction. Curr Eye Res. 2014;39(6):541-52.
177. Iwashita J, Yamamoto T, Sasaki Y, Abe T. MUC5AC production is downregulated in NCI-H292 lung cancer cells cultured on type-IV collagen. Mol Cell Biochem. 2010 337:65-75.
178. Öhlund D, Franklin O, Lundberg E, Lundin C, Sund M. Type IV collagen stimulates pancreatic cancer cell proliferation, migration, and inhibits apoptosis through an autocrine loop. BMC Cancer. 2013;13(154).
179. Rama P, Matuska S, Paganoni G, Spinelli A, Luca MD, Pellegrini G. Limbal stem-cell therapy and long-term corneal regeneration. N Engl J Med. 2010;363(2):147-55.
180. Takács L, Tóth E, Berta A, Vereb G. Stem cells of the adult cornea: from cytometric markers to therapeutic applications. Cytometry A. 2009;75(1):54-66.
181. Li D-Q, Chen Z, Song XJ, Paiva CSd, Kim H-S, Pflugfelder SC. Partial enrichment of a population of human limbal epithelial cells with putative stem cell properties based on collagen type IV adhesiveness. Exp Eye Res. 2005;80(4):581-90.

182. Igarashi T, Shimmura S, Yoshida S, Tonogi M, Shinozaki N, Yamane G-y. Isolation of oral epithelial progenitors using collagen IV. Oral Dis. 2008;14(5):413-8.
183. Vuoristo S, Virtanen I, Takkunen M, Palgi J, Kikkawa Y, Rousselle P, et al. Laminin isoforms in human embryonic stem cells: synthesis, receptor usage and growth support. J Cell Mol Med. 2009;13(8B):2622-33.
184. Miyazaki T, Futaki S, Hasegawa K, Kawasaki M, Sanzen N, Hayashi M, et al. Recombinant human laminin isoforms can support the undifferentiated growth of human embryonic stem cells. Biochem Biophys Res Commun. 2008;375(1):27-32.
185. Singh P, Schwarzbauer JE. Fibronectin and stem cell differentiation - lessons from chondrogenesis. J Cell Sci. 2012;125(Pt 16):3703-12.
186. Kalaskar D, Downes JE, Murray P, Edgar DH, Williams RL. Characterization of the interface between adsorbed fibronectin and human embryonic stem cells. J R Soc Interface. 2013;10(83):20130139.
187. Hughes CS, Radan L, Betts D, Postovit LM, Lajoie GA. Proteomic analysis of extracellular matrices used in stem cell culture. Proteomics. 2011;11(20):3983-91.
188. Nistor G, Poole AJ, Draelos Z, Lupo M, Tzikas T, Liu JH, et al. Human Stem Cell-Derived Skin Progenitors Produce Alpha 2-HS Glycoprotein (Fetuin): A Revolutionary Cosmetic Ingredient. J Drugs Dermatol. 2016;15(5):583-98.
189. Polisetti N, Zenkel M, Menzel-Severing J, Kruse FE, Schlötzer-Schrehardt U. Cell adhesion molecules and stem cell-niche-interactions in the limbal stem cell niche. Stem Cells. 2016;34(1):203-19.
190. Dziasko MA, Daniels JT. Anatomical features and cell-cell interactions in the human limbal epithelial stem cell niche. Ocul Surf. 2016;14(3):322-30.
191. Nakamura R, Nakamura F, Fukunaga S. Diverse functions of perlecan in central nervous system cells in vitro. Anim Sci J. 2015;86(10):904-11.
192. Ohta K, Ito A, Tanaka H. Neuronal stem/progenitor cells in the vertebrate eye. Dev Growth Differ. 2008;50(4):253-9.
193. Cattavarayane S, Palovuori R, Ramanathan JT, Manninen A. α6β1- and αV-integrins are required for long-term self-renewal of murine embryonic stem cells in the absence of LIF. BMC Cell Biol. 2015;16:3.
194. Higashi K, Yagi M, Arakawa T, Asano K, Kobayashi K, Tachibana T, et al. A novel marker for undifferentiated human embryonic stem cells. Monoclon Antib Immunodiagn Immunother. 2015;34(1):7-1.
195. Nanba D, Toki F, Barrandon Y, Higashiyama S. Recent advances in the epidermal growth factor receptor/ligand system biology on skin homeostasis and keratinocyte stem cell regulation. J Dermatol Sci. 2013;72(2):81-6.
196. Williams K, Motiani K, Giridhar PV, Kasper S. CD44 integrates signaling in normal stem cell, cancer stem cell and (pre)metastatic niches. Exp Biol Med (Maywood). 2013;238(3):324-38.
197. Li J, Xin J, Zhang L, Wu J, Jiang L, Zhou Q, et al. Human hepatic progenitor cells express hematopoietic cell markers CD45 and CD109. Int J Med Sci. 2013;11(1):65-79.
198. Bulstrode H, Jones LM, Siney EJ, Sampson JM, Ludwig A, Gray WP, et al. A-Disintegrin and Metalloprotease (ADAM) 10 and 17 promote self-renewal of brain tumor sphere forming cells. Cancer Lett. 2012;326(1):79-87.
199. Imaizumi Y, Sakaguchi M, Morishita T, Ito M, Poirier F, Sawamoto K, et al. Galectin-1 is expressed in early-type neural progenitor cells and down-regulates neurogenesis in the adult hippocampus. Mol Brain. 2011;4:7.
200. Hsieh W-C, Mackinnon AC, Lu W-Y, Jung J, Boulter L, Henderson NC, et al. Galectin-3 regulates hepatic progenitor cell expansion during liver injury. Gut. 2015;64(2):312-21.
201. Nakatsu MN, Ding Z, Ng MY, Truong TT, Yu F, Deng SX. Wnt/β-catenin signaling regulates proliferation of human cornea epithelial stem/progenitor cells. Invest Ophthalmol Vis Sci. 2011;52(7):4734-41.

202. Jirsova K, Dudakova L, Kalasova S, Vesela V, Merjava S. The OV-TL 12/30 clone of anti-cytokeratin 7 antibody as a new marker of corneal conjunctivalization in patients with limbal stem cell deficiency. Invest Ophthalmol Vis Sci. 2011;52:5892-8.
203. Kawano K, Uehara F, Sameshima M, Ohba N. Application of lectins for detection of goblet cell carbohydrates of the human conjunctiva. Exp Eye Res. 1984;38(5):439-47.
204. Ito Y, Iwashita J, Kudoh A, Kuramata C, Murata J. MUC5B mucin production is upregulated by fibronectin and laminin in human lung epithelial cells via the integrin and ERK dependent pathway. Biosci Biotechnol Biochem. 2015;79(11):1794-801.
205. Iwashita J, Ito Y, Yokoo M, Takahashi S, Murata J. Akt induces down regulation of MUC5AC production in NCI-H292 human airway epithelial cells cultured on extracellular matrix. Biosci Biotechnol Biochem. 2014;78(2):212-21.
206. Turpie B, Yoshimura T, Gulati A, Rios JD, Dartt DA, Masli S. Sjögren's syndrome-like ocular surface disease in thrombospondin-1 deficient mice. Am J Pathol. 2009;175(3):1136-47.
207. Yu H, Li Q, Zhou X, Kolosov VP, Perelman JM. Role of hyaluronan and CD44 in reactive oxygen species-induced mucus hypersecretion. Mol Cell Biochem. 2011;352(1-2):65-75.
208. Hodges RR, Bair JA, Carozza RB, Li D, Shatos MA, Dartt DA. Signaling pathways used by EGF to stimulate conjunctival goblet cell secretion. Exp Eye Res. 2012;103:99-113.
209. Wu Q, Jiang D, Chu HW. Cigarette smoke induces growth differentiation factor 15 production in human lung epithelial cells: implication in mucin over-expression. Innate Immun. 2012;18(4):617-26.
210. Deshmukh HS, Case LM, Wesselkamper SC, Borchers MT, Martin LD, Shertzer HG, et al. Metalloproteinases mediate mucin 5AC expression by epidermal growth factor receptor activation. Am J Respir Crit Care Med. 2005;171(4):305-14.
211. Yu HM, Li Q, Perelman JM, Kolosov VP, Zhou XD. Effects of endogeny polypeptide elafin on MUC5AC overexpression in human airway epithelial cells. Zhonghua Jie He He Hu Xi Za Zhi. 2010;33(11):801-5.
212. Deshmukh HS, McLachlan A, Atkinson JJ, Hardie WD, Korfhagen TR, Dietsch M, et al. Matrix metalloproteinase-14 mediates a phenotypic shift in the airways to increase mucin production. Am J Respir Crit Care Med. 2009;180(9):834-45.
213. Xu R, Li Q, Zhou X, Perelman JM, Kolosov VP. Annexin II mediates the neutrophil elastase-stimulated exocytosis of mucin 5ac. Mol Med Rep. 2014;9(1):299-304.
214. DIez-Ajenjo MA, GarcIa-Domene MC, Peris-MartInez C, Artigas JM, Felipe A. Effect of the color of the intraocular lens on optical and visual quality. Indian J Ophthalmol. 2014;62(11):1064-68.
215. Chen G, Kawazoe N, Tateishi T. Effects of ECM proteins and cationic polymers on the adhesion and proliferation of rat islet cells. Open Biotechnol J. 2008;2:133-7.
216. Saltzman WM, Kyriakides TR. Cell interactions with polymers. In: Lanza R, Langer R, Vacanti J, editors. Principles of tissue engineering: Academic Press; 2014.
217. Katoa D, Takeuchia M, Sakuraia T, Furukawab S-i, Mizokamib H, Sakataa M, et al. The design of polymer microcarrier surfaces for enhanced cell growth. Biomaterials. 2003;24(23):4253-64.